UNIVERSITY OF THESSALY

POLYTECHNIC SCHOOL

DEPARTMENT OF MECHANICAL ENGINEERING

Postgraduate Thesis

Review of parameters affecting emission factors

CHARIKLEIA RAMPAOUNI

Dipl. Computer and Telecommunications Engineer, University of Thessaly 2010

Υπεβλήθη για την εκπλήρωση μέρους των

απαιτήσεων για την απόκτηση του

Μεταπτυχιακού Διπλώματος Ειδίκευσης

2013

Institutional Repository - Library & Information Centre - University of Thessaly
09/12/2017 02:36:50 EET - 137.108.70.7

© 2013 Charikleia Rampaouni

Η έγκριση της μεταπτυχιακής εργασίας από το Τμήμα Μηχανολόγων Μηχανικών της Πολυτεχνικής Σχολής του Πανεπιστημίου Θεσσαλίας δεν υποδηλώνει αποδοχή των απόψεων του συγγραφέα (Ν. 5343/32 αρ. 202 παρ. 2).

Institutional Repository - Library & Information Centre - University of Thessaly
09/12/2017 02:36:50 EET - 137.108.70.7

Εγκρίθηκε από τα Μέλη της Τριμελούς Εξεταστικής Επιτροπής:

Πρώτος Εξεταστής (Επιβλέπων)	Δρ. Γεώργιος Κ.Δ. Σαχαρίδης Διδάσκων Π.Δ. 407/80, (εκλεγμένος) Λέκτορας Τμήμα Μηχανολόγων Μηχανικών, Πανεπιστήμιο Θεσσαλίας
Δεύτερος Εξεταστής	Δρ. Αναστάσιος Σταμάτης Αναπληρωτής Καθηγητής, Τμήμα Μηχανολόγων Μηχανικών, Πανεπιστήμιο Θεσσαλίας
Τρίτος Εξεταστής	Δρ. Δημήτριος Παντελής Επίκουρος Καθηγητής, Τμήμα Μηχανολόγων Μηχανικών, Πανεπιστήμιο Θεσσαλίας

Institutional Repository - Library & Information Centre - University of Thessaly
09/12/2017 02:36:50 EET - 137.108.70.7

Ευχαριστίες

Οφείλω να ευχαριστήσω θερμά για τη βοήθεια που μου προσέφεραν στα πλαίσια της μεταπτυχιακής μου εργασίας:

Τον κύριο Γεώργιο Σαχαρίδη, Λέκτορα του Τμήματος Μηχανολόγων Μηχανικών του Π.Θ. για την καθοδήγηση και συμπαράσταση που μου προσέφερε καθ' όλη τη διάρκεια εκπόνησης της μεταπτυχιακής εργασίας.

Τα υπόλοιπα μέλη της εξεταστικής επιτροπής της μεταπτυχιακής εργασίας μου, κύριο Αναστάσιο Σταμάτη, Αναπληρωτή Καθηγητή του Τμήματος Μηχανολόγων Μηχανικών του Π.Θ., και κύριο Δημήτριο Παντελή, Επίκουρο Καθηγητή του Τμήματος Μηχανολόγων Μηχανικών του Π.Θ. για την προσεκτική ανάγνωση της εργασίας μου και για τις πολύτιμες υποδείξεις τους.

Την οικογένειά μου για την αδιάκοπη στήριξη και αγάπη της καθώς και τους φίλους μου για την συμπαράστασή τους.

Institutional Repository - Library & Information Centre - University of Thessaly
09/12/2017 02:36:50 EET - 137.108.70.7

ACRONYMS LIST

PEMS	portable emissions monitoring systems
GPS	global positioning system
EPA	United States Environmental Protection Agency
MEET	Methodologies for estimating air pollutant emissions from transport
UBA	German Environmental Protection Agency in Berlin
BUWAL	Swiss Environmental Protection Agency in Bern
HDM	Maintenance Standards Model
PHEM	Passenger car and Heavy duty Emission model
HDV	Heavy Duty Vehicle
MOVES	Motor Vehicle Emission Simulator model
CSTT	Centre for Surface Transportation Technology
IRI	International Roughness Index
ECRPD	Energy Conservation in Road Pavement Design, Maintenance and Utilisation
MIRIAM	Models for rolling resistance in road infrastructure asset management systems
HBEFA	Handbook on Emission Factors for Road Traffic
LIDAR	Light Detection and Ranging
VSP	Vehicle Specific Power
LDV	Light Duty Vehicle
HDV	Heavy Duty Vehicle
VSTV	Very Specific Type of Vehicle
HOV	High occupancy vehicle
LCV	Light commercial vehicle

Institutional Repository - Library & Information Centre - University of Thessaly
09/12/2017 02:36:50 EET - 137.108.70.7

TCMs	Transportation control measures
CATI	Clean Air Technologies International, Inc.
NYCC	New York City Cycle
FTP	Federal test procedure
UBA	German Environmental Protection Agency
BUWAL	Swiss Environmental Protection Agency
COST	Co-operation in the field of Scientific and Technical Research
NAS	National Academy of Sciences
GHG	Green House Gas emission
GWP	Global Warming Potential
NOAA	National Oceanic and Atmospheric Administration of USA
NYDEC	New York State Department of Environmental Conservation
SFTP	Supplemental Federal Test Procedure
ATL	Automotive Testing Laboratories
ACCF	A/C Correction Factor
CSTT	Centre for Surface Transportation Technology
OBDII	OnBooard Diagnostic
RBF	Radial basis function
MPH	Miles Per Hour
RR	Rolling resistance
CFD	Computation Fluid Dynamics
NMHC	Non-methane Hydrocarbons
CPF	Catalyst pass fraction
NEDC	New European Driving Cycle

Institutional Repository - Library & Information Centre - University of Thessaly
09/12/2017 02:36:50 EET - 137.108.70.7

ZDRAG	Averaged Drag Power
FC	Fuel Consumption
Ztot	Trip Averaged Total Power (kW)
Zlev	Instantaneous Level Power (kW)
Zgrad	Instantaneous Gradient Power (kW)
BEV	Battery Electric Vehicle
PHEV-FC	Plug-in Hybrid Fuel Cell Electric Vehicle
ICEV	Internal Combustion Engine Vehicle
AADT	Annual Average Daily Traffic
VDOT	Virginia Department of Transportation
CO	Carbon Monoxide
HC	Hydrocarbons
FWHS	Freeway High Speed road
ARTC	Arterial LOS C-D road
ADC	Average Degree of Curvature (rad/km)
PI	Performance Index
RF	Rise and Fall (m/km)
ArcGIS	Geographic Information System
CMEM	Comprehensive Modal Emissions Model
FMS	Fleet Management System
CUTE	Clean Urban Transport for Europe

Institutional Repository - Library & Information Centre - University of Thessaly
09/12/2017 02:36:50 EET - 137.108.70.7

Institutional Repository - Library & Information Centre - University of Thessaly
09/12/2017 02:36:50 EET - 137.108.70.7

Institutional Repository - Library & Information Centre - University of Thessaly
09/12/2017 02:36:50 EET - 137.108.70.7

Figures

Institutional Repository - Library & Information Centre - University of Thessaly
09/12/2017 02:36:50 EET - 137.108.70.7

Institutional Repository - Library & Information Centre - University of Thessaly
09/12/2017 02:36:50 EET - 137.108.70.7

Institutional Repository - Library & Information Centre - University of Thessaly
09/12/2017 02:36:50 EET - 137.108.70.7

Institutional Repository - Library & Information Centre - University of Thessaly
09/12/2017 02:36:50 EET - 137.108.70.7

Institutional Repository - Library & Information Centre - University of Thessaly
09/12/2017 02:36:50 EET - 137.108.70.7

Tables

Institutional Repository - Library & Information Centre - University of Thessaly
09/12/2017 02:36:50 EET - 137.108.70.7

Institutional Repository - Library & Information Centre - University of Thessaly
09/12/2017 02:36:50 EET - 137.108.70.7

Institutional Repository - Library & Information Centre - University of Thessaly
09/12/2017 02:36:50 EET - 137.108.70.7

Institutional Repository - Library & Information Centre - University of Thessaly
09/12/2017 02:36:50 EET - 137.108.70.7

INTRODUCTION

The fuel consumption of a vehicle and the emissions produced are two subjects of high importance that have occupied scientists and researchers for many years. A great amount of studies has been published dealing with these two subjects, taking as data different circumstances, different types of vehicles and other parameters that might affect the emissions produced or the fuel economy of these vehicles.

There are many factors that impact the energy/fuel consumption for a vehicle and also the emissions level. These factors can be divided into following parts:

- Thermodynamic efficiency of the engine to transfer heat into mechanical power,
- Rolling resistance: due to tire/pavement effect for each wheel,
- Air resistance: effect of speed and aerodynamic shape,
- Gradient resistance: effect of road slope and vehicle mass,
- Inertia resistance: effect of vehicle mass and acceleration,
- Driveline losses in the vehicle,
- Use of auxiliaries/accessories.

In the chapters below, we are going to deal with four very important parameters and their consequences taking also into account other factors like the type of vehicle and its speed, the type of road and external conditions (e.g. weather conditions). These parameters are:

- The Gradient,
- The Rolling Resistance,
- The Aerodynamic Drag (Air Resistance) and
- The use of A/C.

Each of the chapters below (Chapter 1- Chapter 4) deals with one of the above parameters and contains studies that examine the effects of this specific parameter. All these studies are categorized by the type of vehicle used for examination, so that the presentation is more comprehensible by the reader. Also, in Chapter 5 there are some studies presented that examine more than one of the above parameters in correlation so that we can export even more valid and realistic general conclusions.

Institutional Repository - Library & Information Centre - University of Thessaly
09/12/2017 02:36:50 EET - 137.108.70.7

Chapter 1 : THE GRADIENT

1.1 Introduction

The gradient of a road is an important factor that affects the exhaust emissions and the fuel consumption of a vehicle. It has the effect of increasing or decreasing the resistance of a vehicle to traction. As it has been shown during the development of emission functions, the power employed during the driving operation is the decisive parameter for the pollution emission of a vehicle. Even in the case of large-scale considerations, however, it cannot be assumed that - for example - the extra emission when travelling uphill is compensated by correspondingly reduced emission when travelling downhill. In principle the emissions and fuel consumption of both light and heavy duty vehicles are affected by road gradient. Nevertheless, the overall gradient effect on the behavior of light duty vehicles (passenger cars and light duty trucks) was found to be in some cases less important e.g. (Keller, Evequoz, Heldstab, & Kessler, 1995) compared to the heavy duty vehicles because of their higher masses. Roadway grades are one of the highway-related factors affecting fuel consumption and emission rates. It is a well-accepted fact that vehicles consume more energy and emit higher emissions as they travel along roadway upgrades and there is enough literature that has attempted to study the effect of roadway grades on vehicle fuel consumption and emission rates. Most of the studies concentrate on a specific types of vehicles, load, weather conditions etc. so there are no general results. (Pierson W. , et al., 1994) conducted a field study that aimed to quantify the environmental impacts of driving modes using a large in-use vehicle fleet through remote sensor measurements. The emission factors for a 3.76% uphill and downhill grade were measured in the Fort McHenry area. The study demonstrated that uphill grade emissions were higher than downhill emissions by a factor of 1.52, 1.86, and 2.19 for non-methane hydrocarbons (NMHC), CO and NO_x emissions, respectively. Other places that may promote emissions excursions include ramps where hard accelerations plus grade effects may interact. Ramps have varied designs including the following factors: curvature, length, auxiliary lanes, grades and metering which may include different queue and merging lengths or the presence of a dedicated carpool lane (Sullivan & Edward, 1993).

The road grade, g (percent), between two benchmark points can be calculated as:

$$g = \frac{e_i - e_{i-1}}{\left(\sqrt{(x_i - x_{i-1})^2 + (y_i - y_{i-1})^2}\right)} \times 100 \qquad [1]$$

Institutional Repository - Library & Information Centre - University of Thessaly
09/12/2017 02:36:50 EET - 137.108.70.7

where x and y are the latitude and the longitude values of these points (given in meters from the base station), *e* is the elevation (in meters). The index *i* is the current benchmark point, and i-1 is the previous benchmark point (Boriboonsomsin & Barth, 2009).

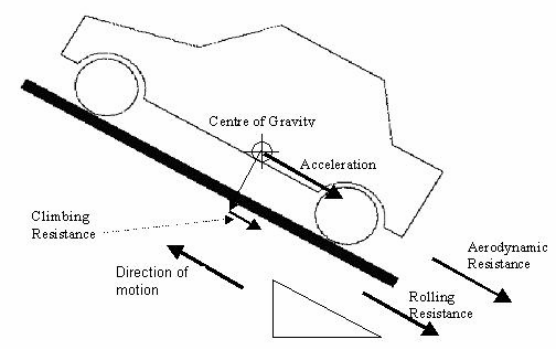

Figure 1: Existing forces on a vehicle moving on a road with grade

Road grade is an important variable with respect to emissions but sometimes is difficult to obtain with high accuracy compared to speed and acceleration. Many methods of measuring road gradients are presented as patents, and some devices are commercially produced. Studies are still under way with regard to measuring road gradients, but most commercial devices are gravity sensors which measure only the acceleration of gravity. These devices operate reasonably well when vehicle moves at a constant speed or accelerates very slowly. However, when the vehicle accelerates or decelerates, these devices measure road gradients poorly. Because the acceleration of gravity and the vehicle acceleration have the same physical properties, gravity sensors cannot discriminate one from the other (Park J. , Kong, Jo, Park, & Lee, 2001).

According to (Zhang & Frey, 2005), a method for estimating road grade was described based upon bivariate regression using Light Detection and Ranging (LIDAR) data. LIDAR data provides 3D coordinates of a geographic point on bare earth. Vehicle Specific Power (VSP) can be used for second-by-second characterization of highway vehicle emissions based upon measurements with portable emissions monitoring systems (PEMS). VSP is calculated based upon vehicle speed, acceleration, and road grade to estimate engine power demand accounting for grade, rolling resistance, and aerodynamic resistance. Road grade is an important input but is more difficult to measure directly using PEMS compared to speed and acceleration. The calculation of VSP requires acquisition of speed, acceleration and road grade data. Speed and acceleration can be measured directly by PEMS while road grade cannot. However, road grade can be approximated using Global Positioning System (GPS) data. However, GPS data can be imprecise for road grade approximation unless a sufficiently sophisticated (and costly) GPS system and data analysis procedures are used (Zhang & Frey, 2005).

Institutional Repository - Library & Information Centre - University of Thessaly
09/12/2017 02:36:50 EET - 137.108.70.7

In 2008, the thesis of (Sahlholm, 2008) presented a new method for iterative road grade estimation based on sensors that are commonplace in modern heavy duty vehicles. It was mentioned that when a highway contains segments with an uphill grade so steep that a vehicle cannot maintain the desired speed, there is a potential for decreasing the fuel consumption compared to a standard cruise controller, with unchanged trip time. The same happens on a very steep downhill grade that overspeeding will occur unless the brake system is used. It is mentioned that to achieve a reduction in the fuel consumption it is necessary to lower the vehicle speed over hill crests and increase it ahead of steep uphill segments. Thus the number of steep hill segments as well as the traffic load of the road affect the fuel consumption gain that can be achieved. However, only theoretical assumptions were presented (Sahlholm, 2008).

In the past there have been many researches about how the gradient of a road can contribute to the fuel consumption and emission rates of a vehicle. There are a lot of papers and reports published that refer to different options of this subject. Although, there is no research that reviews all the options together. In the following section, there will be a presentation of the published work, in chronological order, examining the impact of the road gradient on the fuel consumption, the power consumption and the emission rates of different types of vehicles.

Most of the existing studies, usually examine one type of vehicle or a group of different types of vehicles but there are only a few of them that refer generally to all vehicles giving average conclusions. Therefore, we divided our studies in three main categories that refer to a specific type of vehicles so we can have an even better view of our research. During our review we distinguished three different categories related with the type of the vehicle: (1) papers and reports examining LDVs (Light Duty Vehicles), (2) those examining HDVs (Heavy Duty Vehicles), (3) those that can be applied to many different but specific types of vehicles taking in account the type of vehicle given (VSTV – Very Specific Type of Vehicles). This category also refers to papers and reports that give results about the average behavior of many vehicles (ex. experiments carried out in a daily traffic of a road).

For these three categories we gave all the information concerning the case developed in each study: (1) The type of road examined, if for example is an urban road or a highway, (2) the consequences due to the gradient, that can refer to (a) the Fuel Consumption (FC) of the vehicle, (b) the produced Emissions and/or (c) the Power needed to overcome the gradient resistance, (3) The way that we come to the conclusion of which consequences of the three above exist, if for example there are mathematical expressions that proved that there is an impact on these due to the gradient or there were experiments carried out that gave results about these consequences (see Figure 2).

Institutional Repository - Library & Information Centre - University of Thessaly
09/12/2017 02:36:50 EET - 137.108.70.7

Through all these studies, and by using this categorization, we were able to come to some interesting conclusions about the relation of the gradient with the fuel consumption and the emissions produced from the vehicles. Figure 2 describes schematically our review.

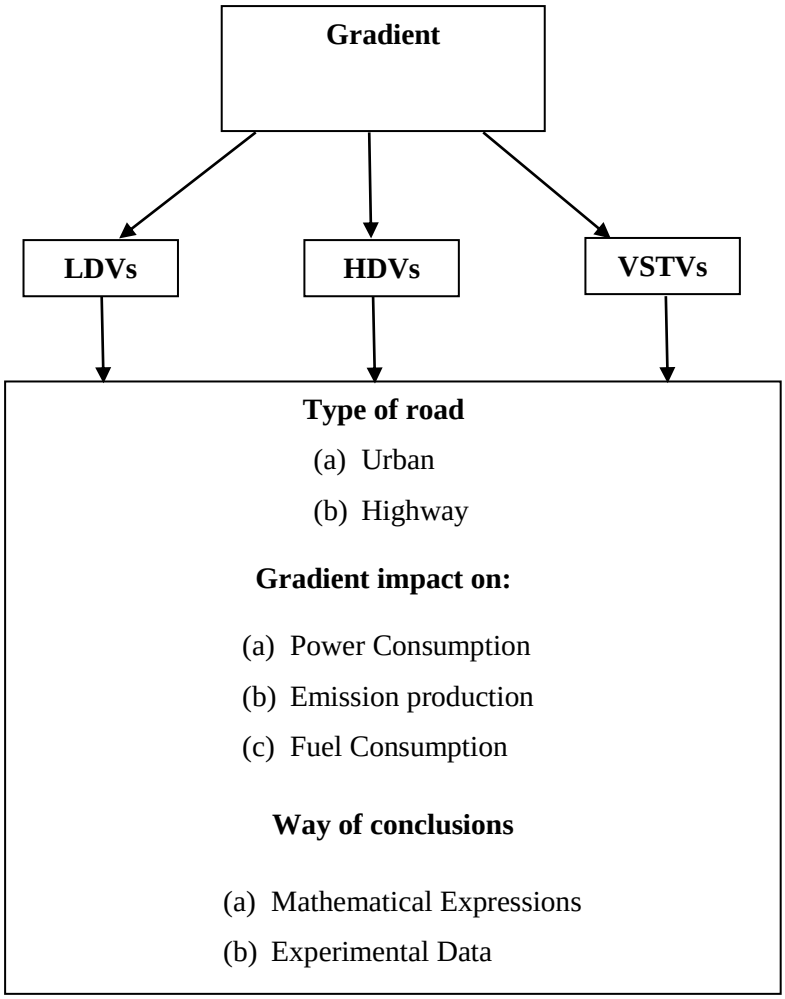

Figure 2: Diagram of our review – categorization of studies

1.2 Review of research on gradient parameter

1.2.1 Light Duty Vehicles (LDVs)

(Pierson W. R., et al., 1996) made some motor vehicle emission rates measurements in under investigation mountain tunnels and presented values for light duty and heavy duty vehicles. The study took place in the tunnels of a highway road and not an urban area and examined the emissions produced by the vehicles in different tunnels and roadway grades. No conclusions were given about fuel consumption or power requirements and no mathematical expressions

Institutional Repository - Library & Information Centre - University of Thessaly
09/12/2017 02:36:50 EET - 137.108.70.7

were used for the emission results. All the data presented below are results from experiments held in the tunnels under study.

Motor vehicle emission rates of CO, NO, NO_x, and gas-phase specified nonmethane hydrocarbons and carbonyl compounds were measured in 1992 in the Fort McHenry Tunnel under Baltimore Harbor and in the Tuscarora Mountain Tunnel of the Pennsylvania Turnpike. Both tunnels represent a high-speed setting at relatively steady speed. The cars at both sites tended to be newer than elsewhere (median age was < 4 years), and much better maintained as judged by low CO/CO_2 ratios and other emissions characteristics. The Tuscarora Mountain Tunnel was flat, making it advantageous for testing automotive emission models, while in the underwater Fort McHenry Tunnel the impact of roadway grade could be evaluated.

The effect of roadway grade on emissions was large (as great as on fuel economy or greater). In general, emissions rated uphill (grades 0 to + 3.76%, average + 3.3%) were double the emission rated downhill (0 to - 3.76%, average - 1.8%). In Table 1 and Table 2, the results referring to light duty vehicles are presented as the case of heavy duty vehicles will be presented later.

	Light Duty	
	Downhill	**Uphill**
CO_2 mi^{-1}	237 ± 9	370 ± 32
CO g×mi^{-1}	4.90 ± 0.26	9.1 ± 1.1
NMHC mi$^{-1c,d}$	0.52 ± 0.04	0.79 ± 0.22
Formaldehyde mi^{-1}	0.006 ± 0.002	0.009 ± 0.004
NO g×mi^{-1} as NO_2^e	0.53 ± 0.06	1.11 ± 0.20
NO_x g×mi^{-1} as NO_2^e	0.58 ± 0.06	1.27 ± 0.19
Mi×gal^{-1f}	36.2 ± 1.4	23.0 ± 1.9

Table 1: Effect of grade; emission rates downhill and uphill in the Fort McHenry Tunnel, June 1992 (Bore 3 and 4 data combined)
[Table 3, (Pierson W. R., et al., 1996)]

where

Light Duty: motorcycles, automobiles, sport/utility vehicles, pickup trucks;

c: Probably 10-20% low;

d: Calculated on the assumption of empirical formula $C_nH_{1.825n}$;

e: Calculated from mol×mi^{-1} using NO_2 molecular weight (molecular weight helps to change between grams and mols when needed);

f: Calculated from total carbon emission rate (ΣCO_2 + CO + organics), assuming empirical formula $C_nH_{1.825n}$ for gasoline and C_nH_{2n} for diesel fuel, and assuming gasoline density 0.7406 g×cm^{-3} and diesel fuel density 0.77331 (cetane).

Institutional Repository - Library & Information Centre - University of Thessaly
09/12/2017 02:36:50 EET - 137.108.70.7

	Light Duty		
	Fort McHenry		Tuscarora (level)
	Down	Up	
CO_2	8569	8520	8589
CO	177 ± 9	210 ± 24	181 ± 18
NMHC	19 ± 2	18 ± 5	11 ± 2
HCHO	0.21 ± 0.06	0.21 ± 0.10	0.23 ± 0.08
NO_x	21 ± 2	29 ± 4	14 ± 10

Table 2: Fuel-specific emission rates ($g \times gal^{-1}$): effect of roadway grade [Table 6, (Pierson W. R., et al., 1996)]

Also (Cicero-Fernandez & Long, 1996) developed a project to assess driving patterns likely to promote emission excursions greater than those encountered in current dynamometer driving cycles. The study was referring to highway road experiments and the strategy involved three phases: The use of an instrumented vehicle to measure on-board emissions; the use of an instrumented vehicle to develop ramp driving cycles; and the dynamometer testing of 10 vehicles on a simulated ramp, both metered and unmetered. The study was concentrated in giving conclusions about the emissions and not the fuel consumption or the power demands of the vehicle. No mathematical expressions were provided for the emission results as all the data presented below were given through experiments.

The first phase of the experiment included a fully occupied vehicle (4 passengers) while driving on a hill (4.5% grade) by a factor of 2, both for hydrocarbons and CO. A simulation was performed for a trip of 10 miles with a hill (3% grade) (including cold starts). During the second phase, two cycles simulated an on-ramp. The RAMP1- free flow and RAMP2-metered flow. Both cycles had the same distance and included three subcycles representing the simulated ramp. Each subcycle had 3 distance-based modes: on-ramp, merging, and the remainder of the cycle. These subcycles included accelerations up to 4.8 MPH/second for RAMP1 and up to 6.3 MPH/second for RAMP2. During the third phase, there was testing of 2 carbureted and 8 fuel injected vehicles, ranging from 1976 to 1992 model year on the RAMP1 and RAMP2 cycles.

Dynamometer testing has shown that significant emissions excursions occur due to hard accelerations, particularly when going from low speed to speeds exceeding 45 MPH. Additionally, driving on grades also increases exhaust emissions. Conditions like this are commonly encountered on on-ramps, and may be exacerbated when the merging distance is short or the ramp has a positive grade.

Institutional Repository - Library & Information Centre - University of Thessaly
09/12/2017 02:36:50 EET - 137.108.70.7

The existing data show that vehicle emission rates are significantly increased when the vehicle is fully occupied and driven under certain high load conditions, such as on a hill. This suggests that high occupancy vehicles (HOVs) may have a lesser effect on improving air quality than has been commonly assumed in air quality management plans in which significant tons per day credits for CO and HC have been given to such transportation control measures (TCMs). The effect of grade on the above emissions is shown in Table 3.

HC			
	Speed	0.08 g/mile	at 30 mph
	Cold Start	0.42 g/mile	for 3.6 miles
	Grade	0.12 g/mile	for a 3% grade
	AC	0.08 g/mile	while operating (on-grades)
	Full Occupancy	0.07 g/mile	4 passengers (on-grades)
CO			
	Speed	1.9 g/mile	at 30 mph
	Cold Start	3.0 g/mile	for 3.6 miles
	Grade	9.0 g/mile	for a 3% grade
	AC	32.9 g/mile	while operating (on-grades)
	Full Occupancy	10.2 g/mile	4 passengers (on-grades)

Table 3: Grade and associated effects on emissions
[Table 1, (Cicero-Fernandez & Long, 1996)]

To calculate the benefits of person trips avoided, a scenario for multiple carpool occupants was evaluated. The scenario assumed a trip of 10 miles that included a hill with a positive grade of 3% for 3.6 miles, and included a cold start. First, the emission rates per occupant were calculated assuming only the incremental emissions from a cold start and emissions from the 10 mile distance trip at 30 MPH assuming the basic emission rates given by current modeling assumptions (e.g. EMFAC7F). Additionally, emissions due to grade and full occupancy (when pertinent) were included to assess the effectiveness of carpooling for hilly areas. The results of this analysis are presented in Table 4. This analysis indicates that grade and full occupancy increases CO emission rates by a factor of three for a fully occupied vehicle, and by a factor of two for lower vehicle occupancy when compared to current modeling. A fully occupied vehicle emits 20% less CO per occupant than the same vehicle with 2 passengers, but 19% more per occupant than with 3 passengers.

Institutional Repository - Library & Information Centre - University of Thessaly
09/12/2017 02:36:50 EET - 137.108.70.7

	Number of occupants	Emission rate (g/mile/passenger)	
		0% grade	3% grade
HC			
	1	0.23	0.27
	2	0.11	0.14
	3	0.08	0.09
	4	0.06	0.08
CO			
	1	3.01	6.25
	2	1.51	3.12
	3	1.00	2.08
	4	0.75	2.48

Table 4: Modeled results for high vehicle occupancy with and without a hill [Table 3, (Cicero-Fernandez & Long, 1996)]

In 1997, (Hassel & Weber, 1997) studied the gradient influence on emission behavior, fuel consumption and power demand of light and heavy duty vehicles. The methods were different for light and heavy duty vehicles and experiments were carried out using highway roads. Also, mathematical expressions were used to come to the conclusions and they are presented below. The results and conclusions concerning heavy duty vehicles will be presented later in another section of our review (as we examine separately these different types of vehicles and as it also include correlation with other parameters). Results and mathematical expressions concerning the power are given only for the case of the heavy duty vehicles that will be presented in the next section of our review. There are specific results and analytical figures provided about the emission rates given below. The impact on the fuel consumption is shown on the figures presented below.

Emission measurements for gradient classes of -6%, -4%,-2%, 0%, 2%, 4% and 6% were conducted. In the case of the +2% gradient classes, the US Test 72 (series of tests defined by EPA to measure tailpipe emissions and fuel economy of passenger cars) with warm start was operated. For the +4 % and +6 % gradient classes special driving cycles derived from the driving behavior data collected in Switzerland were operated. Nine passenger cars with 3 way-catalyst and controlled air/fuel mixture, three conventional spark-ignition passenger cars and three diesel passenger cars were used.

Stratum factors for the gradient classes +2 % can be calculated as follows (German Emission Factor Programme):

$$SE_{G,D} = SE_D \times GF_{G,D} \quad [2]$$

where

Institutional Repository - Library & Information Centre - University of Thessaly
09/12/2017 02:36:50 EET - 137.108.70.7

$SE_{G,D}$: Stratum emission factor for the gradient class G, for the driving pattern D;

$GF_{G,D}$: Gradient factor for the gradient class G, for the driving pattern D;

SE_D: Stratum emission factor for driving pattern D (gradient class 0 %).

The above mathematical expression is valid for gradient classes +4 % and +6 % if stratum factors for driving patterns with mean speeds below 50 km/h are used.

In the case of steeper gradients and mean speeds above 50 km/h one cannot assume that gradient does not affect driving behavior. So stratum factors for the gradient classes +4 % and +6 % should only be calculated for special gradient driving patterns. In comparison to the above mathematical expression, SE_D has been replaced by BGV_D:

$$SE_{G,D} = BGV_D \times GF_{G,D} \quad [3]$$

where

BGV_D: Basis gradient value of a vehicle stratum for gradient driving pattern D.

Basis gradient values were calculated with the representative emission function of a vehicle stratum and a gradient driving pattern. The term BGV instead of SE shall pay attention to the fact that gradient driving patterns do not occur on level roads and is only needed for the calculation of stratum emission factors for the gradient classes +4 % and +6 %.

The gradient factors of the pollutant components and the fuel consumption are presented in Figure 3 toFigure 5, for the vehicle concepts investigated, as a function of the gradient classes and the average vehicle speed of all the driving patterns and speed classes which had to be taken into account for uphill and downhill sections.

Institutional Repository - Library & Information Centre - University of Thessaly
09/12/2017 02:36:50 EET - 137.108.70.7

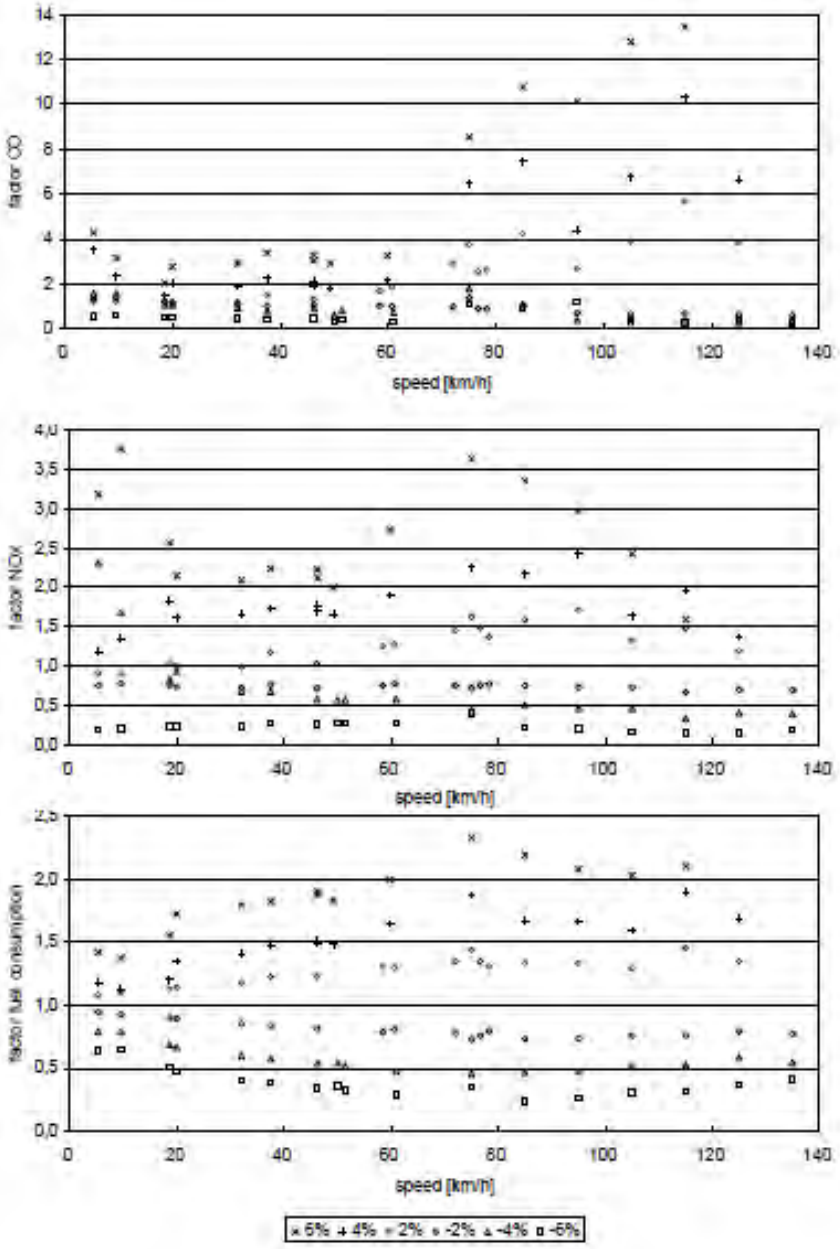

Figure 3: Gradient factors of the spark-ignition passenger cars with regulated catalyzer for CO and NOx and for consumption as a function of the gradient classes and the average vehicle speed [Figure 1, (Hassel & Weber, 1997)].

Institutional Repository - Library & Information Centre - University of Thessaly
09/12/2017 02:36:50 EET - 137.108.70.7

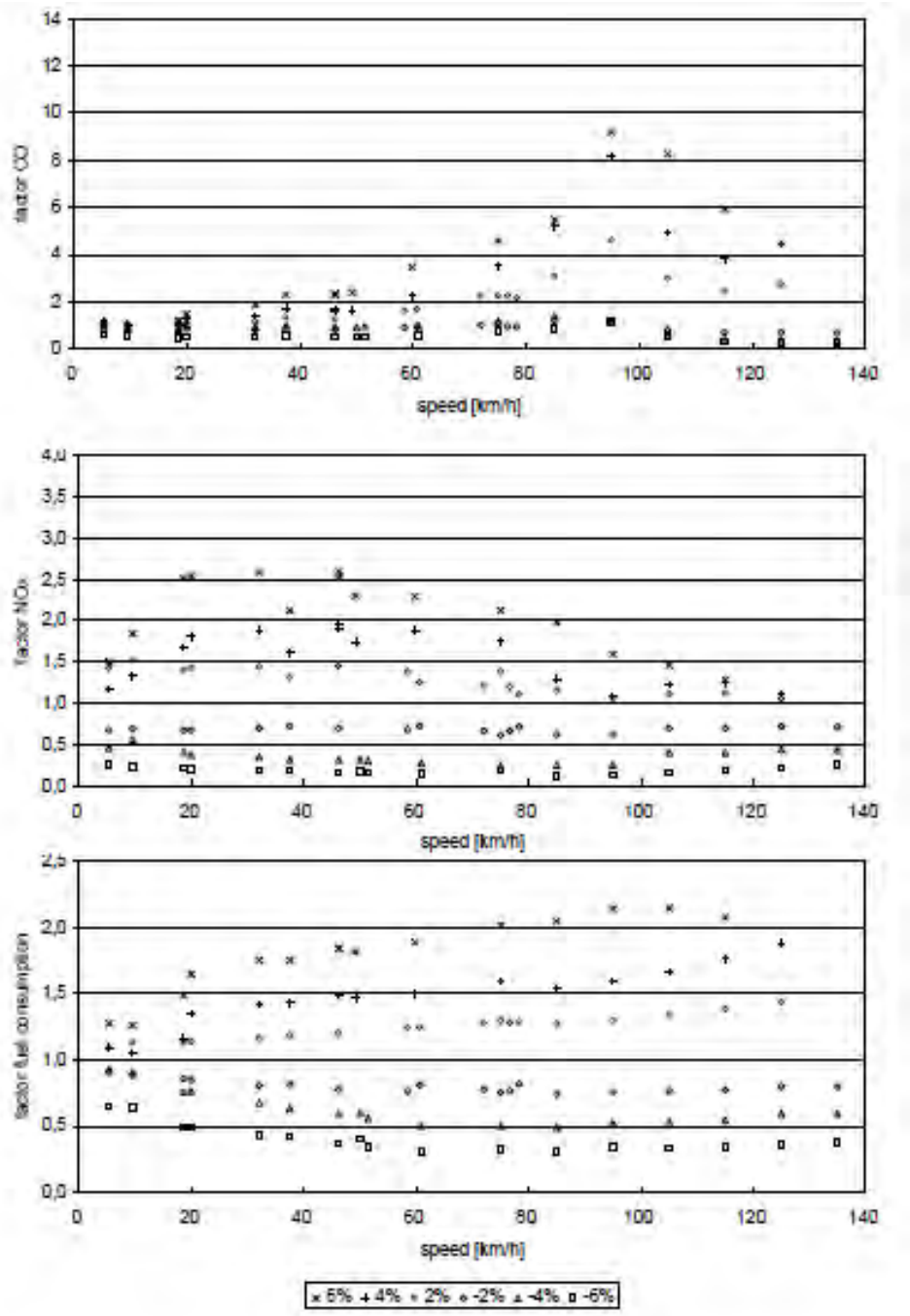

Figure 4: Gradient factors of the conventional spark-ignition passenger cars for CO and NOx and for consumption as a function of the gradient classes and the average vehicle speed [Figure 2, (Hassel & Weber, 1997)]

In the case of the 2% to 6% slope classes, the different driving patterns greatly influenced the gradient factor for CO, HC and NO_x both in the case of conventional spark-ignition passenger cars and in the case of regulated catalyzer passenger cars. The gradient factors of CO and HC in the slope ranged between 2% and 6% are greater in the case of the regulated catalyzer passenger cars than they were in the case of the conventional spark-ignition passenger cars.

Institutional Repository - Library & Information Centre - University of Thessaly
09/12/2017 02:36:50 EET - 137.108.70.7

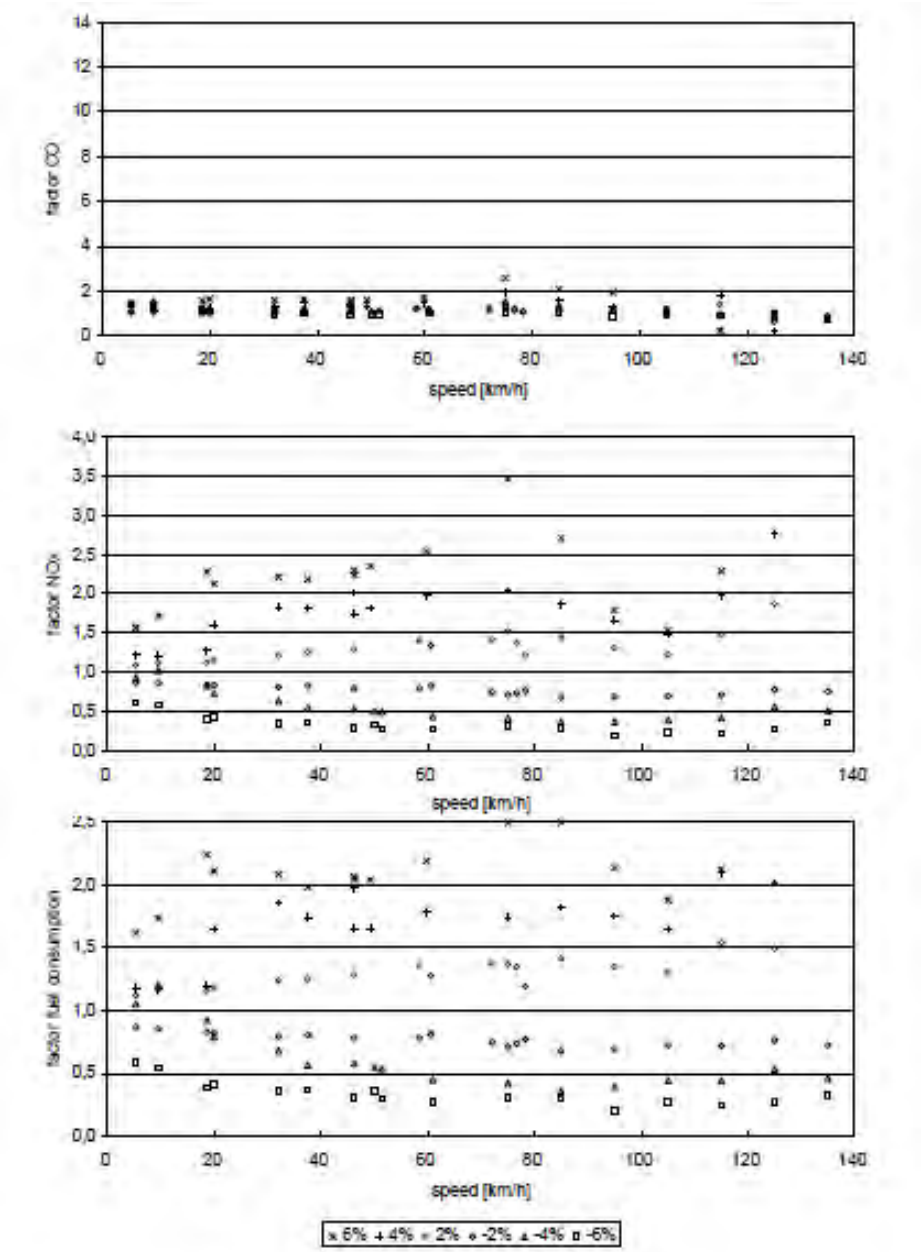

Figure 5: Gradient factors of the conventional diesel passenger cars for CO and NOx and for consumption as a function of the gradient classes and the average vehicle speed [Figure 3, (Hassel & Weber, 1997)]

The gradient factor exhibited the same order of value for all three pollutant components and for the consumption. In contrast with the spark-ignition passenger cars, the gradient factor for consumption in the case of the diesel passenger cars was more strongly influenced by the driving pattern in the case of the 4% and 6% slope classes.

In 2003, a study was carried out by (Frey, Unal, Rouphail, & James D., 2003) for the deployment of portable onboard tailpipe emissions measurement systems for selected highway vehicles fueled by gasoline and E85 (a blend of 85% ethanol and 15% gasoline).

Institutional Repository - Library & Information Centre - University of Thessaly
09/12/2017 02:36:50 EET - 137.108.70.7

There were experimental results given concerning the impact of the gradient to the emission rates but also to the fuel consumption of the tested vehicles, but there was no reference in the power requirements. Data collection, screening, processing, and analysis protocols were developed to assure data quality and to provide insights regarding quantification of real-world intravehicle variability in hot-stabilized emissions. The study provided no specific mathematical expressions for computations.

The instrument used for onboard data collection in this study was the OEM-2100 manufactured by the Clean Air Technologies International, Inc. (CATI). The system was comprised of a five-gas analyzer, an engine diagnostic scanner, and an onboard computer. Three light-duty gasoline vehicles were tested by the New York State Department of Environmental Conservation (NYDEC) using the I/M 240 and New York City Cycle (NYCC) driving cycles and two light-duty vehicles by EPA using the federal test procedure (FTP), US06, NYCC, and freeway high-speed driving cycles at Ann Arbor.

The study design featured two primary drivers who both operated two primary vehicles on each of two corridors. The largest number of driver/vehicle/route data collection runs was made with primary drivers and vehicles to characterize intravehicle variability and to compare emissions of the same vehicle with two different drivers.

Corridors are primary arterials with heavy traffic flow during peak travel times, road grades ranging well within ±5%. An example of time traces of vehicle speed, emissions of CO, NO, HC, and CO_2, and fuel consumption is given in Figure 6. The travel time on the corridor was 14 min. The instantaneous speed ranged from 0 to 45 mph, and the average speed was 10 mph. The longest waiting times occurred in the queue before the Morrisville Parkway intersection. For all four pollutants, it is clear that the highest emission rates, on a mass per time basis, occurred during small portions of the trip. The largest peak in the emission rate occurred at the same time at the acceleration from 0 to 40 mph as the vehicle cleared the intersection with Aviation Parkway. Most of the peaks in CO emission rate tended to coincide with accelerations. The CO emission rate during idling or crawling was low compared with the CO emission rate during acceleration.

Vehicle emissions are episodic in nature, indicating that average emissions for a trip are often dominated by short-term events. In general, the time traces indicate that there is a significant contribution to total emissions from short-term events that occur within the trip. This implies that efforts to reduce on-road emissions should be aimed at understanding and mitigating these short-term events. Below, the figure shows the experimental results concerning several emissions and the fuel consumption of the vehicle.

Institutional Repository - Library & Information Centre - University of Thessaly
09/12/2017 02:36:50 EET - 137.108.70.7

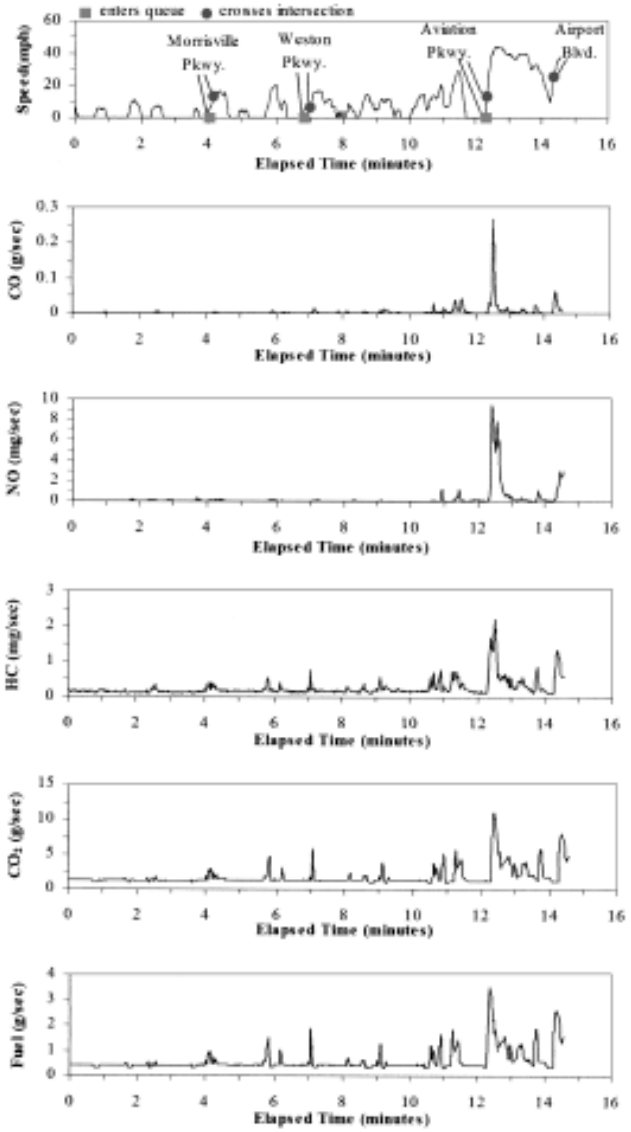

Figure 6: Time traces of vehicle speed, emission rates, and fuel consumption for a 1999 Ford Taurus driven on Chapel Hill Road on August 29, 2000
[Figure 2, (Frey, Unal, Rouphail, & James D., 2003)]

In 2005, (Zhang & Frey, 2005) used a highway road to investigate how the gradient can affect the emission rates and estimated the power needed to be used for the vehicle to overcome the resistance caused by the gradient (Vehicle Specific Power – VSP). This power needed is also the reason why the vehicle needs to consume more fuel, or generally, more energy when driving on roadway grades. The methodology followed included: (1) sensitivity analysis to evaluate the importance of road grade with respect to VSP and emissions, (2) evaluation of alternatives for road grade estimation and (3) development and validation of a reliable and accurate method for road grade estimation.

Institutional Repository - Library & Information Centre - University of Thessaly
09/12/2017 02:36:50 EET - 137.108.70.7

Provided experiments and mathematical expression gave the conclusion that a vehicle needs to use more power to cope with the roadway grades and therefore its emissions rates increase.

A generic VSP estimation mathematical expression was reported by EPA based upon coefficients typical of many light duty vehicles:

$$VSP = v \times [1.1 \times a + 9.81 \times (\sin(a \times (tan(\theta))) + 0.132] + 0.000302 \times v^3 \quad [4]$$

where

v: Vehicle speed (m/s);

a: Acceleration (m/s^2);

θ: Road grade (in degrees);

9.81: The gravitational constant (c_g);

r: Road grade (slope).

To evaluate the sensitivity of emissions to road grade, emissions were estimated using a VSP binning approach. Each VSP bin referred to one of 14 "modes." For each VSP mode, an average emissions rate was estimated based upon PEMS or other second-by-second data (see Table 5).

VSP mode	Definition
1	VSP < -2
2	-2 <= VSP < 0
3	0 <= VSP < 1
4	1 <= VSP < 4
5	4 <= VSP < 7
6	7 <= VSP < 10
7	10 <= VSP < 13
8	13 <= VSP < 16
9	16 <= VSP < 19
10	19 <= VSP < 23
11	23 <= VSP < 28
12	28 <= VSP < 33
13	33 <= VSP < 39
14	39 <= VSP

Table 5: Definition of Vehicle Specific Power (VSP) Modes [Table 1, (Zhang & Frey, 2005)]

For a given speed, larger positive road grades leaded to an increase in VSP, in turn leading to higher mode and average emissions rate. For example, estimated average emissions for a road grade of 0.06 are approximately a factor of two greater than for no road grade. In the tables below, the effect of road grade and speed to VSP and NO_x emissions is presented.

Institutional Repository - Library & Information Centre - University of Thessaly
09/12/2017 02:36:50 EET - 137.108.70.7

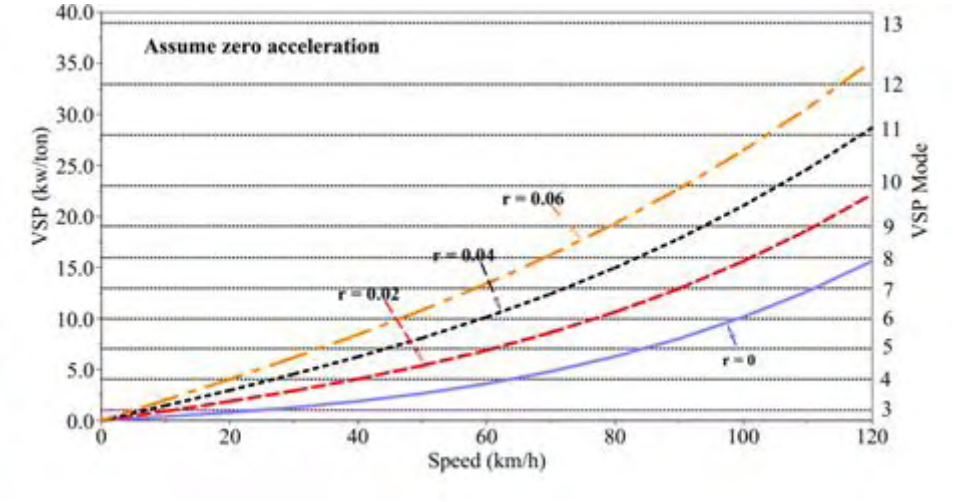

Figure 7: Sensitivity of VSP to Road Grade and Speed
[Figure 1, (Zhang & Frey, 2005)]

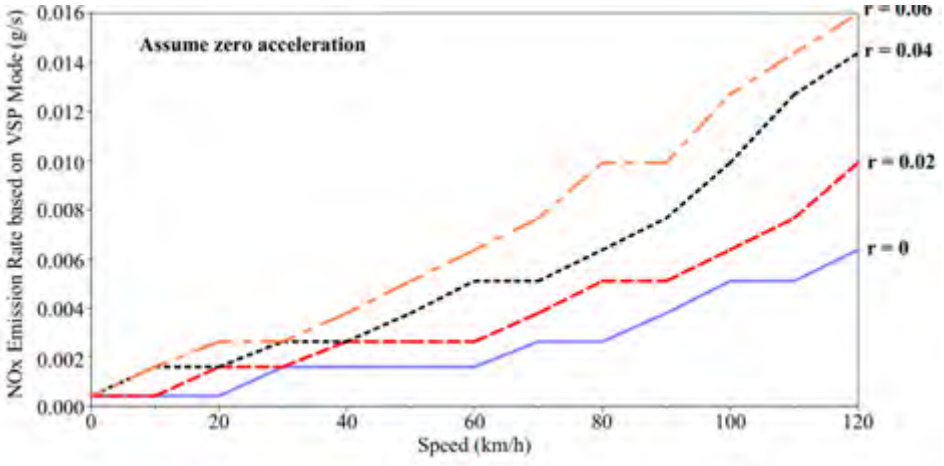

Figure 8: Sensitivity of NOx Emissions to Road Grade and Speed
[Figure 2, (Zhang & Frey, 2005)]

In 2008, a new research tried to quantify the variability in emissions, fuel consumption and power demand of selected light duty gasoline vehicles by routes, time of day, road grade, and vehicle with a focus on the impact of routes and road grade (Frey, Zhang, & Rouphail, 2008). Field experiments on urban roads using a portable emission measurement system were conducted under real world driving cycles. The study area included two origin/destination pairs, each with three alternative routes. Total emissions varied from trip to trip and from route to route due to variations in average speed and travel time. The study was concentrated to find the VSP to come to these conclusions. Experiments were carried out but there were also mathematical expressions provided, that calculate the Vehicle Specific Power.

Institutional Repository - Library & Information Centre - University of Thessaly
09/12/2017 02:36:50 EET - 137.108.70.7

To reduce the effects of factors that cannot be controlled, such as local traffic and ambient conditions, a standardized vehicle specific power (VSP)-based modal average rate of fuel use and emissions was derived to compare the emissions and fuel use by vehicle, route, driver, and time of day, as discussed later. VSP explains a substantial portion of variability in fuel use and tailpipe emissions. VSP accounts for power demand, rolling resistance, road grade, and aerodynamic drag and can be estimated based upon second-by-second speed, acceleration and road grade. VSP may be estimated generically for a typical light-duty vehicle based on representative coefficient values:

$$VSP = 0{,}278 \times v \times \left[0.305 \times \mathrm{a} + 9.81 \times \left(\sin(\mathrm{a} \times tan\left(\frac{r}{100}\right)\right) + 0.132\right] + 0.0000065 \times v^3 \quad [5]$$

where:

v: vehicle speed (km/h);

a: acceleration (km/h/s);

r: road grade (%);

9.81: The gravitational constant (c_g);

VSP: vehicle specific power (kw/ton).

VSP-based modal rates were used to calculate the total emissions on a trip basis for two cases. In one case, the actual road grade for a specific route was taken into account, while in the other case road grade was assumed to be zero. Furthermore, the effect of road grade was assessed on two different scales. One was focused on a "micro-scale", such as short segments, i.e., typically having a length of 30-570 m, of positive or negative grade on the route. The other was at the meso-scale, as represented by the average grade over the entire route. The average NO_x emission rate for grades of 5% or more was higher by a factor of 4 compared to grades of 0% or less; the corresponding increases in HC emission, CO emission, and fuel use rates ranged from 40% to 100%. Because of the substantial variability in traffic conditions, coupled with the localized nature of variations in road grade during short segments of a trip, it is mentioned to be difficult to conduct purely empirical and statistical comparisons of the effect of road grade for situations other than cruising at the indicated range of speeds.

In 2009, an important study evaluated the effect of road grade on light-duty vehicle fuel consumption using both (a) an analytical approach based on a sophisticated energy and emissions model that is going to be presented later in Chapter 5 because it also involves other

Institutional Repository - Library & Information Centre - University of Thessaly
09/12/2017 02:36:50 EET - 137.108.70.7

parameters in correlation and (b) an empirical approach based on real-world measured data (Boriboonsomsin & Barth, 2009).

The real-world experimental results showed that road grade did have significant effects on the fuel economy of light-duty vehicles both at the roadway link level and at the route level. Comparison of the measured fuel economy between a flat route and example hilly routes revealed that the vehicle fuel economy of the flat route is superior to that of the hilly routes by approximately 15% to 20%. This road grade effect will certainly play a significant role in advanced ecorouting navigation algorithms, in which the systems can guide drivers away from steep roadways to achieve better fuel economy and reduce CO_2 emissions.

For a given roadway network, link-based energy and emission factors that can be indexed by link characteristics, such as traffic speed and density, are developed. This is illustrated by Figure 9. By using a large data set of velocity trajectories collected from probe vehicles that have been spatially and temporally correlated with traffic parameters extracted from the freeway performance measurement system (PeMS), the fuel consumption and emission values of each velocity trajectory were estimated by use of a comprehensive modal emissions model (CMEM) for multiple vehicle categories in the model. Also, given appropriate link-based energy and emission factors, network wide routing algorithms are then used to select the optimal routes that minimize fuel consumption and emissions for a designated trip in a geographic information system (ArcGIS) environment.

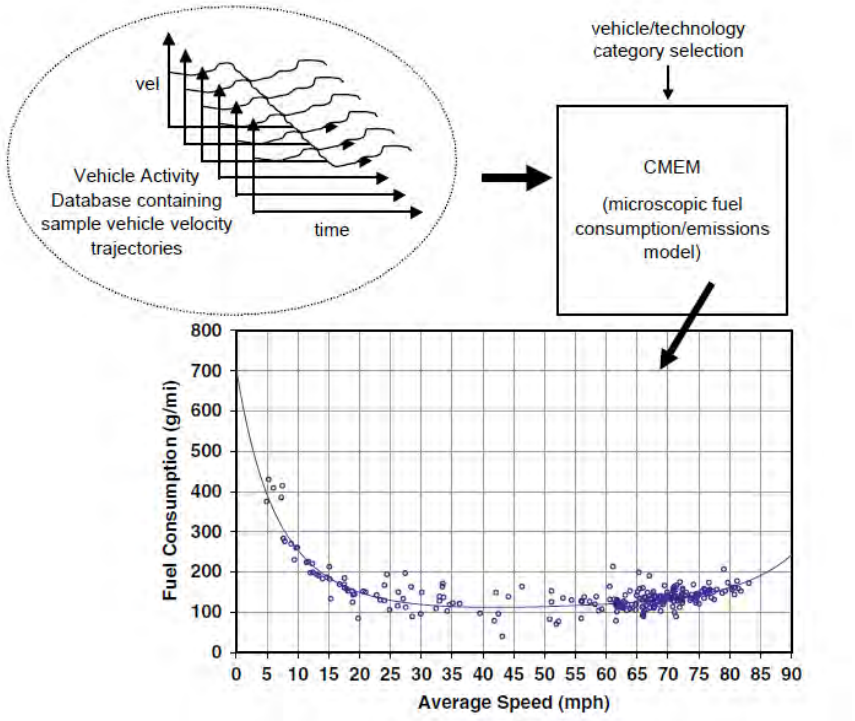

Figure 9: Link-level fuel consumption modeling methodology [Figure 1, (Boriboonsomsin & Barth, 2009)].

Institutional Repository - Library & Information Centre - University of Thessaly
09/12/2017 02:36:50 EET - 137.108.70.7

Figure 9 verifies that the steeper that the road is, the more fuel that the vehicle consumes (controlled for speed). It can also be seen that the optimal speed range for fuel consumption shifts when the road grade changes. According to Figure 10, the optimal speed range on the steepest upgrade of +8% is about 30 to 35 mph. It increases monotonically with lower road grade and reaches 80 to 85 mph on the steepest downgrade of -8%. This is because when a vehicle is going uphill, the increased power required for the vehicle to climb the grade must be compensated for by contributing less power to the speed of the vehicle to keep the same total power requirement at the most efficient engine operating point.

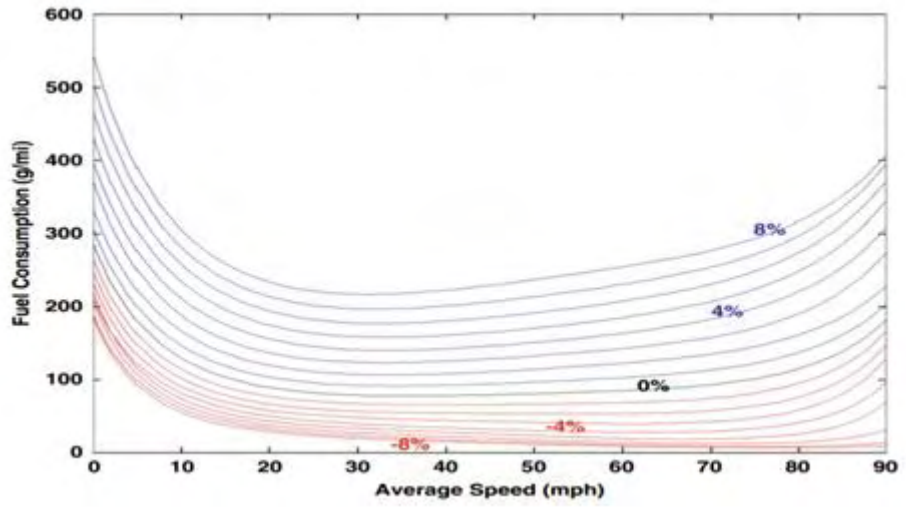

Figure 10: Fuel consumption–versus-speed curves for different road grades [Figure 3, (Boriboonsomsin & Barth, 2009)].

By using the fuel measurement data that were indexed by road grade, the fuel economy of the test vehicle was analyzed in several aspects. The relationship between fuel consumption and road grade was examined. This is illustrated in Figure 11 for each of the three runs. It is shown that the relationship between fuel consumption and road grade is nonlinear. Because the vehicle speed was held constant at 60 mph, the speed and acceleration variable were controlled across all runs. Although these runs were made on different days, which could have affected the values of the mass density of air, the rolling resistance coefficient and the aerodynamic drag coefficient, large variations in these variables were not expected. This is because the runs were made on consecutive days, at a similar time of day, and on the same routes. For the vehicle mass, Run 1 had a driver and a passenger, whereas Runs 2 and 3 had only the driver. Hence, the total mass of Run 1 and those of the other two runs were different by 160 lb (about 5% of the vehicle's curb weight). On the basis of the information in **Σφάλμα! Το αρχείο προέλευσης της αναφοράς δεν βρέθηκε.**, this slight difference in the total mass adversely affects the vehicle's fuel economy, ranging from 5% on the +1% upgrade to almost 20% on the +6% upgrade. However, it helps the vehicle's fuel economy very little (less than 5%) on the downgrades.

Institutional Repository - Library & Information Centre - University of Thessaly
09/12/2017 02:36:50 EET - 137.108.70.7

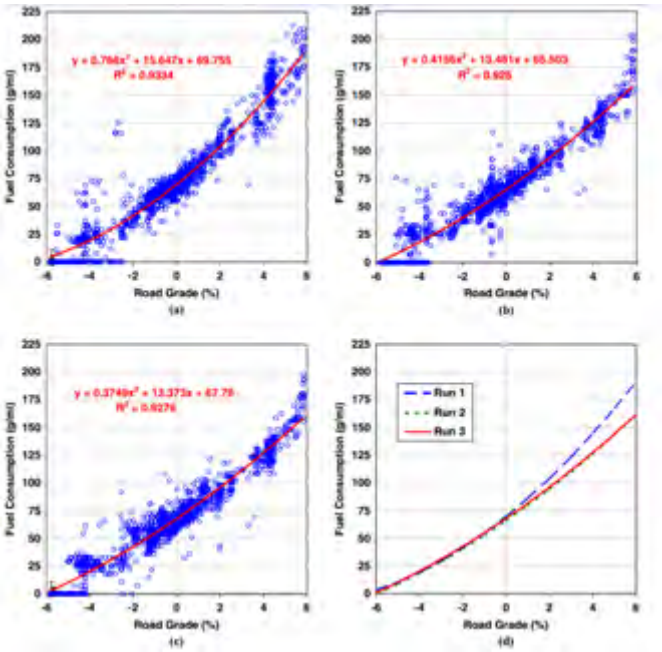

Figure 11: Fuel consumption versus road grade for steady speed of 60 mph: (a) Run 1, (b) Run 2, (c) Run 3,and (d) all [Figure 37, (Boriboonsomsin & Barth, 2009)].

In Figure 12, the mean measured fuel consumption for each integer road grade value and the associated 95% confidence interval were plotted in comparison with the modeled fuel consumption for a speed of 60 mph. The modeled values were consistently higher than the measured values. This trend was expected because the modeling methodology presented earlier in the background section for the study was based on real-world driving patterns that involved speed variations (i.e., acceleration and deceleration). In contrast, the measured fuel consumption was based on driving at a constant speed. The impact of the difference in driving patterns was about 10% at an average speed of 60 mph for CO_2 emissions, which was highly correlated to fuel consumption. The fuel consumption modeled for the -5% and -6% road grade values was considerably overestimated. Furthermore, by examining the plotted 95% confidence intervals of the measured fuel consumption, it was found that the adverse impact of the passenger weight on the vehicle's fuel economy was statistically significant for grades of +2% and higher.

Institutional Repository - Library & Information Centre - University of Thessaly
09/12/2017 02:36:50 EET - 137.108.70.7

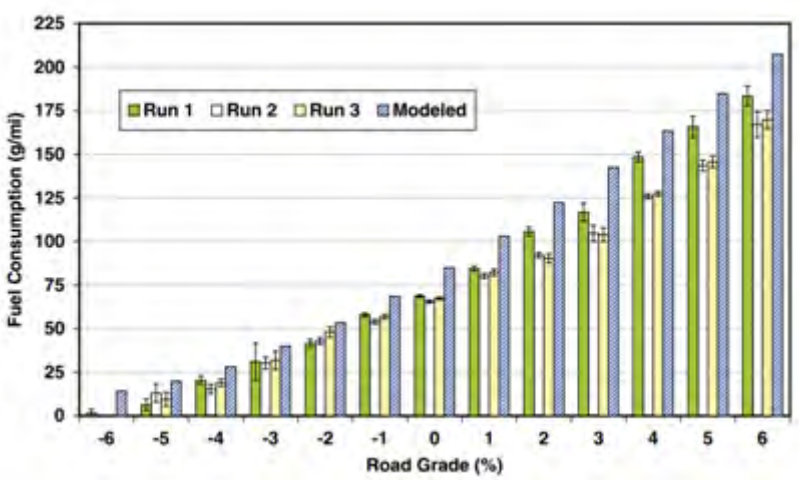

Figure 12: Comparison between real-world and modeled fuel consumption [Figure 8, (Boriboonsomsin & Barth, 2009)].

Finally, the road grade effect on the vehicle's fuel economy at the route level was examined. The fuel economy results (in miles per gallon) for each test section are presented in Figure 13. The overall fuel economy for the hilly route (i.e., uphill and downhill combined) is also given. According to the information in Figure 13, it is not surprising that the downhill section has the best fuel economy, followed by the flat section. More important, the overall fuel economy of the flat route is superior to that of the hilly route by approximately 15% to 20%. At the same speed (i.e., 60 mph), one can save fuel by taking a longer but flat route, given that it is less than 15% to 20% longer than the hilly routes.

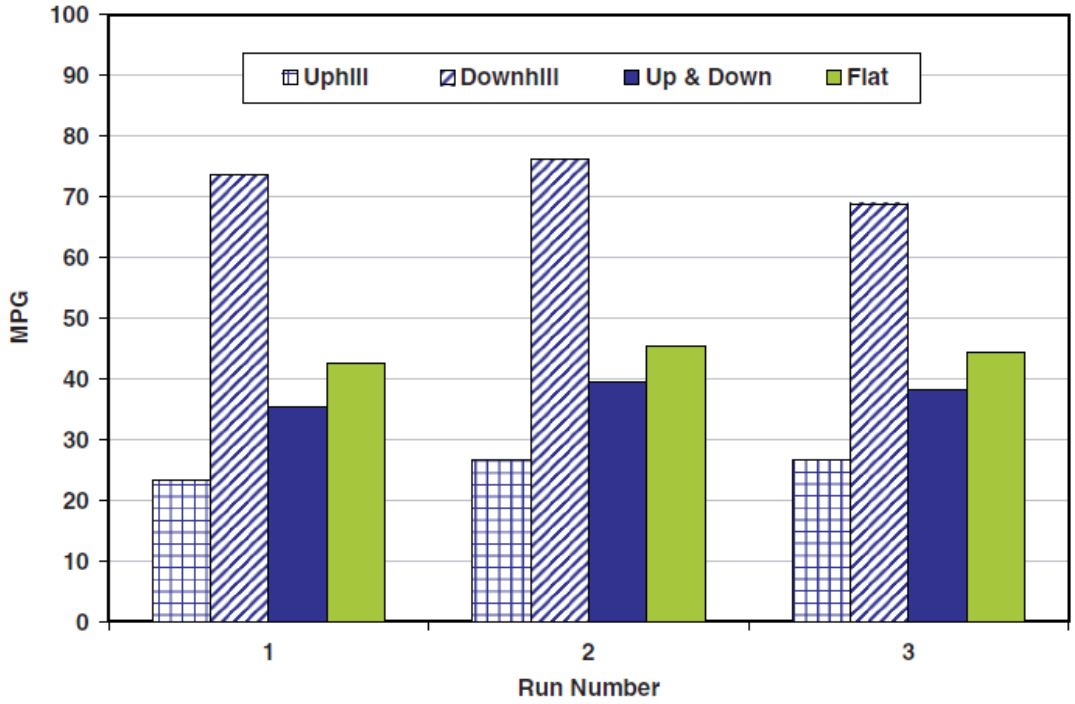

Figure 13: Fuel economy comparison of routes with different road grade (MPG _ miles per gallon) [Figure 9, (Boriboonsomsin & Barth, 2009)].

Institutional Repository - Library & Information Centre - University of Thessaly
09/12/2017 02:36:50 EET - 137.108.70.7

1.2.2 Heavy Duty Vehicles (HDVs)

(Jest, Hassel, & Sonnbrn, 1995) introduced a new method for developing realistic emission functions for heavy duty trucks and buses, independent of driving behavior. This method improved a method developed about 10 years ago by TiiV Rheinland, for representing the emission behavior of heavy commercial vehicles, based on steady state engine maps, vehicle data and driving curves (Hassel, Brosthaus, Dursbeck, Jost, Sonnborn, & Rheinland, 1983). The study concentrated on experiments on urban and also highway roads. Exhaust gas emissions and fuel consumption of 34 different diesel engines were measured on dynamic engine test benches. Exhaust emission behavior of more than 300 different types of trucks and buses could be simulated on the basis of a newly developed method. This new method allowed the determination of exhaust emission and fuel consumption factors for a broad range of different scales, from the emission simulation for a single vehicle up to global emission assessments. There were specific results provided for the emissions but not for the fuel consumption or the power requirements of the vehicles tested. Experimental results and no mathematical expressions were used to come to the conclusions below.

The Emission Factor Program was sponsored by the German Environmental Protection Agency (UBA) in Berlin and the Swiss Environmental Protection Agency (BUWAL) in Bern. The duration of the Project was 5 years. The whole project was divided into three parts:

- collection of emission data, conducted by TiiV Rheinland, Kiiln,
- collection of driving behaviour data, conducted by FIGE GmbH, Herzogenrath,
- collection of vehicle mileage data, conducted by Heusch-Boesefeldt, Aachen.

Institutional Repository - Library & Information Centre - University of Thessaly
09/12/2017 02:36:50 EET - 137.108.70.7

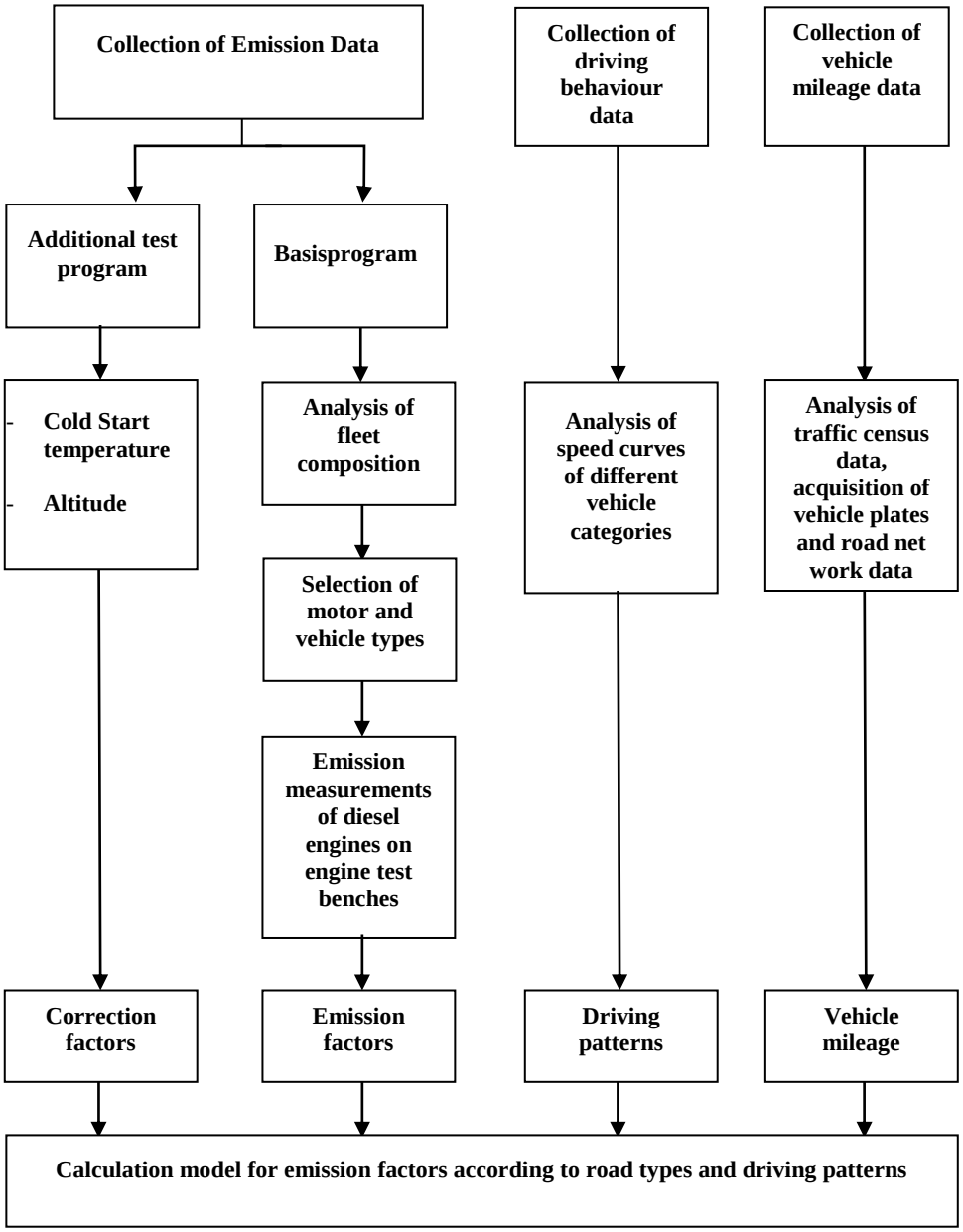

Figure 14: Project structure for heavy duty emission factor determination [Figure 1, (Jest, Hassel, & Sonnbrn, 1995)]

The result of the fleet analysis was the definition of layers which cover the whole range of the heavy duty fleet in Germany and Switzerland. Each vehicle category was divided into five to seven mass classes, and each mass class was classified into up to four body style classes. In addition, each body style class was divided into two model year groups. The total number of layers for the German fleet was 157 and for the Swiss fleet 72. As mentioned above, all these layers could be covered by 300 different heavy duty vehicle types. The principle idea for the emission model is the fact that the emissions of a vehicle are proportional to the engine power.

The figure below shows, as an example, the NO_x, emission factors for one layer (lorry < 7.5 tons, load 90%) as a function of the mean speed of the driving patterns and the road gradients.

Institutional Repository - Library & Information Centre - University of Thessaly
09/12/2017 02:36:50 EET - 137.108.70.7

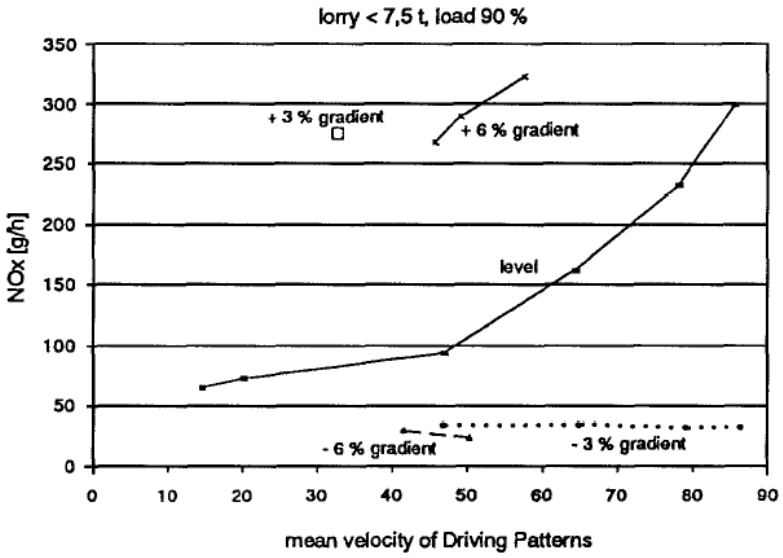

Figure 15: NO,-emissions for mean velocities of driving patterns and road gradient, layer: lorry < 7.5 ton, load 90 %
[Figure 4, (Jest, Hassel, & Sonnbrn, 1995)].

In order to assess the emission model, a verification program was carried out, during the course of which three commercial vehicles, a distribution vehicle, an urban bus and a coach were examined. For this purpose, the three vehicles were run on the chassis dynamometer and the emissions measured at the Institute for Internal Combustion Engines and Thermodynamics at the Technical University of Graz, following driving cycles which had been measured in Switzerland during real runs on the road. The engines were then removed and mounted on the transient engine test bench, the transient emission data and the steady-state engine maps recorded. With these data sets it was possible to determine emission functions for each vehicle. So the emissions of the vehicles could be calculated for each cycle driven on the chassis dynamometer. As can be seen in Figure 16, the agreement between calculation and measurement is satisfactory for CO and NO_x. For CO, and fuel consumption it is even better, whereas the quality of agreement for HC and particulate matter is similar to that of CO.

Institutional Repository - Library & Information Centre - University of Thessaly
09/12/2017 02:36:50 EET - 137.108.70.7

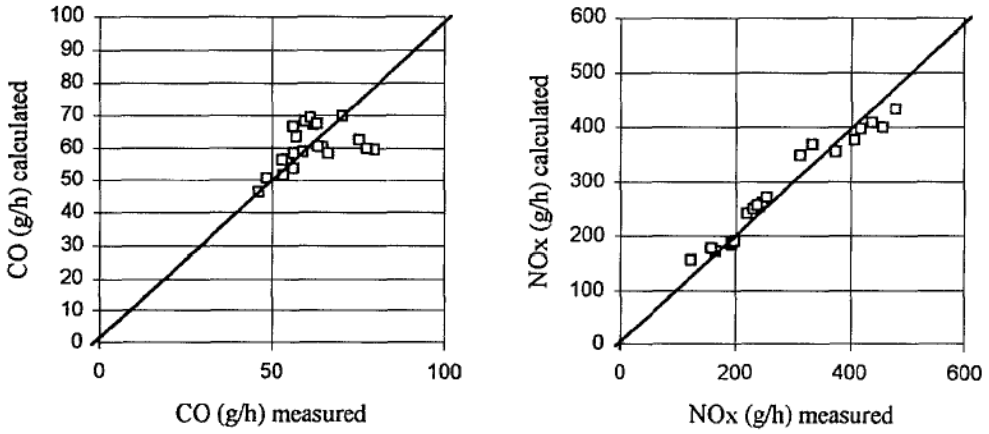

Figure 16: Comparison between calculated and measured CO and NO, emissions for the distribution vehicle [Figure 5, (Jest, Hassel, & Sonnbrn, 1995)].

This model made possible for the first time to separate the data of emission functions (steady-state engine test rigs and non-steady-state correction function) from the data of driving behavior.

In 1996, the study of William R. Pierson, Alan W. Gertler, Norman F. Robinson, John C. Sagebiel, Barbara Zielinska, Gary A. Bishop, Donald H. Stedman, Roy B. Zweidinger and William D. Ray (mentioned before during the presentation of the light duty vehicles) made some motor vehicle emission rates measurements in under investigation mountain tunnels and presented some experimental results (Pierson W. R., et al., 1996). The study took place in the tunnels of a highway road and not an urban area and examined the emissions produced by the vehicles in different tunnels and roadway grades. All the data presented below are results of experiments held in the tunnels. No mathematical expressions were used for the emission computation and there was no reference to the impact on fuel consumption or power demands of the vehicles.

Motor vehicle emission rates of CO, NO, NO_x, and gas-phase specified nonmethane hydrocarbons and carbonyl compounds were measured in 1992 in the Fort McHenry Tunnel under Baltimore Harbor and in the Tuscarora Mountain Tunnel of the Pennsylvania Turnpike. Both tunnels represent a high-speed setting at relatively steady speed. The cars at both sites tended to be newer than elsewhere (median age was < 4 years), and much better maintained as judged by low CO/CO_2 ratios and other emissions characteristics. The Tuscarora Mountain Tunnel was flat, making it advantageous for testing automotive emission models, while in the underwater Fort McHenry Tunnel the impact of roadway grade could be evaluated.

Institutional Repository - Library & Information Centre - University of Thessaly
09/12/2017 02:36:50 EET - 137.108.70.7

The effect of roadway grade on emissions was large (as great as on fuel economy or greater). In general, emissions rated uphill (grades 0 to + 3.76%, average + 3.3%) were double the emission rated downhill (0 to - 3.76%, average - 1.8%). The results below refer to the heavy duty vehicles as the light duty vehicles have been already presented before. In Table 6 and Table 7, the results referring to heavy duty vehicles are presented.

	Heavy Duty	
	Downhill	**Uphill**
CO_2 mi^{-1}	897 ± 48	1897 ± 168
CO g mi^{-1}	6.8 ± 1.5	14.3 ± 5.5
NMHC mi^{-1}[c,d]	0.92 ± 0.21	2.55 ± 1.05
Formaldehyde mi^{-1}	0.039 ± 0.008	0.075 ± 0.022
NO g×mi^{-1} as NO_2[e]	8.73 ± 0.33	20.2 ± 1.0
NO_x g×mi^{-1} as NO_2[e]	9.66 ± 0.32	22.5 ± 1.0
Mi×gal^{-1}[f]	10.1 ± 0.5	4.8 ± 0.4

Table 6: Effect of grade; emission rates downhill and uphill in the Fort McHenry Tunnel,June 1992 (Bore 3 and 4 data combined) [Table 3, (Pierson W. R., et al., 1996)].

where

Heavy duty: buses and heavy-duty trucks, mostly diesel;

c: Probably 10-20% low;

d: Calculated on the assumption of empirical formula $C_nH_{1.825n}$;

e: Calculated from mol×mi^{-1} using NO_2 molecular weight (molecular weight helps to change between grams and mols when needed);

f: Calculated from total carbon emission rate (ΣCO_2 + CO + organics), assuming empirical formula $C_nH_{1.825n}$ for gasoline and C_nH_{2n} for diesel fuel, and assuming gasoline density 0.7406 g cm^{-3} (national average test fuel; see Stump et al., 1992) and diesel fuel density 0.77331 (cetane).

	Heavy Duty		
	Fort McHenry		
	Down	**Up**	**Tuscarora (level)**
CO_2	9043	9029	9163
CO	68 ± 15	68 ± 26	35 ± 9
NMHC	9 ± 2	12 ± 5	4 ± 1
HCHO	0.40 ± 0.08	0.35 ± 0.11	0.25 ± 0.04
NO_x	97 ± 3	107 ± 5	112 ± 5

Table 7: Fuel-specific emission rates (g×gal^{-1}): effect of roadway grade [Table 6, (Pierson W. R., et al., 1996)].

Institutional Repository - Library & Information Centre - University of Thessaly
09/12/2017 02:36:50 EET - 137.108.70.7

In 2006, Hinrich Helms and Udo Lambrecht presented the relation between vehicle weight and energy (fuel) consumption (linear correlation) (Helms & Lambrecht, 2006). Available estimates and measurement data for ground vehicles and also for aircraft and high-speed ferries, have been analyzed in respect to system boundaries and methodologies through experiments. No mathematical expressions were presented and no results of the impact on the emissions and power requirements were given. Generally, energy consumption of vehicles is due to the physical resistance factors which the vehicle has to overcome during its operation. The gradient resistance is proportional to mass and gradient.

The experiments were carried out on different type of highway and urban roads taking also in account the fuel consumption results due to the correlation between the gradient and the type of road. Simulation values for fuel savings in the New European Driving Cycle (NEDC) with adjustments in the rear axle transmission range from 0.34 to 0.48 l/(100 km*100 kg) for gasoline cars can even reach 0.510 l/(100 km*100 kg) in case of sportive driving. A similar level of fuel savings is also indicated by other sources, e.g. (Schmidt, et al., 2004): 0.38 l/(100 km*100 kg). Fuel savings for diesel vehicles turn out to be slightly lower, in the range of 0.29 to 0.33 l/(100 km*100 kg) in the NEDC (Eberle 2000).

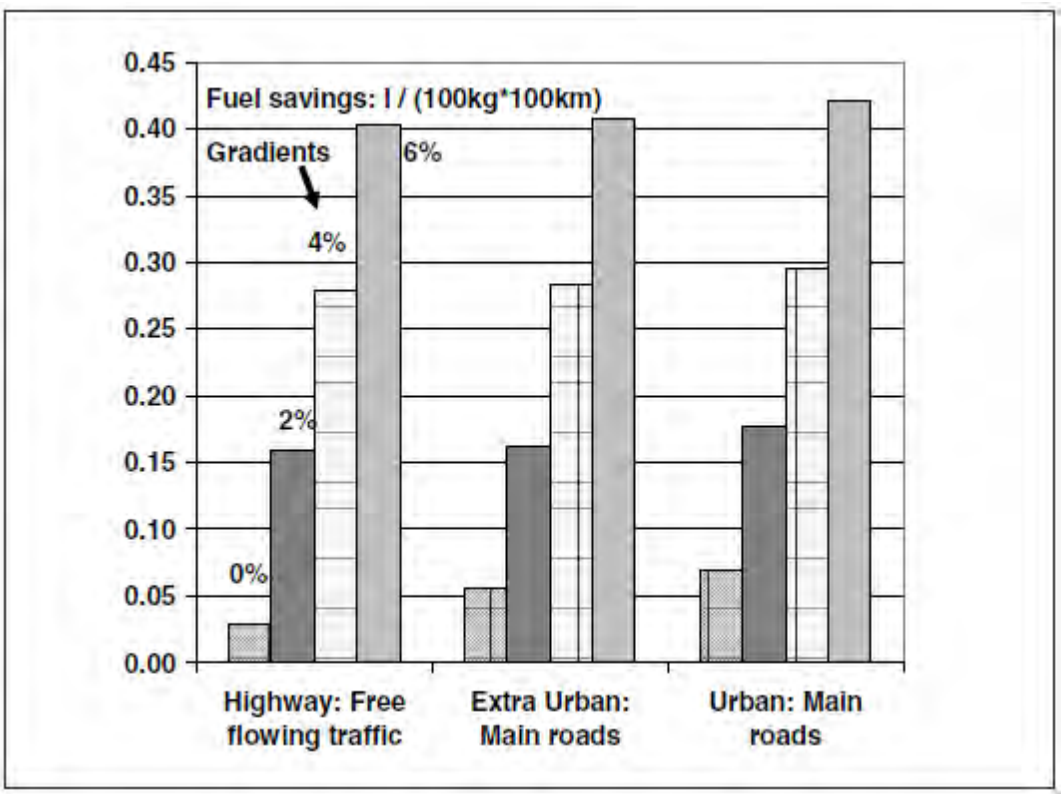

Figure 17: Fuel savings for articulated trucks in different traffic situations and for different gradients [Figure 1, (Helms & Lambrecht, 2006)].

Fuel savings on a flat highway are about 0.03 l per 100 km for a 100 kg weight reduction, but can be up to over 0.1 l/ (100 km*100 kg) in urban traffic situations, due to frequent

Institutional Repository - Library & Information Centre - University of Thessaly
09/12/2017 02:36:50 EET - 137.108.70.7

accelerations. Fuel savings are much higher on uphill roads: For a 2% gradient on a highway, fuel savings are about 5 times higher, for a 4% gradient almost 10 times higher compared to the level road. For downhill roads, no significant change in weight induced fuel savings has been found (Figure 17).

In order to derive average fuel savings for articulated trucks, the differentiated fuel savings data have been weighted according to the average mileage shares for the traffic situation and gradients in Germany. Germany has been selected due to its central location and shares of mountainous, hilly and flat roads. Average fuel savings for articulated trucks turn out to be about 0.06 l per 100 km for a 100 kg weight reduction.

In 2009, Delorme, Dominik Karbowski and Phil Sharer prepared a report about the evaluation of fuel consumption potential of medium & heavy duty vehicles through modeling and simulation on highway roads (Delorme, Karbowski, & Sharer, 2009). During the experiments, four vehicles were modeled and evaluated: Pickup Truck, Utility Truck, Transit Bus, and Line Haul Truck. All presented results came out through these experiments and no by using mathematical expressions. Also, no results about emissions and power requirements were presented in this study.

Due to the lack of real world drive cycles that included grade, to illustrate the potential benefits of hybridization in a "hilly" terrain, idealized sinusoidal road profiles were created. The elevation of such a road was a sinusoidal function of the horizontal distance, with a "hill" period varying between 1 and 3 km. Maximum grades also varied from 0 to 4 %. All combinations of maximum grade and period were analyzed.

Figure 18 shows an example of elevation change as a function of horizontal distance for roads with same maximum grades but different hill periods. The hill period can be seen as twice the approximate distance traveled between the bottom of the hill ("valley") and the top of the hill ("summit"). The vehicle speed target was 60 mph. The maximum positive grade was achieved halfway to the "summit", and the maximum negative grade halfway between the "summit" and the "valley" – there is a (horizontal) phase difference of a quarter of a period between the grade and the elevation.

Institutional Repository - Library & Information Centre - University of Thessaly
09/12/2017 02:36:50 EET - 137.108.70.7

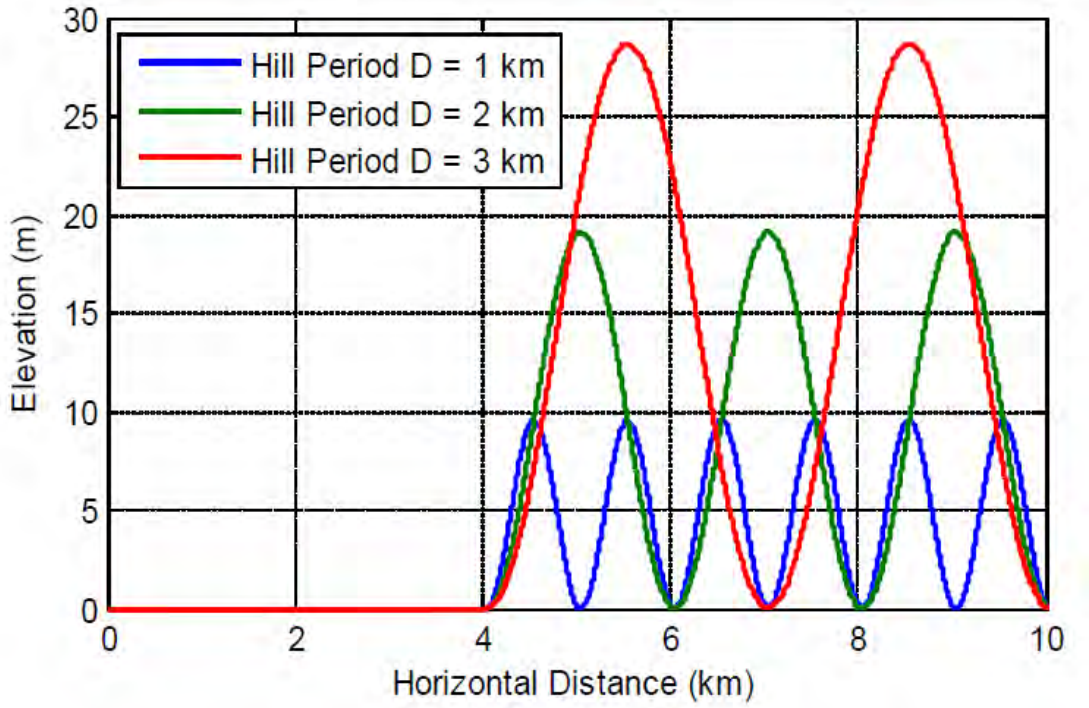

Figure 18: Sectional view of roads (partial) with the same maximum (3%) grade but 3 different hill periods[Figure 38, (Delorme, Karbowski, & Sharer, 2009)].

Figure 19 shows the fuel consumption of the three versions of the trucks on various hills. With a 1% grade, there is no need for the driver to brake in order to stay at 60 mph and regenerative braking is not possible, so hybridization gains are limited. At 2% grade, there is some limited amount of braking, but even at full recuperation rate, the energy recovered is not enough to supply the energy for the accessory load. Charge balancing is hard to achieve in that mode, and charging from engine may occur, which explains the difference in trends. At or above 2.5 %, the downhill grade is steep enough to recover enough energy for the accessory load and for some torque assist. Above 3% grade, the mild-hybrid savings stop increasing because the additional braking energy available cannot be recovered by the small motor. For high grades, the fuel savings for the full hybrid are all the higher that the hill period is shorter. This is not due to the hybrid itself, but to the conventional, which consumes more fuel when the hill period is shorter (and elevation is lower).

Institutional Repository - Library & Information Centre - University of Thessaly
09/12/2017 02:36:50 EET - 137.108.70.7

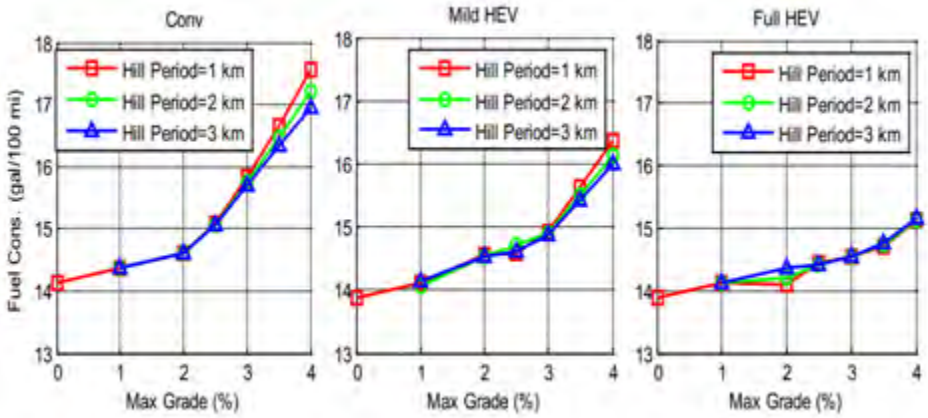

Figure 19: Fuel Consumption of Conventional, Mild-hybrid and full hybrid trucks on sinusoidal road as a function of grade (and for various hill periods) [Figure 41, (Delorme, Karbowski, & Sharer, 2009)].

1.2.3 Very Specific Type of vehicles (VSTVs)

In 1984, K. Post, J. Tomlin and N. Carruther, in the University of Sydney, created a model about emissions and fuel consumption based upon the instantaneous power demand experienced by a vehicle and made a comparison with other existing models (Post, Kent, Tomlin, & Carruther, 1984). The model had been developed from chassis dynamometer experiments on 177 in-use Australian vehicles using urban and highway roads. Their aim was to accurately model motor vehicle emissions and fuel consumption for trips of any length. Two sources of experimental data formed the basis of this work but also mathematical expressions were used to come to numerical conclusions. They were the measured emission and fuel consumption characteristics of a range of different cars and the measurements of traffic driving patterns in Sydney. Fuel consumption and emission rate characteristics were obtained by continuous exhaust gas analysis of vehicles as they were driven on a chassis dynamometer. The instantaneous emission or fuel consumption rate was correlated with vehicle speed and acceleration and subsequently with power. On-road driving pattern measurements recorded instantaneous vehicle speed, acceleration, road gradient and link length. Urban links were defined as that section of the trip between two consecutive traffic control lights and non-urban links were sections of intercity routes. These intercity routes were of 1 km or more in length, contained no stops, and had an average velocity in excess of 60 km/h. Instantaneous power demand was the key parameter which allowed the on-road emission or fuel consumption performance of any specified vehicle fleet to be calculated from the chassis dynamometer data.

Fuel consumption characteristics for 177 different spark ignition and diesel vehicles were measured in the laboratory. During the test, exhaust emissions were sampled by a constant volume sampler and continuously analyzed. The emissions were recorded at one-second

Institutional Repository - Library & Information Centre - University of Thessaly
09/12/2017 02:36:50 EET - 137.108.70.7

intervals together with the vehicle's instantaneous speed and acceleration and sent to an on-line computer for analysis. Important mathematical expressions were presented.

The overall instantaneous total power demand Z_{tot} for 1360 kg vehicle was given by:

$$Z_{tot} = (0.04 \times v + 0.5 \times 10^{-3} v^2 + 10.8 \times 10^{-6} v^3) + \frac{1360}{1000} \times \frac{v}{3.6} \left(\frac{a}{3.6} + 9.81 \times sin\theta\right) kW \quad [6]$$

where θ is the road gradient (in degrees), a is the acceleration of the vehicle (km/h×s) and v is the velocity of the vehicle (km/h).

Instantaneous fuel consumption can now be calculated for any vehicle from above mathematical expressions for any on-road trip. Also,

$$Z_{tot} = Z_{grad} + Z_{lev} \quad [7]$$

where Z_{grad} is the instantaneous gradient power and Z_{lev} the instantaneous level power, Z_{tot} is the instantaneous total power, never allowed to be negative, as the sum is affected accordingly.

Hydrocarbon and oxides of nitrogen emission rates for spark ignition vehicles showed a linear relationship with power similar in form to that found for fuel consumption. Carbon monoxide emission rate however, did not show any simple power demand relationship.

Hydrocarbon emission rate were given by:

$$HC\left(\frac{g}{min}\right) = a + \beta \times Z_{tot}(kW) \ for\ Z_{tot} \geq 0\ kW = a \ for\ Z_{tot} < 0\ kW \quad [8]$$

Altitude was derived from the velocity and total acceleration records obtained by instrumented vehicle.

The instantaneous fuel consumption-power relationship was given by:

$$FC\left(\frac{ml}{min}\right) = \left(a + \beta \times Z_{tot}(kW)\right) for\ Z_{tot} \geq 0\ kW = a\ (\mathrm{ml}/min)\ for\ Z_{tot} < 0\ kW \quad [9]$$

For test vehicle, a = 39.2 ml/min and β = 9.2 ml/min kW from the test data.

Institutional Repository - Library & Information Centre - University of Thessaly
09/12/2017 02:36:50 EET - 137.108.70.7

The coefficients a and β for all cars tested can be found in (Post, et al., 1981) and it should be noted that a and β for each vehicle can vary as the vehicle's condition and state of tune alters.

TRIP LENGTH (km)	TRIP TIME (s)	POSITIVE ALTITUDE (m)	AVERAGE TOTAL POWER (kW)	a (ml/min)	β (ml/min)	ON ROAD MEASURED FUEL (l)	FUEL PREDICTED/ MEASURED
11,7	1331	180	4,83	33,06	10,24	1,795	1.02
8,7	913	170	5,1	33,06	10,24	1,285	1.01
10,2	1522	149	3,54	32,76	10,38	1,800	0.98
10,3	1212	200	4,87	32,76	10,38	1,650	1.02
9,4	1097	206	4,66	32,76	10,38	1,440	1.03

Table 8: Comparison of predicted and measured fuel consumption of Commodore for on-road round-trip tests including gradients (Road data collected on 26/I/82-27/1/82; a and β parameters determined by dynamometer tests on day of trip)
(Post, Kent, Tomlin, & Carruther, 1984)

The predicted fuel consumption in the above table is calculated through the mathematical expressions [9].

Z_{tot}, the trip averaged total power is equal to the sum of all the non-negative one-second total powers, Z_{tot} divided by the total trip time. The coefficients a and β for the examined vehicle were determined several times on the dynamometer to check for changes in engine tune.

Elemental models have been developed in an attempt to isolate individual components of a trip and account for the whole trip fuel consumption in terms of these elements. Important elements are normally considered to be "cruise", "delay" and "stops". (Akcelik, 1980), (Akcelik, 1981) and (Akcelik, 1982) presents an elemental model based on his review of the literature and cast in the fuel usage per unit time form, it can be expressed as follows:

$$FC = \frac{(f_1 \times L + f_2 \times t_s + f_3 \times h)}{T} \qquad [10]$$

where FC is the vehicle trip fuel consumption rate in ml/min, f_1 is the cruise fuel consumption rate in ml/km, f_2 is the idle fuel consumption rate in ml/min, f_3 is the fuel consumption per complete stop in ml/stop, L is the trip cruise distance in km, t_s, is the trip stopped delay time in min, h is the number of stops in the trip and T is the trip time in min. The parameters f_1 and f_3, are dependent upon the cruise speed and f_1, is considered to include the effects of speed fluctuations (i.e. potential stops), gradient, and other environmental factors. In practice, this kind of model has been limited in its use because there has not been an adequate data base from which the vehicle specific parameters f_1, f_2 and f_3 could be determined.

Cruise fuel consumption rate: [11]

Institutional Repository - Library & Information Centre - University of Thessaly
09/12/2017 02:36:50 EET - 137.108.70.7

$$f_1 = F60 \times \frac{(a + \beta \times Z_{DRAG})}{V_c}\ ml/km$$

where Z_{DRAG} is the link averaged drag power in kW and V_c is the cruise velocity adjacent to the stop.

$$Z_{DRAG}(kW) = \frac{1}{T} \times \sum (Z_{drag}) \quad [12]$$

where Z_{drag} is the instantaneous drag power in kW.

Cruise distance:

$$L = V_c \times cruise\ time\ (km) \quad [13]$$

where

$$cruise\ time = [link\ time - t_s - h_d\,(1.14 + 0.28 \times V_c)] \quad [14]$$

h_d and h_a are the number of decelerations and accelerations which occur to and from the stops within each link, t_s is given below.

Idle fuel consumption rate:

$$f_2 = \alpha\ \text{ml/min} \quad [15]$$

Stopped delay time:

$$t_s = Number\ of\ minutes\ spent\ with\ v < 5\ km/h \quad [16]$$

Fuel consumption due to stops:

$$f_3 \times h = f_{3d} \times h_d + f_{3a} \times h_a\ ml \quad [17]$$

where

$$f_{3d} = \frac{(\alpha + \beta\,(-0.45 + 0.02\,V_c))(1.14 + 0.28\,V_c)}{60}\ ml \quad [18]$$

$$f_{3a} = \frac{(\alpha + \beta\,(-1.2 + 0.25\,V_c))(0.22 + 0.34\,V_c)}{60}\ ml \quad [19]$$

Institutional Repository - Library & Information Centre - University of Thessaly
09/12/2017 02:36:50 EET - 137.108.70.7

The performance of all alternative fuel consumption prediction models has been assessed by using 2281 links and 956 km of urban on-road driving pattern data. It was shown that all models can be made to perform well for long trips. The elemental model, however, suffers from an inability to adequately describe the fuel usage of different stop-start manoeuvres and requires some calibration in order to account for cruise speed fluctuations. For short trips, 3.5 km in length or less, the on-road power demand method is superior. Under these conditions, both the simple *v* and elemental models are unable to adequately describe the fuel usage relating to inertial power demands. It is shown that for short trips, inertial power demand does not correlate with average velocity and may range from near zero to up to twice the total trip averaged power.

In 2005, Bryan Harris presented some comments on modeling procedure and proposed a partial one-way traffic-flow system using urban roads to carry out experiments and conclusions about how the gradient can affect the emission rates of different types of vehicles (Harris, 2005). In this work, there have been applied corrections based on experimental data published in a number of scientific reports, including, particularly, one commissioned by the European Environmental Agency through the COST (Co-operation in the field of Scientific and Technical Research) program. There were no computations based on mathematical expressions, just experiments that were carried out and the results are presented below and concern the emission rates and not the fuel consumption and the power requirements.

The results of the COST research program which had been used in this modeling work are shown in Figure 74Figure 20, where they have been graphed directly from the tabulated data in the report. In this graph, positive road gradients relate to traffic travelling uphill, and negative gradients are for downhill traffic. The essential feature of the graph, which includes data from a wide range of vehicle types, is that the general relationship is non-linear. It is clear that uphill driving generates more emissions than downhill driving.

Institutional Repository - Library & Information Centre - University of Thessaly
09/12/2017 02:36:50 EET - 137.108.70.7

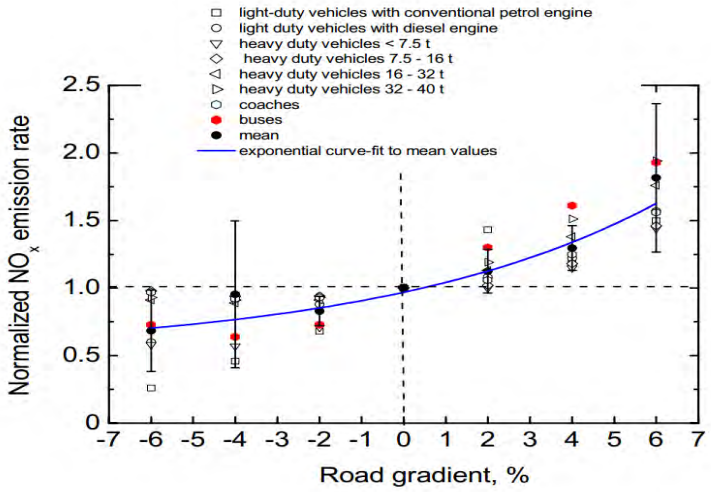

Figure 20: Variation of normalized NOx emission factors for various vehicles as a function of road gradient. Data of Hassel and Weber3 (COST 319 project). The data graphed directly from the tables in the report listed in footnote 1. The road gradients are in %, and the mean gradient of Masons Lane and Market Street is approximately 8%
[Figure 1, (Harris, 2005)]

Dr. Cowan had extracted a number of graphs from the COST report which these were very similar to those in Figure 20. There was one major point of difference, however, because his graph for buses was almost symmetrical about the level driving value (gradient = 0), which suggested that buses travelling downhill generated just as much emissions as those travelling uphill, both being greater than the emissions for level driving. This is represented schematically in Figure 21 (the blue line represents the function also shown as blue in Figure 20), while the red line represents roughly the form of the data for buses exhibited by Dr. Cowan. This is very puzzling because there seems no technical reason for such a phenomenon.

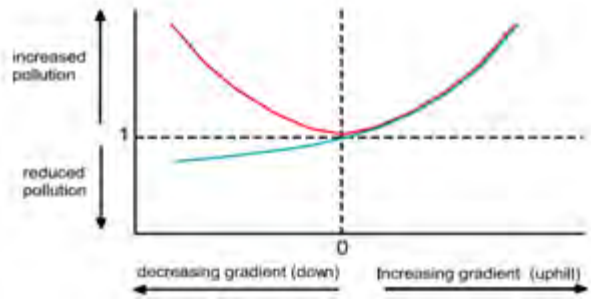

Figure 21: Schematic diagram showing effects of street gradient on traffic emissions. The full blue line is what is expected from published work, and the red line is roughly the shape used by Dr Cowan for buses
[Figure 2, (Harris, 2005)]

Institutional Repository - Library & Information Centre - University of Thessaly
09/12/2017 02:36:50 EET - 137.108.70.7

In 1999, A.J. Hickman presented a summary of all the individual methodologies and corresponding emission factors and functions produced in the MEET project **(**Methodologies for estimating air pollutant emissions from transport) for use in estimating pollutant emissions and energy consumption from transport (Hickman, 1999). Different mathematical expressions were presented concerning emission rates and also hot emission factors when driving probably on urban roads but no experiments were held. No mathematical expressions concerning power or fuel consumption were presented and no experimental results are given. Other factors were also taken into account for the hot emissions computation.

In this report a function of emission rates depending on the average speed of the vehicle was given:

$$\varepsilon = K + acoeff \times v + bcoeff \times v^2 + ccoeff \times v^3 + \frac{dcoeff}{v} + \frac{ecoeff}{v^2} + \frac{fcoeff}{v^3} \quad [20]$$

where

ε:	the rate of emission in g/km for an unloaded goods vehicle, or for a bus or coach carrying a mean load, on a road with a gradient of 0%
K:	a constant
α_{coeff}- f_{coeff}:	coefficients
v:	the mean velocity of the vehicle in km/h

Coefficients and constants for these mathematical expressions are presented in the Appendix of the paper (Hickman, 1999). The gradient of a road has the effect of increasing or decreasing the resistance of a vehicle to traction. In principle the emissions and fuel consumption of both light and heavy duty vehicles are affected by road gradient. However, because of their higher masses, the gradient influence is much more significant in the case of heavy duty vehicles.

For each vehicle category, gradient and pollutant, the gradient factor can be calculated as a polynomial function of the vehicle's mean speed:

$$as_{i,j,k} = A6_{i,j,k} \times v^6 + A5_{i,j,k} \times v^5 + A4_{i,j,k} \times v^4 + A3_{i,j,k} \times v^3 + A2_{i,j,k} \times v^2 + A1_{i,j,k} \times v + A0 \quad [21]$$

Institutional Repository - Library & Information Centre - University of Thessaly
09/12/2017 02:36:50 EET - 137.108.70.7

where

$as_{i,j,k}$:	the correction factor (used in the following mathematical expression);
v:	the mean speed;
$A0_{i,j,k}$... $A6_{i,j,k}$:	constants for each pollutant, vehicle and gradient class.

Hence, it is proposed to correct the emission factor calculated for vehicle's use on a flat road according to the following mathematical expression, in order to incorporate the influence of the road gradient:

$$ec_{hot,i,j,k} = as_{i,j,k} \times e_{hot,i,j,k} \quad [22]$$

where

$ec_{hot,i,j,k}$:	the corrected emission factor of the pollutant *i*, in g/km, of the vehicle of category *j* driven on roads of type *k* with hot engines ;
$e_{hot,i,j,k}$:	the emission factor of the pollutant *i*, in g/km, of the vehicle of category *j* driven with hot engines on roads of type *k* with zero gradient;
$as_{i,j,k}$:	the gradient correction factor of the pollutant *i* of the vehicle of category *j* driven on roads of type *k* for the appropriate gradient class, gradient classes are 0%, 2%, 4%, 6%, -2%, -4% and -6%.

The driving resistance of a vehicle is influenced by vehicle mass, i.e. higher vehicle mass requires higher power from the engine during driving, especially in acceleration modes. Because of the well-known fact that emissions and fuel consumption are proportional to the engine power, the calculations have to take into account, in principle, vehicle load.

In the case of heavy duty vehicles the vehicle load has an important influence on emissions and fuel consumption as the load can contribute significantly to the total weight of the vehicle.

Functions to correct for load have been determined for goods vehicles so that:

$$\varepsilon_l = \varepsilon_u \times \Phi(\gamma, v) \quad [23]$$

where

Institutional Repository - Library & Information Centre - University of Thessaly
09/12/2017 02:36:50 EET - 137.108.70.7

ε_l: the emission factor when loaded in g/km;

ε_u: the emission factor when unloaded in g/km;

$\Phi(\gamma, v)$: the load correction factor function;

γ: the gradient in percent;

v: the mean velocity of the vehicle in km/h.

Load correction factor functions ($\Phi(\gamma, v)$) are of the form:

$$\Phi(\gamma, v) = \kappa + n \times \gamma + p \times \gamma^2 + q \times \gamma^3 + r \times v + s \times v^2 + t \times v^3 + \frac{u}{v} \quad [24]$$

where

κ: a constant;

n - u: Coefficients.

Hot emission factors were calculated firstly as a function of the average vehicle speed. Depending on the vehicle type, a number of corrections may be made to allow for the effects of road gradient, vehicle load, vehicle mileage and ambient temperature. Thus, for one vehicle type and pollutant:

$$e_{hot} = f(v) \times GC \times LC \times MC \times TC \quad [25]$$

where

e_{hot}: the corrected hot emission factor

f(v): the average speed (v) dependent emission rate for standard conditions

GC, LC, MC & TC: correction factors for gradient, load, mileage and temperature respectively

Hot emissions were analyzed and a function of computation was given. It is mentioned that hot emissions are the emissions produced when the engine and the pollution control systems of the vehicle (e.g. catalyst) have reached their normal operating temperature. They can be calculated if the emission per unit of activity and the total activity over the time scale of the calculation are known, using the formula:

Institutional Repository - Library & Information Centre - University of Thessaly
09/12/2017 02:36:50 EET - 137.108.70.7

$$E_{hot} = e \times m \quad [26]$$

where

E_{hot}:	the emission, in units of mass per unit of time (usually in t/a)
e:	the hot emission factor in g/km
m:	the activity, in distance travelled per time unit (usually in km/a)

In 2010, João P. Ribau, Carla M. Silva, Tiago L. Farias published their study "Electric and hydrogen consumption analysis in plug-in road vehicles" (Ribau, Silva, & Farias, 2010). Using different type of vehicles on highway roads, tried to experiment and show the consequences of the gradient on the energy (fuel) consumption. The main goal of the presented study was to analyze some of the capabilities and behavior of two types of plug-in cars: battery electric and hydrogen fuel cell hybrid electric, facing different driving styles, different road gradients, different occupation rates, different electrical loads, and different battery´s initial state of charge. There were experiments carried out that gave some conclusions about the emissions but there is no reference to the behavior of the vehicle concerning the fuel consumption and the power demands. All data presented were results of experiments and no mathematical expressions were used.

Four vehicles with different power/weight (kW/kg) ratio (0.044 to 0.150) were simulated in the software ADVISOR, which gave predictions of energy consumption and behavior of vehicle's powertrain components (including energy regeneration) along specified driving cycles. The examined vehicles were:

(a) Veh A (PHEV-FC, hybrid with hydrogen fuel cell, Plug-in Hybrid Fuel Cell Electric Vehicle),
(b) Veh B-D (BEV, Battery Electric Vehicle),
(c) Veh E (hybrid with gasoline combustion engine),
(d) Veh F (Conventional Gasoline ICEV, Internal Combustion Engine Vehicle),

and the examined gradients ware -15.5%, 0%, 5.75%, 11.5% and 17.25%.

For each vehicle there were two kinds of simulation in every case study: cycle and autonomy. Cycle, simulated the vehicle running once only in the driving cycle. Autonomy, simulated the vehicle running in the driving cycle constantly, till all energy in the vehicle ends up (battery, hydrogen for PHEV-FC´s, or gasoline for HEV and ICEV).

Institutional Repository - Library & Information Centre - University of Thessaly
09/12/2017 02:36:50 EET - 137.108.70.7

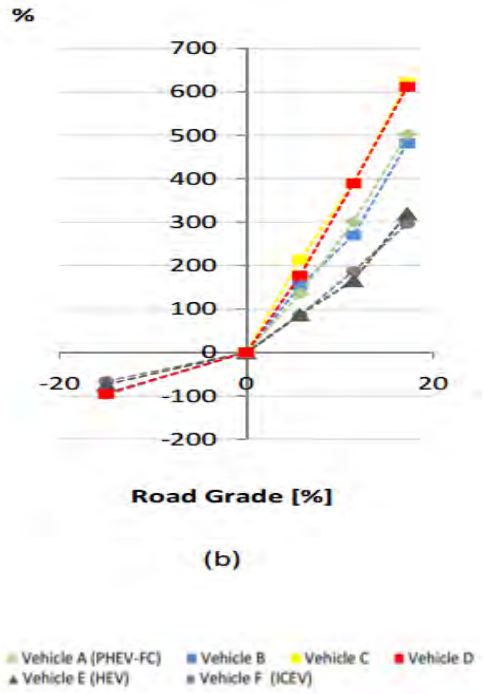

Figure 22: Energy consumption variation, Cascais-Lisboa driving cycle (34.2km) [Figure 5(b), (Ribau, Silva, & Farias, 2010)].

According to the results shown in Figure 22, the heavier the vehicle is, greater the force must be produced by the electric motor on the rise. Vehicles with lower torque/weight ratio present higher increases in the energy consumption.

Vehicle C and vehicle D could not complete the driving cycles for road grades above 11.5% and 5.75% respectively. For these road grades their energy consumption was so high that the autonomy became lower than the driving cycle distance. The variations of energy consumption relatively to original route are shown in Table 9 (marked with bold).

Institutional Repository - Library & Information Centre - University of Thessaly
09/12/2017 02:36:50 EET - 137.108.70.7

		Vehicle A		Vehicle B		Vehicle C		Vehicle D	
		1 Cycle	Aut	1 Cycle	Aut	1 Cycle	Aut	1 Cycle	Aut
Average Acceleration [m/ s^2]	0.43	3.80	4.37	2.74	2.91	1.73	2.62	1.73	1.73
	0.45	3.79	4.34	2.74	2.90	1.73	2.62	1.73	1.73
	0.47	3.78	4.34	2.70	2.93	1.82	2.65	1.82	1.82
	0.69	**4.00**	**4.54**	**2.95**	**3.16**	**1.92**	**2.88**	**1.92**	**1.92**
	0.71	4.22	4.74	3.04	3.24	1.97	3.08	1.97	1.97
	2.13	6.48	6.83	4.33	4.21	3.40	4.43	3.40	3.40
Road Grade [%]	-15	0.06	0.00	0.18	0.18	0.09	0.12	0.09	0.09
	0	**4.00**	**4.54**	**2.95**	**3.16**	**1.93**	**2.74**	**1.93**	**1.93**
	5.75	9.41	9.93	7.48	10.50	…	8.59	…	…
	11.5	16.02	16.71	10.90	10.97	…	13.40	…	…
	17.25	24.09	24.26	17.15	21.03	…	19.76	…	…
Cargo Weight [kg]	**70**	**3.67**	**4.30**	**2.82**	**3.07**	**1.77**	**2.86**	**1.77**	**1.77**
	140	3.80	4.43	2.96	3.20	1.88	2.99	1.88	1.88
	210	3.97	4.58	3.13	3.33	2.00	3.14	2.00	2.00
	280	4.19	4.68	3.25	3.42	2.11	3.26	2.11	2.11
Accessory Electrical Load [W]	**784**	**3.67**	**4.30**	**2.82**	**3.07**	**1.77**	**2.86**	**1.77**	**1.77**
	5235	5.66	6.24	4.25	4.52	3.02	4.54	3.02	3.02
Initial SOC [%]	**100**	**3.67**	**4.30**	**2.82**	**3.07**	**1.77**	**2.86**	**1.77**	**1.77**
	75	3.86	4.33	2.96	3.08	1.83	2.89	1.83	1.83
	50	4.15	4.33	3.15	3.08	1.92	2.87	1.92	1.92
	25	4.68	4.37	2.99	2.93	1.93	2.80	1.93	1.93

		Vehice E		Vehice F	
		1 Cycle	Aut	1 Cycle	Aut
Average Acceleration [m/ s^2]	0.43	5.78	5.93	8.33	8.25
	0.45	5.76	5.92	8.32	8.22
	0.47	5.72	5.89	8.26	8.32
	0.69	**6.10**	**6.28**	**8.43**	**8.36**
	0.71	6.13	6.30	8.68	8.62
	2.13	7.60	7.83	11.09	11.00
Road Grade [%]	-15	1.57	1.24	2.82	2.76
	0	**6.10**	**6.28**	**8.32**	**8.22**
	5.75	11.41	12.79	15.47	15.40
	11.5	16.21	19.37	23.88	23.81
	17.25	25.61	34.18	32.94	32.85
Cargo Weight [kg]	**70**	**6.28**	**6.36**	**8.19**	**8.18**
	140	6.55	6.57	8.36	8.39
	210	6.61	6.67	8.64	8.60
	280	6.67	6.80	8.73	8.68
Accessory Electrical Load [W]	**784**	**6.28**	**6.36**	**8.19**	**8.18**
	5235	8.19	8.46	11.13	11.16

Table 9: Results: energy consumption, 1 Cycle and autonomy,[Lgeq/100km] for plug-in vehicles (A, B, C, D) and conventional vehicles (E, F) [Table 7, (Ribau, Silva, & Farias, 2010)].

Institutional Repository - Library & Information Centre - University of Thessaly
09/12/2017 02:36:50 EET - 137.108.70.7

When the road gradient was positive, it was required more torque (and consequently more power) to the vehicle leading to more energy consumption. An aggressive driving style, higher road gradient and increase of weight, required more energy and power to the vehicle and presented consumption increases near to 77%, 621%, 19% respectively. Higher electrical load and battery´s initial state of charge, did not affect directly vehicle´s dynamic.

1.3 Conclusions

All the above studies, reports and papers have given important information about how the gradient of a road can affect the fuel consumption of a vehicle and the emission rates. We can also find other studies that do not present certain results and experiments but make comparison of data that other studies have given in the past. Such studies were held by (Colberg, et al., 2005), (Colberg, et al., 2005) and (Cadle S. , et al., 2007). Another interesting study conducted by J H Park, J H Kong, H S Jo, Y I Park and J M Lee proposed new driving modes which include road gradients and algorithms to measure road gradients in real time were studied. There have been conducted on-road car tests and then there have made comparisons between the wordwide driving modes and the new driving modes (Park J. , Kong, Jo, Park, & Lee, 2001).

It is commonly accepted that driving in positive grades has a higher cost than driving in negative roadway grades. Driving uphill needs much more power for the vehicle to use which means more energy consumption. Although, the amount of fuel or emissions released are not proportional when driving in a certain positive grade and in the corresponding negative grade (e.g. if the emission rates in +5% grade are +3%, the emission rates in -5% grade will not be -3%). The weight of a vehicle does affect the fuel consumption and the emission rates as heavy duty vehicles or vehicles with load consume more that light duty vehicles or vehicles with fewer passengers and less loads when driving in (positive) grades. Speed also has a significant role when combining with the gradient. Pollutants, for example, are affected in a different way depending on the speed of the vehicle. HC, CO and NO_x, CO_2 emissions may be more sensitive to different roadway grades or different speeds during certain grades.

It is shown that road grades affect undoubtedly the fuel consumption and the emission rates and that in positive grades the numbers are much higher than in negative ones.

Institutional Repository - Library & Information Centre - University of Thessaly
09/12/2017 02:36:50 EET - 137.108.70.7

Chapter 2 THE ROLLING RESISTANCE

3.1 Introduction

One more factor that can affect the fuel consumption and the emissions of a vehicle is the rolling resistance. There are many definitions given about what the rolling resistance is.

In the past, the rolling resistance was defined as an energy loss that is caused due to the friction between the tires and the road and also due to other factors that have to do with the tire of the vehicle.

The U.S. Department of Energy estimates that approximately 4.2 percent of the total energy available in the fuel put in a tank is lost to rolling resistance during the operation of the vehicle (Department of Energy, 2009). However, Duleep and NAS (Duleep, November, 2005) point out that the peak first law (thermodynamic) efficiency of a modern spark-ignited gasoline engine is in the 3436 percent range (40-42% for diesels), and therefore tire rolling resistance consumes about a third of the usable energy actually transmitted to the wheels (i.e., 1/3 of the available tractive energy). Therefore, considering rolling resistance in terms of the energy in the fuel tank is not a useful measure. For instance, in Figure 23 only 12.6 percent of the energy in the fuel is finally transmitted to the wheels. The 4.2 percent of original fuel energy used by rolling resistance is actually 33 percent (4.2%/12.6%) of the total usable energy available to the wheels. Generally, only about 15 percent of the energy from the fuel put in a tank gets used to move a car down the road or run useful accessories, such as air conditioning. The rest of the energy is lost to engine and driveline inefficiencies and idling. Therefore, the potential to improve fuel efficiency with advanced technologies is enormous.

Institutional Repository - Library & Information Centre - University of Thessaly
09/12/2017 02:36:50 EET - 137.108.70.7

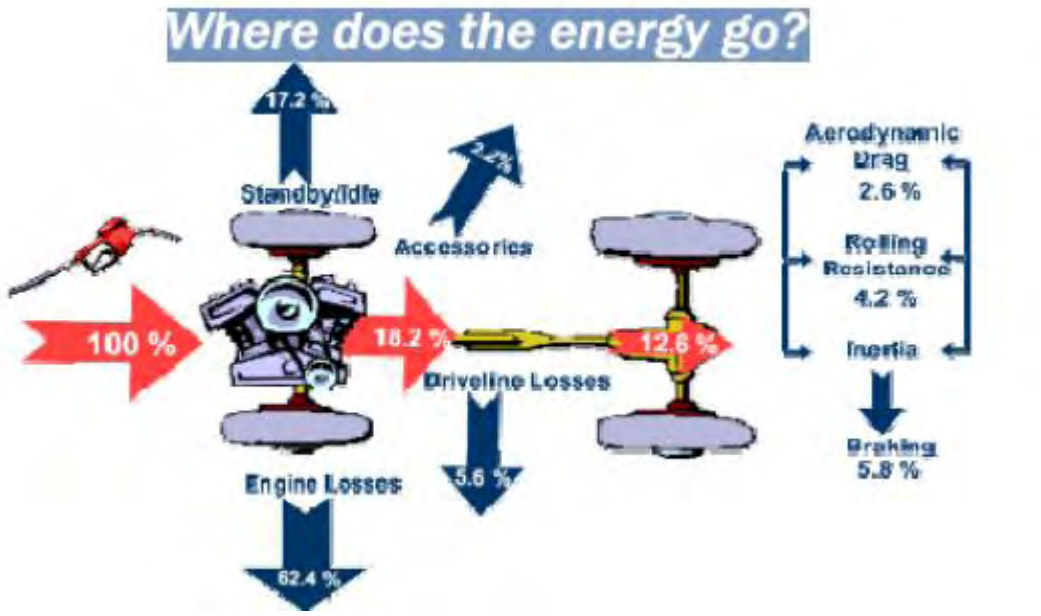

Figure 23: Where Does the Energy Go? (Department of Energy, 2009).

Additionally, the contribution of tire rolling resistance to fuel economy varies with the speed of the vehicle. At lower speeds, tire rolling resistance represents a larger percentage of the fuel consumption (see Figure 24) than at higher speeds (Reimpell, Stoll, & Betzler, 2001).

Another definition for the rolling resistance was given by (Biggs, 1988) :

The total of all forces, apart from aerodynamic drag, acting on a freewheeling vehicle (i.e., with the clutch disengaged). Thus, it includes all frictional forces from the output of the gear box to the wheels and tire resistance forces.

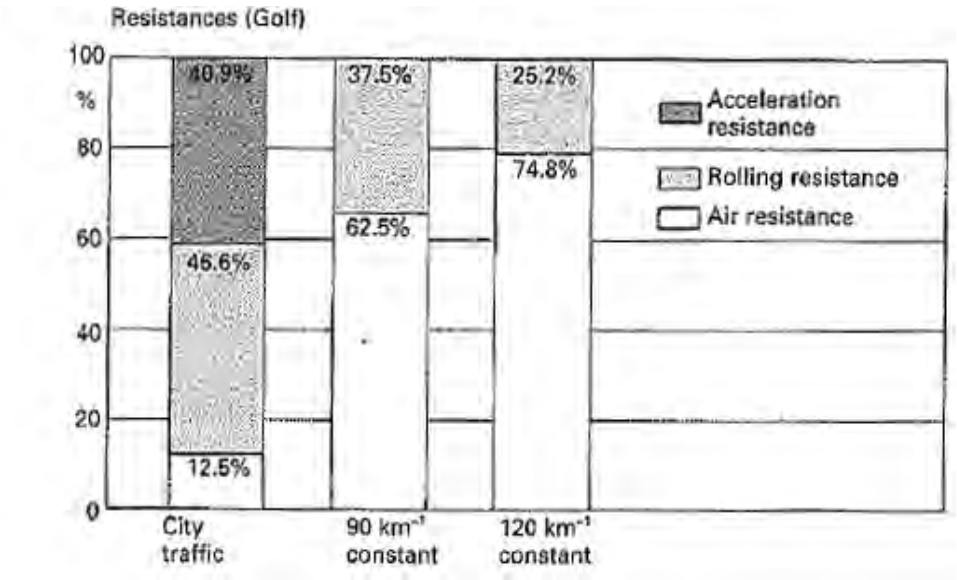

Figure 24: Contribution of Tire Rolling Resistance to Vehicle Fuel Economy Versus Speed (Reprinted with permission from the Automotive Chassis: Engineering Principles, 2nd Edition, Reed Educational and Professional Publishing Ltd., 2001) (Larry, et al., 2009).

Institutional Repository - Library & Information Centre - University of Thessaly
09/12/2017 02:36:50 EET - 137.108.70.7

Concerning the relation between the rolling resistance and the type of road, Studies in Sweden and Canada reveal that energy consumption during construction, maintenance and operation of roads is lower for asphalt pavements than for concrete pavements. Green House Gas emission (GHG) and Global Warming Potential (GWP) are therefore always lower for asphalt. However the bulk of energy is consumed by traffic using the road and only 2 to 5% of the total consumption is required for construction, maintenance and operation of the road. Fuel consumption on different road surfaces is therefore the logical subject of several studies. Of particular interest are road related factors such as surface characteristics (texture), bearing capacity and viscoelastic behavior.

All studies confirm that surface texture is a predominant factor. However, the outcome of various studies is sometimes conflicting regarding differences in fuel efficiency on asphalt and concrete roads. It is fair to say that the differences between pavement types as such – asphalt or concrete - are not significant. The condition of the pavement (good surface characteristics) is more important in this respect for both asphalt and concrete roads. Optimal maintenance of roads is therefore a tool to reduce fuel consumption and GHG emission. The main type of roads that we also examine during our review is:

Asphalt: A viscous cementitious material composed principally of high molecular weight hydrocarbons (typically 300-2000 g/mol). It is composed of aggregates bound together with asphalt cement. The aggregate is heated and mixed with hot (275º F) asphalt cement then taken to the construction site (Gibbons, 1999).

Concrete: Material composed of binding material called cement, that contains lime, silica, alumina and gypsum, that is mixed with sand, aggregate and water (Gibbons, 1999).

Composite: A structure comprising two or more layers that combine different characteristics and that act as one composite material (Smith, 1963). Pavements with asphalt concrete surfaces and Portland cement concrete beneath the surface are the most common ones (Ongel & Aybike, 2007).

At Mairepav'03 Symposium in July 2003 in Portugal, A. Woodside, University of Ulster, Northern Ireland, presented a paper about rolling resistance of surface materials affected by surface type, tire load and inflation pressure (Woodside & al., 2003). In Table 10 different factors affecting rolling resistance are presented.

Institutional Repository - Library & Information Centre - University of Thessaly
09/12/2017 02:36:50 EET - 137.108.70.7

Tyre characteristics	Tyre Operating Conditions	Environment Conditions	Rad Surface Characteristics
Construction: • Cross ply • Bias-belted • Radial Tread: • Compound • Pattern • Depth • fragmentation	Inflation pressure Load Speed Slip angle Camber angle Driving/breaking force Wheel/axle configuration	Temperature Water Snow Ice	Micro-texture Macro-texture Mega-texture Uneveness

Table 10: Factors affecting rolling resistance (EAPA & EUROBITUME, March 2004).

Road surface characteristics affect both the rolling resistance and the suspension losses. Both of these factors affect the fuel consumption. Road surface characteristics can be defined in terms of the following surface textures:

- Microtexture is the texture with wavelengths shorter than 0.5 mm
- Macrotexture is the texture with wavelengths in the range 0.5 to 50 mm
- Megatexture is the texture with wavelengths in the range 50 to 500 mm
- Unevenness is the "texture" or roughness with wavelengths longer than 500 mm

Road pavement roughness has traditionally been regarded as a measure of the ride quality perceived by occupants of passenger cars. It has also been found to provide a good measure of overall pavement condition. For these reasons, and because of the relatively low cost of data collection, road roughness has become the most commonly used measure of pavement condition at the network level. IRI (International Roughness Index) is an index that is obtained from measured longitudinal road profiles (McLean & Ramsay, October 1996).

Besides the type of pavement which definitely influences the fuel consumption and the emission production, there is another important factor that affects the rolling resistance. This factor is the age of pavement.

In the WesTrack facilities in Nevada, according to a record of fuel consumption of two test vehicles before and after the pavement restoration in 1998, there was found that a reduction of 10% of the average IRI was followed by a 4.5% reduction in the fuel consumption of the trucks. The results of a check of the Ministry of Transport of Florida mentioned that a 10% reduction of the roughness can raise the fuel economy by 1.3%. Experimental results of the

Institutional Repository - Library & Information Centre - University of Thessaly
09/12/2017 02:36:50 EET - 137.108.70.7

National Center for Asphalt Technology in tests in Alabama, showed that a 10% reduction of the roughness will lead to a 10% reduction in fuel consumption.

Another thing that has an impact on the rolling resistance and therefore the fuel consumption is the tire use. It is reported in literature that a tire's rolling resistance level, and therefore its effects on vehicle fuel economy, can decrease by more than 20% from a new tread to completely worn (LaClair, 2006), (Council, 2006). Therefore, calculations of the benefits of lower tire rolling resistance derived from measurements of new tires will likely understate the benefits to a vehicle in terms of absolute fuel economy over the lifetime of the set of tires. However, since both new vehicle fuel economy and new-tire rolling resistance change with time, and are dependent on usage conditions, age, and maintenance levels, attempts to calculate lifetime benefit can vary widely.

Tire rolling resistance is measured in a laboratory under controlled conditions. The test conditions vary between the various SAE and ISO test standards, but the basic premise is the same in that a tire is mounted on a free-rolling spindle with no camber or slip angle, loaded against a large-diameter powered test drum, turned by the drum to simulate on-road rolling operation, and some measure of rolling loss evaluated. Referring to the book The Pneumatic Tire (LaClair, 2006):

Rolling resistance is the effort requireed to keep a given tire rolling. Its magnitude depends on the tire used, the nature of the surface on which it rolls, and the operating conditions - inflation pressure, load and speed.

This description is important because it emphasizes that rolling resistance is not an intrinsic property of the tire, rather a function of many operating variables. Its definition is that it represents the energy dissipated by the tires per unit of distance travelled. One other way to express this is (EAPA & EUROBITUME, March 2004):

$$Tyre\ power\ loss = (Power\ input\ at\ the\ week\ axle) - (Power\ output\ to\ the\ ground) \quad [27]$$

As it was mentioned before, the rolling resistance depends both on how the tire is designed (tire factors) and on different characteristics in the road pavement. Many different tire factors influence the rolling resistance:

- Different shape of the tire gives different rolling resistance at higher speeds.
- Higher air pressure in the tire reduces rolling resistance.
- Higher vehicle load gives higher rolling resistance.
- The tire manufacturers can change the composition of the tires to achieve a lower rolling resistance.

Institutional Repository - Library & Information Centre - University of Thessaly
09/12/2017 02:36:50 EET - 137.108.70.7

- A higher ambient temperature reduces rolling resistance.

This is why multi-point laboratory tests measure a tire's rolling resistance over a range of inflation pressures, loads, and for some tests, a range of speeds. Conversely, single point rolling resistance test methods use a single set of these variables to estimate the rolling resistance of the tire under nominal, straightline, steady state operating conditions (the vast majority of a tire's rolling operation). In the case of a laboratory test, rolling resistance (energy loss) is calculated by measuring the amount of additional force, torque, or power necessary to keep the tire rolling at the test conditions. A fourth method, which is not widely used, is a deceleration method in which the energy source is decoupled from the system and the rate of loss of angular momentum (energy loss) imparted by the tire is measured (Larry, et al., 2009).

Using the force method, the machine measures a reaction force at the axle of the test tire & wheel assembly (Figure 25). The drum is brought up to speed and the tire is warmed up to an equilibrium temperature. The tire is then lightly loaded to measure "parasitic" losses caused by the tire spindle friction, aerodynamic losses, and the test drum/drive system bearings. The tire is then loaded to the test load and successive readings are taken until consistent force values are obtained. During the test, the loaded radius (r_L) of the tire is measured during the steady-state conditions. In ISO 28580 the Rolling Resistance (Fr) at the tire/drum interface is calculated from the measured force at the spindle (F_t), multiplied by a ratio of the loaded tire radius (r_L) to the test wheel radius (R), minus the skim load (F_{pl}):

$$F_r = F_t[1 + r_L/\mathrm{R}] - F_{\mathrm{pl}} \quad [28]$$

Institutional Repository - Library & Information Centre - University of Thessaly
09/12/2017 02:36:50 EET - 137.108.70.7

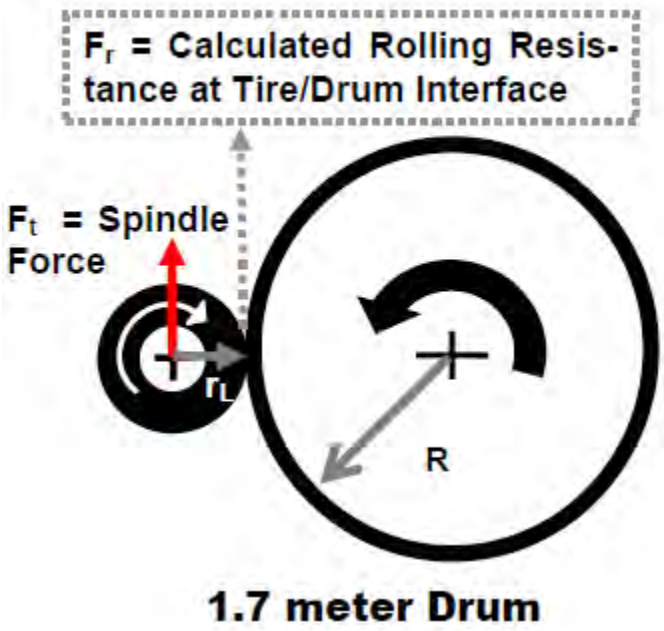

Figure 25: Force Method Rolling Resistance Test Machine (Larry, et al., 2009).

Using a torque method machine, the torque required to maintain the rotation of the drum is measured (Figure 26). The drum is connected to the motor through a "torque cell". The drum is brought up to speed and the tire is warmed up to an equilibrium temperature. The tire is then lightly loaded to measure the losses caused by the axle holding the tire and aerodynamic losses from the tire spinning. The tire is then loaded to measure the losses caused by the axle holding the tire and aerodynamic losses from the tire spinning. The tire is then loaded to the test load and successive readings are taken until consistent torque (T_t) values are obtained:

$$F_r = T_t/\mathrm{R} - F_{\mathrm{pl}} \qquad [29]$$

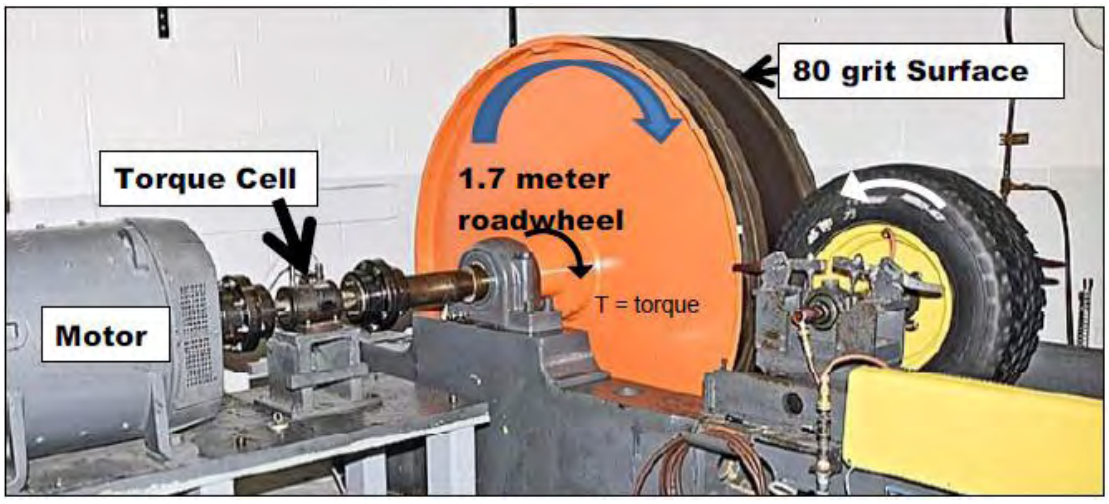

Figure 26: Torque Method Rolling Resistance Test Machine (Larry, et al., 2009).

Traditionally the rolling resistance is calculated as:

Institutional Repository - Library & Information Centre - University of Thessaly
09/12/2017 02:36:50 EET - 137.108.70.7

$$Fr = m \times a_g \times C_r \quad [30]$$

where

m: the mass of the vehicle in kg;

Fr: the rolling resistance in N;

a_g: the acceleration due to gravity in m/s² ;

C_r: the coefficient of rolling resistance.

There is an alternative formulation for this mathematical expression which takes into account vehicle lift. This aerodynamic effect serves to reduce the normal load on the pavement and therefore reduce the rolling resistance.

In HDM-III (Watanatada, Lima, & Dhareshwar, 1987b) only roughness was considered to influence C_r. This led to the following mathematical expressions:

$$C_r = 0.0218 + 0.00061\, IRI\ for\ cars\ and\ LCVs \quad [31]$$

$$C_r = 0.0139 + 0.00026\, IRI\ for\ buses\ and\ HCVs \quad [32]$$

where IRI is the roughness in IRI m/km. (International Ltd., 1995).

A project named ECRPD (Energy Conservation in Road Pavement Design, Maintenance and Utilisation) measured the rolling resistance based on coastdown measurements (Hammarstrom, Karlsson, & Sorenssen, 2008)(see Table 11).

C_r01	C_r02	C_2	C_3	C_4	C_5
0.00926	0.0000695	0.000380	3.47E-05	0.00221	0.000111

Table 11: Parameter values for a car in the general model (Hammarstrom, Karlsson, & Sorenssen, 2008).

Where the general model is described as:

$$C_r = C_{r_{01}} + C_{r_{02}} \times V + dC_r(IRI, v) + dC_r(mpd); \quad [33]$$

$$dC_r(IRI, v) = C_2 \times IRI + C_3 \times IRI \times (v - 20); \quad [34]$$

$$dC_r(mpd) = C_4 \times mpd + C_5 \times mpd\ v(V - 20); \quad [35]$$

where

mpd The macrotexture;

IRI The international roughness index.

Institutional Repository - Library & Information Centre - University of Thessaly
09/12/2017 02:36:50 EET - 137.108.70.7

There have also been estimations of parameters for temperature adjustment and for the side force resistance. The road surface effects have not been estimated as temperature dependent. Instead there is a separate term for temperature adjustments included in the C_r function. The main objective in most measurements of rolling resistance and road surface influence is to reach a general model representative for one category of vehicles. In ECRPD the parameters C_2–C_5 represent the test vehicle and C_{r01} and C_{r02} are most rough estimations for an average car. The ECRPD project, the Swedish part, included 28 test routes for coastdown measurements. These were selected to cover most of the existing variation in *IRI* and *mpd*. The range of variation is a function of the road length the measure represents. In the ECRPD case the finest resolution is 20 m, see Table 12.

	IRI (m/km)		mpd (mm)	
	At 20m average	At 400m average	At 20m average	At 400m average
Min	0.59	0.79	0.26	0.39
Max	8.75	3.66	2.74	2.54

Table 12: Data range in ECRPD at coastdown measurements (28 routes) (Hammarstrom, Karlsson, & Sorenssen, 2008).

In order to estimate exhaust emission factors using the program ARTEMIS/HBEFA there is need for driving resistance parameters including rolling resistance. Coastdown measurements were performed with a 60t truck with trailer and a box vehicle body, see (Hammarstrom & Yanya, 2011). In order to isolate transmission losses from C_r two vehicle loads were used. The estimated rolling resistance parameters were:

$$C_r = (0.00375 + 0.0000916 \times IRI \times v + 0.000695 \times mpd) \quad [36]$$

the mpd parameter is not significant different from zero (95%))

Fuel efficiency and greenhouse gas emission of different road pavements has been the object of research projects and studies all over the world. The total energy consumption during construction, maintenance and operation of roads is lower for asphalt pavements than for concrete pavements. Also the greenhouse gas emissions during construction, maintenance and operation are lower for asphalt pavements.

However the energy consumption of the traffic itself on a road is during its lifetime of overwhelming importance (95 to 98%). Depending on the traffic volume the energy use for construction, maintenance and operating the road is less than 2 to 5% of the energy used by the traffic itself. Therefore, it is legitimate to focus on how different road pavement surfaces effect the fuel consumption of vehicles driving on it (EAPA & EUROBITUME, March 2004).

Institutional Repository - Library & Information Centre - University of Thessaly
09/12/2017 02:36:50 EET - 137.108.70.7

The impact of the rolling resistance to the fuel consumption is very important. In the table below you can find the results of a study (OECD, 2004) about the influence of the rolling resistance in the fuel consumption of three different types of vehicles and two different road types.

Type of vehicle	**Medium-sized family car**		**Electric car**		**Hybrid car**	
Type of road	**Urban**	**Highway**	**Urban**	**Highway**	**Urban**	**Highway**
Rolling resistance	4%	7%	5%	8%	5%	8%

Table 13: Analysis of the influence of the rolling resistance to the fuel consumption (OECD, 2004).

In this table we can see that there is some stability in the energy consumption of each type of road for all type of vehicles. This observation shows us that we could consider that the rolling resistance is similar for an every vehicle at a specific type of road. The different percentages between urban and highway roads happen because on highways, the vehicles travel bigger distances than in urban roads so the wear of the tire due to the road is higher. Although there the fuel consumption, in general, can be higher in urban roads because of other factors e.g. traffic.

In the following section we are going to present previous studies, in chronological order, that examine the impact of the rolling resistance on the fuel consumption, the power consumption and the emissions of a vehicle. In contrast with the gradient parameter, the literature is limited. It has to be noted that there are no studies found that examine only the rolling resistance impact on heavy duty vehicles so our categorization was simpler than the gradient factor. Our review was focused on two different categories related with the type of the vehicle: (1) papers and reports examining LDVs (Light Duty Vehicles), (2) those that can be applied to many different but specific types of vehicles taking in account the type of vehicle given (VSTV – Very Specific Type of Vehicles). As we also said in the previous chapter, this category also refers to papers and reports that give results about the average behavior of many vehicles (for example in experiments carried out in a daily traffic of a road).

For all of the studies presented, we gave all the information concerning the case developed in each study: (1) The type of road examined: asphalt, concrete, composite, (2) the age of the pavement if there was reference to it, (3) the consequences due to the rolling resistance, that can refer to (a) the Power Consumption , (b) the Fuel Consumption (FC) of the vehicle, (c) the produced Emissions, (4)The way that we come to the conclusion of which consequences of the three above exist, if for example there are mathematical expressions that proved that

Institutional Repository - Library & Information Centre - University of Thessaly
09/12/2017 02:36:50 EET - 137.108.70.7

there is an impact on these due to the rolling resistance or there were experiments carried out that gave results about these consequences (see Figure 27).

Through all these studies, we were able to export some interesting conclusions about the relation of the rolling resistance with the fuel consumption, the power consumption and the emissions produced from the vehicles. As there were no studies found that examine only the rolling resistance impact on heavy duty vehicles , in Chapter 5 we will examine cases that study the impact of the rolling resistance parameter on HDVs but in correlation with other parameters as well.

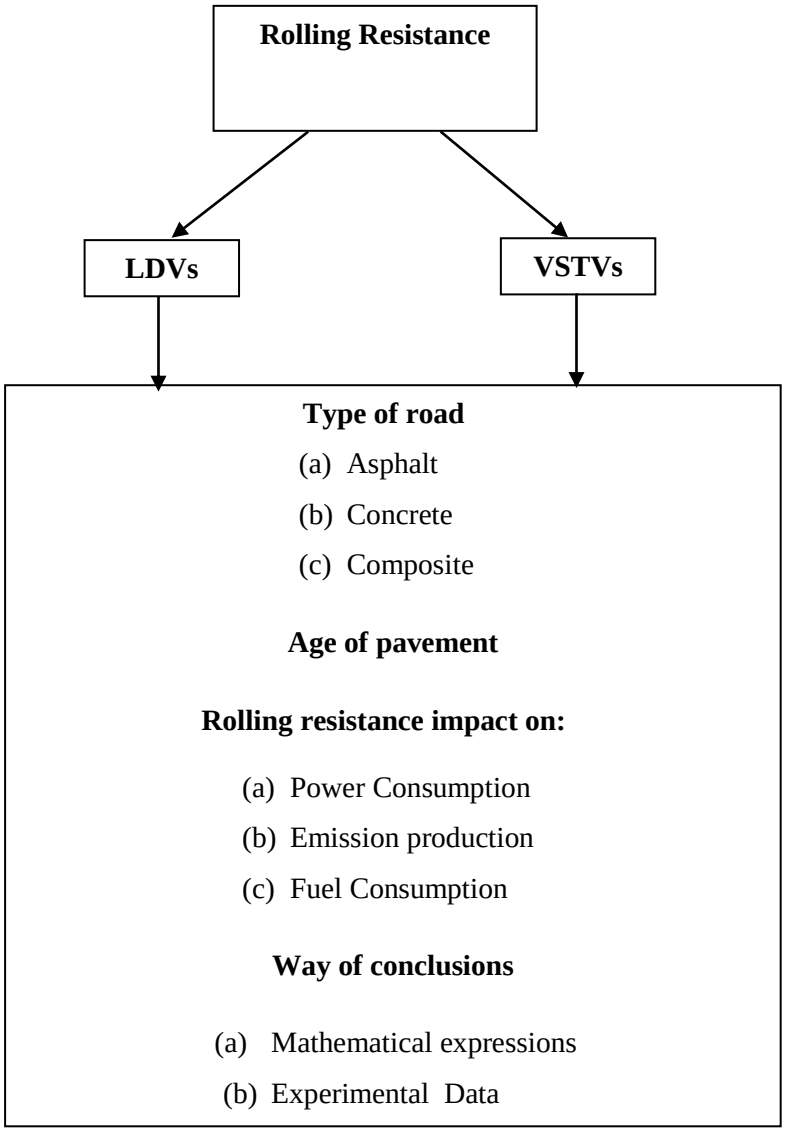

Figure 27: Diagram of our review – categorization of studies.

Institutional Repository - Library & Information Centre - University of Thessaly
09/12/2017 02:36:50 EET - 137.108.70.7

3.2 Review of Rolling Resistance research

3.2.1 Light Duty Vehicles (LDVs)

In 1990 a study in Sweden presented the effects of different textures on rolling resistance and therefore the fuel consumption of the vehicle through experimental data on a light duty vehicle (Sandberg U. S., 1990). The experiment presented in the study concerned the influence of road macro- and megatexture on fuel consumption and had been performed by VTI (Swedish Road and Traffic Research Institute) in Sweden. In the experiment a specially instrumented Volvo passenger car was run at 50, 60 and 70 km/h constant speed over 20 test sites with various surfaces textures. Macro- and megatexture as well as shorter wavelengths of unevenness were measured by a mobile laser profilometer. The fuel consumption data at each speed and averaged for the three speeds were regressed on the texture profile spectrum data. Some of the results from the experiment are shown in Table 14.

In the paper there is no reference to the impact on the power consumption or the emission rates and no mathematical expressions are given in the study. Although there are data concerning different texture of different road types like asphalt and concrete but there is no reference to the age of pavement.

Institutional Repository - Library & Information Centre - University of Thessaly
09/12/2017 02:36:50 EET - 137.108.70.7

Pavement type and aggregate size	**Texture Data**				**Fuel Consumption (ml/10 km)**		
	Macro scale* 0-9	Macro L_{MA}** dB	Mega L_{ME}** dB	Short-wave unevenness L_{SU} ** dB	50 km/h	60 km/h	70 km/h
Dense Asphalt 0/8	6	48.0	45.0	54.4	695	676	736
Dense Asphalt 0/16	3	50.2	48.5	54.0	714	692	732
Cement Concrete 0/25	2	52.0	56.3	58.6	720	710	756
Δ[Dense Asphalt 0/8- Cement Concrete 0/25]	4	-4	-11.3	-4.2	-25	-34	-20
Δ[Dense Asphalt 0/16- Cement Concrete 0/25]	1	-1.8	-7.8	-4.6	-6	-18	-24

* Estimated microtexture on a scale 0 – 9 where 0 = perfectly smooth and polished and 9 = very harsh

**The following wavelength ranges were used in the study:

- L_{MA}: level of macrotexture, range 2 to 50 mm
- L_{ME}: level of megatexture, range 63 to 500 mm
- L_{SU}: level of shortwave unevenness, range 0.63 to 3.15 m

Table 14 Texture data and fuel consumption for different Pavement Types .The values are normalized with respect to speed and temperature (Sandberg U. S., 1990).

Some of the conclusions in the report were:

- Clear correlation between fuel consumption and macrotexture;
- Good correlation between fuel consumption and shortwave unevenness;
- An uneven road may increase fuel consumption by up to 12% relative to an even road;
- A rough macrotexture, may increase fuel consumption by 7% relative to a very smooth macrotexture;
- Fuel consumption for a car may be influenced as much as 12% by road surface characteristics within the tested range;
- Clear correlation between fuel consumption and macrotexture.

Institutional Repository - Library & Information Centre - University of Thessaly
09/12/2017 02:36:50 EET - 137.108.70.7

There were strong indications that there are three different sources of energy losses due to road surface effects:

- Vehicle suspension losses excited by the longest wavelengths;
- Tire-bulk vibration losses at wheel hop frequencies (at 0.5-1.3 m texture wavelength);
- Tire impact hysteresis losses at the typical macrotexture wavelength (chipping sizes and spacing). The latter is pronounced only at 60 and 70 km/h and seems to be more important the higher the speed is.

In 1999 a study in Netherlands examined different types of textures and pavements to see the effects on the fuel consumption of a specially instrumented Volvo V70 passenger car loaded with two persons and full fuel tank that was run at 90 km/h constant speed over the test sections (De Graaff, 1999). There was no reference to the emissions or the power consumption of the vehicle and the pavements examined were different types of asphalt and concrete. There is a reference to the impact that the age of pavement (the quality and the maintenance) on the rolling resistance and during the experiments there is also a new road compared among others. No mathematical expressions were presented as all data were part of experimental procedures. During the study there were specific environmental conditions taken into account so the results presented refer might not be generalized. The results of the experiment are shown in Table 15.

Road surface type	**Fuel consumption relative to Dense Asphalt Concrete 0/16 [%]**
Dense Asphalt Concrete 0/16	0
Porous Asphalt 6/16	$-0.0\ (\pm 3.5)$
Stone Mastic Asphalt	$+3.4\ (\pm 3.6)$
Double-layered Porous Asphalt 4/8 + 11/16*	$+1.2\ (\pm 3.3)$
Cement Concrete, broomed transversely	$+0.4\ (\pm 3.4)$
Cement Concrete treated with a surface epoxy durop	$+2.7\ (\pm 4.5)$
Brick-layered pavement	$+5.3\ (\pm 6.6)$
*New road surface; bitumen film still present Mean value on long measuring sections, corrected to 20℃, weather without wind and a Volvo V70 passenger car loaded with two persons and full fuel tank. Between brackets it shows the 95% confidence level of the difference	

Table 15: Fuel consumption at 90 km/h on different types of road pavement relative to Dense Asphalt Concrete 0/16 (EAPA & EUROBITUME, March 2004).

The conclusions from this study were mainly three:

Institutional Repository - Library & Information Centre - University of Thessaly
09/12/2017 02:36:50 EET - 137.108.70.7

- There was no significant difference in fuel consumption found between porous and dense road surfaces. The positive and the negative effects, found in the literature, cancel one another roughly;
- From a statistical point of view there is no significant difference in fuel consumption found between asphalt and cement concrete road surfaces. Additionally it was mentioned that dense road surfaces that are used in the Netherlands are for the greater part in the category fine textured road surfaces. The differences in fuel consumption that could be expected within this category are, according to the literature, up to 10%;
- Another conclusion of the report was that the condition of the road surface especially those that influence the texture and the evenness (like the quality of the construction and the maintenance), seem to have a strong influence on the rolling resistance and therefore on the fuel consumption of the traffic driving on this road surface.

In 2009, (Sumitsawan, Romanoschi, & Ardekani, August 2009) the effect of pavement type on fuel consumption was investigated. Significant differences in fuel consumption and emissions rates were observed on rigid versus flexible pavement surfaces. The pavement sections were a Portland cement concrete (PCC) and an asphalt concrete (AC) section. During the study there was no reference about how the rolling resistance can affect the power consumption of the vehicle. The data provided were experimental results and there is only one mathematical expression concerning the CO_2 emissions given. The age of pavement was not a factor that was taken into account during the experiments.

The study emphasis was on urban driving cycles at non-highway speeds and fuel consumption measurements were made on multiple runs by driving an instrumented van over two new pavement sections: a rigid and a flexible section of two parallel city streets. The two sections were both tangent sections with identical gradients and similar roughness, they had similar geometric characteristics and differed only in the type of pavement. All other factors that could influence fuel consumption (weight, fuel tank level, tire pressure, ambient temperature, humidity, and wind speed and direction) were either controlled or kept the same during the test runs. Two different driving modes were also performed: constant speed of 30 mph and acceleration from zero to 30 mph at a rate of 3 mph/second. All tests were conducted under dry pavement conditions with a four factor-level experimental design—two pavement types and two driving modes. The differences in fuel consumption rates were determined to be statistically significant at 10% level of significance for the constant speed runs with the rate for the rigid section being lower. The experimental design had two factors (pavement type and driving mode) and two levels for each factor (PCC versus AC and constant speed of 30

Institutional Repository - Library & Information Centre - University of Thessaly
09/12/2017 02:36:50 EET - 137.108.70.7

mph versus a 3 mph/sec acceleration mode). The experimental factors and combinations are also shown in Table 16.

Factor-Level Combination	Pavement Type	Driving Mode
1	PCC	Constant Speed
2	PCC	Acceleration
3	AC	Constant Speed
4	AC	Acceleration

Table 16: The four factor-level combinations (Sumitsawan, Romanoschi, & Ardekani, August 2009).

Table 17 summarizes the average fuel consumption rate for each of the four dry pavement and driving mode runs. In the constant speed mode, a cruise speed of 30 mph was maintained throughout the test section. Under the acceleration driving mode, the fuel data were collected while accelerating from zero to 30 mph in 10 seconds, yielding an average acceleration rate of 3 mph/second. For each driving mode, the total fuel consumed was recorded, and the corresponding consumption rate in gallons per mile was computed. In Table 17, we can see the results concerning the two different types of pavement: asphalt (AC) and cement (PCC) during the two driving modes: constant speed and acceleration and their differences between.

	Average Fuel Consumption (10^{-3} gals/mile)	Test Conditions
PCC, Constant Speed	40.7	**Date:** November 7, 2008 **Temperature:** 69 °F **Pressure:** 30.08 in. Hg **Wind:** 7 mph W (tailwind) **Engine:** Warm **Tire Pressure:** 50 psi **Tank Level:** Full **IRI (in./mi):** 174.6 (PCC), 180.6 (AC) **Longitudinal Slope:** +1.2% (PCC) + 1.2% (AC)
AC, Constant Speed	42.7	
Δ[PCC, Constant Speed - AC, Constant Speed]	-2.0	
PCC, Acceleration	236.4	
AC, Acceleration	236.9	
Δ[PCC, Constant Speed - AC, Constant Speed]	-0.5	

Table 17: Average fuel consumption rates for PCC versus AC sections (Sumitsawan, Romanoschi, & Ardekani, August 2009).

In both driving modes, the fuel consumption rate for the PCC pavement was observed to be lower than the rate for the AC pavement. These observed differences in fuel consumption

Institutional Repository - Library & Information Centre - University of Thessaly
09/12/2017 02:36:50 EET - 137.108.70.7

rates were, however, tested for statistical significance at 10% level of significance. One-sided tests were conducted to probe whether the fuel rates on the PCC section were statistically lower than the rates on the AC section. It was determined that in the constant speed mode, the lower fuel consumption rate on the PCC section was in fact statistically significant at 10% level of significance. However, this was not the case under the acceleration mode. Therefore, it can be concluded that under constant travel speed of 30 mph, the PCC section results in statistically lower fuel consumption rate than the AC section. Under an acceleration of 3 mph/sec, while the PCC still resulted in a slightly lower consumption rate, the difference in consumption rate was found not to be statistically significant. The CO_2 emissions in the PCC case were estimated using the following empirically derived regression model (Afotey, 2008):

$$CO_2 \; amount \; in \; gram/\sec = 0.867 + 0.011 \times v + 1.172 \times \mathrm{a} + 0.208 \times \mathrm{a} \times v \qquad [37]$$

where v is the velocity in mph and a is the acceleration rate in mph/second. The CO_2 emissions for all other cases were estimated as a ratio of the fuel consumption rate for each respective case relative to the field-measured rate for the PCC section.

Under dry surface conditions at urban driving speed of 30 mph, fuel consumption per unit distance is lower on concrete pavement than on asphalt pavement. Moreover, the observed difference in fuel consumption rate is statistically significant at 10% level of significance with the rate for the concrete pavement being lower. The potential savings in fuel consumed and CO_2 emissions over the life of the project could be substantial and should be considered in the life cycle cost analysis of alternative projects and in sustainable development considerations such as the carbon footprint of a roadway project.

3.2.2 Very Specific Type of vehicles (VSTVs)

In 2007, a study presented the relationship between pavement roughness and fuel consumption. This paper has its origin in an inquiry into the impact of contractual pay adjustments for smoothness, known formally as the special provision for rideability, on maintenance contract prices for hot-mix asphalt and on the roughness of new asphalt overlay. The paper estimated the agency and motorist costs on a selected segment of I-64 highway road in Virginia, with and without the special provision, for resurfacing cycles of from 1 to 12 years. Experimental data concerning the fuel consumption are presented in the study but there is no reference to the power consumption or the emission rates, neither any mathematical expressions provided.

Table 18 presents the evolution of the roughness for a typical pavement with or without the driving behavior parameter. The annual evolution of the fuel consumption is shown as well,

Institutional Repository - Library & Information Centre - University of Thessaly
09/12/2017 02:36:50 EET - 137.108.70.7

having as data the Annual Average Daily Traffic – AADT in miles/day of 14000 vehicles for two traffic lanes. It shows the same two quantities for a pavement overlaid with the special provision.

	Without Spec. Provision		**With Spec. Provision**	
Year	**IRI (inche/mi)**	**Annual Fuel Consumption**	**IRI (inche/mi)**	**Annual Fuel Consumption**
0	76.2	288.456	67.4	283.890
1	77.4	289.035	68.6	284.524
2	78.6	289.616	69.8	285.159
3	79.8	290.198	71.0	285.796
4	81.1	290.782	72.2	286.434
5	82.3	291.366	73.4	287.074
6	83.6	291.366	74.7	287.715
7	86.2	293.126	76.0	288.357
8	86.2	293.126	77.3	289.001
9	87.6	293.715	78.7	289.646
10	88.9	294.306	80.0	290.293
11	90.3	294.897	81.4	290.941
12	91.7	295.490	82.8	291.591

Table 18: Roughness and fuel consumption depending on the pavement age maintenance for Fuel Consumption Elasticity=0,13 (passenger cars, vans)* (Gillespie & McGhee, 2007).

***FuelConsumptionElasticity=The ratio of the change of the fuel consumption to the unit change of the pavement roughness.**

The International Roughness Index (IRI) for the years 0-7 has been concluded through average data of the Virginia Department of Transportation (VDOT) and it is considered to increase in a stable mode. The fuel consumption of a vehicle per mile is expected to be increased by 0.13% for every 1% increase of IRI.

Institutional Repository - Library & Information Centre - University of Thessaly
09/12/2017 02:36:50 EET - 137.108.70.7

	Without Spec. Provision		With Spec. Provision	
Year	**IRI (inche/mi)**	**Annual Fuel Consumption**	**IRI (inche/mi)**	**Annual Fuel Consumption**
0	76.2	287.415	67.4	282.702
1	77.4	288.027	68.6	283.345
2	78.6	288.643	69.8	283.994
3	79.8	289.264	71.0	284.647
4	81.1	289.889	72.2	285.306
5	82.3	290.518	73.4	285.969
6	83.6	291.151	74.7	286.638
7	86.2	291.789	76.0	287.312
8	86.2	292.432	77.3	287.991
9	87.6	293.079	78.7	288.675
10	88.9	293.730	80.0	289.365
11	90.3	294.386	81.4	290.060
12	91.7	295.046	82.8	290.760

Table 19: Roughness and fuel consumption depending on the pavement age maintenance for Fuel Consumption Elasticity=0,45 (only trucks) (Gillespie & McGhee, 2007).

The table above demonstrates the evolution of the pavement roughness and the fuel consumption taking in account that the fuel consumption of the trucks (that constitute the 13% of the traffic) increases by 0.45% for every 1% increase of IRI. This projection ignores any impact on the fuel economy of cars and light utility vehicles.

The general conclusion that comes out by the above tables is that as the roughness increases due to the pavement aging, with or without the driving mode parameter, we have an analogous increase of the annual fuel consumption.

3.3 Conclusions

The above studies show that the rolling resistance is a parameter that undoubtedly influences the fuel consumption of a vehicle. Although many factors influence the level of the rolling resistance and therefore the size of its impact. These factors are the type of vehicle, the type of road (asphalt, concrete, composite), the roughness of the pavement, the condition of the pavement (the age of pavement and maintenance), the speed of the vehicle, the condition of the tires and other factors like the ambient temperature or the weather (e.g. if the pavement is wet or dry, hot or cold).

Institutional Repository - Library & Information Centre - University of Thessaly
09/12/2017 02:36:50 EET - 137.108.70.7

Different textures of road surfaces influence fuel consumption for passenger cars by up to 10%. The roughness of the road is playing a significant role in influencing the rolling resistance. According to the previous studies, an uneven road may increase fuel consumption by up to 12% relative to an even road. A rough macrotexture, may increase fuel consumption by 7% relative to a very smooth macrotexture. Fuel consumption for a car may be influenced as much as 12% by road surface characteristics.

The type of road may also influence the fuel consumption. For example the PCC pavement was observed to be lower than the rate for the AC pavement. Generally, studies showed differences in the fuel consumption when testing vehicles in different types of roads.

Another important conclusion is that the condition of the road surface especially factors that influence the texture and the evenness (like the quality of the construction and the maintenance), seem to have a strong influence on the rolling resistance and therefore on the fuel consumption of the traffic driving on this road surface. Therefore, the age of pavement that influences the quality is an important factor that has to be taken into account. More important for the fuel efficiency are pavements in good condition with good surface characteristics (texture and roughness). Optimal maintenance of the roads is therefore the means to limit fuel consumption and greenhouse gas emission.

Institutional Repository - Library & Information Centre - University of Thessaly
09/12/2017 02:36:50 EET - 137.108.70.7

Chapter 3 THE AIR RESISTANCE

3.1 Introduction

A third parameter that can affect the fuel consumption and the emissions of a vehicle is the air resistance or aerodynamic drag. This parameter depends on the wind and the air density.

The air flow over a vehicle transmits an aerodynamic force to the vehicle through pressure and shear stress distribution acting on the surface of the vehicle. Pressure and shear stress act at every point on the body. The net effect of the aerodynamic force includes drag D, lift L, side force component S, and various forces PM, RM, YM as shown in Figure 28 acting on a principal axis of a vehicle. Each one is described as follows.

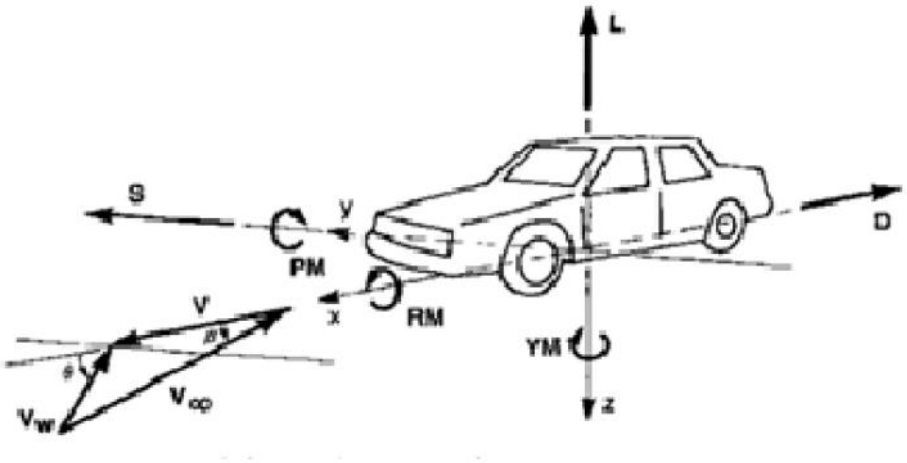

Figure 28: Aerodynamic force and moments acting on a vehicle (Adem, 2009).

Aerodynamic lift (i.e. L) that is mentioned above is the component of aerodynamic force perpendicular to the free stream velocity. It is mainly created by the pressure difference on the top and bottom surface of a vehicle.

Drag (i.e. D) is the force acting on the surface of the vehicle by the flow in direction opposing the motion of the vehicle. The drag is the integral of local stream-wise component of normal (pressure) and tangential (skin friction) surface forces over all surface exposed to the stream. Direct evaluation of drag requires knowledge of the detailed stress distribution and also integrating the pressure distribution over the complex surface of the vehicle which is extremely difficult to obtain.

According to (U.S. Department of Energy), in urban driving, aerodynamic drag accounts for 2.6% of the 12.6% of fuel energy being used to propel the car. Since the aerodynamic drag increases at higher speeds, the aerodynamic drag on a highway driving accounts for 11% of

Institutional Repository - Library & Information Centre - University of Thessaly
09/12/2017 02:36:50 EET - 137.108.70.7

20% fuel energy needed to propel the vehicle. Therefore improving vehicle aerodynamics is one of the factors that play crucial role for getting better mileage and better performance including the handling of the vehicle especially at high speeds.

The shape of the vehicle plays a significant role to the size of the drag impact. According to (Hucho, 1998) the contribution of the front body of a vehicle to drag is usually small. The rear shape of the vehicle contributes greatly to the aerodynamic drag because of the fact that the low pressure turbulent wake region is formed at the rear creating large pressure difference between the front and rear ends of the vehicle.

Aerodynamic drag is generated by the interaction of a solid body with a fluid which results in the difference in velocity between the solid object and the fluid. It can be regarded as aerodynamic resistance to motion of the object through the fluid medium. To reduce the aerodynamic drag of a ground vehicle, it is very important to understand the source of aerodynamic drag for a flow over a vehicle which is described as follows:

1. Skin friction: the interaction between the flowing air molecule and the solid object causes friction drag on the object. Skin friction is dominant on streamlined objects like airplane wings while pressure drag is dominant on bluff bodies.
2. Boundary layer pressure loss: as the air flows over the body, a boundary layer is developed. The boundary layer is a thin layer over the body where the velocity of the flow varies from zero on the surface of the object to free flow velocity at the edge of the boundary layer. The viscous effect within the boundary layer is very important. Boundary layer gets thicker as it progresses from the front to rear of the vehicle. The thicker boundary layer at the rear of the vehicle makes the rear stagnation pressure of the flow less than the front stagnation pressure, so there is effective pressure drop along the length of the body, which causes flow separation. For non-streamlined bluff bodies such as pickup trucks immersed in a flow, the flow separates from the body near sharp edges and creates a region of turbulence. Pressure will drop in the turbulence region, resulting in the pressure difference between the front and rear of the vehicle – the pressure the drag. Since blunt bodies have a larger rear area, they have larger pressure drag. For streamlined body, this term is less significant.
3. Induced drag: when a body such as a vehicle spoiler is immersed in a flow it generates a lift which also induces drag. The drag on a body increases as lift increases. Thus minimum drag occurs when the lift on the body is zero. As road vehicles are bluff bodies in close proximity to the ground and the pressure difference between the under body and upper surface of the vehicle create lift which could induce drag.

Institutional Repository - Library & Information Centre - University of Thessaly
09/12/2017 02:36:50 EET - 137.108.70.7

4. Interference drag: it is caused by imperfection on the body of the vehicle surfaces as windshield wipers, door handles.

There are some mathematical expressions provided in several studies for the calculation of the aerodynamic force, which is the force needed to overcome the air resistance. This force represents the force required to push an object through the air. It is calculated as (International Ltd., 1995):

$$Fa = 0.5 \times \rho \times CD \times A_{Frontal} \times vr^2 \quad [38]$$

where

Fa: the aerodynamic force opposing motion in N;
ρ: the mass density of air in kg/m^3;
CD: the aerodynamic drag coefficient;
$A_{Frontal}$: the projected frontal area of the vehicle in m^2;
vr: the speed of the vehicle relative to the wind in m/s.

Below all the factors of the above mathematical expression are analyzed.

Mass Density of Air (i.e. ρ)

The density of moist air varies with pressure and temperature. Several researchers ((John & Kobett, 1978), (Visser & Curtayne, 1985), (Biggs, 1990)) have related the density of air to either temperature, altitude or a combination of the two. The default value recommended is 1.2 kg/m^3, which is based on a standard temperature of 15℃ at an altitude of 200 m (Biggs, 1987). Adjustments to the default value are made using the following mathematical expression (Bennett, 1989a):

$$\rho = 0.0566 + 1.225 \times (1 - 2.23 \times 10^{-5} \times ALT)^{4.225} - 0.00377 \times \text{TAIR} \quad [39]$$

where

ALT: the altitude above sea level in m
TAIR: the temperature of the air in ℃

Aerodynamic Drag Coefficient and Relative Velocity (i.e. CD)

The aerodynamic drag coefficient (CD) is a measure of three sources of air resistance:

- form drag caused by turbulent air flow around the vehicle;

Institutional Repository - Library & Information Centre - University of Thessaly
09/12/2017 02:36:50 EET - 137.108.70.7

- skin friction between the air and the vehicle;
- interior friction caused by the flow of air through the vehicle.

Form drag and skin friction make up approximately 85 % and 10 % respectively of the total air resistance (Manning & Kilareski, 1990). Accordingly, large square shaped vehicles have higher CD values than small rounded ones.

The CD is a function of vehicle direction relative to the wind. The apparent direction of the wind, which is the vector resultant of the vehicle direction and the wind direction, is termed the yaw angle (ψ). This is illustrated in Figure 29. The values of CD reported in the literature are usually from wind tunnel tests conducted with a 0 degree yaw (i.e. front on to the wind) and accordingly are the minimum for the vehicle.

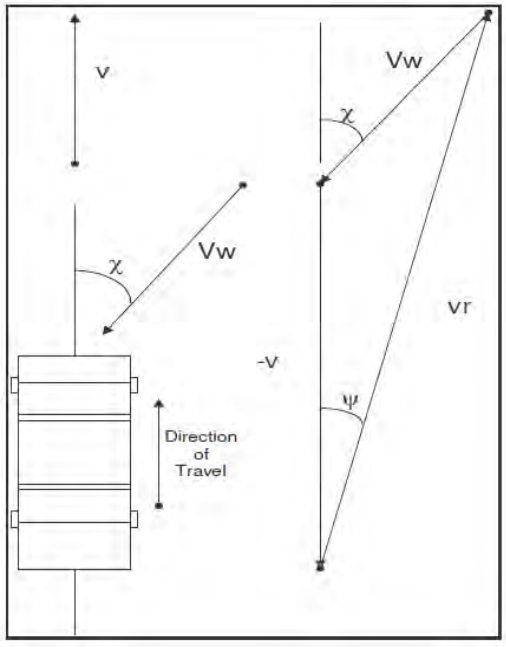

Figure 29: Wind Forces Acting on a Vehicle (International Ltd., 1995).

To obtain typical values of CD which would be found on roads, it is therefore necessary to adjust for the variation in wind direction. This can be done using a "typical" wind angle which increases the 0 degree yaw CD, leading to wind averaged CD, or CD(ψ). The ratio of CD(ψ)/CD is termed the CD multiplier (i.e. CDmult). The mathematical expression below is therefore rewritten as:

$$Fa = 0.5 \times \rho \times CD(\psi) \times vr^2 \quad [40]$$

$$Fa = 0.5 \times \rho \times CDmult \times CD \times A_{Frontal} \times vr^2 \quad [41]$$

where

Institutional Repository - Library & Information Centre - University of Thessaly
09/12/2017 02:36:50 EET - 137.108.70.7

CD(ψ): the wind averaged CD

CDmult: the CD multiplier

(Biggs, 1988) presented an approach for calculating CDmult, however (Biggs, 1995) recommended the use of the methodology presented by (Sovran, 1984). The (Sovran, 1984) approach gave a value of zero for CDmult when the yaw angle was 90°, whereas the method presented by (Biggs, 1988) gave a non-zero value. The (Sovran, 1984) approach for calculating CDmult is as follows:

For 0 <ψ < ψc:

$$CDmult = 1 + h \times \left[sin\frac{90\psi}{\psi c}\right]^2 \quad [42]$$

For ψc < ψ < 180- ψc:

$$CDmult = (1 + h) \times cos\left[\frac{90(\psi - \psi c)}{90 - \psi c}\right] \quad [43]$$

For 180- ψc < ψ < 180:

$$CDmult = -\left(1 + h \times \left(sin\left[\frac{90(180 - \psi)}{\psi c}\right]\right)^2\right) \quad [44]$$

where

ψc: the yaw angle in degrees at which CDmult is a maximum;

ψ: the yaw angle (i.e. the apparent direction of the wind);

h: the proportionate increase in CD at angle yc (see Figure 30).

The yaw angle is given by:

$$\psi = sin^{-1} \times (Vw \times \sin(\chi)/vr) \quad [45]$$

where

V_w: the wind velocity in m/s;

χ: the direction of the wind relative to the direction of travel.

The velocity of the vehicle relative to wind can be calculated from Figure 30 as:

$$vr^2 = v^2 + Vw^2 + 2 \times Vw \times \cos(\chi) \quad [46]$$

Institutional Repository - Library & Information Centre - University of Thessaly
09/12/2017 02:36:50 EET - 137.108.70.7

(Sovran, 1984) gave the value of ψc as 30° and had 0.4 for passenger cars. Figure 30 is a plot of CDmult for ψc = 30° and h=0.4. (Wong, 1993) indicated that ψc is approximately 30° for heavy vehicles also. (Biggs, 1995) gave the value of h for trucks as:

0.6 rigid trucks;

0.8 single trailer trucks;

1.2 double trailer trucks.

These values compare well with the data in (Wong, 1993).

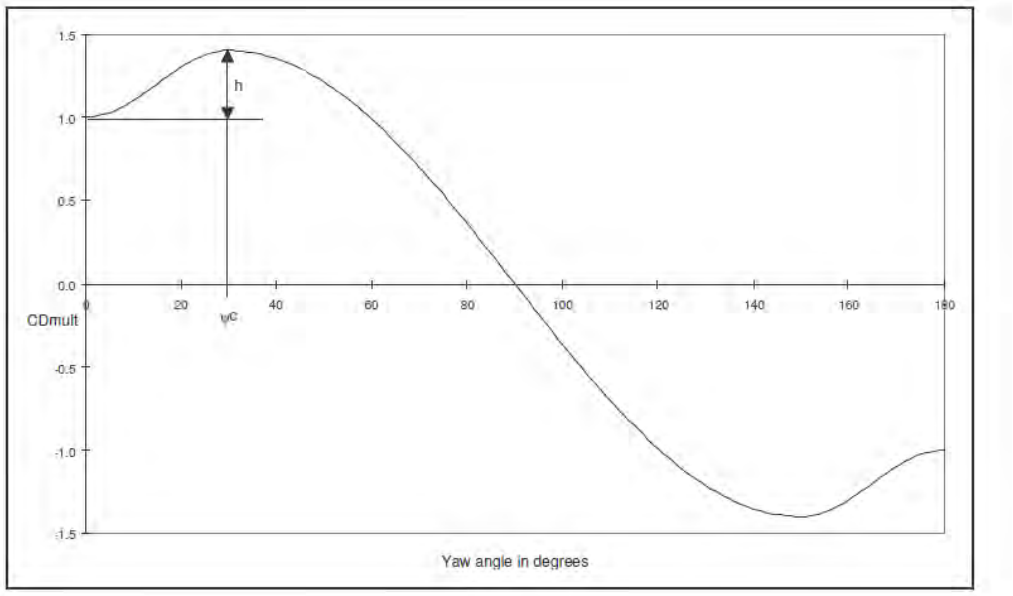

Figure 30: CDmult versus Yaw Angle (International Ltd., 1995).

In order to calculate an average value for CDmult it is necessary to allow for the distribution of wind directions acting on a vehicle. (Ingram, 1978) calculated wind-averaged values of CD for heavy goods vehicles by establishing the distribution of wind speeds and directions imposed on a vehicle on various motorways around Britain. He compared his detailed values with those which would have arisen under the assumption that on a network there is an equal probability of wind arriving at all angles relative to the center line of the roads. He concluded that:

The approximation reached by assuming that the national average wind speed is equally probable from all directions is quite adequate, giving an error of less than one per cent.

This does not imply that the wind has an equal probability of arriving from all directions, as most localities have predominant wind patterns, but rather that the combined distribution of

Institutional Repository - Library & Information Centre - University of Thessaly
09/12/2017 02:36:50 EET - 137.108.70.7

wind and road angles is equally distributed. Consequently, there is little utility in undertaking a detailed analysis of wind direction, such as that done by (Ingram, 1978).

Using the approximation that wind has an equal probability of arriving at any angle relative to the center line of the road within a network in conjunction with the above mathematical expressions, a wind-averaged CD multiplier can be ascertained. By considering the relative velocity of the vehicle in these calculations it is possible to rewrite the mathematical expression [41] as:

$$Fa = 0.5 \times \rho \times CDmult \times CD \times AF \times v^2 \quad [47]$$

Thus, the value of CDmult implicitly models the ratio of vr^2/v^2.

Under the assumption that ψc is a constant value of 30^o for all vehicle classes, a series of calculations was performed to calculate the CD multiplier. To simplify the use of the aerodynamic resistance mathematical expression, CDmult was assumed to be a constant value for all vehicle speeds. The vehicle velocity chosen for calibration of CDmult was 21 m/s (75 km/h). The results were not very sensitive to the chosen speed (International Ltd., 1995).

This approximation results in a slight under prediction of the aerodynamic resistance at low vehicle speeds, and a slight over prediction at high vehicle speeds. At low vehicle speeds, the tractive force is dominated by rolling resistance, whereas at high vehicle speeds aerodynamic resistance dominates. Hence, it is more important to accurately model aerodynamic resistance at higher vehicle speeds.

Table 20 presents values of CDmult based on a vehicle velocity of 21 m/s. As the value of the ψc is constant for all vehicle classes, only one series of values are presented. The CD multiplier was calculated for angles of χ between 0 and 180 degrees, in intervals of 1 degree. From the 181 values of yaw angle, the value of the CD multiplier and relative velocity were calculated for each angle. The average of these values was then divided by the square of vehicle speed. As can be seen from Table 20, CDmult increases both with increasing wind speed and an increasing value of h.

Institutional Repository - Library & Information Centre - University of Thessaly
09/12/2017 02:36:50 EET - 137.108.70.7

h	Wind Speed in km/h					
	0	10	20	30	40	50
0.0	1.00	1.01	1.07	1.16	1.28	1.43
0.2	1.00	1.03	1.12	1.26	1.42	1.60
0.4	1.00	1.04	1.18	1.36	1.56	1.78
0.6	1.00	1.06	1.23	1.46	1.71	1.95
0.8	1.00	1.07	1.29	1.57	1.85	2.13
1.0	1.00	1.09	1.34	1.67	1.99	2.30
1.2	1.00	1.10	1.40	1.77	2.14	2.47
1.4	1.00	1.12	1.45	1.88	2.28	2.65

Table 20: CDmult for a Range of Wind Speeds and Values of 'h' (International Ltd., 1995).

From the data presented in Table 20, an analysis was carried out to construct a mathematical expression which would predict the CDmult for a vehicle speed of 21 m/s and a critical yaw angle of 30°. CDmult was found to be linear with respect to h, with both the intercept and the slope been dependent on the wind speed. The resulting mathematical expression (adjusted Rsquared = 0.99, S.E. = 0.01) was:

$$CDmult = a_0 \times Vw^2 + (a_1 \times Vw^3 + a_2 \times Vw^2) \times h + 1.0 \quad [48]$$

where a_0 to $_{a2}$ are regression constants as follows:

a_0= 2234 x 10^{-6}
a_1= -507 x 10^{-6}
a_2= 11.525 x 10^{-3}

Table 20: CDmult for a Range of Wind Speeds and Values of 'h' .Table 20 presents the recommended default values of h and CDmult for use with mathematical expression [47] based on the default wind speed.

Projected Frontal Area (i.e $A_{Frontal}$)

The projected frontal area $A_{Frontal}$, is calculated as product of the maximum width of the vehicle by the maximum height less the area under the axles. (Biggs, 1988) indicated that the area under the axles is between 5 and 15 per cent for most vehicles. As with the aerodynamic drag coefficient, the projected frontal area is proportional to the yaw angle. However, these considerations have been included with the wind averaged aerodynamic drag coefficient so are not repeated here.

(Wong, 1993) gave the following approximation for calculating the frontal area of a passenger car from the vehicle mass:

Institutional Repository - Library & Information Centre - University of Thessaly
09/12/2017 02:36:50 EET - 137.108.70.7

$$A_{Frontal} = 1.6 + 0.00056 \times (m - 756) \quad [49]$$

where m is the vehicle mass in kg.

Vehicle Number	Type	h	CD_{mult}	CD	AF(m^2)
1	Motorcycle	0.4	1.10	0.70	0.8
2	Small Car	0.4	1.10	0.40	1.8
3	Medium Car	0.4	1.10	0.42	1.9
4	Large Car	0.4	1.10	0.45	2.0
5	Light Delivery Vehicle	0.5	1.11	0.50	2.9
6	Light Goods Vehicle	0.5	1.11	0.50	2.8
7	Four Wheel Drive	0.5	1.11	0.50	2.8
8	Light Truck	0.6	1.13	0.55	4.0
9	Medium Truck	0.6	1.13	0.60	5.0
10	Heavy Truck	0.7	1.14	0.70	8.5
11	Articulated Truck	1.2	1.22	0.80	9.0
12	Mini-bus	0.5	1.11	0.50	2.9
13	Light Bus	0.6	1.13	0.50	4.0
14	Medium Bus	0.7	1.14	0.55	5.0
15	Heavy Bus	0.7	1.14	0.65	6.5
16	Coach	0.7	1.14	0.65	6.5

Table 21: Default CDmult Values for HDM-4 Vehicle Classes

Another way to calculate the air resistance is through some mathematical expressions that were provided after experiments that were carried out for different types of vehicles by simulations using the model PHEM (Passenger car and Heavy duty Emission model).

The emission model PHEM is interpolating the fuel consumption and the emissions from the engine maps according to the course of engine power demand and engine speed in the driving cycles. The method is therefore capable of making use of the data from all engines from the data collection campaign.

PHEM was primarily developed to simulate the HDV emission factors in the HBEFA 2.1 and the ARTEMIS inventory model. In these applications emission factors for more than 600 000 combinations of HD vehicle segments (separated according to vehicle categories, vehicle weight classes and engine technologies) with different vehicle loadings based on representative driving cycles at different road gradients had to be simulated according to certification level (EURO 0 to EURO 5). From the beginning of the research it was obvious,

Institutional Repository - Library & Information Centre - University of Thessaly
09/12/2017 02:36:50 EET - 137.108.70.7

that it would be impossible to cover such an extensive number of HDV operation conditions directly with a representative number of experimental emission tests (e.g. by emission tests at a chassis dynamometer). Thus a suitable model had to be elaborated. It was decided to set the model on physical basis according to the longitudinal dynamics of vehicles to allow a reliable simulation of all relevant influences such as driving behavior, road gradients, vehicle loading, etc. and to use engine emission maps as basis for the simulation of fuel consumption and emissions. This structure makes PHEM capable of including all sources of actual and past measurement campaigns to a large extent (Sturm & Hausberger, 2005).

In the meantime the model PHEM was extended to be applicable for passenger cars and for light commercial vehicles (LCVs) too. This task mainly required an extension to be able to obtain the PHEM engine maps not only from steady state engine tests but also from transient driving cycles of the entire vehicle (Hausberger , Rexeis, Zallinger, Luz , & Eichlsede, 2009).

For a proper simulation of the actual engine power all relevant driving resistances occurring in real world cycles have to be taken into consideration. Limit for the details to be covered is mainly the availability of data necessary for the simulation of the forces caused by single parts of a vehicle.

The power demand Fa to overcome the air resistance for LCVs in PHEM is given by the Mathematical expression [50]:

$$Fa = CD \times A_{Frontal} \times p/2 \times v^3 \qquad [50]$$

where,

CD: the air resistance coefficient [dimensionless];

$A_{Frontal}$: the frontal area [m^2] of the vehicle;

ρ: the density of the air [kg/m^3];

v: the wind velocity [m/s].

The CD and $A_{Frontal}$ are given by the tables below according to the engine type (gasoline or diesel), the euro class, the reference mass (N1-I, N1-II, N1-III) and the loading of each vehicle.

Institutional Repository - Library & Information Centre - University of Thessaly
09/12/2017 02:36:50 EET - 137.108.70.7

N1_I	EURO 0	EURO 1	EURO 2	EURO 3	EURO 4	EURO 5	EURO 6
Vehicle mass [kg]	1025	1100	1100	1100	1100	1100	1100
Loading [kg]	275	275	275	275	275	275	275
CD-value	0.35	0.34	0.33	0.32	0.31	0.31	0.30
$A_{Frontal}$[m^2]	2.40	2.40	2.40	2.40	2.40	2.40	2.40
Related Power [kW]	50	50	50	50	60	62	64
N1_II	EURO 0	EURO 1	EURO 2	EURO 3	EURO 4	EURO 5	EURO 6
Vehicle mass [kg]	1500	1500	1500	1500	1500	1500	1500
Loading [kg]	285	285	285	285	285	285	285
CD-value	0.35	0.34	0.33	0.32	0.31	0.31	0.30
$A_{Frontal}$[m^2]	4.00	4.00	4.00	4.00	4.00	4.00	4.00
Related Power [kW]	62	65	65	68	70	72	74
N1_III	EURO 0	EURO 1	EURO 2	EURO 3	EURO 4	EURO 5	EURO 6
Vehicle mass [kg]	2100	2050	2050	2050	2050	2050	2050
Loading [kg]	360	360	360	360	360	360	360
CD-value	0.35	0.34	0.33	0.32	0.31	0.31	0.30
$A_{Frontal}$[m^2]	5.00	5.00	5.00	5.00	5.00	5.00	5.00
Related Power [kW]	68	70	75	79	90	90	90

Table 22: Vehicle data used as input for the model PHEM to simulate emission factors for average diesel LCV (not all parameters listed) (Hausberger , Rexeis, Zallinger, Luz , & Eichlsede, 2009).

Institutional Repository - Library & Information Centre - University of Thessaly
09/12/2017 02:36:50 EET - 137.108.70.7

N1_I	EURO 0	EURO 1	EURO 2	EURO 3	EURO 4	EURO 5	EURO 6
Vehicle mass [kg]	1000	1000	1090	1060	1100	1100	1100
Loading [kg]	228	228	228	228	228	228	228
CD-value	0.35	0.34	0.33	0.32	0.31	0.31	0.30
$A_{Frontal}$[m^2]	1.97	1.97	2.00	2.00	2.00	2.00	2.00
Related Power [kW]	50	50	50	51	55	55	55
N1_II	EURO 0	EURO 1	EURO 2	EURO 3	EURO 4	EURO 5	EURO 6
Vehicle mass [kg]	1400	1475	1400	1310	1300	1300	1225
Loading [kg]	229	229	229	229	229	229	229
CD-value	0.35	0.34	0.33	0.32	0.31	0.31	0.30
$A_{Frontal}$[m^2]	2.25	2.25	2.20	2.10	2.10	2.10	2.10
Related Power [kW]	70	70	70	73	65	65	65
N1_III	EURO 0	EURO 1	EURO 2	EURO 3	EURO 4	EURO 5	EURO 6
Vehicle mass [kg]	1685	1790	1820	1840	1910	1910	1910
Loading [kg]	340	340	340	340	340	340	340
CD-value	0.35	0.34	0.33	0.32	0.31	0.31	0.30
$A_{Frontal}$[m^2]	3.30	3.30	3.30	3.35	3.40	3.40	3.40
Related Power [kW]	85	85	90	95	95	95	95

Table 23: Vehicle data used as input for the model PHEM to simulate emission factors for average gasoline LCV (not all parameters listed) (Hausberger , Rexeis, Zallinger, Luz , & Eichlsede, 2009).

The power for overcoming the air resistance for HDVs is simulated according to (Sturm & Hausberger, 2005) is given using the same mathematical expression ([50]). The values for CD and $A_{frontal}$ are taken from the specifications given by the manufacturer. If no manufacturer specifications for the CD value are available the CD is set according to those of a similar HDV in a data bank of the TUG Institute (see Table below).

Institutional Repository - Library & Information Centre - University of Thessaly
09/12/2017 02:36:50 EET - 137.108.70.7

Vehicle class		Gross vehicle weight rating [tons] / category	$A_{Frontal}$ [m^2]	CD	$CD \times A_{Frontal}$ [m^2]
Rigid truck		Up to 7.5	5.8	0.64	3.71
		7.5 to 12	6.7	0.64	4.31
		12 to 14	6.9	0.64	4.40
		14 to 20	7.4	0.63	4.66
		20 to 26	7.5	0.63	4.76
		26 to 28	7.5	0.64	4.77
		28 to 32	7.9	0.66	5.18
		Larger 32	8.0	0.66	5.25
Truck trailers and articulated trucks		Up to 28	6.9	0.56	3.87
		28 (Switzerland)	7.6	0.56	4.26
		28 to 34	7.7	0.55	4.23
		34 to 40	9.0	0.50	4.50
		40 to 50	9.0	0.52	4.71
		50 to 60	8.1	0.63	5.07
Urban bus	Midi	Up to 50	5.7	0.55	3.14
	Standard	15 to 18	6.5	0.58	3.77
	Articulated	Larger 18	6.5	0.62	4.04
Coach	Standard	Up to 18	7.1	0.45	3.20
	Three axle	Larger 18	7.4	0.45	3.33

Table 24: Average values for DC and $A_{Frontal}$ for the different vehicle categories (EURO 3 vehicles) (Sturm & Hausberger, 2005).

Concerning the air resistance, there were no studies found that examine only this parameter. There are although studies that examine the impact of the air resistance on the behavior of a vehicle in correlation with other parameters but they are going to be presented later in another Chapter where the correlation between these parameters is going to be analyzed in detail and the corresponding bibliography is going to be given.

Institutional Repository - Library & Information Centre - University of Thessaly
09/12/2017 02:36:50 EET - 137.108.70.7

Chapter 4 USE OF A/C - TEMPERATURE

4.1 Introduction

The influence of air-conditioning activity on the emissions and fuel consumption of passenger cars is an important issue, since fleet penetration and use of these systems have reached a high level nowadays. It is a fact that CO_2 emissions and fuel consumption rise with the thermal load. This also causes a notable rise in CO and hydrocarbons (HCs). However, apart from studies involving MOBILE6 in the United States and other U. S. and European studies, air-conditioning activity in relation to meteorological conditions has not been thoroughly investigated. MOBILE6 includes revised estimates of exhaust emissions resulting from air conditioning operation. For the European situation, with its different climatic conditions and different vehicle air-conditioning (A/C) technologies, most available studies are based on simulations, on measurements covering only a small temperature range or older vehicle technologies, or else they deal with particular questions (Weilenmann, Vasic, Stettler, & Novak, 2005).

The air conditioning compressor generally cycles on and off depending on the ambient temperature, humidity, solar load and the length of time that the vehicle has been operating. The greater the temperature and humidity, the more often drivers turn the air conditioning on. The greater the temperature and humidity, the more frequent the compressor needs to operate in order to keep the cabin at a comfortable temperature; the shorter the trip, the more relevant any solar loading of the vehicle. Therefore it is important to keep the interior climate of the vehicle stable at the desired comfort temperature (EPA, 2006).

In central Europe, typical summer temperatures range from 15 to 35℃, humidity varies in a narrower range than in the United States, usually being between 50% and 80% relative humidity, and even at hot temperatures the percentage of time with clouds, and therefore no direct solar radiation, has to be considered. Technically, the European car fleet consists of smaller cars with smaller engines, smaller passenger compartments, and thus smaller A/C devices than the U. S. fleet. A high percentage of the A/C systems are automatic or semiautomatic; i.e., the driver only has to set the desired temperature or has to set both the desired temperature and the fan speed. In addition, more and more vehicles are equipped with A/C systems that modulate the stroke of their compressor or have other modulation capabilities. It is therefore not possible to relate compressor activity data from real-world studies to chassis dynamometer tests where the A/C systems are off or at full load (Weilenmann, Vasic, Stettler, & Novak, 2005).

Institutional Repository - Library & Information Centre - University of Thessaly
09/12/2017 02:36:50 EET - 137.108.70.7

Although, according to (Hugrel & Joumard, September 17-19, 2001), the development of air-conditioning has a very limited effect on CO_2 emissions at the passenger car fleet scale. At fleet level the difference between passenger cars equipped with air conditioning and passenger cars without air-conditioning is not such as at vehicle level (Figure 31).

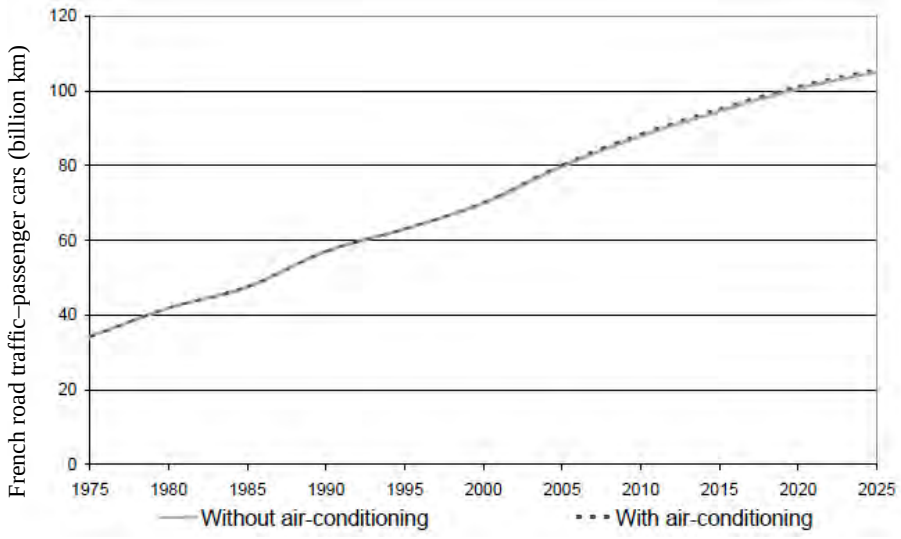

Figure 31: Influence of air-conditioning on passenger car CO_2 emissions (10^6 t) (Hugrel & Joumard, September 17-19, 2001).

Temperature and humidity are the most important drivers of A/C system demand. While temperature is a widely recognized influence, the load placed on the air conditioning system by humidity can account for over half of the total load under the ambient conditions. It is considered important, therefore, to develop a demand factor methodology which incorporates both temperature and humidity. Figure 32 shows relative humidity at the start of each trip as a function of temperature.

Institutional Repository - Library & Information Centre - University of Thessaly
09/12/2017 02:36:50 EET - 137.108.70.7

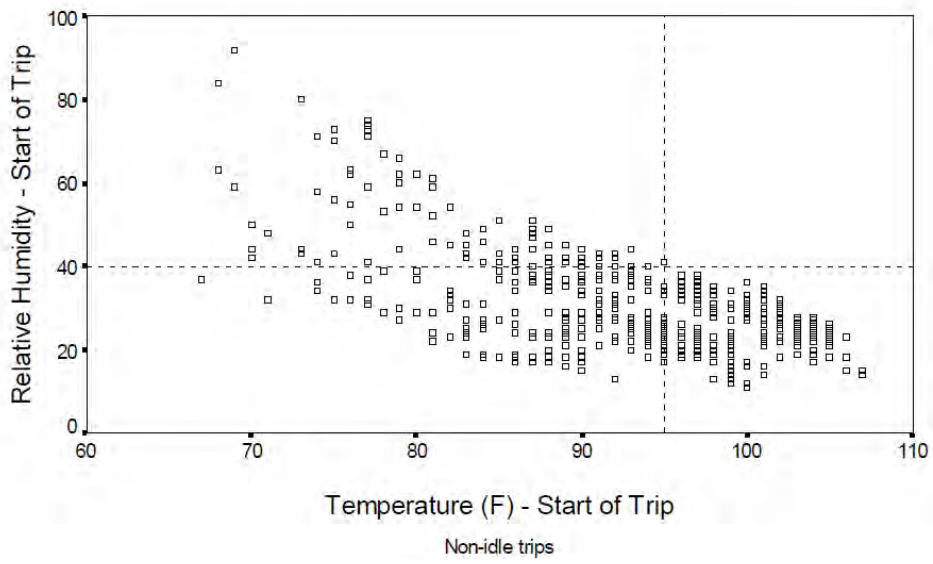

Figure 32: Humidity vs. Temperature for Phoenix Dataset (Koupal J. , 2001).

The emission data used in the development of the MOBILE6 air conditioning factors were gathered using a test procedure intended to represent extreme ambient conditions. From these data, emission factors were developed which represented emission levels at full air conditioning load (referred to as "full-usage" emission factors). These emission factors cannot appropriately be applied to all ambient conditions, since less severe conditions will result in only partial A/C loading and hence lower emissions. A method for modeling air conditioning effects under intermediate ambient conditions was required. This method was generally not inducing full load on the engine 100% of the time the A/C is turned on under intermediate ambient conditions. An ideal model of this sort would link ambient conditions and emissions by modeling changes in compressor load (torque) as a function of changes in ambient conditions. MOBILE6 includes revised estimates of exhaust emissions resulting from air conditioning operation. This requires air conditioning behavior and the resulting emission levels to be predicted over a wide range of ambient conditions.

Using air conditioning activity data collected in Phoenix, a methodology was developed which related temperature and humidity levels to air conditioner load using a combined measure known as the heat index. This methodology also incorporated some solar load impact and allowed adjustments for cloud cover if desired by the user. In MOBILE6 approach a compressor which is engaged 100% of the time would result in the full-usage emission factor. If the compressor is engaged only 50% of the time, 50% of the full-usage emission factor would be applied. This scaling factor is termed by MOBILE6 the "demand factor" (Koupal J. , 2001). All the studies that have been made were based on full use of A/C so it is necessary to use this demand function in order to multiply the experimental data with a correction factor which is going to be the heat demand.

Institutional Repository - Library & Information Centre - University of Thessaly
09/12/2017 02:36:50 EET - 137.108.70.7

The key to this approach is the assumption that the relative emission impact due to A/C correlates 1:1 with compressor-on fraction for all pollutants. It should be noted that air conditioning system experts from the automotive industry have identified several limitations with this assumption. Specifically, compressor load fluctuates significantly when the compressor is engaged, depending on a number of factors including ambient conditions, vehicle speed, vehicle cabin temperature, and A/C system setting (e.g. fan setting, recirculation vs. outside air); A/C system response to changes in all of these factors is highly vehicle-specific. Using only compressor-on fraction is a rough estimate of actual compressor load since it assumes that fluctuations in relative compressor load average out over periods when the compressor is engaged. Further, the impact of compressor load on emissions is likely not linear. However, the complexity and data demands of a compressor-load based model are prohibitive within the timeframe and scope of MOBILE6. Future research activity will need to address this lack of information.

To assess the effect of ambient variables (temperature, humidity, heat index) on air conditioning demand, the Phoenix dataset was analyzed by "binning" trips according to the variable being analyzed. For example in (Koupal J. , 2001), for temperature, all trips at a given temperature were combined, and the compressor-on fraction was calculated at each temperature as total time with the compressor engaged at that temperature divided by total trip time at that temperature. This aggregation step was taken to reduce the variability from individual vehicle and driver behavior, since the operation of air conditioning over the "composite" fleet and population is of more concern for MOBILE6. In an attempt to more accurately assess the relative impacts of temperature and humidity on air conditioning load, a metric known as the heat index was used in developing the demand factors. Heat index is used by the National Weather Service to quantify discomfort caused by the combined effects of temperature and relative humidity. The basis of the index is the human body's ability to maintain thermal equilibrium through perspiration, taking into account numerous factors including clothing thickness, atmospheric pressure and ambient conditions. Mathematical expressions have been developed which allow heat index to be calculated using only temperature and relative humidity; these expressions s are proposed for use in MOBILE6 to compute heat index based on temperature and humidity values input by the user. An attractive feature of this approach is that the air conditioning activity component of MOBILE6 would be based directly on driver discomfort, the most likely factor impelling a driver's A/C behavior and thus a strong determinant in the vehicle's emission response. As shown in Figure 33, the Phoenix data exhibits a strong correlation between compressor-on fraction and heat index.

Institutional Repository - Library & Information Centre - University of Thessaly
09/12/2017 02:36:50 EET - 137.108.70.7

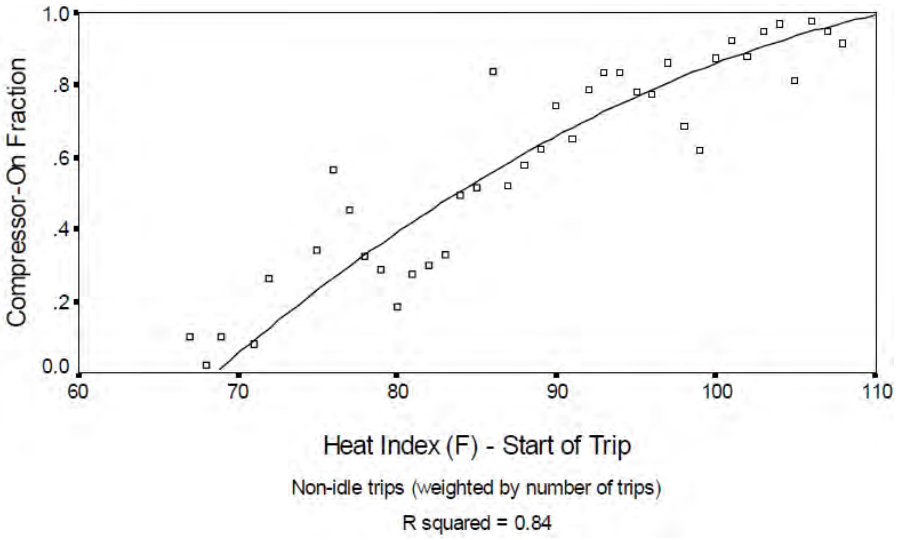

Figure 33: Compressor-On vs. Heat Index (Koupal J. , 2001).

In MOBILE6 approach using heat index or temperature provides the same result for low humidity conditions. The intent of using the heat index is to introduce a more equitable balance in the effect of temperature and humidity on air conditioning load. The underlying assumption of this methodology is that the temperature-driven effects seen at high temperatures are replicated under lower temperature but higher humidity conditions. Given the stated importance of humidity on air conditioning load, this assumption is believed to be more reasonable than ignoring or understating the impact of humidity altogether. Many proposals for air conditioning effects did not include any accounting for solar load. MOBILE 6 is the first approach which indicates that a solar load impact can be discerned, and consequently a method which accounts for solar load and cloud cover should be used. Four "period" bins were created: night (sunset-sunrise), morning (sunrise - 10 am), peak sun (10 am - 4 pm), and afternoon (4 pm - sunset). A regression across all trips of compressor-on fraction by heat index was performed within each bin, with the results shown in

Figure 34.

Institutional Repository - Library & Information Centre - University of Thessaly
09/12/2017 02:36:50 EET - 137.108.70.7

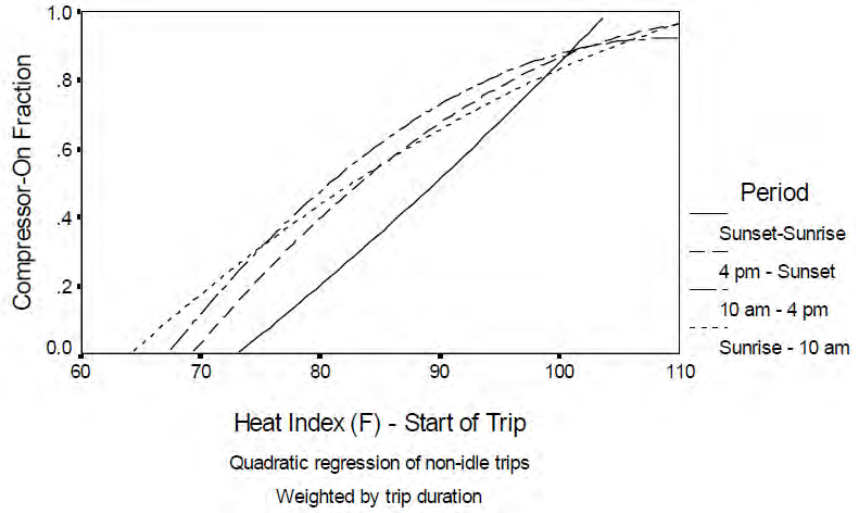

Figure 34: Compressor-On vs. Heat Index by Time of Day (Koupal J. , 2001).

Three demand factor mathematical expressions were developed for MOBILE6: night time, morning/afternoon and peak sun. The "raw" mathematical expression for each period, as well as for all daytime trips and all trips, are shown in Table 25.

Period	Constant	a	b	R^2
Morning/Afternoon	-2.930273	0.059110	-0.000213	0.54
Peak Sun	-5.307355	0.113973	-0.000521	0.17
Daytime Combined	-4.101082	0.086382	-0.000367	0.43
Night	-1.257412	0.006753	0.000143	0.52
All Combined	-3.631541	0.072465	-0.000276	0.44

Table 25: Proposed "Raw" Demand Factor mathematical expressions (Demand Factor = Constant + a*(Heat Index) + b*(Heat Index)2) (Koupal J. , 2001).

These mathematical expressions were developed by fitting a quadratic mathematical expression through all trips by period, weighting by trip length. This was because it was favored over more complex forms because it provides a balance between goodness of fit and more reasonable behavior at the high and low ends of the heat index range. Still, because a smaller sample of trips occurred at the high and low ends (only 5% of trips occurred when the heat index was less than 75^{o}) the behavior of the fitted curves at these ends tends to defy engineering judgment. In particular the morning/afternoon curve is higher than the peak curve below 75^{o}, and the night curve is higher than the daytime curves above 100^{o}. To rectify this, separate demand mathematical expressions are applied only in the middle of the heat index range, while the higher and lower ends are modeled with composite mathematical expressions. The "daytime combined" is used for all daytime periods at the lower end, and all

Institutional Repository - Library & Information Centre - University of Thessaly
09/12/2017 02:36:50 EET - 137.108.70.7

individual curves are modeled with the "all combined" mathematical expression at the high end. The heat index values at which the composite mathematical expressions and period-specific expressions diverge (at the low end) or converge (at the high end) are determined based on the respective points of intersection. This progression is outlined in Table 26, with the revised equation forms for each period shown in Figure 34.

Heat Index	Morning/Afternoon	Peak Sun	Night
65 & below	Constant=0	Constant=0	Constant=0
66	Daytime	Daytime	Constant=0
74	Morning/Afternoon	Daytime	Night
76	Morning/Afternoon	Peak Sun	Night
96	All	Peak Sun	Night
101	All	Peak Sun	All
104	All	All	All
110 % above	Constant=1	Constant=1	Constant=1

Table 26: Proposed Demand Factor Equation Forms (Koupal J. , 2001).

Since MOBILE6 calculates emission factors on an hourly basis, changes in solar load throughout the course of a full day are modeled by applying the appropriate demand mathematical expressions at each hour. The night mathematical expression is applied from sunrise to sunset, the morning/afternoon mathematical expression applies from sunrise - 10 am and 4 pm - sunset, and the peak mathematical expression applies from 10 am - 4 pm. The peak sun cutpoints were determined based on analysis of the NOAA data on different days throughout the summer months, which indicated that direct solar radiation levels stay relatively high from 10 am to 4 pm but tend to drop off rapidly before 10 am and after 4 pm. However, the user is allowed to input alternate time for which peak sun demand mathematical expressions are applied if desired. Default sunrise/sunset times of 6 am and 9 pm are used in MOBILE6 to approximate a typical summer day with daylight savings time. The user also has the option of inputting alternative sunrise/sunset times in order to alter the hours for which the morning/afternoon and nighttime demand mathematical expressions are applied.

Institutional Repository - Library & Information Centre - University of Thessaly
09/12/2017 02:36:50 EET - 137.108.70.7

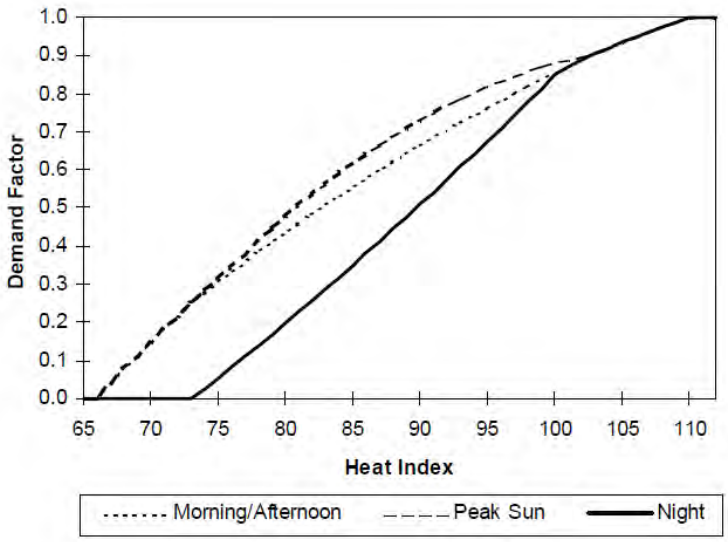

Figure 35: Proposed Demand Factor Functions (Koupal J. , 2001).

MOBILE6 incorporates an optional input for percent cloud cover on a daily basis. The method for handling cloud cover input is to scale back the default daytime demand mathematical expressions. Analysis of National Oceanic and Atmospheric Administration of USA (NOAA) solar radiation data indicates that direct solar radiation is reduced to zero when the sun is obstructed by clouds (Figure 36). Based on these data, the nighttime demand mathematical expression is proposed to represent 100% cloud cover. For intermediate cloud cover inputs, the model interpolates between the appropriate daytime demand mathematical expression and the nighttime demand mathematical expression. Thus, 50% cloud cover at noontime results in a demand factor halfway between the demand calculated with the peak and nighttime mathematical expressions at the appropriate heat index (Koupal J. , 2001).

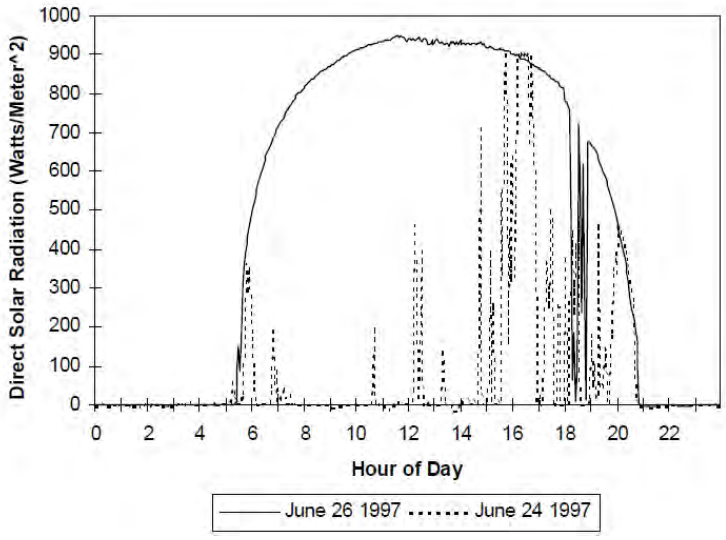

Figure 36: Solar Radiation - Sunny and Cloudy Day (Fort Peck, MT) (Koupal J. , 2001).

Institutional Repository - Library & Information Centre - University of Thessaly
09/12/2017 02:36:50 EET - 137.108.70.7

In order to define the heat index, the NOAA's Heat Index Values approach can be used (Figure 37). The Heat Index, sometimes referred to as the apparent temperature could be given in degrees Fahrenheit. The Heat Index is a measure of how hot it really feels when relative humidity is factored with the actual air temperature. To find the Heat Index temperature, the following table can be used.

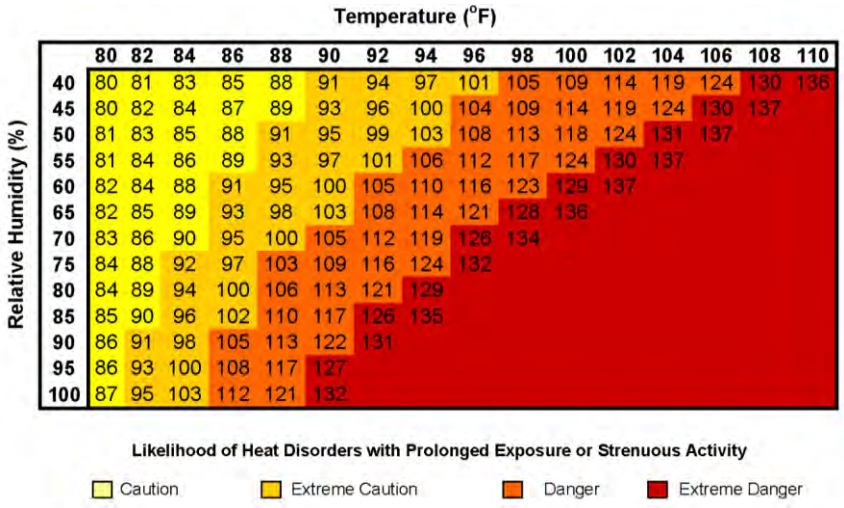

Figure 37: NOAA's National Weather Serrvice – Heat Index (NOAA website).

As an example, if the air temperature is 96°F and the relative humidity is 65%, the heat index--how hot it feels--is 121°F. The Weather Service will initiate alert procedures when the Heat Index is expected to exceed 105°-110°F (depending on local climate) for at least 2 consecutive days.

The use of A/C plays a significant role on the fuel consumption and emission rates of a vehicle. It is important, therefore, to study different cases and come to conclusions that will help limiting its impact in a reasonable level. The studies presented below show more details about this impact. Through the experimental data and the mathematical expressions provided, some general results can be exported.

As for the previous parameters, a review of studies about the impact of the A/C use on the fuel consumption, the power consumption and the emissions of a vehicle is going to be presented, in chronological order,. The number of studies presented, though, is more limited than the other parameters presented above. In contrast with the previous parameters studied, all the papers below, concerning the use of A/C, examine only cases of light duty vehicles (passenger cars and light trucks). No studies for HDVs were found.

For these studies found, we gave all the information concerning the case developed in each study: (1) The type of road examined: urban or highway, (2) the consequences due to the use of A/C, that can refer to (a) the Power Consumption , (b) the Fuel Consumption (FC) of the

Institutional Repository - Library & Information Centre - University of Thessaly
09/12/2017 02:36:50 EET - 137.108.70.7

vehicle, (c) the produced Emissions, (3) The way that we come to the conclusion of which consequences of the three above exist, if for example there are mathematical expressions that proved that there is an impact on these due to the use of A/C or there were experiments carried out that gave results. The figure below describes schematically our review.

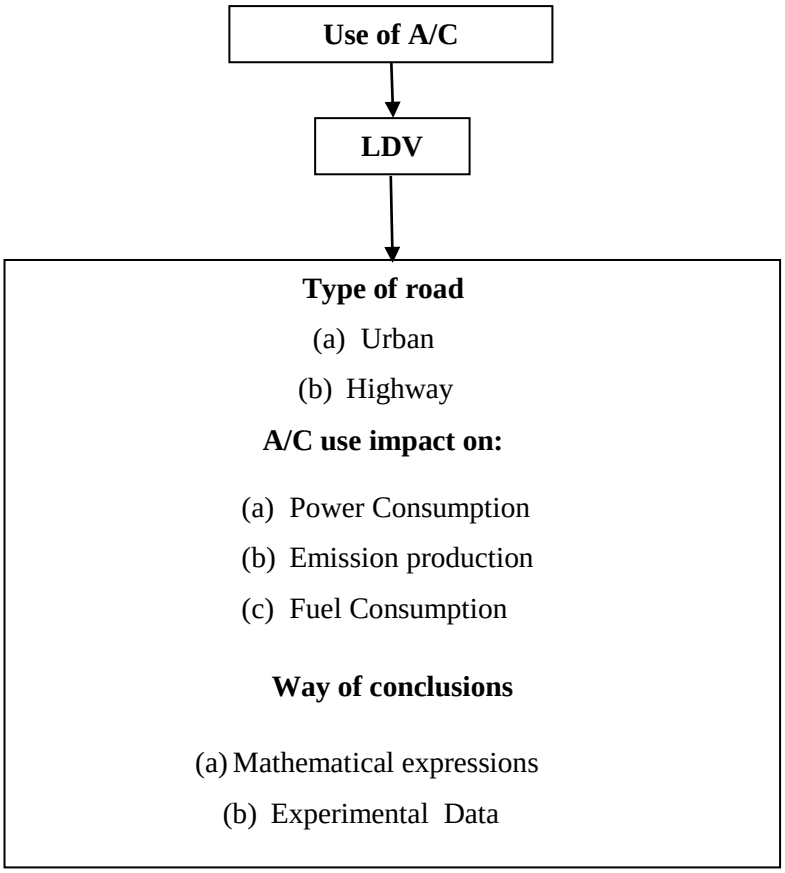

Figure 38: Diagram of our review – categorization of studies.

4.2 Review of A/C Use - Temperature

In 2001 revised air conditioning exhaust emission correction factors were calculated, based on testing of 38 vehicles at two locations, using a test procedure meant to simulate air conditioning emission response under extreme "real world" ambient conditions (Koupal & Kremer, 2001). These factors are meant to predict emissions which would occur during full loading of the air conditioning system. In general, running emissions were found to increase during air conditioning operation, but under some conditions HC and CO emissions decreased. The sample of vehicles tested included LDV cars and trucks and simulations took part in highway-road conditions. Emission results for the four cycles tested at all three locations are shown in Table 27.

Institutional Repository - Library & Information Centre - University of Thessaly
09/12/2017 02:36:50 EET - 137.108.70.7

The data used for this analysis was generated through testing performed at EPA's National Vehicle and Fuel Emissions Laboratory and through an EPA contractor, Automotive Testing Laboratories (ATL), in East Liberty, Ohio. A correlation vehicle was run over all test cycles using the simulation procedure at EPA and ATL, and on a subset of cycles under the SFTP test conditions (Supplemental Federal Test Procedure) at GM's environmental chamber in Rochester, New York.

Besides the experimental results, there were also some mathematical expressions provided for each pollutant. The results presented in the study concerned the fuel consumption and the emissions of the vehicle. There is no reference to the power consumption of the vehicle.

NMHC pollutant:

$$A/C\ Effect = 0.001162 \times v\ ;\ R^2 = 0.44 \quad [51]$$

CO pollutant:

$$Light\ Duty\ Vehicle\ \ A/C\ Effect = 0.815 \times (A/C\ \ base) + 0.05272 \times v;\ R^2 = 0.255 \quad [52]$$

$$Light\ Duty\ Truck\ \ A/C\ Effect = 0.104 \times v\ ;\ R^2 = 0.059 \quad [53]$$

NOx pollutant:

$$A/C\ Effect = \Big(4.867 \times Log(NOx\ base + 1) - 2.296 \times \big(Log(\bar{v})\big) \times Log(NOx\ base + 1)\Big);\ R^2 = 0.612 \quad [54]$$

where

v: speed of the vehicle [m/s];

$\bar{v}$: average speed of the vehicle [m/s].

Institutional Repository - Library & Information Centre - University of Thessaly
09/12/2017 02:36:50 EET - 137.108.70.7

		NMHC		CO		NOx		Fuel Consumption	
		Off	On	Off	On	Off	On	Off	On
NYCC	ATL	0.07	0.67	1.36	4.34	0.03	0.33	214.1	281.6
	EPA	0.07	0.07	0.98	3.32	0.11	0.25	208.6	275.4
	GM	0.06	0.07	0.60	7.71	0.11	0.28	217.8	283.5
	Average	0.066	0.27	0.98	5.123	0.083	0.287	213.5	280.16
LA92	ATL	0.04	0.10	0.39	7.92	0.38	0.21	115.3	138.7
	EPA	0.02	0.02	0.15	0.53	0.38	1.51	110.1	133.0
	GM	0.04	0.03	0.54	1.83	0.67	1.04	216.8	267.2
	Average	0.033	0.05	0.36	3.426	0.476	0.92	147.4	179.63
FWHS	ATL	0.08	1.32	2.82	100.04	0.25	0.03	88.2	120.7
	EPA	0.05	1.33	4.63	112.24	0.22	0.00	82.7	120.0
	GM	0.02	0.03	0.82	241	0.30	0.62	82.0	85.9
	Average	0.05	0.893	2.756	151.1	0.256	0.216	84.3	108.87
ARTC	ATL	0.04	0.04	1.70	1.41	0.11	0.16	120.0	145.3
	EPA	0.03	0.05	1.41	3.00	0.13	0.28	116.7	144.4
	GM	0.01	0.03	0.33	2.99	0.19	0.37	120.2	144.5
	Average	0.027	0.04	1.146	2.47	0.143	0.27	119	144.7

Table 27: Correlation vehicle emission results (g/mi). where NYCC: New York City Cycle road, LA92: California "Unified" Cycle road, FWHS: Freeway High Speed road and ARTC: Arterial LOS C-D road. The average of all the results for each case are calculated (Koupal & Kremer, 2001).

		Compressor Fraction	Average High Pressure $[lb/in^2]$	Average Low Pressure $[lb/in^2]$
NYCC	ATL	1.00	311.5	49.7
	EPA	0.99	306.4	58.1
	GM	0.97	320.9	44.5
LA92	ATL	0.99	334.2	48.2
	EPA	0.97	339.4	48.2
	GM	0.99	312.1	40.3
FWHS	ATL	1.00	361.1	43.7
	EPA	0.99	367.3	50.3
	GM	1.02	264.8	34.3
ARTC	ATL	1.00	310.7	46.4
	EPA	0.98	315.3	54.7
	GM	0.99	310.8	39.0

Table 28: Correlation Vehicle Compressor Behavior (Koupal & Kremer, 2001).

Table 28 contains compressor behavior data, expressed in terms of the compressor fraction (the fraction of time the compressor in engaged during the test), and average high and low side compressor pressures, on which compressor torque in based. The data indicate that a) the compressor was engaged at all locations 97% or more of the time on each of the cycles, and

Institutional Repository - Library & Information Centre - University of Thessaly
09/12/2017 02:36:50 EET - 137.108.70.7

b) for the New York City, Unified and Arterial cycles a strong difference is not observed in the compressor pressures. The exception again is the High Speed Freeway cycle, for which the GM data shows significantly lower compressor pressures than ATL or EPA. From these data and the fuel consumption results, it is apparent that the A/C system load on the high speed freeway cycle in the full environmental cell was much less than that produced by the simulation at EPA or ATL. The most plausible explanation for this is the use of a variable speed fan in the full environmental cell, which would create a much higher airflow than produced by the standard one-speed fan used on the simulation. Higher air flow across the vehicle's A/C system can increase system efficiency, reducing relative load demand on the engine.

In 2005 a study about the influence of air-conditioning activity on the emissions and fuel consumption of passenger cars was published (Weilenmann, Vasic, Stettler, & Novak, 2005). Since weather conditions and A/C technologies both differ from those in the U. S., a test series was designed for the European setting. A fleet of six modern gasoline passenger cars was tested in different weather conditions. Separate test series were carried out for the initial cool down and for the stationary situation of keeping the interior of the vehicle cool. As assumed, CO_2 emissions and fuel consumption rise with the thermal load. This also causes a notable rise in CO and hydrocarbons (HCs). Moreover, A/Cs do not stop automatically at low ambient temperatures; if necessary, they produce dry air to demist the windscreen. A model was proposed that shows a constant load for lower temperatures and a linear trend for higher temperatures.

The test cycle used was CADC, which originates from the ARTEMIS project under the EU Fifth Framework Program and represents real-world driving in Europe. The study consisted of three phases that describe urban, rural, and highway situations; the exhaust gas of each phase was measured separately and there are results and conclusions concerning the fuel consumption, the power and the emissions of the vehicles. All measurements were performed at a relative humidity of 50%. Besides the experimental data, there were also mathematical expressions provided. This test was repeated with each car at ambient temperatures of 13, 23, 30, and 37 °C. The lowest temperature was intentionally chosen to obtain information on the situation where the A/C is not needed to cool the passenger compartment but just to create dry air in the event of windscreen misting. At each temperature, one reference test was run with A/C off, one with A/C on and no solar radiation (shade), and one with A/C on and solar radiation on (sun). In Figure 39, we see on Y axis the increase(%) in CO_2 emissions with the

Institutional Repository - Library & Information Centre - University of Thessaly
09/12/2017 02:36:50 EET - 137.108.70.7

use of A/C and on the X axis the temperature. The red cross is "sun" and the green rhombus "shade".

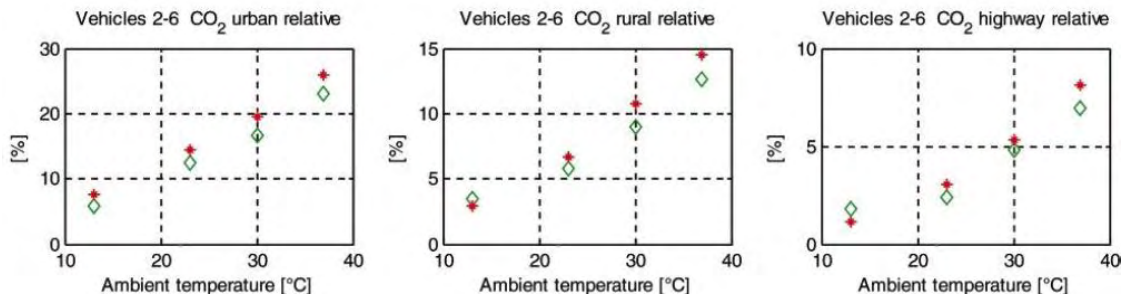

Figure 39: Average CO2 emissions of vehicles 2-6 in CADC at different temperatures and in different irradiation scenarios for different A/C settings (Weilenmann, Vasic, Stettler, & Novak, 2005).

Also, the power demand due to the use of A/C is shown in Figure 40.

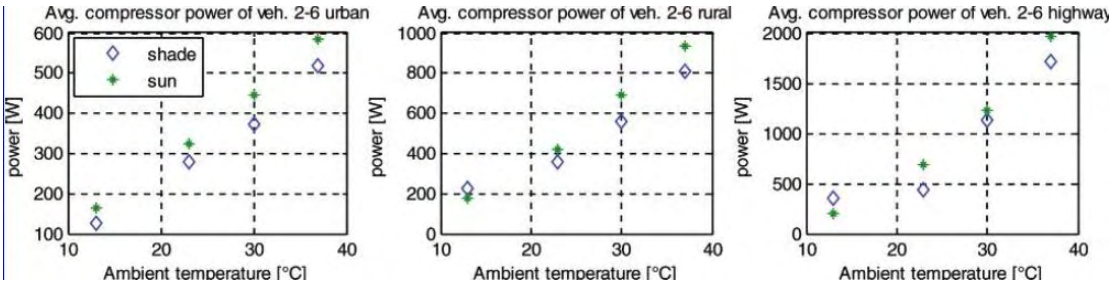

Figure 40: Stationary keep-cool test of the passenger compartment, average of estimated mechanical compressor power for A/C activity (Weilenmann, Vasic, Stettler, & Novak, 2005).

CO, NOx and HC emissions due to A/C use are shown in the figures below.

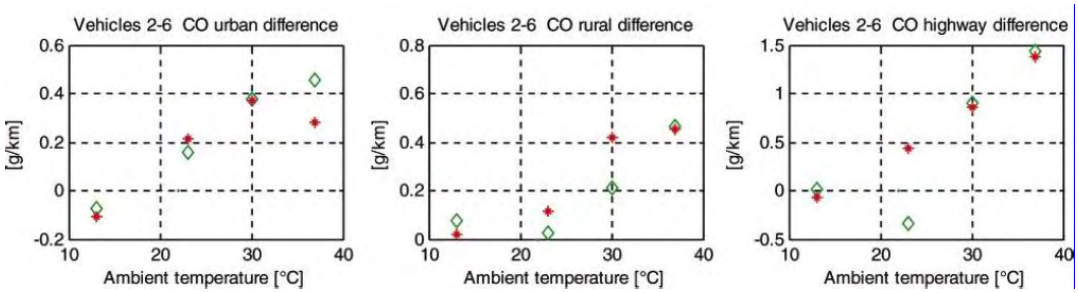

Figure 41: Average CO emissions of vehicles 2-6 in CADC at different temperatures and in different irradiation scenarios for different A/C settings (Weilenmann, Vasic, Stettler, & Novak, 2005).

Institutional Repository - Library & Information Centre - University of Thessaly
09/12/2017 02:36:50 EET - 137.108.70.7

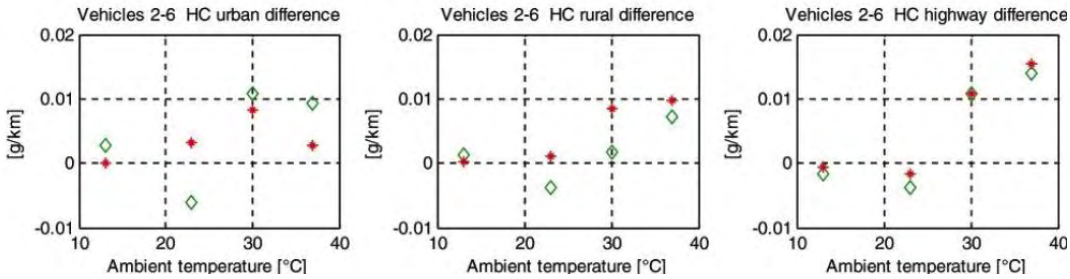

Figure 42: Average HC emissions of vehicles 2-6 in CADC at different temperatures and in different irradiation scenarios for different A/C settings (Weilenmann, Vasic, Stettler, & Novak, 2005).

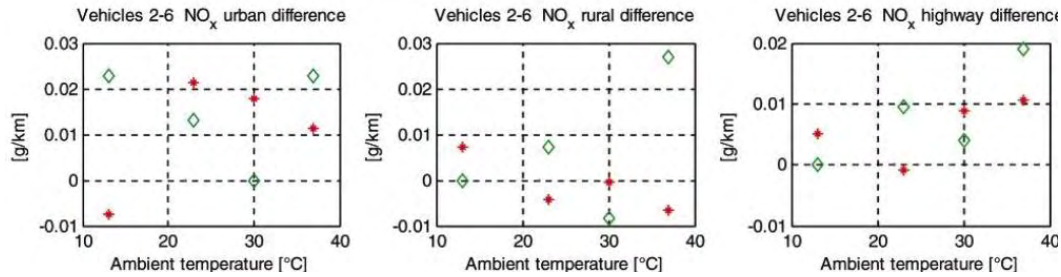

Figure 43: Average NOx emissions of vehicles 2-6 in CADC at different temperatures and in different irradiation scenarios for different A/C settings (Weilenmann, Vasic, Stettler, & Novak, 2005).

It should be noted that for the following simplified discussion, fuel consumption (FC) and CO_2 emission are considered to be proportional since CO and HC emissions are quite low (0.3148 g fuel ↔ g CO_2), and CO_2 and FC are treated as synonymous in relative comparisons. The fuel consumption is correctly calculated as:

$$m_{FC} = 13.85 \times \left(\frac{m_{CO_2}}{44} + \frac{m_{CO}}{28} + \frac{m_{HC}}{13.85}\right) \quad [55]$$

Institutional Repository - Library & Information Centre - University of Thessaly
09/12/2017 02:36:50 EET - 137.108.70.7

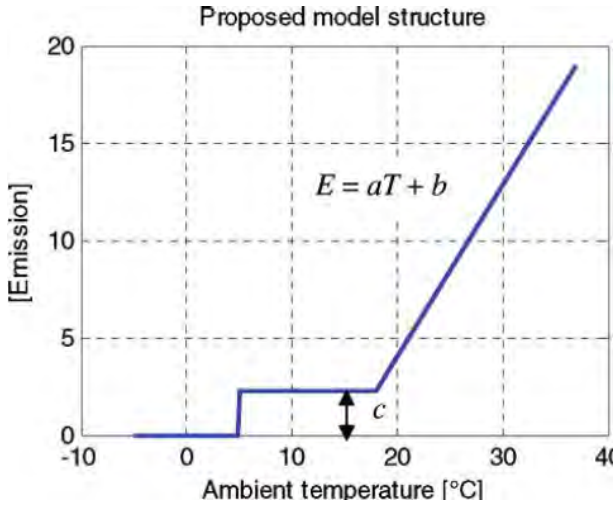

Figure 44: Suggested model structure for the extra emission due to the A/C activity for the keep-cool case (Weilenmann, Vasic, Stettler, & Novak, 2005).

A model with the basic shape shown in Figure 50 is proposed. It consists of no A/C activity for temperatures below 5 °C and a constant A/C load (thus CO_2 and FC) for temperatures above 5 °C for demisting. Its value is given by the tests at 13 °C. The above model is to be applied individually to both sunny and shady scenarios and to urban, rural, and highway driving situations. The question arises as to whether it is to be applied to the absolute difference in emissions in g/km or to the relative emissions in percentages. For CO_2 and FC it could be argued that it is meaningful to use the relative emissions since cars with larger engines usually also have larger passenger compartments and thus need more cooling power than small vehicles. However, the relative standard deviations of the absolute and relative extra emissions are comparable and do not show either approach to be superior. For the pollutant emissions (CO, HC, and NO_x) no purpose is served by considering the relative emissions for the model since the basic values are quite low and thus uncertain. On this basis, it is proposed that the model be applied to the absolute extra emissions in g/km.

For CO_2 and fuel consumption (FC) the average parameters c and the parameters a and b derived by least-squares regressions are given in Table 29. The intersection of the two straight lines is not fixed; it is defined as:

- If $T > 5$℃, then (if $c > aT + b$, then emission) c, else emission) $aT + b$)
- If $T < 5$ ℃ extra emission = 0.

Institutional Repository - Library & Information Centre - University of Thessaly
09/12/2017 02:36:50 EET - 137.108.70.7

CO_2		shade			sun		
parameter	**unit**	**urban**	**rural**	**highway**	**urban**	**rural**	**highway**
a	$g/(km/℃)$	2.4422	0.8522	0.6842	2.6889	0.9863	0.7778
b	g/km	-18.7718	-9.9298	-10.9286	-17.1977	-11.2158	-12.1216
c	g/km	18.4666	6.2840	3.6224	23.7000	5.0084	2.1753
FC		shade			sun		
parameter	**unit**	**urban**	**rural**	**highway**	**urban**	**rural**	**highway**
a	$g/(km/℃)$	0.7804	0.2847	0.2793	0.8488	0.3231	0.2790
b	g/km	-6.0888	-3.5017	-5.0211	-5.3366	-3.7406	-4.3917
c	g/km	5.7801	2.0163	1.1428	7.4062	1.5853	0.6512

Table 29: Parameters for Proposed CO2 and Fuel Consumption (FC) Model (Weilenmann, Vasic, Stettler, & Novak, 2005).

In 2006, a study made changes to EPA's fuel economy test methods to bring the fuel economy estimates closer to the fuel economy consumers are achieving in the real-world (EPA, 2006). The analysis concerned passenger cars and light duty trucks and was focused both on urban and highway roads. Additional tests were made and parameters like the driving cycle effects, trip length, air conditioner compressor-on usage, and operation over various temperatures were weighted according to how much they occur over average real-world city or highway driving. There were experiments carried out but also some mathematical expressions given throughout the study. There were results concerning the fuel consumption and the emissions of the vehicle but not the power requirements.

The new test methods brought into the fuel economy estimates the test results from the five emissions tests in place today: FTP, HFET, US06, SC03, and Cold FTP. The US06 test is designed to represent high speed highway driving and aggressive (i.e., rapid accelerations and decelerations) urban driving. The SC03 test is designed to represent the impact of air conditioner operation at high temperatures. The Cold FTP, which is conducted at 20°F, is designed to reflect the impact of cold temperatures. The FTP test consists of three distinct measurements, called bags because the emissions produced during each portion of the test are literally collected in separate plastic "bags". Bags 1 and 3 consist of the exact same driving pattern, while Bag 2 consists of a different pattern.

The performance of emission controls while the air conditioning system is operating was assessed via the SC03 test. The SC03 test begins with a hot start (i.e., the engine has been turned off for 10 minutes after having been fully warmed up prior to engine shutdown). The test cell was at 95°F and 40% relative humidity, with a solar load of 850 Watts per square

Institutional Repository - Library & Information Centre - University of Thessaly
09/12/2017 02:36:50 EET - 137.108.70.7

meter on the vehicle. The vehicle was also pre-heated at this solar load for 10 minutes prior to the test, so the air conditioning compressor was generally engaged throughout the entire test. The driving pattern of the SC03 test was designed to represent driving performed immediately after vehicle start-up, so it was a relatively low speed cycle. The driving pattern contained in the SC03 test is similar to that of the cold FTP (Federal Test Procedure), but not identical.

The impact of air conditioning operation on fuel economy based on the difference in fuel use was estimated over the SC03 and Bags 2 and 3 of the FTP.

It was proposed to estimate the incremental fuel use due to the operation of the air conditioner at 95°F and 40% relative humidity at an average speed of 21.5 mph as the difference in fuel consumption measured over the SC03 versus this combination of fuel consumption over Bags 2 and 3 of the standard FTP. The following expression depicts this mathematically:

$$Excess\ fuel\ use\ due\ to\ air\ conditioning\ at\ 95°F = \left[\frac{1}{Fuel\ economy\ over\ the\ SC03test} - \frac{1}{\left(\frac{0.39}{(FueleconomyoverBag2)}\right) + \left(\frac{0.39}{(FueleconomyoverBag3)}\right)}\right] \quad [56]$$

The next factor to address is that of compressor operation. The length of the SC03 test is 10 minutes. Since the vehicle has been sitting at 95°F for some time and has been under a solar load of 850 Watts per square meter for 10 minutes, the air conditioning compressor is usually engaged throughout the test. Here it is assumed that the air conditioning compressor is engaged during 100% of the SC03 test. However, this estimate could be too high. The air conditioning compressor generally cycles on and off depending on the ambient temperature, humidity, solar load and the length of time that the vehicle has been operating. The greater the temperature and humidity, the more often drivers

The Draft MOVES2004 model, which includes estimates of ambient temperature by hour of the day for each month of the year for each county in the U.S., contains an algorithm which estimates the percentage of time which the compressor is engaged as a function of heat index. Heat index is a complex combination of ambient temperature and humidity which was developed to predict degrees of personal comfort. Heat index is used by the National Weather Service to quantify discomfort caused by the combined effects of temperature and relative humidity. Figure 45 is reproduced from the MOBILE6 report and shows how heat index varies with both temperature and humidity.

Institutional Repository - Library & Information Centre - University of Thessaly
09/12/2017 02:36:50 EET - 137.108.70.7

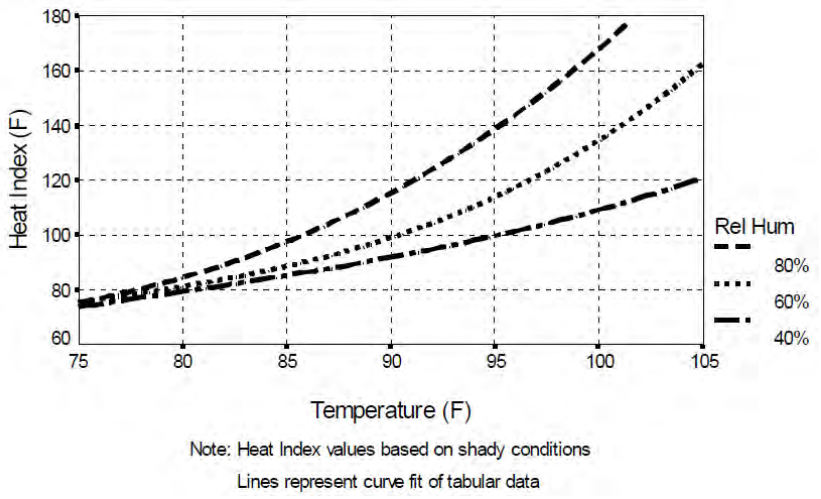

Figure 45: Heat Index vs. Temperature and Humidity (EPA, 2006).

The Draft MOVES2004 algorithm of compressor on fraction versus heat index was developed from the direct measurement of air conditioning operation of over 1000 trips by 20 vehicles in Phoenix, Arizona during the summer and fall of 1992. The algorithm considers both the frequency that the system is turned on by the driver and the frequency that the compressor is engaged once the system is turned on. The algorithm is of the form:

$$A/C\ compressor\ on\ fraction = A + B \times HeatIndex + C \times HeatIndex^2 \quad [57]$$

The above coefficients vary depending on time of day, basically causing the predicted compressor use to increase when the sun rises higher in the sky for a given level of heat index. The coefficients are shown in Table 30.

Heat Index	**7-10 am, 5-9 pm**			**11 am – 4 pm**			**10 pm – 6 am**		
	A	**B**	**C**	**A**	**B**	**C**	**A**	**B**	**C**
≤ 65	0	0	0	0	0	0	0	0	0
65-74	-4.101	0.0864	-0.00367	-4.101	0.0864	-0.00037	0.000	0.0000	0.000000
74-76	-2.930	0.0591	-0.000213	-4.101	0.0864	-0.00037	-1.257	0.0068	0.000143
76-96	-2.930	0.0591	-0.000213	-5.307	0.1140	-0.00052	-1.257	0.0068	0.000143
96-101	-3.632	0.0725	-0.000276	-5.307	0.1140	-0.00052	-1.257	0.0068	0.000143
101-104	-3.632	0.0725	-0.000276	-5.307	0.1140	-0.00052	-3.632	0.00725	-0.000276
104-110	-3.632	0.0725	-0.000276	-3.632	0.0725	-0.00028	-3.632	0.00725	-0.000276
>110	A/C compressor is engaged 100% of the time								

Table 30: Coefficients for A/C Compressor Usage mathematical expressions (EPA, 2006).

Since emissions and fuel economy are affected by the operation of the air conditioning compressor and not simply whether the switch is turned on or off, the MOBILE6 analysis did not develop analogous correlations for drivers turning their air conditioning systems on as a function of heat index. However, whether the switch was turned on or off was recorded during the test program. In order to provide a point of comparison with other studies, which

Institutional Repository - Library & Information Centre - University of Thessaly
09/12/2017 02:36:50 EET - 137.108.70.7

have focused on the frequency that the switch is turned on, this parameter was estimated, as well. Using the data collected during the 1992 study in Phoenix (U.S. Environmental Protection Agency, 1994), a regression of the average percentage of time during each trip that the A/C system was turned on against the ambient temperature at the time of the trip was performed. For 5 degree F intervals, the average percentage of time that the air conditioning system was turned on and that the air conditioning compressor was engaged was calculated. These data are plotted in Figure 46.

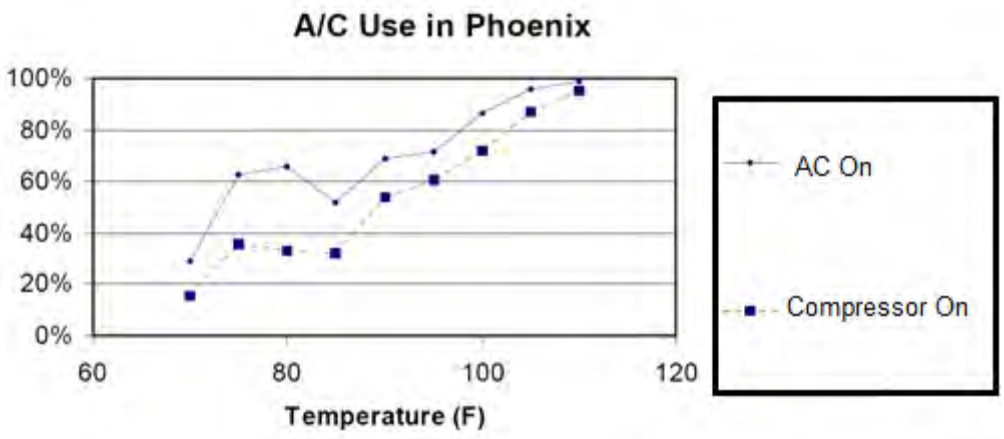

Figure 46: Air conditioning use in Phoenix (EPA, 2006).

Then the ratio of the percentage of time that the compressor was engaged to the percentage of time that the air conditioning system was turned during each temperature interval was calculated. This ratio is essentially the percentage of time that the compressor was engaged while the system was turned on. These ratios are plotted in Figure 47.

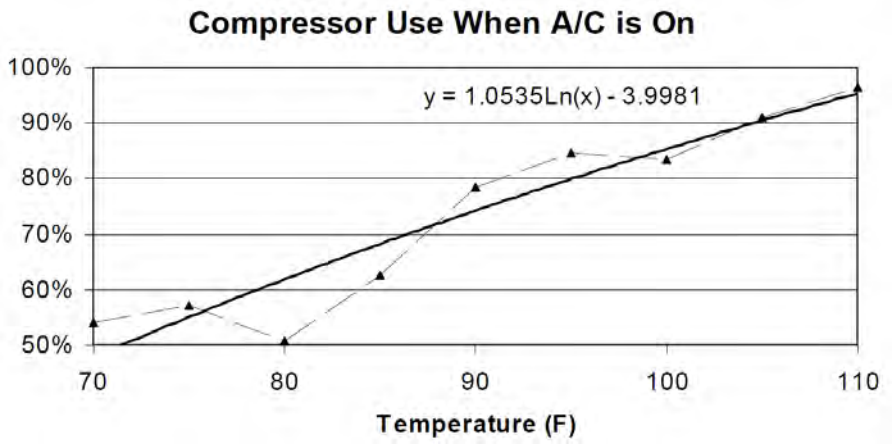

Figure 47: Compressor Engagement as a Function of Ambient Temperature (EPA, 2006).

Then a simple regression of these percentages was performed as a function of temperature. The result was:

Institutional Repository - Library & Information Centre - University of Thessaly
09/12/2017 02:36:50 EET - 137.108.70.7

$$Compressor\ Engagement(fraction) = 1.0535 \times \ln\big(ambient\ temperature(F)\big) - 3.9981 \quad [58]$$

Then the MOBILE6 estimate of compressor on fraction and this estimate were divided in order to convert the fraction of time that the compressor is on to the fraction of time that the air conditioning system is on.

Three other interesting studies that were carried out, are presented below. All of these three studies ((Roujol, 2005), (Roujol & Joumard, 2008) (Roujol & Joumard, 2009) were based on the Artemis (Assessment and Reliability of Transport Emission Models and Inventory Systems) study that was aiming at developing a harmonized emission model for road, rail, air and ship transport to provide consistent emission estimates at the national, international and regional level. A workspace aimed at improving the exhaust emission factors for the passenger cars and light duty vehicles by enlarging the emission factor database, especially for effects of auxiliaries. Various data from European laboratories were used and analyzed. Parameters linked to technology and climatic conditions investigated. The main distinction was made between gasoline and diesel vehicles. There were experimental data analyzed but also mathematical expressions provided and the results concerned the fuel consumption and not the power demand of the vehicles. Although, there were some results presented concerning the emissions of the tested vehicles.

A physical model of excess fuel consumption due to AC seemed to be complex to be implemented in an inventory software as Artemis. Therefore there had been a computation of the physical model with weather data of 91 regions all over Europe (urban and highway roads). Then by statistical regressions a relationship between calculated hourly fuel consumption and the following variables was found: ambient temperature, humidity, solar radiation (direct and diffuse) and position of sun in the sky. Solar radiations can be quite difficult to obtain, so the use of the hour in the day than the use of solar radiation was preferred. There were 4 types of vehicles distinguished for the test. Technological parameters analysed were parameters connected to the vehicle engine, to the AC system and to the body shape of the vehicle. The data are displayed according to the engine size, the fuel type, the vehicle size, the type of compressor and the type of regulation (Table 33).

The general form of the simplified model was:

$$hfc = a_{1,wf} + a_{1,wf} \times T_{ex,t,wf} + a_{3,wf} \times T_{int} + a_{4,wf} \times h + a_{5,wf} \times h^2 \quad [59]$$

$$with\ hfc \geq 0$$

Institutional Repository - Library & Information Centre - University of Thessaly
09/12/2017 02:36:50 EET - 137.108.70.7

where

hfc: hourly excess fuel consumption (l/h);

$T_{ext,wf}$: external temperature provided by hourly, daily or monthly weather data (wf: weather format) (°C), hourly weather format contains 8760 values, daily weather format contains 365 values and monthly weather data contains 12 values;

T_{int}: set temperature in the cabin; default value is 23°C;

h: the hour (between 1 and 24);

$a_{1,\ldots 5}$: coefficients depending on the location.

The system distinguished 6 major climatic types, designated by a capital letter (see Table 31).

Koppen climate type	Description
A	Tropical moist climates (average temperature of each month is above 18℃)
B	Dry climates
C	Moist mid-latitude climates with mild winters
D	Moist mid-latitude climates with cold winters
E	Polar climates
H	Highland area

Table 31: Major climatic types of Koppen climate classification (Roujol, 2005).

Each major climatic type was sub-divided into sub-categories based on temperature and precipitation. For the considered locations, there were 6 Köppen climate classes:

- Cfa : "C" indicates the "mild mid-latitude" type, the second letter, "f" comes from the German word "feucht" which means moist and the last letter "a" indicates that the average temperature of the warmest month is above 22°C;
- Cfb: this climate is similar to Cfa with a cooler warmest month;
- Csa: the group of letter "Cs" indicates a Mediterranean climate, "a" indicates that the average temperature of the warmest month is above 22°C;
- Csb: this climate is similar to Csa with a cooler warmest month;
- Dfb: "D" indicates a moist continental mid-latitude climates, "f" indicates that the climate is wet at all seasons and "b" that the average temperature of warmest month is below 22°C and average temperature of the 4 warmest months is above 10°C;
- Dfc: This climate is close to Dfb, "c" means that average temperature of 1 to 3 warmest months is above 10°C.

Institutional Repository - Library & Information Centre - University of Thessaly
09/12/2017 02:36:50 EET - 137.108.70.7

The Köppen classes of European locations are given in Annex 1 of (Roujol, 2005).

Type of weather data	Koppen classes	a_1	a_2	a_3	a_4	a_5
Hourly weather format	Cfa	-1.0368	0.0436	-0.0404	0.0455	-0.00189
	Cfb	-0.8575	0.0343	-0.0315	0.0480	-0.00202
	Csa/Csb	-0.9618	0.0393	-0.0380	0.0482	-0.00203
	Dfb	-0.7937	0.0333	-0.0319	0.0417	-0.00185
	Dfc	-0.6450	0.0242	-0.0250	0.0431	-0.00181
	average	-0.886	0.0363	-0.0339	0.0458	-0.00195

Table 32: Values of hourly fuel consumption simplified model for hourly weather format for 6 modified Koppen climate classes and an average (Roujol & Joumard, 2008).

In Table 33 there are the results of the AC fuel consumption of the 4 vehicles tested. The results show that the fuel consumptions were quite close with large standard deviations. Therefore it was assumed that the fuel consumption of AC does not depend on technical parameters.

Vehicle type			Nber veh.-tests	Fuel consumption	
	fuel	AC regulation		average	Standard deviations
Small, Medium 1	Gasoline	manual	38	0.7	0.2
	Diesel		55	0.68	0.22
Medium 2, Large, SUV	Gasoline	automatic	25	0.75	0.34
	Diesel		28	0.85	0.35

Table 33: Average fuel consumption due to AC (l/h) for the 4 vehicle types (Roujol & Joumard, 2008).

As it was shown in this study, AC system is running quite close to the full load at the test conditions (outside temperature higher than 28°C). Pollutants emissions are assumed to be pollutants emissions at full load. For the modeling of pollutants emissions, we assume that pollutants emissions at part load are a fraction of pollutant emissions at full load; this fraction is equal to the demand factor. The demand factor is the ratio of hourly fuel consumption to the hourly fuel consumption at full load. Excess pollutant emission at part load of one vehicle was expressed as a function of excess pollutant emission at full load and demand factor.

$$ef_{pollutant,AC} = ef_{pollutant,ACfull} \times \tau_{AC} \quad [60]$$

where

Institutional Repository - Library & Information Centre - University of Thessaly
09/12/2017 02:36:50 EET - 137.108.70.7

efpollutant, AC:	excess pollutant emission due to AC at given conditions (g/km);
efpollutant, ACfull:	excess pollutant emission due to AC at full load (g/km);
τ_{AC}:	demand factor; ratio of hourly fuel consumption at given condition to hourly fuel consumption at full load.

$$\tau_{AC} = \frac{hfc}{hfc_{full_{load}}} \quad [61]$$

where hfc is the hourly fuel consumption at full load = 0.85 l/h.

4.3 Conclusions

The above studies presented show us the impact of the use of A/C in the fuel consumption, power consumption and emissions of a vehicle. The study of its impact is very important as the use of these systems has reached a high level nowadays. A European Climate Change Programme working group estimated that the usage of AC systems under average European conditions causes an increase of fuel consumption between 4 and 8% in 2020.

The air conditioning compressor generally cycles on and off depending on the ambient temperature, humidity, solar load and the length of time that the vehicle has been operating. The greater the temperature and humidity, the more often drivers turn the air conditioning on. The greater the temperature and humidity, the more frequent the compressor needs to operate in order to keep the cabin at a comfortable temperature; the shorter the trip, the more relevant any solar loading of the vehicle. For high humidities the load of A/C almost doubles and for low humidities the load is reduced by some 10-50% in relation to the measured case of 50% relative humidity. Therefore, it is important to study all these ambient conditions in order to come to conclusions for the right use of the A/C inside a vehicle. According to the comfort theory, it is important to keep the interior climate of the vehicle stable at the desired comfort temperature. This ideal temperature is assumed to be 23°C for all the vehicles equipped with A/C.

There are available models that can be used with relatively high confidence to predict fuel consumption and CO_2 emissions. However, the models are more limited in their ability to accurately predict short-term variations in emissions of HC, CO, and NOx. While these emissions depend in some part on engine power demand, they depend in a more complex way on other factors, and thus are more difficult to model accurately. The case studies illustrate that the models can make predictions of average emission rates over many runs that are

Institutional Repository - Library & Information Centre - University of Thessaly
09/12/2017 02:36:50 EET - 137.108.70.7

accurate to within 10% to 20% in some cases. However, the trip average emissions of these pollutants can be very sensitive to short-term episodic events that produce large emissions peaks. Models like the MOVES and the MOBILE6 are used to examine all the above factors and come to conclusions about the vehicle's behavior in energy consumption and emissions. Although most studies concern the U.S. fleets. The A/C systems of European cars are based on a variety of different technologies, so that it is not possible to link compressor activity data collected by tests on the road with emission results from A/C full-load tests on the chassis dynamometer. Fuel consumption and exhaust emissions have to be measured directly in tests where the cars are exposed to simulated weather conditions on the test bench.

Concerning warm conditions, the excess fuel consumption due to AC is well-known because of the large number of experiments. It is quite different in usual climatic conditions with solar radiation, because of the reduced number of experiments.

Institutional Repository - Library & Information Centre - University of Thessaly
09/12/2017 02:36:50 EET - 137.108.70.7

Chapter 5 Correlation

5.1 Introduction

In the four previous Chapters we presented some parameters that have an impact on the behavior of a vehicle as they can affect the fuel consumption, the power demand and also the emission level of the vehicle. Although, in real traffic conditions, more than one of these parameters act at the same time. It is important, therefore, to present some studies that examine the impact of two or more of the above parameters together and how they can have even more visible results in the behavior of the vehicle.

As we said also in the previous chapters, when a vehicle is moving, several resisting forces must be overcome. Resisting forces that arise from the interaction between the vehicle, the air and the road are:

- Aerodynamic drag, which depends on the shape of the vehicle and the frontal area and is proportional to the square of the speed.
- Rolling resistance, which depends on the tires, on the tire pressure and on the quality of road and is proportional to the weight of the vehicle.
- Resisting forces related to the weight of the vehicle: Inertia during acceleration, which depends on the weight of the vehicle, but also on all the rotating pieces (wheels, components of the engine and of the gearbox).
- Gravity along a slope.

These forces are a function of the use of the vehicle and can vary considerably. At high speeds, the aerodynamic resistance is preponderant (more than 75% of the total), while in urban use the inertia resistance is more than 95% of the total. As well, the absolute values of the forces differ significantly from model to model. An indication of the power required to overcome the above forces is provided in Table 34 for a conventional passenger car. The table refers to a passenger car of 100 kg with a frontal area of $1.75m^2$ and an air resistance coefficient of 0.45. For urban use the weight of the vehicle is a very important determinant of the power requirements (and the fuel consumption) for passenger cars. This is also the case for delivery vans and buses.

Institutional Repository - Library & Information Centre - University of Thessaly
09/12/2017 02:36:50 EET - 137.108.70.7

Use of the vehicle	Rolling	Aerodynamic	Inertia	Gravity	Total
Urban 20 km/h (mean speed)	0.7 (4.2%)	0.09 (0.5%)	15.9 (95.2%)	0	16.7
60 km/h constant horizontal	2.5 (51%)	2.4 (49%)	0	0	4.9
140 km/h constant horizontal	9.4 (24%)	30.1 (76%)	0	0	39.5
80 km/h constant slope 5%	3.7 (17.4%)	5.6 (26.3%)	0	12.0 (56.3%)	21.3

Table 34: Power (kW) required to overcome various forms of resistance to forward movement of the vehicle (OECD, 2004).

Drag, rolling resistance and weight are major parameters influencing fuel consumption, which are explained in the policy report. Accessories generally have only accounted for a moderate part of the fuel consumption. However, traditionally, accessories did not include an air conditioner or an auxiliary heater. Modern cars are increasingly equipped with an air conditioner. In addition, modern diesel cars with highly efficient engines require additional heating and are equipped with an auxiliary heater.

The breakdown of the energy consumption of a traditional mid-size family car powered by a petrol engine is given as an example in Table 35.

Type of road		Urban	Highway
Energy content of fuel	**Energy consumption**	**100%**	**100%**
Drivetrain losses	Thermodynamic losses	60%	60%
	Engine losses	12%	3%
	Transmission losses	4%	5%
	Total	**76%**	**68%**
Used for components	Auxiliaries	2%	1%
	Accessories	1%	1%
	Air conditioning (when in use)	10%	10%
	Total	**13%**	**12%**
Used for propulsion	Air resistance	2%	11%
	Roll resistance	4%	7%
	Kinetic losses/braking – no inclination	5%	2%
	Total	**11%**	**20%**

Table 35: Energy breakdown of a traditional standard mid-size family car (OECD, 2004).

The breakdown of the energy consumption of a typical hybrid vehicle is given in Table 36. In a hybrid electric vehicle, an electrical machine and battery are used to improve the drivetrain losses.

Institutional Repository - Library & Information Centre - University of Thessaly
09/12/2017 02:36:50 EET - 137.108.70.7

Type of road		Urban	Highway
Energy content of fuel	**Energy consumption**	**100%**	**100%**
Drivetrain losses	Thermodynamic losses	51%	56%
	Engine losses	11%	3%
	Transmission losses	6%	5%
	Total	**68%**	**65%**
Used for components	Auxiliaries	3%	1%
	Accessories	1%	1%
	Air conditioning (when in use)	15%	11%
	Total (with air conditioning)	**19%**	**11%**
	Total (no air conditioning)	**4%**	**2%**
Used for propulsion	Air resistance	2%	12%
	Roll resistance	5%	8%
	Kinetic losses/braking – no inclination	6%	2%
	Total (with air conditioning)	**13%**	**22%**
	Total (no air conditioning)	**28%**	**33%**

Table 36: Energy breakdown of a typical hybrid vehicle (OECD, 2004).

According to (Hammarstrom, Eriksson, Karlsson, & Yahya, 2012) , fuel consumption is a function of driving resistance and engine efficiency. Driving resistance is a function of the road conditions and driving behavior. The driving resistance (*Fx*) constitutes a sum of forces:

$$Fx = Fb + Fair + Facc + Fgr + Fside + Fr \quad [62]$$

where

Fx: total driving resistance
Fb: wheel bearing resistance (N)
Facc: acceleration resistance from vehicle mass (N)
Fair: air resistance (N)
Fgr: gradient resistance (N)
Fside: resistance caused by the side force (N)
Fr: rolling resistance (N)

Below the functions that compute all the above factors are presented:

Wheel bearing resistance Fb

In the wheel bearings there will be a resistance proportional to the vertical force (Mitschke, 1982):

Institutional Repository - Library & Information Centre - University of Thessaly
09/12/2017 02:36:50 EET - 137.108.70.7

$$Fb = Cb \times Fz \quad [63]$$

where

Cb: parameter for bearing resistance

Fz: vertical load per tyre (N)

Air resistance Fair

The air resistance at calm wind conditions is expressed by:

$$Fair = CD \times A_{Frontal} \times \rho \times v^2/2 \quad [64]$$

where

ρ: the density of air (kg/m^3) where ρ=(348.7/1000)*(Pair/(T+273))

v: the vehicle velocity (m/s)

$A_{Frontal}$: the projected frontal area of the vehicle (m^2)

CD: the air dynamic coefficient (dimensionless)

Pair: the air pressure (mbar)

T: the ambient temperature (°C)

Inertial force Facc

$$Facc = macc \times \frac{dv}{dt} \quad [65]$$

$$macc = m + m_J \quad [66]$$

where

dv/dt: the acceleration level (m/s^2)

m: the total mass of the vehicle (kg)

m_J: sum(K_J*J/rwh^2), where sum means summation over the wheels (kg)

rwh: the wheel radius (m)

J: the inertial moment per wheel (kgm^2)

K_J (set to 1.0 in this study): a correction factor of J to include moving parts in the transmission system

Institutional Repository - Library & Information Centre - University of Thessaly
09/12/2017 02:36:50 EET - 137.108.70.7

Gradient resistance Fgr

$$Fgr = m \times 9.81 \times \sin(gr) \quad [67]$$

Where

gr: the longitudinal slope (rad).

Side force resistance Fside

$$Fside = Fy \times Cr3 \quad [68]$$

$$Fy = m \times \left(\cos\left(\frac{crf}{100}\right) \times \frac{v^2}{R - 9.81} \times \sin\left(\frac{crf}{100}\right) \times \cos(gr)\right) \quad [69]$$

$$Cr3 = \frac{1}{C_A} \quad [70]$$

where

Fy:	the side force acting on the vehicle (N)
C_A:	the tire stiffness parameter (N/rad)
crf:	the crossfall (%)
gr:	the longitudinal slope (rad)
R:	the radius of the road curvature (m)
Cr3:	the estimated parameter for the stiffness inverse (rad/N)

The cross fall causes a driving resistance (*Fside*) because the tyre will not be parallel to the vehicle movement direction. *Fside* is a function of *Fy* and C_A. C_A is a non linear function of the tyre load. Because of the cross fall one can expect different Fside on different wheels on the same wheel axle. This level of detail has not been used in the analysis. The cross fall of the road will influence the normal force distribution from left to right. Higher vertical force on the right side is expected to give higher tire temperature and pressure on the right hand side of the vehicle.

Rolling resistance Fr

Institutional Repository - Library & Information Centre - University of Thessaly
09/12/2017 02:36:50 EET - 137.108.70.7

$$Fr = C_r \times m \times 9.81 \quad [71]$$

There are several alternatives to express C_r as a function of other variables, one of them is:

$$C_r = C_r0 + IRI \times C_r1 + mpd \times C_r2 \quad [72]$$

$$C_r0 = C_r00 + CtTemp \times (5 - T) \quad [73]$$

where

IRI:	the road roughness measure (m/km)
mpd:	the macrotexture measure (mm)
m:	the vehicle mass (kg)
v:	the vehicle velocity (m/s)
C_r0, C_r1 and C_r2:	the rolling resistance parameters.

By combining all the above mathematical expressions, it's possible to develop an *Fc* function able to describe most of the effects of interest in road planning. The main problems to solve are that direct information about engine speed and torque not are available. Instead these variables are expressed indirectly by vehicle speed and driving resistance.

An *Fc* function based on the above mathematical expressions is:

$$Fct = c0 \times Mind^{e1} Mindel \times \mathrm{NRs}^{e2} \quad [74]$$

Where Fct = Fc per time unit and,

$$Mind = PFR + PME \,/\, (NRs \times 6.28) \quad [75]$$

$$PME = PAUX + PTRM + PMdriv \quad [76]$$

$$PMdriv = Fx \times v \quad [77]$$

$$PFR = k1 \times NRs \quad [78]$$

$$PAUX = k2 \quad [79]$$

$$PTRM = k3 \times NRs \quad [80]$$

$$Mind = \frac{k1 \times NRs + k2 + k3 \times NRs + Fx \times \frac{v}{VGVX}}{NRs \times 6.28} \quad [81]$$

In a simplified Fc model engine speed and torque need to be expressed indirectly.

Institutional Repository - Library & Information Centre - University of Thessaly
09/12/2017 02:36:50 EET - 137.108.70.7

$$k4 = \frac{k1 + k3}{6.28} \quad [82]$$

$$Mind = k4 + \frac{k2}{NRs \times 6.28} + k5 \times Fx = k4 + \frac{k21}{NRs} + k5 \times Fx \quad [83]$$

$$Fct = c0 \times (k4 + \frac{k21}{v} + k5 \times Fx)_{e1} \times (k6 \times v)_{e2} \quad [84]$$

This function can be expressed in an alternative way:

$$Fct = c1 \times (1 + \frac{k21}{v} + k7 \times Fx)_{e1} \times v_{e2} \quad [85]$$

$$Fcs = Fct \times v \quad [86]$$

The function is only valid for *Mind≥0*. *Mind<0* represents a situation when full engine brake is used in combination with the use of wheel brakes. *Fct* then should be approximately equal to zero.

Depending on what demand for use of the function *Fx* can be expressed to meet that demand. In order to describe *Fx* representative vehicle parameters are used as far as possible. The other parameters – *c0, k4, k21, k5, k6, e1* and *e2* – are possible to estimate if *Fct* for different driving conditions are available. Such values are possible to calculate by use of for example VETO (computer program). To a great extent this function approach should be able to describe the same effects as programs like VETO. What cannot be described is that the vehicle situation in one road and time position is a function of the conditions in the position before. The transmission losses and the relation between vehicle speed and engine speed are described in a most simplified way with loss of accuracy. The function approach is possible to use as a base for functions on different levels of complexity. When developing an *Fc* function one can state that the big difference is between driving modes and integrated driving modes along a road. In the second alternative driving modes need to be described in some way for example by average speed. In the function *Fx* needs to be expressed by measures possible to use in practice. At least *IRI* and mpd needs to be included.

Fuel consumption is a function of power required at the wheels and overall engine-accessories driveline efficiency. The horsepower required for a vehicle to sustain a given speed is a function of the vehicle's total drag. The greater the drag, the more horsepower is required. The total vehicle drag can be broken into two main components; aerodynamic drag and tire drag. Both aerodynamic drag and tire drag are influenced by vehicle speed. Consider a typical tractor and van combination operating at 80,000 lb. gross combination weight and at 55 MPH on a level highway. No aerodynamic drag reduction devices are used on either the tractor or

Institutional Repository - Library & Information Centre - University of Thessaly
09/12/2017 02:36:50 EET - 137.108.70.7

the trailer. Using bias ply tires in all wheel positions, the approximate distribution of horsepower requirements is as follows:

Item	HP Requirement	Percent
Aerodynamic drag	104	40
Tire Roll Resistance	97	38
Driveline Losses	36	14
Engine Accessories	20	8
Total	**257**	**100**

Table 37: Distribution of horsepower requirements for a typical tractor and van combination on a highway road (Goodyear, 2012).

Conditions external to the vehicle can have a strong influence on the fuel economy achieved by a given driver and tractor-trailer/tire combination. Some of the greater influences are exerted by:

Winds: Headwinds and crosswinds reduce truck fuel economy by increasing truck airspeed and/or yaw angle, thus increasing aerodynamic drag.

Road Surface: The type of road surface can affect tire rolling resistance. Smooth-textured highway surfaces provide the lowest rolling resistance, while coarse-textured surfaces give the highest tire rolling resistance and the lowest fuel economy.

Ambient Temperature: High ambient temperatures reduce tire rolling resistance. High temperatures also reduce atmospheric density, resulting in lower aerodynamic drag. However, fuel economy performance of non-turbocharged diesel engines may be adversely affected by high ambient temperatures, and this would tend to negate some of the gains resulting from lower tire drag and lower aerodynamic drag. Cold weather operation has an opposite effect: tire drag and aerodynamic drag increase at the lower ambient temperatures.

Terrain (road grade and altitude): Most proving grounds fuel economy testing is done on level terrain, and most simplified calculations relating various truck and tire parameters to truck fuel economy also assume level terrain. The effect of traveling up a grade is very significant in terms of reducing truck fuel economy. As altitude increases, air density and atmospheric pressure decrease. At 5,000 ft. altitude, for example, air density in a standard atmosphere is 14 percent less than at sea level. This percent reduction in air density also applies to reduction in aerodynamic drag, all else being equal. Tire rolling resistance is not affected by altitude, unless cold inflation pressure is set at lower altitudes and not changed as altitude of operation increases during the course of the trip (Goodyear, 2012).

Institutional Repository - Library & Information Centre - University of Thessaly
09/12/2017 02:36:50 EET - 137.108.70.7

In the following section, we will present studies that correlate two or more of the parameters that were presented in the previous chapters and their effect on the fuel consumption, the emissions and the power demands of different types of vehicles.

For a better understanding, we also kept the same mode of categorization as in the previous chapters so we divided our studies in those that examine (1) LDVs (Light Duty Vehicles), (2) HDVs (Heavy Duty Vehicles) and (3) Very Specific Type of Vehicles (VSTVs). We also divided the above sections in subcategories that concerned the number of the correlated factors. The diagram of our review is shown in **Σφάλμα! Λανθασμένη αναφορά σελιδοδείκτη στον εαυτό του.**.

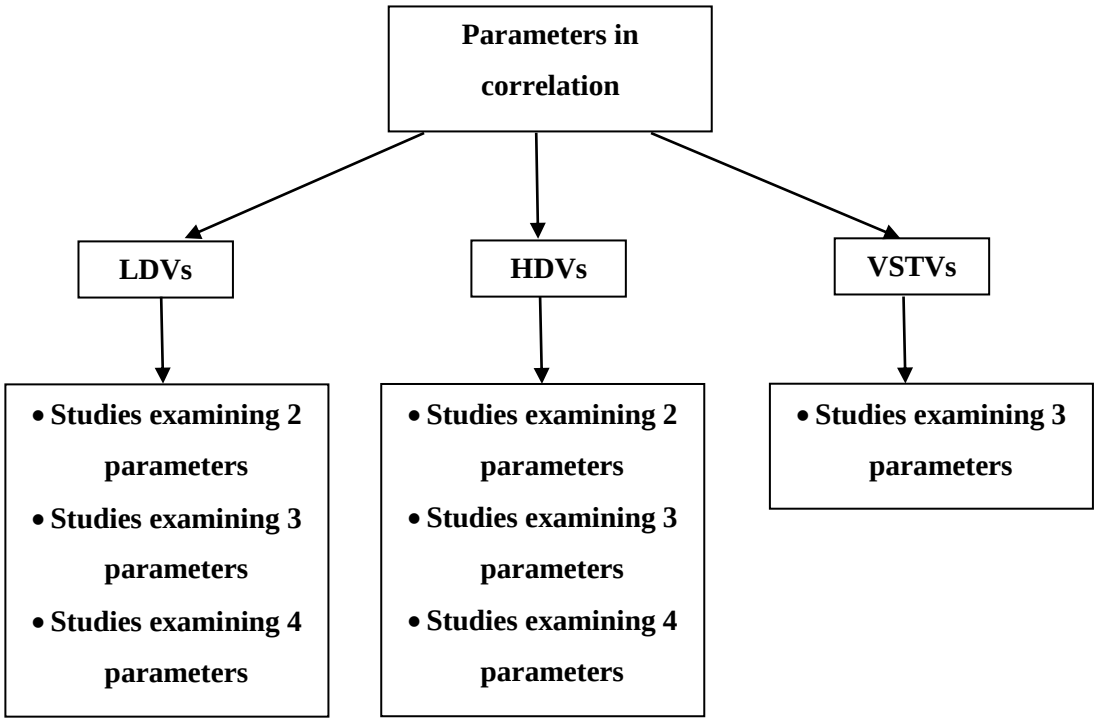

Figure 48: Diagram of our review – categorization of studies.

5.2 Review of studies with correlated parameters

5.2.1 Light Duty Vehicles (LDVs)

5.2.1.1 Studies examining two parameters

In 1995, Pablo Cicero-Fernandez and J.R. Long developed a project to assess driving patterns likely to promote emission excursions greater than those encountered in current dynamometer driving cycles, using an instrumented vehicle equipped for on-road testing on highway road hills (Cicero-Fernandez & Long, 1995). Their study was focused on two parameters: the road

Institutional Repository - Library & Information Centre - University of Thessaly
09/12/2017 02:36:50 EET - 137.108.70.7

gradient and the A/C use and how they influence the vehicle's behavior. Also, the passenger load was a less significant parameter that was taken into account. Their study was mostly concerned on uphill driving but they presented some comparing results with downhill driving presenting. It also took as a datum the use or not of the air-conditioning system of the examined vehicle. The tested vehicle was a 1991 GM Lumina and was equipped with an on-board data-logger and analyzers for hydrocarbons and carbon monoxide, along with sensors for basic driving parameters such as speed, manifold pressure, throttle position, and grade. The on-board emission instrumentation was compared to dynamometer tests by performing parallel sampling. The results were carried out by experiments and one mathematical expression provided and concerned the emissions of the vehicle as there was no study held about the fuel consumption and the power demands. High correlation among emission rates was shown: CO (R^2=0.82), Hydrocarbons (R^2=0.72). Controlled runs with predetermined cruises and accelerations were conducted on flat terrain and hills on grades ranging from 0% to 7%. The hills were located in metropolitan Los Angeles, both on freeways and arterials.

The selected roads with grades included Montebello (FWY 60), Kellogg Hill (FWY10), Sepulveda Hill (FWY405), Colima Hill (in Whittier), Crenshaw (in Palos Verdes), and Las Tunas Canyon (in Malibu). Driving on the hills was primarily composed of constant speeds at targeted low accelerations. Three nominal speeds were tested per hill, these nominal speeds were 35, 45 and 55 mph. The final run was designed to follow the general car flow on the road. A summary of the driving routes is presented in Table 38, the hill profiles are presented in Figure 49.

Location	**Grade (percent feet)**	**Elevation Change**
Telstar Avenue in El Monte	≈0	0
Highway 58 near Barstow	<0.3	20
Montebello Hill Freeway 60	2	160
Sepulveda Hill Freeway I-405	3.5	620
Kellogg Hill Freeway I-10	4.3	330
Colima Hill in Whittier	4.5	100
Crenshaw Canyon in Palos Verdes	6.7	420
Tuna Canyon in Malibu	11	1350

Table 38: Driving Routes [Table 2, (Cicero-Fernandez & Long, 1995)].

Institutional Repository - Library & Information Centre - University of Thessaly
09/12/2017 02:36:50 EET - 137.108.70.7

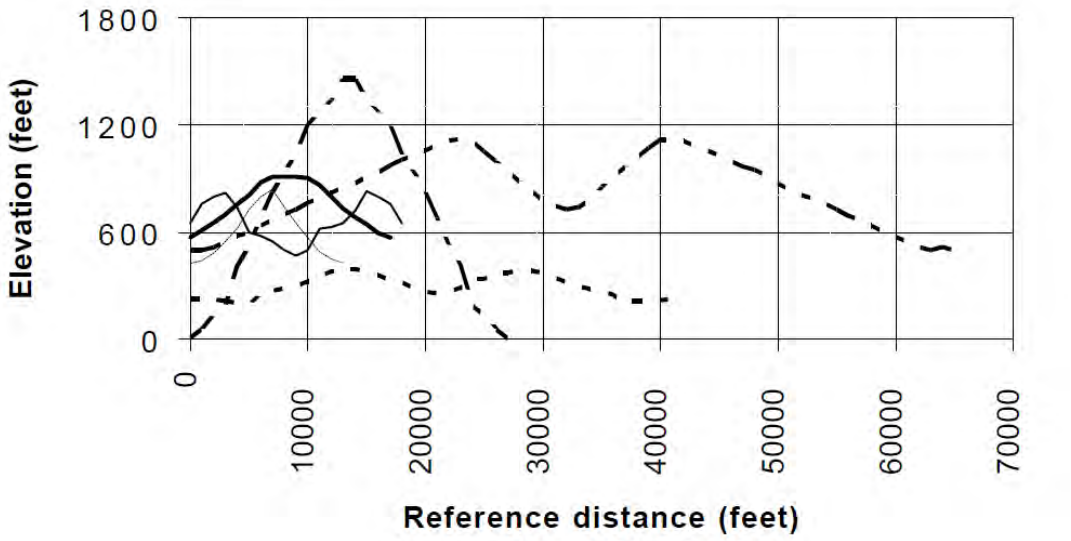

Figure 49: Hill Profiles [Figure 2, (Cicero-Fernandez & Long, 1995)].

Three tests were presented with running speeds of 32, 38 and 43 mph. The additional emissions imposed by the positive grade compared to the downhill fraction were evident, even for the low speed tests, for HC. The effects on CO were very dramatic for the higher speed run, showing typical open-loop or enrichment behavior (Figure 50, Figure 51). To analyze the effects of different grades, each run was desegregated into idle (less than 5 mph), driving on flat terrain (less than ±0.5% grade), positive grade, and negative grade.

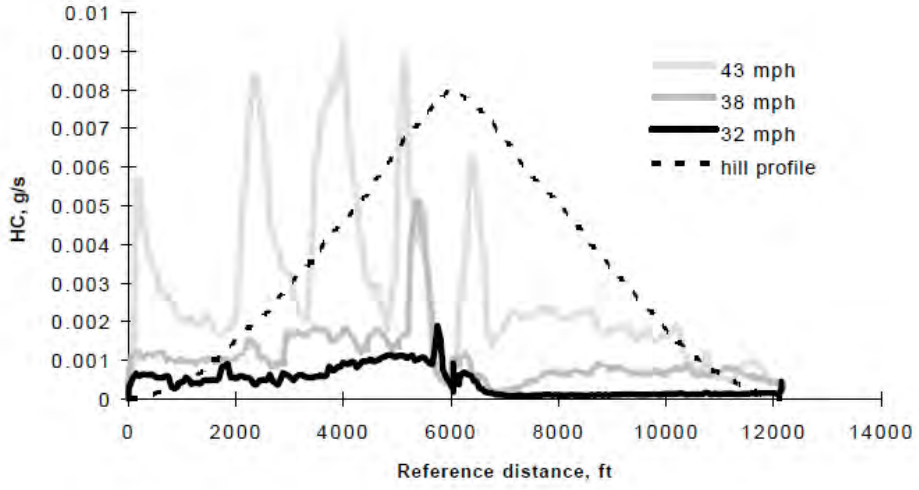

Figure 50: HC vs Time [Figure 3, (Cicero-Fernandez & Long, 1995)].

Institutional Repository - Library & Information Centre - University of Thessaly
09/12/2017 02:36:50 EET - 137.108.70.7

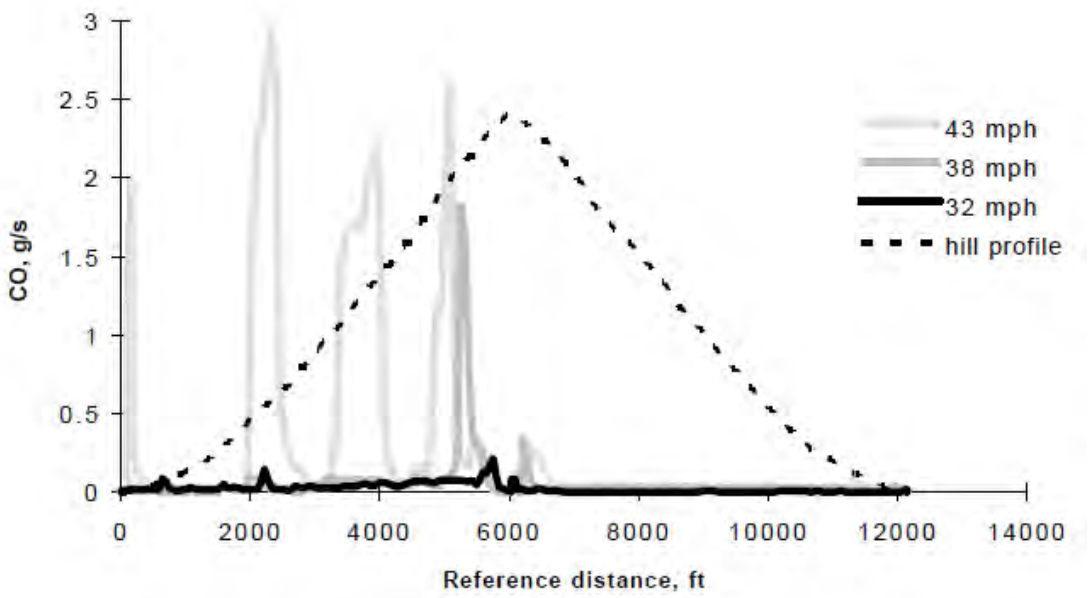

Figure 51: CO vs Time [Figure 4, (Cicero-Fernandez & Long, 1995)].

The impact of speed and grade on emission rates (HC, CO/s and /mile) was evaluated using multiple regression on the positive grade fraction of each run, the results are presented in Table 39.

		HC/s	CO/s	HC/mile	CO/mile
	R	0.668	0.616	0.635	0.603
	R	0.446	0.379	0.403	0.364
	a_0	-0.00494	-0.70833	-0.31338	-49.35373
	p-a_0	0.003	0.002	0.022	0.004
Speed	a_1	0.00011	0.01687	0.00689	117.734
	p-a_1	0.002	0.001	0.018	0.001
Grade	a_2	0.00049	0.03827	0.04283	299.567
	p-a_2	0.001	0.048	0.001	0.037
	n	29	29	29	29

Table 39: Estimated impact of speed and grade on emission rates using regression. The data points correspond to the positive grade fraction of the run [Table 4, (Cicero-Fernandez & Long, 1995)].

The values of the emission rates in Table 39 were calculated using the mathematical expression below:

$$Emission\ Rate = a_0 + a_1 \times v + a_2 * \text{Grade} \quad [87]$$

where

v: The speed of the vehicle

There were also some simulations conducted that included other parameters such as the passenger load and the use of air conditioning.

Institutional Repository - Library & Information Centre - University of Thessaly
09/12/2017 02:36:50 EET - 137.108.70.7

A commuter car was simulated on a hill with passenger loads of one to four passengers. Each passenger load was driven at three different nominal speeds. In a similar fashion air conditioning effects were tested using three nominal speeds for no air-conditioning operation and for air-conditioning operation at maximum setting.

For air conditioning operation, tests were performed on two hills (4.5 and 6.7%). The emission rates of hydrocarbons showed an increase of 57% when air conditioning at a maximum setting was used. For CO the increase was 268% for air conditioning operation. For air conditioning operation, tests were performed at three speeds and two positive grades (4.5 and 6.7%). The analysis included the positive grade fraction of the runs. The distance based emission rates of hydrocarbons showed an increase of 57% when air conditioning at a maximum setting was used. For CO the increase was 268% for air conditioning operation.

Example of emissions rates (HC, CO/s and /mile) regarding passenger load (1st case: 1, 2 &3 passengers, 2nd: 4 passengers) at three speeds 32, 38, 43 mph, grade 4.5 % and AC (1st case: off, 2nd: on) at three speeds 32, 38, 43 mph and two grades, 4.5 and 6.7% are shown in Table 40.

		HC/s	CO/s	HC/mile	CO/mile
Passenger load					
	1,2 & 3 passenger	0.0010	0.173	0.08	13.4
	4 passenger	0.0021	0.345	0.16	25.3
	increase	105%	100%	96%	89%
AC					
	off	0.0023	0.190	0.20	15.0
	on	0.0038	0.703	0.31	55.2
	increase	68%	269%	57%	268%

Table 40: Estimated impact of passenger load and air conditioning on emission rates. For passenger load the test was performed at three speeds and a grade of 4.5%. For air conditioning operation the test was performed at three speeds and two grades (4.5 and 6.7%). The data points corresponded to the positive grade fraction of the run [Table 5, (Cicero-Fernandez & Long, 1995)].

The emission rates of HC showed an increase of 57% when air conditioning at a maximum setting was used. For CO the increase was 268% for air conditioning operation.

Controlled runs with predetermined cruises and accelerations were conducted on flat terrain and hills on grades ranging from 0% to 7%. The hills were located in metropolitan Los Angeles, both on freeways and arterials (highway roads). The results were carried out by experiments and concerned the emissions of the vehicle and there is no reference to the fuel consumption or power demand. There were no mathematical expressions provided during the study concerning the use of air conditioning system and the fuel consumption/power demand or emissions of the vehicle.

Institutional Repository - Library & Information Centre - University of Thessaly
09/12/2017 02:36:50 EET - 137.108.70.7

Another report taking into consideration the two above parameters was published in 2010. It was a report that described adjustments that affect running exhaust, start exhaust and extended idling emissions (EPA, 2010). According to the report, the emission rates in the MOVES model database represent a single (base) scenario of conditions for temperature, humidity, air conditioning load and fuel properties. MOVES is designed to adjust these base emission rates to reflect the conditions for the location and time specified by the user. MOVES also includes a methodology for adjusting the base emission rates to reflect the effects of local Inspection and Maintenance (I/M) programs. This report describes how these adjustments for temperature, humidity, I/M and air conditioning were derived. The MOVES model was the evolution of the MOBILE6 model and both of them are systems for calculating the emissions level in country level. Throughout the report there are tests that showed the effect of air conditioning in the fuel consumption and the emissions of the vehicle. Also, there were mathematical expressions, for the calculation of the required power, provided. All tests concerned highway vehicles.

MOVES made adjustments to total energy consumption and exhaust running HC, CO and NOx emissions separately for each operating mode. The criteria pollutants (HC, CO and NOx) were only affected for passenger car, passenger truck and commercial light truck source types. Energy consumption was affected for all source types. The same adjustment values were used for all source use types affected within a pollutant type.

In EPA's previous emissions model (MOBILE6), passenger car and light-duty truck tailpipe emissions were adjusted relative to its base emission rates at 75°F based on:

1. ambient temperature and
2. for start emissions, an adjustment based on the length of the soak time.

MOVES took a similar approach, but substantially altered the nature of the temperature adjustments. The air conditioning adjustments in MOVES are based on the same data as was used in the previous MOBILE6 model, but the adjustments themselves were recalculated to be consistent with the MOVES methodology. The proposed factors are based on a test procedure meant to simulate air conditioning emission response under extreme “real world” ambient conditions. These factors predict emissions which would occur during full loading of the air conditioning system, and will then be scaled down in MOVES according to ambient conditions in a modeling run. The second-by-second emission data were analyzed using the MOVES methodology of binning the data according to vehicle characteristics (source bins in MOVES) and vehicle specific power bins (operating modes in MOVES). The results of the

Institutional Repository - Library & Information Centre - University of Thessaly
09/12/2017 02:36:50 EET - 137.108.70.7

analysis showed statistically significant and consistent results for three bin combinations (deceleration, idle and cruise/acceleration) and the three primary exhaust pollutants (hydrocarbon, carbon monoxide and nitrous oxides). The report showed the results of the analysis for the air conditioning adjustments used in MOVES for HC, CO, NOx and energy consumption.

The data for the MOVES A/C Correction Factor (ACCF) was collected in calendar year 1997 and 1998 in specially designed test programs. In the programs the same set of vehicles were tested at standard FTP test conditions (baseline) and at a nominal temperature of 95 F. Use of the same set of vehicles and test cycles should eliminate most of the vehicle and test procedure variability and highlight the difference between a vehicle operating at extreme ambient conditions and at a baseline condition. The data used to develop the MOVES ACCF consisted of 54 individual cars and light trucks tested over a variety of test schedules. Overall the database consisted of a total of 625 test cycles, and 1,440,571 seconds of emission test and speed / acceleration data.

The overall dataset consisted of a sample of vehicle tests with the A/C system on and a sample of vehicle tests with the A/C system off. Both samples consisted on the same vehicles and all tests were modal with a data sampling of 1 hertz (second-by-second data collection). Prior to analysis the data for each vehicle / test cycle combination was time aligned to insure that the instantaneous vehicle operating mode was in-sync with the emission collection system. Following time alignment, the vehicle specific power (VSP) was calculated for each vehicle test / second combination. This was done using the mathematical expression below:

$$VSP = 985.5357 \times v \times \frac{Acoeff}{Weight} + 440.5729 \times v^2 \times \frac{Bcoeff}{Weight} + 196.9533 \times v^3 \times \frac{Ccoeff}{Weight} + 0.19984476 \times v \times \mathrm{a} + GradeTerm \quad [88]$$

where

VSP: the vehicle specific power for a given second of operation [KW/tonne]

v: the instantaneous vehicle speed for a given second [miles/h]

a: the instantaneous vehicle acceleration for a given second [miles/hr-sec]

Weight: the test vehicle weight [pounds]

$$Acoeff = 0.7457 \times \left(\frac{0.35}{50 \times 0.447}\right) \times ROAD\_HP \quad [89]$$

Institutional Repository - Library & Information Centre - University of Thessaly
09/12/2017 02:36:50 EET - 137.108.70.7

$$Bcoeff = 0.7457 \times \left(\frac{0.10}{50^2 \times 0.447^2}\right) \times ROAD\_HP \quad [90]$$

$$Ccoeff = 0.7457 \times \left(\frac{0.55}{50^3 \times 0.447^3}\right) \times ROAD\_HP \quad [91]$$

where

$$ROAD_{HP} = 4.360117215 + 0.002775927 \times Weight(for\ cars) \quad [92]$$

$$ROAD_{HP} = 5.978016174 + 0.003165941 \times Weight(for\ light\ trucks) \quad [93]$$

$$GradeTerm(kW/tonne) = 4.3809811 \times Speed \times \sin(radians(GradeDeg)) \quad [94]$$

where GradeDeg is the road grade in units of degrees. This term is zero for dynamometer tests.

$$4.3809811 \times \left(m^2 \times \frac{hr}{s^3 \times miles}\right) = 9.80665(m/s^2) \times 1609.34(m/mile)\ /3600(secs/hr) \quad [95]$$

where $\frac{kW}{tonne} = \frac{m^2}{s^3}$ and $9.80665(m/s^2)$ is the gravitational constant.

After computing the VSP for each vehicle test / second combination, the individual seconds to the MOVES VSP bins were assigned. These VSP bins are defined in Table 41. VSP bins 26 and 36 were not defined because bins 27-30 and bins 37-40 overlap them.

Institutional Repository - Library & Information Centre - University of Thessaly
09/12/2017 02:36:50 EET - 137.108.70.7

VSP Label	Definition
0	Braking
1	Idling
11	Low Speed Coasting: VSP<0; 1<=v<25
12	Cruise/Acceleration: 0<=VSP<3; 1<=v<25
13	Cruise/Acceleration: 3<=VSP<6; 1<=v<25
14	Cruise/Acceleration: 6<=VSP<9; 1<=v<25
15	Cruise/Acceleration: 9<=VSP<12; 1<=v<25
16	Cruise/Acceleration: 12<=VSP; 1<=v<25
21	Moderate Speed Coasting: VSP<0; 25<=v<50
22	Cruise/Acceleration: 0<=VSP<3; 25<=v<50
23	Cruise/Acceleration: 3<=VSP<6; 25<=v<50
24	Cruise/Acceleration: 6<=VSP<9; 25<=v<50
25	Cruise/Acceleration: 9<=VSP<12; 25<=v<50
26	Cruise/Acceleration: 12<=VSP; 25<=v<50
27	Cruise/Acceleration: 12<=VSP<18; 25<=v<50
28	Cruise/Acceleration: 18<=VSP<24; 25<=v<50
29	Cruise/Acceleration: 24<=VSP<30; 25<=v<50
30	Cruise/Acceleration: 30<=VSP; 25<=v<50
33	Cruise/Acceleration: VSP<6; 50<=v
35	Cruise/Acceleration: 6<=VSP<12; 50<=v
36	Cruise/Acceleration: 12<=VSP; 50<=v
37	Cruise/Acceleration: 12<=VSP<18; 50<=v
38	Cruise/Acceleration: 18<=VSP<24; 50<=v
39	Cruise/Acceleration: 24<=VSP<30; 50<=v
40	Cruise/Acceleration: 30<=VSP; 50<=v

Table 41: VSP Bin Definitions (EPA, 2010).

An average emission result for each pollutant (HC, CO and NOx) with and without A/C operation was computed for each VSP Bin. An analysis of cars versus trucks was also performed, and showed no statistical difference between the two.

Full A/C adjustments were generated for each of the nine VSP Bin and pollutant combinations. This was done by dividing the mean "With A/C" emission factor by the mean "Without A/C" emission factor for each of the VSP Bin / pollutant combinations. The Full A/C adjustments are shown in Table 42.

Institutional Repository - Library & Information Centre - University of Thessaly
09/12/2017 02:36:50 EET - 137.108.70.7

Pollutant	Operating Mode	Full A/C FC
HC	Braking/Decel	1.0000
HC	Idle	1.0796
HC	Cruise/Accel	1.2316
CO	Braking/Decel	1.0000
CO	Idle	1.1337
CO	Cruise/Accel	2.1123
NOx	Braking/Decel	1.0000
NOx	Idle	6.2601
NOx	Cruise/Accel	1.3808

Table 42: Full Air Conditioning Adjustments for HC, CO and NOx (EPA, 2010).

The use of a vehicle's A/C system will often have a sizeable impact on the vehicle's energy consumption. This was found statistically by analyzing the available second by second data on CO_2 and other gaseous emissions, and converting them to an energy basis using standard EPA vehicle fuel economy certification mathematical expressions. The vehicle emission data were binned by VSPBin (see above). A mean value was computed for each combination of VSPBin. Separate analysis was done as a function of sourcebinid (combination of vehicle type, fuel type and model year), and the results were not statistically different versus sourcebinid given the relatively small sample sizes. As a result, the A/C adjustments for energy are a function of only VSPBin. The mean value of all the VSPBins calculated is: $28.649/24 \approx 1.19371$. This number shows the increase of the VSP demands when the AC is fully used.

The adjustments for each operating mode are weighted together by the operating mode distribution calculated from the driving schedules used to represent the driving behavior of vehicles. Average speed, road type and vehicle type will affect the operating mode distribution:

$$weightedFullACAdjustment = SUM(fullACAdjustment \times opModeFraction) \quad [96]$$

Since not all vehicles are equipped with air conditioning and air conditioning is normally not on all of the time, the full air conditioning effect on emissions is adjusted before it is applied to the emission rate. The SourceTypeModelYear table of the MOVES database (Table 43) contains the fraction of vehicles in each model year that are equipped with air conditioning which is the percentage of vehicles that were designed with an air conditioning system the specific year (Koupal & Kremer, 2001).

Institutional Repository - Library & Information Centre - University of Thessaly
09/12/2017 02:36:50 EET - 137.108.70.7

Model Year	Passenger Cars	All Trucks and Buses
1971*	0.592	0.287
1972	0.592	0.287
1973	0.726	0.287
1974	0.616	0.287
1975	0.631	0.287
1976	0.671	0.311
1977	0.720	0.351
1978	0.719	0.385
1979	0.694	0.366
1980	0.624	0.346
1981	0.667	0.390
1982	0.699	0.449
1983	0.737	0.464
1984	0.776	0.521
1985	0.796	0.532
1986	0.800	0.544
1987	0.755	0.588
1988	0.793	0.640
1989	0.762	0.719
1990	0.862	0.764
1991	0.869	0.771
1992	0.882	0.811
1993	0.897	0.837
1994	0.922	0.848
1995	0.934	0.882
1996	0.9484	0.9056
1997	0.9628	0.9292
1998	0.9772	0.950
1999	0.980	0.950
2000**	0.980	0.950
* 1971 model year fractions are applied to all previous model years. ** 2000 model year fractions are applied to all later model years. Motorcycles are not adjusted for air conditioning.		

Table 43: Fraction of Vehicles Equipped with Air Conditioning (ACPenetration) (EPA, 2010).

Institutional Repository - Library & Information Centre - University of Thessaly
09/12/2017 02:36:50 EET - 137.108.70.7

The fraction of vehicles whose air conditioning is operational varies by age of the vehicle and is stored in the SourceTypeAge table of the MOVES database (Table 44).

Age	Functioning	Age	Functioning	Age	Functioning
1	1.00	11	0.98	21	0.95
2	1.00	12	0.98	22	0.95
3	1.00	13	0.96	23	0.95
4	0.99	14	0.96	24	0.95
5	0.99	15	0.96	25	0.95
6	0.99	16	0.96	26	0.95
7	0.99	17	0.96	27	0.95
8	0.98	18	0.95	28	0.95
9	0.98	19	0.95	29	0.95
10	0.98	20	0.95	30	0.95

Table 44: Fraction of Air Conditioning Units Still Functioning By Age (EPA, 2010).

A mathematical expression is used to predict the fraction of those vehicle owners who have air conditioning available to them that will turn on the air conditioning based on the ambient temperature and humidity (heat index (Koupal & Kremer, 2001)) of the air outside their vehicles. The heat index values are stored in the ZoneMonthHour table of the MOVES database. The effect of the heat index on A/C activity is shown in Table 45.

$$ACOnFraction = ACActivityTermA + heatIndex \times (ACActivityTermB + ACActivityTermC \times heatIndex) \quad [97]$$

Institutional Repository - Library & Information Centre - University of Thessaly
09/12/2017 02:36:50 EET - 137.108.70.7

-3.63154	ACActivityTermA
0.072465	ACActivityTermB
-0.000276	ACActivityTermC
Heat Index	**AC On Fraction**
67.44	0.000
70	0.089
75	0.251
80	0.399
85	0.534
90	0.655
95	0.762
100	0.855
105	0.934
110	1.000

Table 45: Effect of Heat Index on Air Conditioning Activity (EPA, 2010).

The fraction of vehicles equipped with air conditioning, the fraction of operational air conditioning and the fraction of air conditioning use are used to adjust the amount of "full" air conditioning that occurs in each hour of the day.

$$ACAdjustment = 1 + ((weightedFullACAdjustment - 1) \times ACPenetration \times functioningACFraction \times ACOnFraction) \quad [98]$$

The air conditioning adjustment is a multiplicative adjustment applied to the emission rate after it has been adjusted for fuel effects. Air conditioners are employed for defogging at all temperatures, particularly, at lower temperatures. This secondary use of the A/C along with associated emission effects is not addressed in MOVES2010.

In 2006, another study examined the use of numerical models for estimating fuel consumption and emission of HC, CO, NO_x and CO_2 of gasoline vehicles, under urban driving conditions. The study was focused on the impact of road gradient in correlation with the use of A/C. Traffic conditions were also taken into account. Three models were selected for evaluation: EcoGest, CMEM and ADVISOR (Silva & Farias, 2006). The models were used to simulate a sample of 14 urban trips for two 1999 Ford Taurus vehicles. Trip statistics were monitored on-board of the passenger vehicles across a variety of traffic conditions, using a portable

Institutional Repository - Library & Information Centre - University of Thessaly
09/12/2017 02:36:50 EET - 137.108.70.7

emissions measurement device (PEMS). Table 46 shows selected trip statistics. A key conclusion was that the tested models can be used with relatively high confidence to predict fuel consumption and CO_2 emissions. However, results must be viewed with greater caution when it comes to predictions for other pollutants. There was also reference to the power consumption of the tested vehicle. Besides the experiments, there were no mathematical expressions given.

Trip	Road	A/C (on/off)	Km	v (km/h)	A (m/s^2)	#stop-go	FC (l/100 km)	HC (g/km)	CO (g/km)	NOx (g/km)	CO2 (g/km)
1	Chapel hill	On	3.9	17.8	2.2	9	15.2	0.074	0.72	0.023	361
2	Chapel hill	On	3.9	63.3	3.6	1	9.4	0.017	0.23	0.037	225
3	Chapel hill	On	3.9	51.6	3.6	2	11.8	0.035	0.77	0.079	280
4	Chapel hill	On	3.9	35.1	3.6	5	12.6	0.038	0.63	0.073	300
5	Walnut Street	On	3.5	33.7	4.5	4	13.5	0.049	0.66	0.071	322
6	Walnut Street	On	3.4	31.0	4.0	5	13.3	0.0267	0.29	0.041	317
7	Walnut Street	On	3.5	29.5	2.7	4	13.7	0.042	0.34	0.044	326
8	Walnut Street	Off	3.4	30.2	3.6	6	13.5	0.046	0.89	0.071	321
9	Walnut Street	Off	3.5	45.1	2.7	3	9.7	0.024	0.33	0.031	230
10	Walnut Street	Off	3.5	37.0	3.1	4	10.9	0.047	0.68	0.038	259
11	Walnut Street	Off	3.4	42.5	3.6	3	10.5	0.038	0.39	0.056	250
12	Walnut Street	Off	3.5	38.0	3.6	5	10.7	0.039	0.35	0.032	255
13	Walnut Street	Off	3.5	31.9	3.6	4	12.7	0.044	0.38	0.047	301
14	Chapel hill	Off	4.0	17.1	2.2	9	14.9	0.057	0.58	0.036	356
v = average speed / a = maximum acceleration / FC = fuel consumption											

Table 46: Monitored trip statistics (Silva & Farias, 2006).

It was assumed that A/C use increases power consumption by 2 kW, on average, for light-duty vehicles. For cruise speeds of 10–120 km/h, and for several stop and go situations, models predicted an increase of 6–67% in fuel consumption and CO_2 emissions (relatively to the runs without A/C), 3–8% increase in HC%, 6–140% increase in CO and 7–230% in NO_x emission. This is consistent with reported values by (Welstand, Haskew, Gunst, & Bevilacqua, 2003) and (Nam , 2000) which were increases of 25–30% in fuel consumption, no effect on HC, except on few limited cases, with a maximum 10% increase, 0–200% increase in CO emissions and 10–100% increase in NO_x emissions.

Another report conducted by EPA and Eurobitume in 2004, presented the factors that impact the energy/fuel consumption for a vehicle. The rolling resistance and air resistance were examined for their impact on Light Duty and Heavy Duty Vehicles (EAPA & EUROBITUME, March 2004). In this section, we will present the first option as HDVs are going to be presented later in a following section. During the study, there was no reference to the emission rates of the vehicle as the paper was concentrated on the power and the fuel consumption of the vehicle for overcoming the rolling resistance. The results below come

Institutional Repository - Library & Information Centre - University of Thessaly
09/12/2017 02:36:50 EET - 137.108.70.7

from experiments held in the past and no mathematical expressions are presented, they are general and do not depend on a specific type of road surface (asphalt, concrete, composite) or the age of the pavement. Figure 52 taken from a Michelin publication (Michelin, 2003) shows how mechanical power available at the engine crankshaft is distributed as a function of the vehicle speed (no climbing, no acceleration).

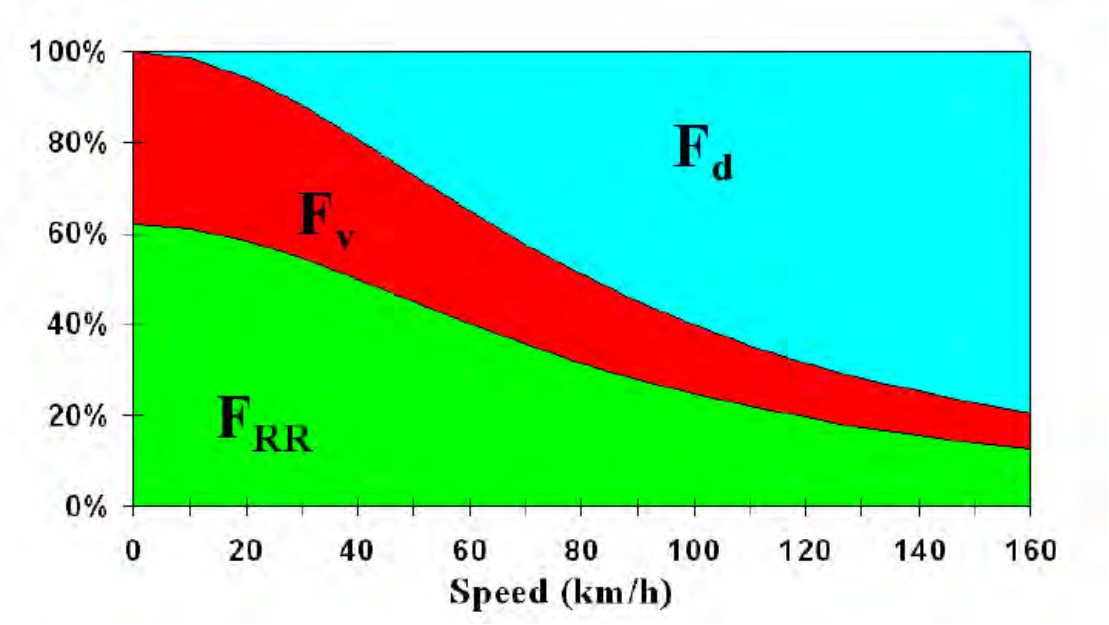

Part of different forces as a function of speed for a passenger car: Fd = Air drag, Fv = Internal friction and FRR = Rolling resistance.

Figure 52: Energy distribution in a passenger car versus speed as a percentage of the available power output at the crankshaft (Michelin, 2003).

For passenger cars driving at a constant speed of 100 km/h, the rolling resistance accounts for 25% of the available mechanical engine power output, air drag represents 60% of energy loss and internal friction (drive line loss) for 15% according to Michelin. Passenger cars are normally overpowered and therefore have less efficient running engines, in particular gasoline fuelled engines. As a percentage of the fossil fuel input it is estimated that rolling resistance losses account for 15 to 20% for such vehicles. At high speeds air drag becomes the largely predominant factor.

In 2006, another report examining the impact of the rolling and the air resistance in combination was published. CSTT (Centre for Surface Transportation Technology) provided an independent third-party evaluation to quantify the potential fuel consumption differences when vehicles are driven over three distinct types of pavements: asphalt, concrete and composite (asphalt top-coat over concrete) (Taylor, Eng, & Patten, 2006). CSTT developed comprehensive performance tests that were conducted between fall 2002 and fall 2003 to quantify these potential fuel consumption differences. There were limited data collected for a passenger car that was tested in one loading condition, winter and summer weather conditions

Institutional Repository - Library & Information Centre - University of Thessaly
09/12/2017 02:36:50 EET - 137.108.70.7

over all three pavement types (asphalt, concrete, composite) independently of the age of pavement. Prior to the commencement of this testing, the National Research Council and the Cement Association of Canada had engaged in two previous pavement fuel efficiency studies. Although the main objective of this Phase III study was to quantify the fuel efficiency of a heavy haul tractor-trailer combination, a passenger car component was added to the test program, to broaden the spectrum of analysis. All results presented concern the fuel consumption and there is no reference to the power consumption or the emission rates of the vehicle. There were also mathematical expressions provided that contained all the variables measured.

The vehicle was equipped with a communication cable connected to the onboard diagnostic (OBDII) engine communication system on the vehicle with laptop computer recording the information. The test conditions included winter and summer temperature ranges. The winter car tests were performed in March 2003. The pavement temperature conditions ranged from -11 to +5℃. The summer tests were undertaken in September 2003. The pavement temperature conditions for the summer tests ranged from +20 to +34℃.

The passenger car was tested in two separate temperature ranges as follows:

Season	**Ambient Temperature Range**
Winter	$< -10℃$
Summer Cool	$> +15℃$ and $< +25℃$

(These temperatures were selected to give a broad range of data, while respecting the limited time allotted for car testing)

Table 47: Ambient conditions for the experiment (Taylor, Eng, & Patten, 2006).

The passenger car was tested using one load condition as follows:

Load Condition	**Weight**
Curb weight, 2 occupants and baggage	1756 kg

Table 48: Load conditions for the experiment (Taylor, Eng, & Patten, 2006).

Pavement structure was represented in the model by two indicator values, Pvash and Pvcomp:

- the first took on a value of one (1) for asphalt and zero (0) otherwise,
- the other took a value of one (1) for composite and zero (0) otherwise.

The analysis developed a model which estimated fuel consumption rate (L/100km) as a function of pavement structure, vehicle load, air or pavement temperature, vehicle speed, wind speed, IRI, grade, and various interactions among these variables.

Institutional Repository - Library & Information Centre - University of Thessaly
09/12/2017 02:36:50 EET - 137.108.70.7

In order to quantify and compare the savings in fuel consumption on concrete relative to asphalt or composite pavements, point estimates and confidence bounds were determined for expected fuel consumption on each surface for a range of temperatures in each seasonal model.

During the winter testing, the regression modeling resulted in the following regression mathematical expression:

$$FC = 12.6 + 0.285 \times Pvash - 0.227 \times Pvcomp - 0.0417 \times IRI + 2.03 \times Grade - 0.0607 \times Pavetemp - 0.0509 \times v + 0.000202 \times AirSpdSq \quad [99]$$

where

FC:	fuel consumption rate in L/100km;
IRI:	International Road Roughness Index;
Grade:	Road grade in percent;
Pavetemp:	Pavement or ambient temperature in degrees Celsius;
v:	Vehicle road speed in km/h;
AirSpdSq:	Absolute air speed (road speed plus relative wind speed) squared.

Each table below gives point estimates. The resulting point estimates are provided along with their 95th percentile confidence for expected fuel consumption for cars on smooth road surfaces. The third column shows the mean value of the estimated fuel consumption between the 95% lower and upper bound. Increases in expected fuel consumption for asphalt and composite surfaces relative to concrete are also given. All calculations are based on an IRI of 1.0, a vehicle speed of 100 km/hr, an air speed of 100 km/hr (assuming a wind speed of 0 km/hr), and a grade of 0.

Institutional Repository - Library & Information Centre - University of Thessaly
09/12/2017 02:36:50 EET - 137.108.70.7

Ambient Temp	Surface	Estimate FC(L/100 km)
0	Asphalt	9.8
-4.2	Asphalt	10.1
-8.5	Asphalt	10.4
0	Composite	9.3
-4.5	Composite	9.6
-8.9	Composite	9.9
0	Concrete	9.5
-4.3	Concrete	9.8
-8.6	Concrete	10.1

Table 49: Car Winter Point Estimates, 100 km/h (Taylor, Eng, & Patten, 2006).

Again, the same model formulation was used as for the summer data and resulted in the following mathematical expression:

$$FC = 14.2 + 0.0263 \times Pvash - 0.125 \times Pvcomp - 0.0772 \times IRI + 1.78 \times Grade - 0.0462 \times Pavetemp - 0.0744 \times v + 0.000252 \times AirSpdSq \quad [100]$$

Ambient Temp	Surface	Estimate FC(L/100 km)
25.4	Asphalt	7.8
21.1	Asphalt	8.1
17	Asphalt	8.3
27	Composite	8.0
22.5	Composite	8.2
18	Composite	8.4
26	Concrete	7.9
21.5	Concrete	8.1
17.2	Concrete	8.3

Table 50: Car Summer Points Estimates, 100 km/h (Taylor, Eng, & Patten, 2006).

CSTT's primary conclusions stemming from the passenger car testing and subsequent statistical models are summarized below and they are also shown in Table 51:

- All models have negative coefficients for pavement and ambient temperature and thus as the temperature increases the fuel consumption decreases.

Institutional Repository - Library & Information Centre - University of Thessaly
09/12/2017 02:36:50 EET - 137.108.70.7

- In winter testing, the passenger car consumed 0.3 l/100 km more (2.9%) on asphalt than on concrete. These savings were all statistically significant.
- In winter testing, the car consumed 0.2 l/100 km less fuel (2.3%) on composite pavement when compared to concrete. These savings were all statistically significant.
- In summer testing, the passenger car consumed 0.1 l/100 km (1.5%) more fuel on composite roads when compared to concrete. These savings were all statistically significant.
- In summer testing, the passenger car consumed 0.05 l/100 km (0.3%) less fuel on asphalt roads when compared to concrete. However, these savings were not
- statistically significant.

Winter	**FC**
Asphalt to Concrete	2.9% more
Composite to Concrete	2.3% less
Summer	**FC**
Asphalt to Concrete	0.3% less
Composite to Concrete	1.5% more

Table 51: General conclusions.

The last study found to examine the rolling and air resistance together was in 2012. A report by (Hammarstrom, Eriksson, Karlsson, & Yahya, 2012) was produced on commission of the Swedish Transport Administration and constitutes one part of the MIRIAM sp2 project. According to it, to evaluate traffic energy changes due to the improvement of road surface standard one needs to describe:

- rolling resistance at different road surface conditions;
- all other driving resistance;
- fuel consumption (*FC*) as a function of driving resistance.

In the study, some mathematical expressions are provided but also experimental data are presented. The type of road and the age of pavement are not specified. No reference to the emissions of the vehicle exists. Based mainly on empirical data from coast down measurements in Sweden, a general rolling resistance model – with roughness (*IRI*), macrotexture (*mpd*), temperature and speed as explanatory variables – was developed and calibrated for three types of vehicle; car; heavy truck and heavy truck with trailer. The passenger car results are going to be presented here as we will refer to HDVs in the next section. This rolling resistance model had been incorporated into a driving resistance based *FC* model with a high degree of explanation. The *FC* function also included variables for horizontal curvature and the road gradient . These functions may appropriately be included in

Institutional Repository - Library & Information Centre - University of Thessaly
09/12/2017 02:36:50 EET - 137.108.70.7

the Swedish road planning system (EVA). In EVA the road alignment standard is classified into four sight classes (*scl 1–4*) from high to low. Rolling resistance caused by IRI is dependent on speed.

- At a speed of 90 km/h, when IRI and *mpd* increase by one unit, the rolling resistance will increase for a car by 4.6% and 15.1%;
- At an average speed of 90 km/h and an alignment standard *scl 1*, *Fc* increases, per unit increase of IRI and *mpd*: 0.8% and 2.8%;
- At the same average speed, 90 km/h, *Fc* increases when the alignment standard decreases from *scl 1* to *scl 4* by 7.1%;
- A wider road at the same alignment standard *scl 1* will increase speed and then also *FC*. A motorway section instead of a two lane section, at a speed limit of 90 km/h, will increase *FC* at free flow conditions for a car 3.8%.

The final rolling resistance (RR) model for a private car, used in this report, heavily rests on the work by (Karlsson, Hammarström, Sörensen, & Eriksson, 2011). Their method was summarized and the modifications of their results that have been done in Miriam were presented.

Basically, the coastdown method was applied to estimate the RR parameters for two different tires. From earlier projects (ECRPD and Production measurements) a large number of coastdown measurement data was available. Essentially, the following model was used:

$$y = Fz \times (Cr00 + CrTemp \times (5 - T) + CrMPD \times mpd + CrIRIV \times iri \times (v - 20)) + CrSide \times Fy^2 + CL \times AIR + CLbeta \times AIR \times \sin(beta) \quad \textbf{(model 1)} \qquad [101]$$

where

Crxx, CLxx:	model parameters to be estimated by regression;
Fz	vertical load per tyre (N);
y:	is the decelerating force acting on the vehicle (adjusted for gravitational; forces and transmission losses);
T:	the air temperature;
mpd:	mean profile depth (road macrotexture);
IRI:	International Roughness Index (road unevenness);
v:	velocity [m/s];
Fy:	side force acting on the vehicle.

Institutional Repository - Library & Information Centre - University of Thessaly
09/12/2017 02:36:50 EET - 137.108.70.7

$$AIR = A_{Frontal} \times v^2 \times \frac{\rho}{2} \times \cos(\theta) \quad [102]$$

where

$A_{Frontal}$:	the frontal area of the vehicle;
v:	the air speed (relative to the vehicle);
ρ:	air density;
θ:	angle between the vehicle velocity and the resultant air velocity vector.

Note that RR only comprises the terms containing C_r00, C_rTemp, C_rMPD, C_rIRI and $C_rIRI \times v$. A disadvantage with this model is that it is unphysical in the sense that the RR contribution from unevenness (IRI) does not tend to zero when IRI tend to zero. In order to avoid this defect, the two IRI terms can be replaced by a single term $C_rIRI\_v\_EXP \times \text{IRI} \times v$. So the second (optimized) model will be:

$$y = Fz \times (C_r00 + CrTemp \times (5 - T) + C_rMPD \times mpd + C_rIRI\_v\_EXP \times \text{IRI} \times v) + C_rSide \times Fy^2 + CL \times AIR + CLbeta \times AIR \times \sin(\theta) \quad \textbf{(model 2)} \quad [103]$$

Another difficulty is that both models require that the decelerating force, *y*, is adjusted for transmission losses. The transmission losses are modeled as a constant force, *C0*, independent of the weight of the vehicle. In the work by (Karlsson, Hammarström, Sörensen, & Eriksson, 2011), transmission losses were estimated using special coastdown measurements with varying vehicle weights. The resulting value, *C0=65.5 N*, was, however, very unreliable. In hindsight, this value is probably too large and a more reasonable value is probably 40 N.

A further circumstance that should be noted is that the above models were estimated for two types of tires only, normal Michelin Energy and stubbed winter tires. Most of the measurements were done using the Michelin Energy tires. For the Miriam project it was desirable to modify the parameters to better correspond to a representative vehicle. From drum measurement data covering 90 different tires, it was found that the *mpd* coefficient, C_rMPD, for the Michelin Energy tire was fairly representative (slightly lower than the average value). On the other hand, the basic rolling resistance was untypically low. Therefore an adjustment of the coefficient C_r00 was done. Drum measurement data indicated that C_r00 for a representative vehicle can be expected to exceed the probe tires by 1.67e-3.

In Table 52 estimated parameters for the model 1 (columns A, B and C) and model 2 (columns D and E) are shown. In column A, the original parameter estimations made in (Karlsson, Hammarström, Sörensen, & Eriksson, 2011) are displayed. In column B,

Institutional Repository - Library & Information Centre - University of Thessaly
09/12/2017 02:36:50 EET - 137.108.70.7

corresponding estimations using a more reasonable value for the transmission losses (*C0=40 N* instead of *65.5 N*). It is evident that only the basic rolling resistance (C_r00) is affected, while all other terms are virtually unchanged. This is due to the large correlation between the transmission resistance and the basic rolling resistance (the vehicle weight varies only by a small amount between the measurements). In column C, C_r00 has been adjusted to a more representative value, as indicated by drum measurement data. In columns D and E, values corresponding to columns B and C are shown, but for the second model (Eq. [103]) instead of the first one (Eq. [102]).

	A	**B**	**C**		**D**	**E**
C0	65.5N	40N	40N		40N	40N
C_r**00**	6.48E-03	8.02E-03	9.69E-03	C_r**00**	7.76E-03	9.43E-03
C_r**Temp**	1.04E-04	1.03E-04	1.03E-04	C_r**Temp**	1.04E-04	1.04E-04
C_r**MPD**	1.72E-03	1.72E-03	1.72E-03	C_r**MPD**	1.72E-03	1.72E-03
CrIRI	4.66E-04	4.66E-04	4.66E-04	C_r**IRI_v_EXP**	2.10E-05	2.10E-05
CrIRI_V	3.65E-05	3.65E-05	3.65E-05			
CrSide	2.52E-05	2.51E-05	2.51E-05	**CrSide**	2.45E-05	2.45E-05
CL	0.4257	4.26E-01	4.26E-01	**CL**	4.36E-01	4.36E-01
CLbeta	0.5446	5.43E-01	5.43E-01	**CLbeta**	5.44E-01	4.36E-01

Table 52: Parameters for model number1 obtained by (Karlsson et al, 2011) and for model number2 computed in Miriam Sp2. Reference temperature is 5°C. (Additional dummy terms included in the regressions are not shown here) (Hammarstrom, Eriksson, Karlsson, & Yahya, 2012).

A general rolling resistance mathematical expression had been estimated representing an ambient temperature of 8° C:

$$Fr = m1 \times curv \times (0.00912 + 0.0000210 \times IRI \times v + 0.00172 \times mpd) \quad [104]$$

where v speed (m/s), mpd the macrotexture and $curv$ the curvature term.

These parameter values have been used both in VETO simulations and in the *Fct* function. For each vehicle category one *FC* function has been calibrated and so has been for the passenger car examining here:

The estimation of parameter values has been based on the *Fct* approach:

$$Fct = c0 \times (1 + k5 \times (Fr + Fair + d1 \times ADC \times v^2 + d2 \times RF + d3 \times RF^2))^{e1} \times v^{e2} \quad [105]$$

where

Institutional Repository - Library & Information Centre - University of Thessaly
09/12/2017 02:36:50 EET - 137.108.70.7

ADC: average degree of curvature (rad/km);

RF: Rise and Fall (m/km)

Fair: $Cd \times Ayz \times \rho \times \frac{v^2}{2}$;

ρ: 1.293 (kg/m3);

Fct: fuel consumption (L/h);

Estimated parameter values in *Fct* are presented in Table 53.

Parameter	**Estimate**	**Lower bound***	**Upper bound***
c0	0.103	0.101	0.105
k5	0.00156	0.001	0.002
d1	0.0516	0.050	0.053
d2	-3.906	-4.103	-3.709
d3	0.1898	0.184	0.196
e1	1.163	1.100	1.225
e2	1.056	1.050	1.063
R^2	1.000		

**95%*

Table 53: Estimated car parameter values in the function approach (Fct) (Hammarstrom, Eriksson, Karlsson, & Yahya, 2012).

One can notice that all estimated parameter values are significant different from zero. The degree of explanation is high. Several approaches in order to describe the interaction between *ADC* respectively *RF* and other variables have been tested.

For a gradient, average upwards and downwards, there is no extra energy use until there is need for use of brakes downwards. The influence of a horizontal curve is most complicated. An approach with "$RF \times v^2$" turned out as the best alternative tested.

The resulting parameter values for *Fcs* are presented in Table 54.

$$Fcs = \frac{Fct}{v \times \frac{3600}{10000}} = c1 \times (1 + k5 \times (Fr + Fair + d1 \times ADC \times v^2 + d2 \times RF + d3 \times RF^2))^{e1} \times v^{e2-1} \quad [106]$$

where

Fcs: fuel consumption (l/10 km)

Institutional Repository - Library & Information Centre - University of Thessaly
09/12/2017 02:36:50 EET - 137.108.70.7

Parameter	Car
c0	0.286
k5	0.00156
d1	0.0516
d2	-3.906
d3	0.1898
e1	1.163
e2	1.056

Table 54: Estimated parameter values in the Fcs (l/10km) function (Hammarstrom, Eriksson, Karlsson, & Yahya, 2012).

The *Fcs* function for the car would then be:

$$Fcs = 0.286 \times ((1.209 + 0.000481 \times iri \times v + 0.0394 \times mpd + 0.000667 \times v^2 + 0.0000807 \times ADC \times v^2 - 0.00611 \times RF + 0.000297 \times RF^2)^{1.163}) \times v^{0.056} \quad [107]$$

In 2010, there was a study published about the effect of pavement type on fuel consumption and emissions in city driving, examining the impact or the rolling resistance in correlation with the existing weather conditions (Ardekani & Sumitsawan, 2010). This study was based on the previous study of (Sumitsawan, Romanoschi, & Ardekani, August 2009) but included also experiments on wet pavements. The main objective of this study has been to investigate any differences that might exist in fuel consumption and CO_2 emissions when operating a motor vehicle on an Asphalt Concrete (AC) versus a Portland Cement Concrete (PCC) pavement under city driving conditions. During the study there was no reference about how the rolling resistance can affect the power consumption of the vehicle. The data provided were experimental results and there were no mathematical expression provided. The age of pavement was not a factor that was taken into account during the experiments. Accordingly, two pairs of street sections in Arlington, Texas (two asphalt sections and two concrete sections) were selected for fuel consumption studies. Each pair of streets (one AC and one PCC) had similar gradients and roughness indices. The streets were also approximately parallel so as to minimize the effect of wind direction and velocity during measurement runs. In the course of the fuel consumption measurements, every attempt was made to either control all other factors that could affect fuel consumption or keep the factors that cannot be controlled the same. Two different driving modes (cruise vs acceleration) were used in the test runs. Under the constant speed mode, a cruise speed of 30 mph was maintained

Institutional Repository - Library & Information Centre - University of Thessaly
09/12/2017 02:36:50 EET - 137.108.70.7

throughout the test run. In the acceleration mode, the fuel consumption data were collected while accelerating from zero to 30 mph in 10 seconds, yielding an average acceleration rate of 3 mph/second. The cases studied are shown in Table 62Table 55.

Factor-Level Combination	Pavement Type	Driving Mode	Surface Ambient Condition
1	PCC	Constant Speed	Dry
2	PCC	Constant Speed	Wet
3	PCC	Acceleration	Dry
4	PCC	Acceleration	Wet
5	AC	Constant Speed	Dry
6	AC	Constant Speed	Wet
7	AC	Acceleration	Dry
8	AC	Acceleration	Wet

Table 55: The Eight-Factor Level Combinations (Ardekani & Sumitsawan, 2010).

As shown in the table below, it was found that the fuel consumption rates per unit distance were consistently lower on the PCC sections regardless of the test section, driving mode (acceleration vs. constant speed), and surface condition (dry vs. wet). In all cases, the differences were found to be statistically significant at 10% level of significance. The fuel consumption rates in this table indicate fuel consumption savings of 3% to 17% on PCC pavements depending on the driving mode, surface conditions, and crown and substructure materials and thicknesses. The percentage savings could also vary depending on the vehicle mix.

Institutional Repository - Library & Information Centre - University of Thessaly
09/12/2017 02:36:50 EET - 137.108.70.7

	Surface Condition	
	Dry	**Wet**
	Average Fuel Consumption (10^{-3} gals/mile)	**Average Fuel Consumption (10^{-3} gals/mile)**
Road to Six Flags (PCC) Constant Speed of 30 mph	42.2	45.6
Randol Mill Rd (AC) Constant Speed of 30 mph	51.3	55.3
Road to Six Flags (PCC) Acceleration of 3 mph/sec	240.2	226.1
Randol Mill Rd (AC) Acceleration of 3 mph/sec	257.7	259.9
Abram Street (PCC) Constant Speed of 30 mph	45.6	54.1
Pecandale Dr (AC) Constant Speed of 30 mph	49.5	55.9
Abram Street (PCC) Acceleration of 3 mph/sec	232.8	260.6
Pecandale Dr (AC) Acceleration of 3 mph/sec	247.0	269.3

Table 56: Average fuel consumption rates for PCC versus AC sections

An analytical tool in the form of a spreadsheet program was also developed to estimate the fuel consumption and emissions savings or costs based on user-specified project conditions, namely pavement type and expected vehicle mix and miles of travel. It was shown that for a typical metropolitan area, these user cost differences could be substantial over the design life of a city street pavement.

Based on the above objectives, the main outcomes of the study were as follows:

- Statistical comparison of relative fuel economy differences for concrete and asphalt pavement surfaces under urban driving conditions.
- A spreadsheet tool to estimate fuel consumption and emissions for the pavement types and surface conditions studied so that the resulting savings or costs could be quantified and incorporated into the life-cycle cost analysis of different pavement design alternatives.

Institutional Repository - Library & Information Centre - University of Thessaly
09/12/2017 02:36:50 EET - 137.108.70.7

The CO_2 emissions in the PCC case were estimated using the same mathematical expressions as a previous study (Sumitsawan, Romanoschi, & Ardekani, August 2009).

This study aimed at investigating any statistically significant differences which might exist in fuel consumption rates on typical concrete versus asphalt city streets. The study was conducted through field data collections using an instrumented van. The scope of the study was limited to assessing any such differences through field data collection. However, the study scope did not include any theoretical assessment of pavement/tire interactions or other mechanical reasons as to why such differences might exist. It was observed that under urban driving speeds of 30 mph, the fuel consumption per unit distance is lower on concrete pavements compared to asphalt pavements. These findings were based on test runs on two sets of typical PCC and AC street sections in Arlington, Texas, with each pair of study sites having similar gradient and roughness index values. The results were found to hold for either dry or wet surface conditions, although wet surface conditions generally resulted in higher fuel consumption rates compared to dry conditions regardless of pavement type. All observed differences were found to be statistically significant at 10% level of significance.

The potential savings or costs in fuel consumed and CO_2 emissions generated were shown to be substantial over the design life of a project. As a result, it is recommended that these savings or costs be considered in the life cycle cost analysis of alternative projects. Differences in CO_2 emissions should also be considered in life cycle analysis when estimating the carbon footprint of particular pavement materials to be used.

5.2.1.2 Studies examining three parameters

In 2005, Sangiun Park and Hesham Rakha in their paper offered a systematic analysis of the impact of roadway grades on vehicle fuel consumption and emission rates using the INTEGRATION microscopic traffic simulation software taking also in account the influence of the rolling resistance and the air resistance (Park & Rakha, 2005). The energy and emission impacts were quantified for various cruising speeds, under stop and go conditions, and for various traffic signal control scenarios in a highway road. The results demonstrated that the impact of roadway grade is significant with increases in vehicle fuel consumption and emission rates in excess of 9% for a 1% increase in roadway grade. Consequently, a reduction in roadway grades in the range of 1% can offer savings that are equivalent to various forms of advanced traffic management systems. Some mathematical expressions were provided but the results were carried out through experiments. There was no reference to the power demands of the vehicle and how it can be affected by the gradient. Correlation of the gradient with other parameters like the aerodynamic resistance and the rolling resistance were taken into account.

Institutional Repository - Library & Information Centre - University of Thessaly
09/12/2017 02:36:50 EET - 137.108.70.7

The INTEGRATION software computed the effective tractive force as the minimum of two forces; namely: the maximum engine tractive force (F_e) and the maximum frictional force that can be sustained between the vehicle wheels and the roadway surface (F_{max}). The aerodynamic resistance (R_a), rolling resistance (R_{rl}), and the grade resistance (R_g) were also computed each deci-second. Subsequently, the maximum vehicle acceleration was then computed as:

$$a = \frac{\min(F_e\ , F_{max}) - \ (R_a + \ R_{rl} + R_g\ )}{m} \qquad [108]$$

where a is the vehicle acceleration (m/s^2) and m is the vehicle mass (kg).

In estimating vehicle emissions, given that the power required to overcome the aerodynamic and rolling resistance forces were accounted for in the development of the fuel consumption and emission models, the effective vehicle acceleration was adjusted to account for the additional acceleration required to overcome the component of the vehicle weight opposing the vehicle motion as:

$$a_\varepsilon = a + 9.8067\ \times Grade \qquad [109]$$

where a_ε is the effective acceleration (m/s^2) and 9.8067 is the acceleration of gravity (m/s^2).

Firstly, there had been held simulations for constant speed scenarios for both normal and high emitting vehicles. These runs were executed by simulating the motion of a vehicle along a 1-km section at a constant speed. Vehicle fuel consumption and emission rates were computed for the entire trip to compute a distance based fuel consumption and emission rate. The results demonstrated, as would be expected, an increase in the vehicle fuel consumption and emission rate with an increase in the roadway grade, as illustrated in Figure 53. As we can see, the minimum fuel consumption rate occurring at a speed of 75 km/h and the minimum CO_2 rate occurs at a cruise speed of 75 km/h for a 0 to 6% grade. HC, CO, NO_x emissions are more sensitive to roadway grades. NO_x and CO_2 emissions are more sensitive to roadway grades in the 35 to 95 km/h cruise speed range.

Institutional Repository - Library & Information Centre - University of Thessaly
09/12/2017 02:36:50 EET - 137.108.70.7

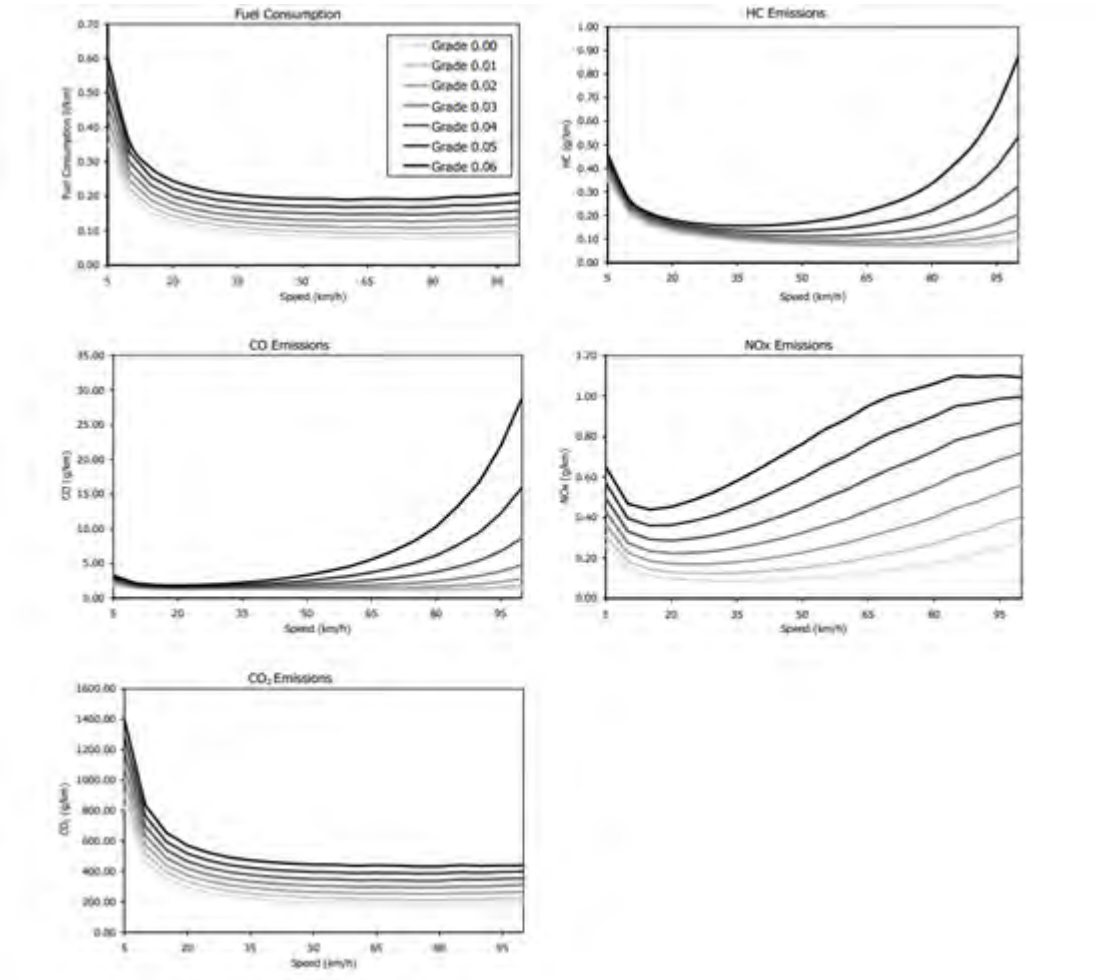

Figure 53: MOE profiles for Normal LDV [Figure 1, (Park & Rakha, 2005)].

The variation in CO_2 emission rates as a function of cruise speed and roadway grade appears to be similar to that of fuel consumption. Specifically, the CO_2 emission rates demonstrate a bowl shaped functional form with respect to cruise speed with the highest rates occurring at low speeds. However, the minimum CO_2 emission rate, unlike the fuel consumption rate, varies as a function of the roadway grade. Specifically, the minimum CO_2 rate occurs at a cruise speed of 75 km/h for a 0 to 6% grade, as demonstrated in Table 57.

Institutional Repository - Library & Information Centre - University of Thessaly
09/12/2017 02:36:50 EET - 137.108.70.7

Grade		Fuel Consumption		HC		CO		NOx		CO_2	
		Speed (km/h)	Rate (l/km)	Speed (km/h)	Rate (g/km)	Speed (km/h)	Rate (g/km)	Speed (km/h)	Rate (g/km)	Speed (km/h)	Rate (g/km)
Max	0%	5	0.354	5	0.347	5	1.876	100	0.283	5	822.71
	1%	5	0.389	5	0.363	5	2.046	100	0.407	5	905.17
	2%	5	0.427	5	0.378	100	2.783	100	0.560	5	992.98
	3%	5	0.467	5	0.395	100	4.764	100	0.719	5	1086.13
	4%	5	0.509	5	0.415	100	8.645	100	0.869	5	1184.83
	5%	5	0.554	100	0.532	100	15.977	100	0.996	5	1288.84
	6%	5	0.601	100	0.872	100	28.881	95	1.102	5	1398.16
Min	0%	75	0.078	75	0.070	80	1.128	30	0.087	75	180.85
	1%	75	0.092	75	0.071	75	1.221	30	0.123	75	212.26
	2%	75	0.108	65	0.080	30	1.359	25	0.169	75	250.99
	3%	75	0.127	60	0.093	20	1.435	20	0.223	75	292.99
	4%	75	0.147	50	0.112	20	1.533	20	0.287	75	337.97
	5%	60	0.168	45	0.133	20	1.660	15	0.360	75	384.94
	6%	60	0.190	35	0.156	20	1.818	15	0.439	75	432.75

Table 57: Max/Min Fuel Consumption and Emission Rates (Normal LDV) [Table 1, (Park & Rakha, 2005)].

Fuel consumption and CO_2 emission rates are found to be more sensitive to variations in cruise speed levels than to variations in roadway grades. Alternatively, HC, CO, NO_x emissions are more sensitive to roadway grades. Furthermore, NO_x and CO_2 emissions are more sensitive to roadway grades in the 35 to 65 km/h and the 65 to 95 km/h cruise speed range, respectively, as illustrated in Figure 54. Alternatively, HC and CO emissions are more sensitive to roadway grades at high cruise speeds (100 km/h).

Institutional Repository - Library & Information Centre - University of Thessaly
09/12/2017 02:36:50 EET - 137.108.70.7

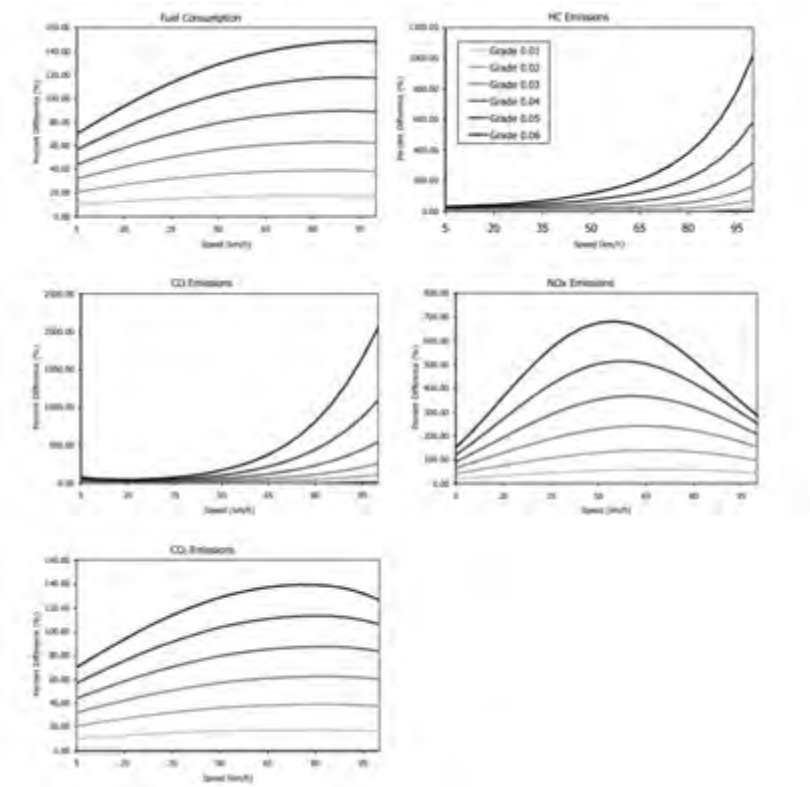

Figure 54: Percent change in MOEs relative to 0% grade for Normal LDV [Figure 2, (Park & Rakha, 2005)].

During the study, there was also a simulation of the signal control scenario. A description of the Performance Index (PI) concept was presented given that it was utilized as an objective function in computing the optimum traffic signal offsets. The PI is computed as:

$$Performance\ Index = number\ of\ Stops\ \times 10 + Total\ \ Delay \quad [110]$$

First, the optimal offsets were computed to maximize the Performance Index PI. Subsequently, the environmental impacts were computed for the identified signal timings. The optimal offset based on the PI was 40 s at 0, 1, 2, and 3% grade and 30 s at 4, 5, and 6% grade. Figure 55 illustrates the variation of MOEs as a function of roadway grades and signal offsets for the Normal LDV. The figures demonstrate that the roadway grade is critical in estimating fuel consumption and emission rates. More specifically NO_x emissions are extremely sensitive to roadway grades.

Institutional Repository - Library & Information Centre - University of Thessaly
09/12/2017 02:36:50 EET - 137.108.70.7

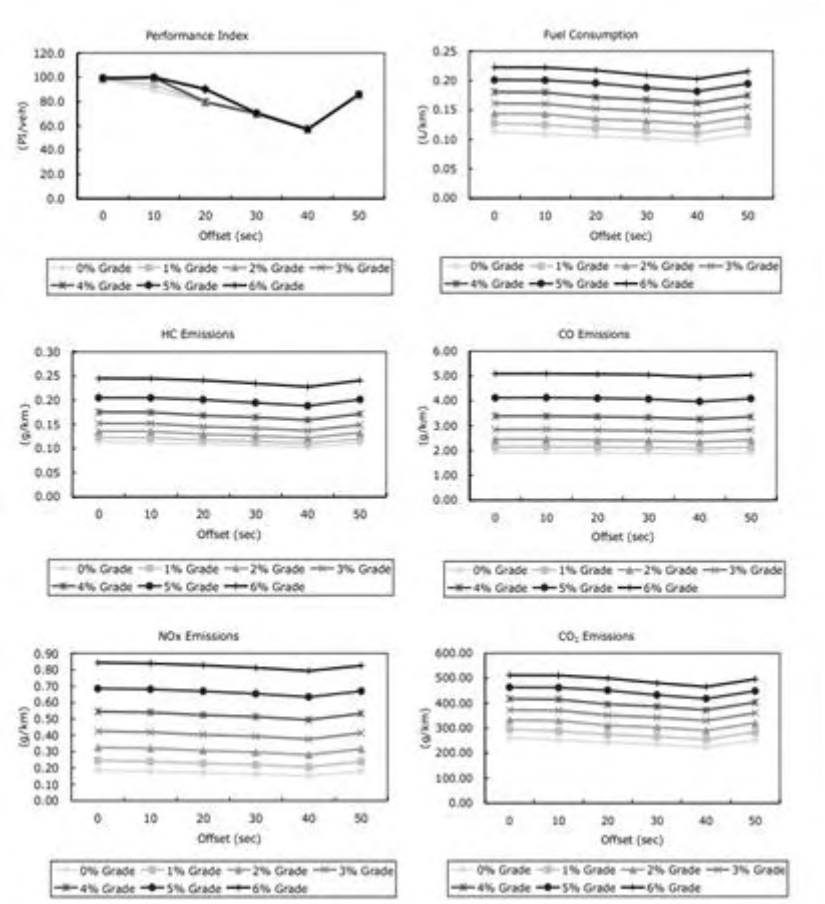

Figure 55: PI and MOEs as a function of signal offsets for Normal LDV [Figure 5, (Park & Rakha, 2005)].

The fuel consumption and vehicle exhaust emissions increased as roadway grade levels increase. The percentage changes in MOEs were significant, even for a 1% increase in roadway grade levels, regardless of the vehicle type (normal versus high emitter), as demonstrated in Table 58 and Figure 56.

Institutional Repository - Library & Information Centre - University of Thessaly
09/12/2017 02:36:50 EET - 137.108.70.7

Grade		Uniform Speed Scenario		Stop Sign Scenario		Signal Scenario	
		Normal	High Emitter	Normal	High Emitter	Normal	High Emitter
0%	Fuel (L/km)	0.801	0.0709	0.0982	0.0802	0.0968	0.0824
	HC (g/km)	0.0720	1.1581	1.1749	1.3674	0.1030	1.5501
	CO (g/km)	1.1625	13.0496	4.3436	15.6208	1.8534	17.0251
	NOx (g/km)	0.1247	1.8709	0.2218	1.9440	0.1514	1.7963
	CO_2 (g/km)	185.2292	141.7317	222.2241	157.7008	223.0919	160.9206
1%	Fuel (L/km)	0.0943	0.0818	0.1109	0.0909	0.1103	0.0928
	HC (g/km)	0.0728	1.2856	0.1939	1.4874	0.1111	1.6693
	CO (g/km)	1.2327	14.6258	5.0308	17.0627	2.0726	18.4108
	NOx (g/km)	0.1980	2.1332	0.2851	2.1803	0.2058	1.9552
	CO_2 (g/km)	218.3178	165.7147	250.7782	181.2075	254.2866	183.0239
6%	Fuel (L/km)	0.1924	0.1511	0.2039	0.1552	0.2027	0.1596
	HC (g/km)	0.2141	2.1307	0.4241	2.2850	0.2276	2.4746
	CO (g/km)	5.3574	29.4986	11.8173	30.0671	4.9459	30.3239
	NOx (g/km)	0.9432	3.8262	0.9400	3.6576	0.7928	3.1558
	CO_2 (g/km)	440.7586	299.8061	456.8297	306.4108	465.4452	317.6261

Table 58: Comparison of scenarios at 0%, 1%, and 6% grade (FFS = 64km/h, Max. Acc. Level = 60%) [Table 2, (Park & Rakha, 2005)].

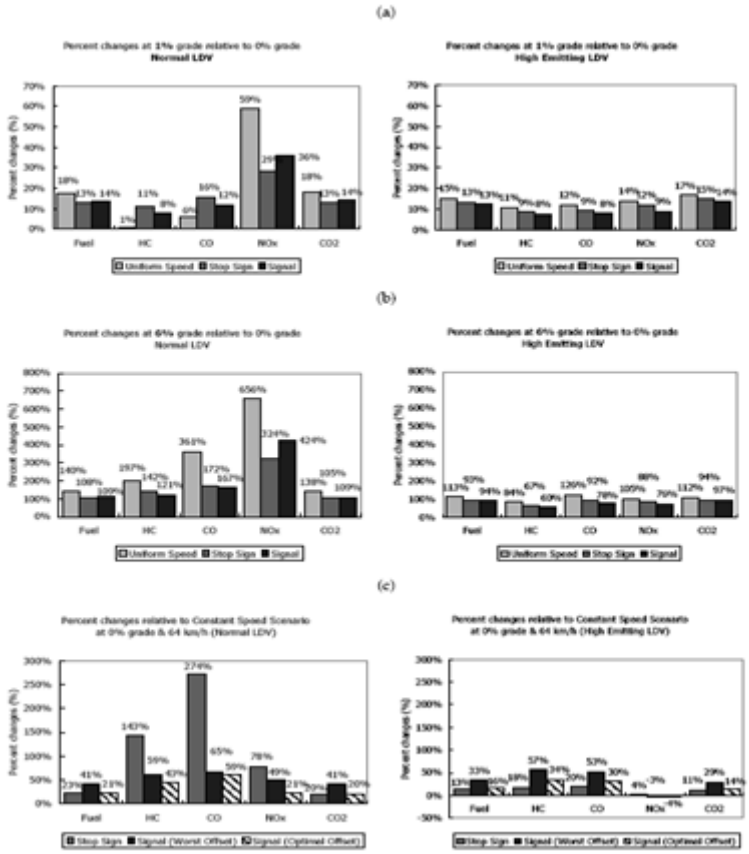

Figure 56: Comparison of MOE Scenarios (Percent Changes) [Figure 6, (Park & Rakha, 2005)].

Institutional Repository - Library & Information Centre - University of Thessaly
09/12/2017 02:36:50 EET - 137.108.70.7

In 2009, an important study evaluated the effect of road grade on light-duty vehicle fuel consumption using both (a) an analytical approach based on a sophisticated energy and emissions model (b) an empirical approach based on real-world measured data (Boriboonsomsin & Barth, 2009).

The empirical approach was already prevented in Chapter 1 because it involved only the gradient parameter and there were no other correlated parameters. In this chapter we present the analytical approach giving the mathematical expressions included in the paper and take into account the effect of road grade, rolling resistance and air resistance on vehicle emissions, fuel consumption and power demand (Boriboonsomsin & Barth, 2009).

It is well known that speed and acceleration have a large impact on a vehicle's fuel economy and tailpipe emissions, as they are the primary variables that determine the power requirements necessary for specific driving maneuvers. In addition, power requirements for a vehicle are also influenced by its weight; the grade of the road on which it travels; and other factors, such as aerodynamic drag and rolling resistance. The total tractive power requirement ($P_{tractive,}$ in kilowatts) placed on a vehicle (at the wheels) is given in simplest form as:

$$P_{tractive} = \frac{m}{100} \times v \times \left(a + c_g \times sin\theta\right) + \left(m \times c_g \times C_r + \frac{\rho}{2} \times v^2 \times A_{Frontal} \times CD\right) \times \frac{v}{1000} \quad [111]$$

where

m:	vehicle mass (kg);
v:	vehicle velocity (m/s);
α:	vehicle acceleration (m/s^2);
c_g:	gravitational constant (9.81 m/s^2);
θ:	road grade angle;
C_r:	rolling resistance coefficient;
P:	mass density of air (1.225 kg/m$_3$, depending on the temperature and altitude);
$A_{Frontal}$:	The frontal area of the vehicle (m^2);
CD:	aerodynamic drag coefficient.

To translate this tractive power requirement to the engine power requirements demanded (P_{engine}), the following simple mathematical expression can be used as a first approximation:

Institutional Repository - Library & Information Centre - University of Thessaly
09/12/2017 02:36:50 EET - 137.108.70.7

$$P_{engine} = \left(\frac{P_{tractive}}{\eta_{tf}}\right) + P_{accessories} \quad [112]$$

where η_{tf} is the combined efficiency of the transmission and final drive and $P_{accessories}$ is the engine power demand associated with the operation of accessories, such as air conditioning, power steering and brakes, and electrical loads. In the final model, $P_{accessories}$ may be modeled as a function of engine speed, and η_{tf} can be modeled in terms of engine speed and $P_{tractive}$. The power requirement on the engine (P_{engine}) is directly related to fuel consumption:

$$\frac{dF}{dt} \approx \lambda \times \left(k \times N \times D + \frac{P_{engine}}{\eta_{engine}}\right) \quad [113]$$

where

F: the fuel consumption;

t: the time;

λ: the fuel–air equivalence ratio;

k: the engine friction factor (which represents the fuel energy used at zero power output to overcome engine friction per engine revolution and unit of engine displacement);

N: the engine speed;

D: the engine displacement;

η_{engine}: a measure of indicated engine efficiency.

This mathematical expression is simple but fairly accurate for determination of the fuel use rate (in kilowatts).

With the above mathematical expression, it is possible to calculate instantaneous fuel consumption for different road grades. Higher levels of fuel consumption (and emissions) will result with a positive grade, and lower levels of fuel consumption (and emissions) will result with a negative grade. If a route contains both uphill and downhill sections, then in many cases, the fuel consumption increases and decreases should mostly balance out.

(Sovran, 1984) made a fuel consumption analysis to determine the impact of the rolling resistance, the air resistance and the use of accessories (i.e. A/C) on fuel economy over the Environmental Protection Agency (EPA) driving schedules. It was based on the tractive energy required by vehicles to negotiate those schedules, specifically on the fraction that was

Institutional Repository - Library & Information Centre - University of Thessaly
09/12/2017 02:36:50 EET - 137.108.70.7

required to overcome the drag. In conjuction with empirical inputs on closed-throttle fuel rate and the fuel consumption fraction for engine and vehicle accessories, an expression for the aerodynamic influence coefficient relating any percentage reduction in drag to the corresponding attainable percentage reduction in on-road fuel consumption had been formulated. The simple formula was used to show the effect of drag changes of various magnitude on EPA Urban, Highway and Composite fuel consumptions. The equivalent reductions in vehicle mass and tire rolling-resistance coefficient required to produce the same fuel saving were also shown. The study was concentrated to passenger cars (LDVs). There were no experiments but there were developed mathematical expressions concerning the power demand and the fuel consumption provided. Notice that in this researcher there is no discussion about the effect of air resistance to the emission rates of the vehicles.

The mathematical expression given represents the total volume of fuel consumed per unit distance traveled according to the EPA schedules used is:

$$g = \frac{G}{S} = \frac{\overline{bsfc}}{\rho_f} = \left[\frac{1}{\overline{\eta_d}} \times \left(\frac{E_{TR}}{S}\right) + \left(\frac{E_{AC}}{S}\right)\right] + \dot{G_0} \times \left[\frac{T_{ID} + T_{BR}}{S}\right] \quad [114]$$

where

- g: The total volume of fuel consumed per unit distance traveled;
- *S:* The total distance of the trip [km];
- *G*: The total volume of fuel consumed;
- $\dot{G_0}$: The instantaneous volumetric rate of fuel consumption;
- bsfc: The break specific fuel consumption of the engine [mass of fuel];
- ρ_f: The fuel density;
- E_{TR}: The total tractive energy delivered to the tire-road interface;
- E_{AC}: The power requirement of accessories;
- T_{ID}: Total duration of the idling period [s];
- T_{BR}: Total duration of the braking period [s].

And

$$\eta_d = \frac{P_{TR}}{(P_B)_{TR}} \quad [115]$$

where

Institutional Repository - Library & Information Centre - University of Thessaly
09/12/2017 02:36:50 EET - 137.108.70.7

$(P_B)_{TR}$: the tractive power delivered to the tire-road patch;

P_B: the part of the brake engine power that is sent to the driveline.

The relationship between the change in fuel consumption resulting from a prescribed change in tractive energy is obtained by the above mathematical expression under appropriate circumstances. The only direct change considered is one in tractive energy E_{TR} resulting from a change in aerodynamic drag. However, changes in other factors of the e mathematical expression may occur as a consequence of that drag change and must be identified and considered.

$$\frac{dg}{g} = \left\{\left[1 + \left(1 + \frac{g_{AC}}{g_{TR}}\right) \times \xi_F\right] \times \left(\frac{g_{TR}}{g}\right) \times \left(\frac{E_A}{E_{TR}}\right)\right\} \times \frac{d(CD \times A_{Frontal})}{CD \times A_{Frontal}} = \xi_A \times \frac{d(CD \times A_{Frontal})}{CD \times A_{Frontal}} \quad [116]$$

where

$$g_{TR} = \frac{\overline{E_{TR}}}{\overline{\eta_d} \times S} \quad [117]$$

$$g_{AC} = \frac{E_{AC}}{\overline{\eta_d} \times S} \quad [118]$$

$$\xi_F = \frac{\overline{\frac{d(bsfc)}{bsfc}}}{\frac{dE_{TR}}{E_{TR}}} \quad [119]$$

and,

CD: the drag coefficient;

$A_{Frontal}$: the frontal area of the vehicle;

g_{TR}: the tractive fuel consumption fraction;

g_{AC}: the fuel consumption due to accessories fraction;

ξ_A: Influence coefficient relating percentage changes in $CD \times A_{Frontal}$ and g.

Influence coefficient ξ_A is vehicle independent. To take full advantage of the fuel economy potential of reductions in aerodynamic drag, the first factor must by unity (i.e. ξ_F must be zero). For new car designs, this means that engine and driveline performance must be

Institutional Repository - Library & Information Centre - University of Thessaly
09/12/2017 02:36:50 EET - 137.108.70.7

maintained at existing levels. For an existing car model, it implies appropriate rematching of the engine-driveline system to recover the original bsfc. Without such control of the drivetrain, the aerodynamic influence coefficient can easily deteriorate to only 60% of its potential value. The coefficient with proper control will be given its own designation, ξ^*_A. Where:

$$\xi^*_A = \left(\frac{g_{TR}}{g}\right)_1 \times \left(\frac{E_A}{E_{TR}}\right)_1 \quad [120]$$

The resultant tractive fuel-consumption fractions are determined in Table 59.

	S [km]	$\boldsymbol{T_{ID}}$ $[s]$	$\boldsymbol{T_{BR}}$ $[s]$	$\frac{\dot{G}_0}{g}$	$\frac{g_{ID}}{g}$	$\frac{g_{BR}}{g}$	$\frac{g_{AC}}{g}$	$\frac{g_{TR}}{g}$
Urban	11.9	249	311	12.4	0.07	0.09	0.10	0.74
Highway	16.50	3	57	17.1	0.00	0.02	0.09	0.89

Table 59: Fuel-Consumption fractions for EPA driving schedules (Sovran, 1984).

Composite fuel consumption is defined by the following weighted average:

$$g \equiv 0.55 \times g_U + 0.45 \times g_H \quad [121]$$

where U and H define the Urban and Highway roads and,

$$\xi_A = 0.63 \times (\xi_A)_U + 0.37 \times (\xi_A)_H \quad [122]$$

The above mathematical expression can be also used for ξ^*_A.

In Figure 57, the attainable aerodynamic influence coefficient, ξ^*_A, for each of the EPA schedules is shown as a function of the vehicle variable $CD \times A_{Frontal}/m$, with tire rolling-resistance coefficient, r_0, as the parameter, where m is the mass of the vehicle.

Institutional Repository - Library & Information Centre - University of Thessaly
09/12/2017 02:36:50 EET - 137.108.70.7

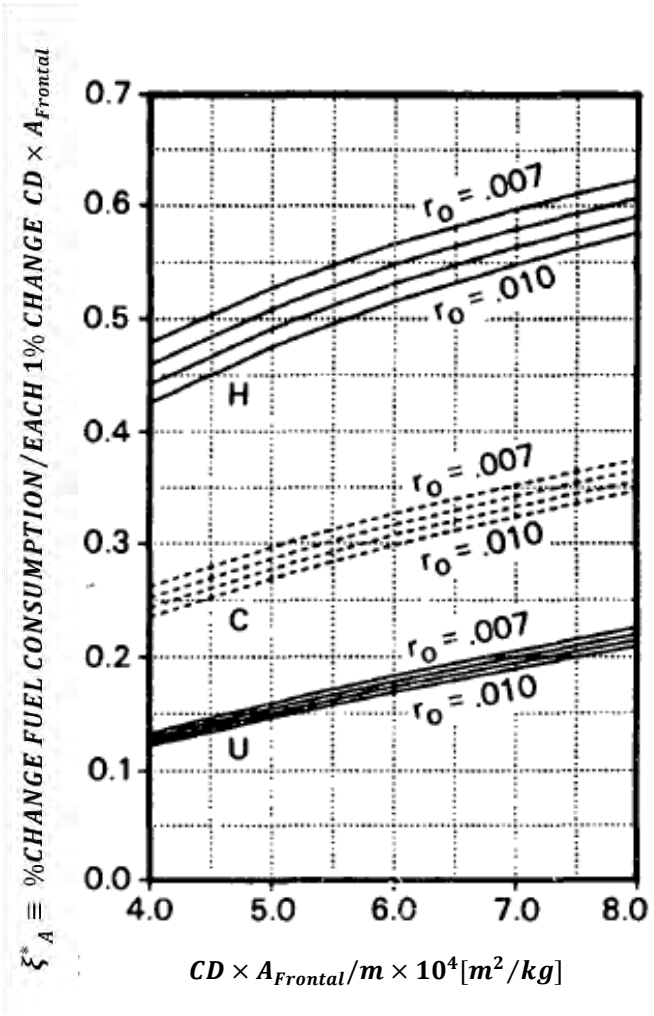

Figure 57: Attainable aerodynamic influence coefficient for EPA driving schedules (U-Urban, C-Composite, H-Highway) (Sovran, 1984).

Federal legislation in the U.S. is written in terms of the reciprocal of fuel consumprion, i.e. fuel econymy. The percentage fuel economy improvement is greater than its corresponding fuel consumption reduction. Figure 58**Σφάλμα! Το αρχείο προέλευσης της αναφοράς δεν βρέθηκε.** shows the the percentage fuel economy improvement using the ξ^*_A.

Institutional Repository - Library & Information Centre - University of Thessaly
09/12/2017 02:36:50 EET - 137.108.70.7

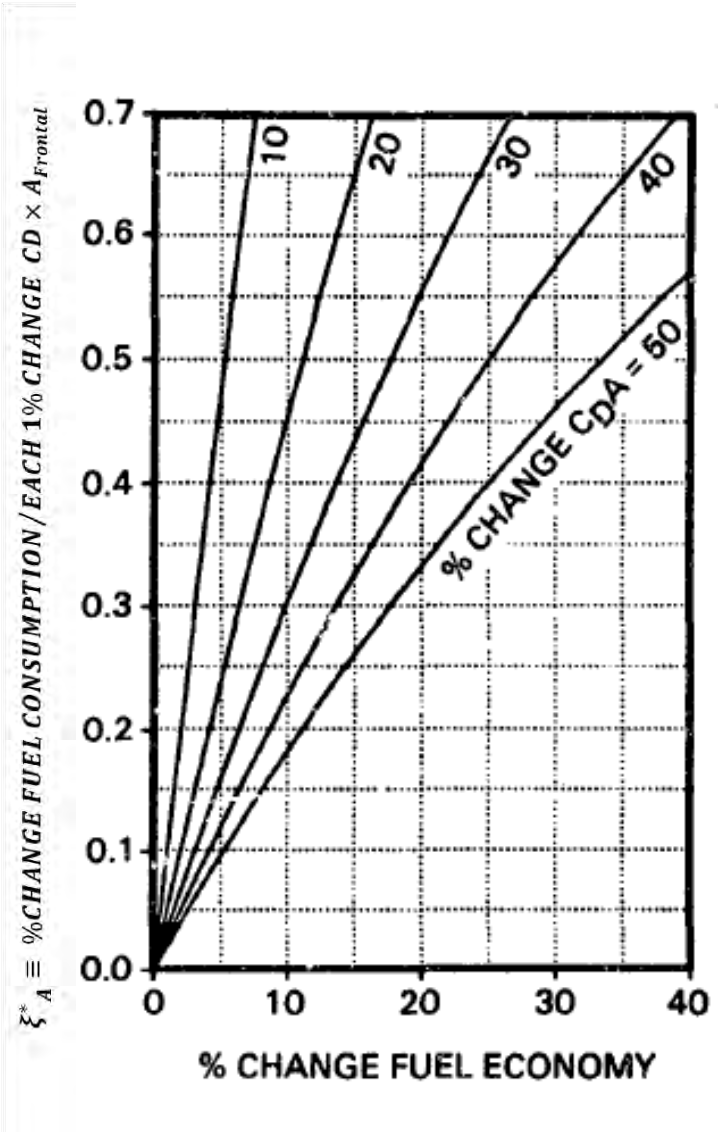

Figure 58: Percentage change in fuel economy corresponding to any correlation of aerodynamic influence coefficient and percentage change in CD × $A_{Frontal}$ (or CDA) (Sovran, 1984)

The results of the study are in influence-coefficient form, relating the percentage changes in the overall vehicle characteristics to corresponding percentage changes in EPA Urban, Highway and Composite fuel consumption economy. These attainable values represent the full conversion of tractive-energy reductions to fuel saving. They highlight the importance of appropriate drivetrain design and matching if full value is to be received for the reduction in energy requirement generated by lower aerodynamic drag.

5.2.1.3 Studies examining four parameters

There was only one study found to study more than three parameters in correlation. In 2000, D.Y.C. Leung and D.J. Williams presented a power based fuel consumption and exhaust emissions model evaluated from testing a wide range of in-use cars on a chassis dynamometer (using a large Australian database - 611 passenger cars) (Leung & Williams, 2000). The study examined the impact of the gradient, the rolling resistance, the air resistance and the use of

Institutional Repository - Library & Information Centre - University of Thessaly
09/12/2017 02:36:50 EET - 137.108.70.7

vehicle's accessories (A/C) in vehicle's behavior. The proposed model was applied to results of on-road fuel consumption measurement using a "floating" car which was driven back and forth on hilly roadways in Sydney with a length of 8.6 km in an urban area. The model is found to predict the fuel consumption well over the standard drive cycles and also for the floating car. Besides the experiments that were carried out, there were also useful mathematical expressions given for the fuel consumption and the power demand computation without giving, though, any results concerning the emission rates. The fact that power is required for a vehicle to overcome all of resistive forces and to run its accessories, made them estimate this power by using some functions. The instantaneous power, Z_t, to propel a vehicle along a road can be expressed as:

$$Z_t = Z_d + Z_r + Z_a + Z_e + Z_m \quad [123]$$

where Z_d , Z_r , Z_a , Z_e and Z_m are, respectively, the power required to overcome vehicle drive-train resistance, the tire rolling resistance, the aerodynamic drag, the inertial and the gravitational resistance, and for the accessories (such as air-conditioning), the major contributions (in kW) are:

$$Z_d = 2.36 \times 10^{-7} \times v^2 \times m \quad [124]$$

$$Z_r = (3.72 \times 10^{-5} + 3.09 \times 10^{-8} \times v^2) \times m \quad [125]$$

$$Z_a = 1.29 \times 10^{-5} \times CD \times A_{Frontal} \times v^3 \quad [126]$$

$$Z_e = 2.78 \times 10^{-4} \times (a + g \sin\theta) \times m \times v \quad [127]$$

where m (kg) is the inertia mass of vehicle, v (km/hr) the vehicle speed, a (m/s^2) the vehicle acceleration, CD the aerodynamic drag coefficient, $A_{Frontal}$ (m^2) the vehicle frontal area, and θ the road gradient. For testing on a chassis dynamometer the tire pressure has to be increased resulting in a reduction in the rolling resistance. Z_r is assumed to reduce 0.3 of the value given by the above mathematical expression. It should be noted that Z_m depends on the type of accessories used and is assumed zero in this study.

Because detailed information of vehicle behavior on the road is not generally available a number of procedures have been developed for estimating fuel consumption under different road and traffic conditions (Watson, 1980). However, when detailed speed time profiles are

Institutional Repository - Library & Information Centre - University of Thessaly
09/12/2017 02:36:50 EET - 137.108.70.7

known, the instantaneous power model can be applied. Good correlation between fuel consumption and power demand was found for vehicles under a standard driving cycle (Post, et al., 1981). It is generally accepted that the fuel consumption rate (in m1/min) is linearly related to the total instantaneous power (in kW) by:

$$FC = a + \beta \times Z_{tot} = \gamma \times EC + \beta \times Z_{tot} \quad [128]$$

where Z_{tot} is the overall instantaneous total power demand, α is the idle fuel consumption rate and β a measure of the thermodynamic efficiency of power generation. The above mathematical expression was also presented in the first paper presented by (Post, et al., 1981).

Fuel consumption for any one vehicle is influenced by the particular frictional resistances inherent to the vehicle and by the engine compression status that affects the thermodynamic efficiency, β. Thus, significant variations would be expected between nominally identical vehicles. The model was further validated by using the on road measurement data of the floating car. The forward trip of the measurement was towards city direction which is subject to downhill slope with an overall descent of about 100m. As expected, more fuel was consumed in the return journey as shown in Figure 59. Despite the difference in the running conditions the fuel consumption of the forward and return trip fall onto a straight line with slope about 1. The overall model accuracy for this measurement is ∓10% with an average of 5%.

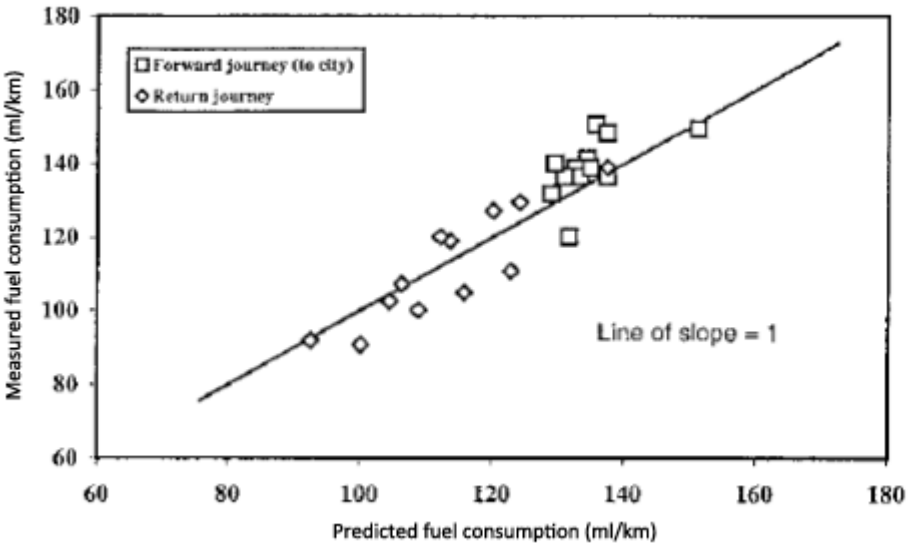

Figure 59: Fuel consumption results of on-road measurement [Figure 3, (Leung & Williams, 2000)].

Institutional Repository - Library & Information Centre - University of Thessaly
09/12/2017 02:36:50 EET - 137.108.70.7

5.2.2 Heavy Duty Vehicles (HDVs)

5.2.2.1 Studies examining two parameters

In 2002, a report provided the results of additional statistical analysis of fuel consumption data collected on a semi-trailer tank truck operating on a variety of highway pavement structures in the Ottawa and Montreal region in 1999 and 2000 (G.W. Taylor Consulting, 2002). This data set consisted of three sets of data:

1. vehicle data (speed, fuel flow, wind speed, temperature) was collected on a continuous (approximately 0.5 Hz) basis,
2. road roughness data measured independently and provided as an International Road Roughness (IRI) rating,
3. precision roadway elevation survey to provide grade information.

The study was concentrated in two important parameters: the rolling resistance and the road gradient. There were experiments carried out but also some mathematical expressions provided during the study. There was no reference to the behavior of the emission rates.

The model presented is described by the mathematical expression below:

$$Y_i = \beta_0 + \beta_1 \times X_{i1} + \beta_2 \times X_{i2} + \beta_3 \times X_{i3} + \beta_4 \times X_{i4} + \beta_5 \times X_{i5} + \beta_6 \times X_{i6} + \beta_7 \times X_{i7} + \beta_8 \times X_{i8} + \varepsilon_i \quad [129]$$

where

Y_i: Fuel economy associated with the *i*-th observation (*FUEL*),

X_{i1}: 1 if the *i*-th observation is measured on asphalt pavement, and 0 otherwise (*PVASH*)

X_{i2}: 1 if the *i*-th observation is measured on composite pavement, and 0 otherwise (*PVCOMP*),

X_{i3}: Load associated with the *i*-th observation (*LOAD*),

X_{i4}: Pavement temperature associated with the *i*-th observation (*PAVETEMP*),

X_{i5}: IRI associated with the *i*-th observation (*IRI*),

X_{i6}: Road grade associated with the *i*-th observation (*GRADE*),

X_{i7}: 1 if the vehicle speed on the *i*-th observation is 75 km/hr, and 0 otherwise (*SPEED75*),

X_{i8}: 1 if the vehicle speed on the *i*-th observation is 100 km/hr, and 0 otherwise (*SPEED100*).

ε_i: error term associated with the *i*-th observation, which is assumed to

Institutional Repository - Library & Information Centre - University of Thessaly
09/12/2017 02:36:50 EET - 137.108.70.7

be normally distributed with a mean of zero and an unknown variance.

The above model was fitted to the data over all seasons, sites, loads, and speeds.

The following variables were found to have the highest statistical significance in predicting the fuel consumption of the vehicle:

- Pavement Structural Type (Concrete, Asphalt, Composite)
- Vehicle Load (mass)
- Pavement Temperature
- Road roughness as measures as IRI
- Road Grade
- Vehicle speed

The test data was used to calibrate a vehicle power model by estimating the aerodynamic drag and rolling resistance coefficients for the test vehicle. The power model then calculated the effect of this magnitude change in rolling resistance on the vehicle's fuel consumption rate. The estimates indicated a maximum percentage change for the fully load configuration of 10.5% at road speeds of between 20 and 50 km/h. At highway speeds is model predicts a 5 to 6 percent change between concrete and asphalt conditions.

In 2007, a paper about comparing real-world fuel consumption for diesel - and hydrogen-fueled transit buses and implication for emissions was published (Frey, Rouphail, Zhai, Farias, & Goncalves, 2007) examining the impact of the road gradient and the rolling resistance combined. It explored the influence of key factors such as speed, acceleration, and road grade on fuel consumption for diesel and hydrogen fuel cell buses under real-world operating conditions in urban roads. The study tried to come to results about how the road gradient and factors concerning the rolling resistance can affect the power needed for a vehicle to move using mathematical expressions and not any experimental data. A Vehicle Specific Power-based approach was used for modeling fuel consumption for both types of buses. Although, there were no numerical results presented about the impact on the fuel consumption and the emissions produced.

The methodology consisted of: (a) conducting an exploratory analysis to assess the relationships between fuel consumption and factors that significantly affect it; (b) developing a VSP-based approach for estimating fuel consumption at a micro-scale level; (c) comparing fuel consumption between different vehicles for a given fuel (i.e. diesel); (d) comparing fuel

Institutional Repository - Library & Information Centre - University of Thessaly
09/12/2017 02:36:50 EET - 137.108.70.7

consumption between buses with differing fuel types; and (e) developing fuel-based emission factors to evaluate tailpipe emission reductions for hydrogen-fueled buses.

$$VSP = v \times [\, a + c_g \times (\sin(\theta) + 0.092\,] + 0.00021 \times v^3 \quad [130]$$

where VSP is the Vehicle Specific Power (m^2/s^3), v is the instantaneous speed at which the vehicle is traveling (m/s), a is the instantaneous acceleration of the vehicle (m/s^2), c_g the gravitational constant(≈ 9.81), θ is instantaneous road grade (decimal fraction), 0.092 is rolling resistance term coefficient, and 0.00021 is the drag term coefficient.

The calibration data were utilized to estimate VSP-based modal average fuel consumption rates. Trip-based fuel consumption was estimated as:

$$\sum_{j=1}^{J} FR_j \times TVSP_j \quad [131]$$

where E is the total trip fuel consumption (in litters for diesel buses and in grams for hydrogen buses), *j* the VSP mode index, *J* is the number of VSP modes (*J* = 8 for diesel buses and 6 for hydrogen buses as explained later), FR_j is fuel consumption rate for VSP mode *j* (l/s for diesel bus and g/s for hydrogen bus) and $TVSP_j$ is the bus trip time spent in VSP mode *j* (s).

The correlation coefficients for speed and fuel consumption rates were higher for diesel than for hydrogen buses, indicating a stronger effect for the former. Road grade was weakly correlated with fuel consumption for both types of buses. Passenger load had almost no effect on fuel consumption during idling, or under very low speeds (610 km/h).

In 2008 (Gandert, Raemdonck, & van Tooren, 2008) studied the impact of the rolling resistance and the air resistance oh heavy duty vehicles. The design, production and verification of a data acquisition system to measure aerodynamic and mechanical characteristics of a tractor-trailer combination, operating in a real life environment, were presented. The main goal of this work was to derive a reference level of a truck with respect to its aerodynamic and mechanical performances. This way, if the truck is equipped with different aerodynamic aids, a correct comparison can be made between the aerodynamic drag reductions obtained by these devices. Also, a relation can be defined which links the

Institutional Repository - Library & Information Centre - University of Thessaly
09/12/2017 02:36:50 EET - 137.108.70.7

aerodynamic drag reduction with fuel consumption savings. The acquisition system consisted of an anemometer, which measured the wind speed and direction, and a two-axis inclination indicator, which was coupled to the FMS (Fleet Management System) of the tractor via the CAN communication system and to the wipers to indicate if it is raining or not. The FMS of the tractor was measuring, for instance, the vehicle speed, the engine torque, the rpm, acceleration pedal position, cruise control, fuel rate, cargo weight and the like. All the measured data were registered on a hard disk and could be accessed through a simple USB connection. The processed data gave insight in the performance of the driver and in the aerodynamic behavior (CD value of 0.430) as well as the mechanical characteristics (power required breakdown; 47% rolling resistance, 39% aerodynamic drag and 15% mechanical losses; average speed of 75 km/h; fuel consumption of 30 liters per 100 km) of the truck. The study was based in measurements of the truck which was transporting cargo in highway roads of West Europe from February to July 2006. The experimental data were weekly downloaded and processed using Matlab. There were also developed some mathematical expressions which are provided below.

The mathematical expression used below describes the measured delivered power in relation to the different required power contributions to overcome the aerodynamic and friction forces and the total losses.

$$P_{req} = D_{aero} \times v + F_{friction} \times v + P_{losses} \quad [132]$$

P_{req} corresponds to the required power that is produced by the engine and is registered by the data acquisition system whereas $D_{aero} \times v$ is the aerodynamic force multiplied by the vehicle velocity. The friction force $F_{friction}$ originates from the friction between the wheels of the truck and the road. The friction force is dependent on the normal force N and the rolling resistance coefficient C_r. The normal force N equals the weight m times the gravitational acceleration g. The weight m is composed out of the weight of the truck together with the trailer and the cargo. The last variable is the total power loss P_{losses} due to mechanical friction. If these total losses are known one can make an estimation of the drag coefficient of the truck with the aid of the measured delivered power and the calculated wheel friction force. In Figure 60 the estimated drag coefficient is plotted together with vehicle speed, the velocities below the 23m/s are filtered away in order to get the maximum constant velocity.

Institutional Repository - Library & Information Centre - University of Thessaly
09/12/2017 02:36:50 EET - 137.108.70.7

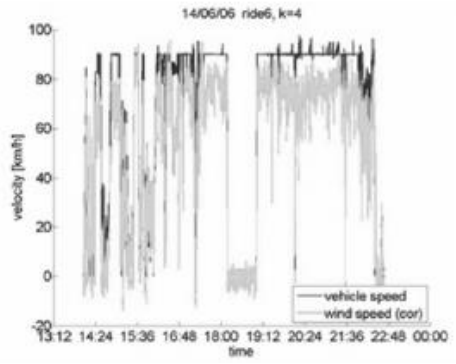

Figure 60: Estimated drag coefficient together with vehicle velocity (Gandert, Raemdonck, & van Tooren, 2008).

The average drag coefficient, based on a frontal area of 10.34 m^2, for the whole testing period of two months was CD=0.430. (van Raemdock, 2006) performed numerical simulations of a full scale symmetrical model of the same truck used during the data acquisition. A drag coefficient CD = 0.384 was obtained after the numerical simulations. The difference between the estimated drag coefficient and the one simulated with the aid of computation fluid dynamics (CFD) was probably related to the fact that the model used during CFD was a simplified semi-model, not equipped with a radiator, no side-winds were simulated and the known short comings of the used turbulence model.

All the different contributions in terms of percentage to the total power required P_{req} are known. If the average for the whole testing period is calculated for the three different contributions, a summarizing pie-chart, Figure 61 , can be made. The figure illustrates that almost 15% of the delivered power is lost into the mechanical friction of the engine, the gearbox and the drive shafts. The rolling resistance is responsible for 47% of the total delivered power, while the aerodynamic forces consume 39%. Only the vehicle velocities which are equal or higher than 23m/s were considered.

Institutional Repository - Library & Information Centre - University of Thessaly
09/12/2017 02:36:50 EET - 137.108.70.7

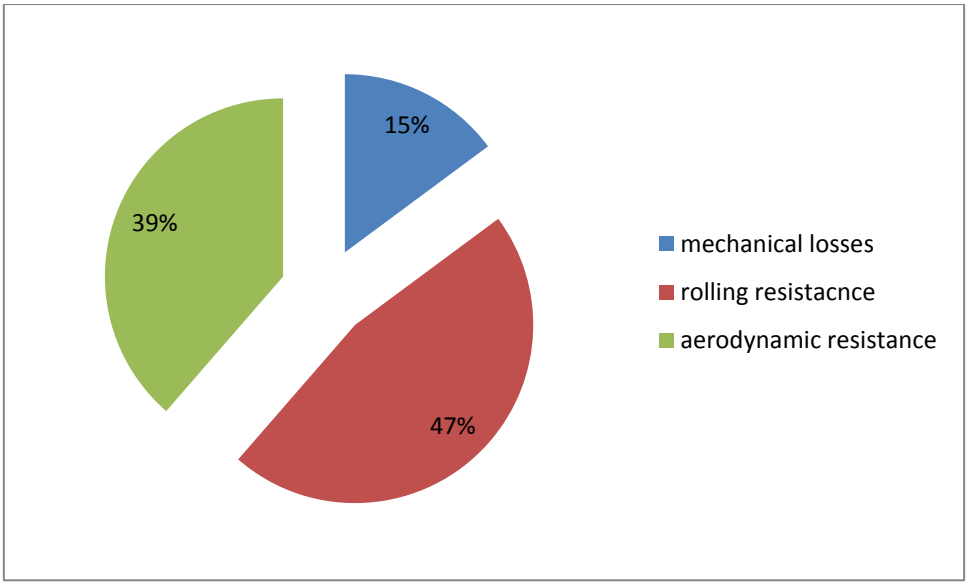

Figure 61 Average contributions for the whole testing period considering velocities higher than 23 m/s (Gandert, Raemdonck, & van Tooren, 2008).

During the test period a reference level of the truck was defined which made it possible to compare different aerodynamic devices and their corresponding fuel economy impact.

In 2012, a report also examined the rolling and air resistance parameters in correlation. The study was produced on commission of the Swedish Transport Administration and constitutes one part of the MIRIAM sp2 project (Hammarstrom, Eriksson, Karlsson, & Yahya, 2012). Based mainly on empirical data from coastdown measurements in Sweden, a general rolling resistance model – with roughness (*IRI*), macrotexture (*mpd*), temperature and speed as explanatory variables – was developed and calibrated for three types of vehicle; car; heavy truck and heavy truck with trailer. Here we will present the conclusions that concern the HDVs. In this study, experimental results are presented for HDVs. The type of road and the age of pavement are not specified. The study focuses on the fuel consumption and there is reference to the emissions of the vehicle exists.

In (Karlsson, Hammarström, Sörensen, & Eriksson, 2011) coastdown measurements were done also for an HGV without a trailer. Unfortunately, due to measurement errors the resulting parameter estimations were rather unstable. For this reason no final model was formulated.

In (Hammarstrom & Yanya, 2011) measurements were done for both a truck and a trailer. Although some interesting results concerning the air resistance were obtained, the results describing the influence of road surface conditions on rolling resistance were very unreliable. In order to obtain some results a renewed analysis based on a merged dataset from the two reports was performed. A crucial difficulty is that the modeling details can be varied in a large

Institutional Repository - Library & Information Centre - University of Thessaly
09/12/2017 02:36:50 EET - 137.108.70.7

number of ways and that the results vary a lot when changing the implementation details. These instabilities make it difficult to confidently determine a final model.

Rolling resistance caused by IRI is dependent on speed. At a speed of 90 km/h, when IRI and *mpd* increase by one unit, the rolling resistance will increase accordingly:

- for a heavy truck by 7.1% and 18.4%
- for a heavy truck with trailer by 7.9% and 20.3%.

At an average speed of 90 km/h and an alignment standard *scl 1*, *Fc* increases, per unit increase of IRI and *mpd*, accordingly*:*

- for a heavy truck: 1.3% and 3.4%;
- for a truck with trailer: 1.7% and 5.3%.

At the same average speed, 90 km/h, *Fc* increases when the alignment standard decreases from *scl 1* to *scl 4* accordingly:

- for a heavy truck: 21%;
- for a truck with trailer: 60%.

The importance of *mpd*, IRI and alignment standard increases with heavier vehicle weight (Hammarstrom, Eriksson, Karlsson, & Yahya, 2012).

The model results for the HGV is unstable in a number of ways. Firstly, an upper limit for acceptable wind speed, Wmax, can be set to different values. The model parameter estimations varied with this choice. Secondly, the temperature coefficient, $C_r Temp$, is unknown for the HGV. The model parameter estimations also vary with this choice. Thirdly, even more alarming, the model was unstable with respect to removing data from a single road strip.

By carefully analyzing the ranges in which the model parameters varied when the above conditions were changed within reasonable limits, a "best" set of parameter values displayed in Table 60 was finally selected for the Miriam model.

Institutional Repository - Library & Information Centre - University of Thessaly
09/12/2017 02:36:50 EET - 137.108.70.7

C0*	260N
C_r00_t	4.14e-03
C_r00_tt	3.65E-03
C_rTemp*	3.00E-05
C_rMPD	1.02E-03
C_rIRI_V_EXP	1.58E-05
CL_t*	0.5358
CLbeta_t*	0.3661
CL_tt*	0.895
CLbeta_tt*	1.411

**Not estimated by regression*

Table 60: Parameters for a modified version of the model. Reference temperature is 8°C. (Additional dummy terms included in the regressions are not shown here.) The suffix "_t"means truck only, while "_tt" denotes truck + trailer (Hammarstrom, Eriksson, Karlsson, & Yahya, 2012).

For the vehicle simulation program the coefficient C_r00_tt for the combination truck+trailer is inconvenient. More appropriate is to separate the basic rolling resistance coefficient for the trailer from that of the truck. This can be achieved by equating the (basic) rolling resistance force acting on the entire vehicle with the corresponding sum of forces for the truck and for the trailer. Using the value for C_r00_t and the mass for the truck (15.1 ton) and for the trailer (12.3 ton), yields:

$$C_r00_{trailer} = 0.00306 \quad [133]$$

It should once again be noted that the estimated values are very uncertain. Also, no consideration to the representativity of the tires was taken.

A general rolling resistance function had been estimated for the two types of trucks representing an ambient temperature of 8° C:

Rolling resistance for a heavy truck:

$$Fr = m1 \times curv \times (0.00414 + 0.0000158 \times IRI \times v + 0.00102 \times mpd) \quad [134]$$

Rolling resistance for a heavy truck with trailer:

[135]

Institutional Repository - Library & Information Centre - University of Thessaly
09/12/2017 02:36:50 EET - 137.108.70.7

$$Fr = m1 \times curv \times (0.00414 + 0.0000158 \times IRI \times v + 0.00102 \times mpd) + m2 \times curv \times (0.000.00306 + 0.0000158 \times IRI \times v + 0.00102 \times mpd)$$

where v speed (m/s), mpd the macrotexture and $curv$ the curvature term.

These parameter values have been used both in VETO simulations and in the *Fct* function. For each vehicle category one *Fc* function has been calibrated and so has been for the passenger car examining here:

The estimation of parameter values has been based on the *Fct* approach:

$$Fct = c0 \times (1 + k5 \times (Fr + Fair + d1 \times ADC \times v^2 + d2 \times RF + d3 \times RF^2))^{e1} \times v^{e2} \quad [136]$$

$$Fr = m1 \times 9.81 \times (Cr0(1) + Cr1(1) \times IRI \times v + Cr2(1) \times mpd) + m2 \times 9.81 \times (Cr0(2) + Cr1(2) \times IRI \times v + Cr1(2) \times mpd) \quad [137]$$

where

(1)	the motor vehicle;
(2)	The trailer;
ADC:	average degree of curvature (rad/km);
RF:	Rise and fall (m/km);
Fair:	$Cd \times Ayz \times dns \times \frac{v^2}{2}$;
ρ:	1.293 (kg/m^3);
Fct:	fuel consumption (L/h).

Estimated parameter values in *Fct* are presented in Table 61 and Table 62.

Institutional Repository - Library & Information Centre - University of Thessaly
09/12/2017 02:36:50 EET - 137.108.70.7

Parameter	Estimate	Lower bound*	Upper bound*
c0	0.246	0.206	0.287
k5	0.000863	0.00045	0.00127
d1	0.171	0.133	0.210
d2	-4.211	-8.206	-0.216
d3	1.390	1.259	1.521
e1	1.027	0.881	1.172
e2	0.960	0.927	0.994
R^2	0.992		

**95%*

Table 61 Estimated heavy truck parameter values in the function approach (Fct) (Hammarstrom, Eriksson, Karlsson, & Yahya, 2012).

Parameter	Estimate	Lower bound*	Upper bound*
c0	0.839	0.794	0.883
k5	0.000466	0.00043	0.00050
d1	1.655	1.545	1.766
d2	148.1	138.9	157.3
d3	1.637	1.374	1.900
e1	1.000		
e2	0.734	0.717	0.751
R^2	0.990		

**95%*

Table 62 Estimated heavy truck+trailer parameter values in the function approach (Fct) (Hammarstrom, Eriksson, Karlsson, & Yahya, 2012).

The resulting parameter values for *Fcs* are presented in Table 63.

$$Fcs = \frac{Fct}{v \times \frac{3600}{10000}} = c1 \times (1 + k5 \times (Fr + Fair + d1 \times ADC \times v^2 + d2 \times RF + d3 \times RF^2))^{e1} \times v^{e2-1} \quad [138]$$

where

Fcs: fuel consumption (L/10 km)

Institutional Repository - Library & Information Centre - University of Thessaly
09/12/2017 02:36:50 EET - 137.108.70.7

Parameter	Heavy truck	Heavy truck+trailer
c0	0.684	2.330
k5	0.000863	0.000466
d1	0.171	1.655
d2	-4.211	148.1
d3	1.390	1.637
e1	1.027	1.000
e2	0.960	0.734

Table 63: Estimated parameter values in the Fcs (L/10km) function (Hammarstrom, Eriksson, Karlsson, & Yahya, 2012).

The last study found that examines the influence of rolling resistance and air resistance was in 2006. CSTT, provided an independent third-party evaluation to quantify the potential fuel consumption differences when vehicles are driven over three distinct types of pavements: asphalt, concrete and composite (asphalt top-coat over concrete) without taking in account the age of pavement (Taylor, Eng, & Patten, 2006). CSTT developed comprehensive performance tests that were conducted between fall 2002 and fall 2003 to quantify these potential fuel consumption differences for a highway tractor pulling a loaded van semi-trailer. The data concerning Light Duty Vehicles were given in the previous section and here we present the results for the HDVs. The highway tractor and tridem van semi-trailer (type of three-axle heavy truck) were tested in three loading conditions, at five distinct seasonal conditions (winter, summer day [hot], summer night [cool], fall and spring) and over all three pavement types. All results presented concern the fuel consumption and there is no reference to the power consumption or the emission rates of the vehicle. There was also an integrated mathematical expression provided that contained all the variables measured.

The tractor semi-trailer was tested in five separate temperature ranges as follows:

Season	Ambient Temperature Range
Winter	< -10 ℃
Spring	> -5 ℃ and $< +10$ ℃
Summer Hot	$> +29$ ℃
Summer Cool	$> +10$ ℃ and $< +25$ ℃
Fall	> -5 ℃ and $< +10$ ℃

Note: Although the ambient temperature range for fall and spring were identical, roads can behave differently in different seasons due to variations in roadbed strength.

Institutional Repository - Library & Information Centre - University of Thessaly
09/12/2017 02:36:50 EET - 137.108.70.7

Table 64: Ambient conditions for the experiment (Singer & Harley, A fuel-based motor vehicle emission inventory, 1996)

The tractor semi-trailer was tested using three separate loading conditions as follows:

Load Condition	CVW
Empty	16,000 kg
Practical Full Load	43,660 kg
Maximum Legal Load in Ontario/Quebec	49,400 kg

Table 65: Load conditions for the experiment (Taylor, Eng, & Patten, 2006).

The load conditions were selected for the following reasons:

Empty: This represented a situation when a trailer has delivered its load and is returning to its point of origin.

Nominal Full Load: This represented a typical situation where a trailer is loaded to its maximum nominal weight with allowances for variations in payload location, snow and rain loading, extra passengers and fuel. This load situation, although not at the legal limit, is the practical limit used by most operators. It is very difficult to configure a vehicle at maximum legal gross weight while simultaneously satisfying individual load restrictions on each axle group.

Maximum Legal Load: This represented the maximum permissible loading as stipulated by the Ministries of Transportation in Quebec and Ontario. Although this load is legal, it is not practical for normal revenue service as it requires delicate balancing of gross weight and individual axle loads.

Multiple regression was used to investigate the effects of pavement structure on fuel consumption rate. Data filtering was employed on the total data set to remove spurious data and also to constrain the data within designated speed zones (removing speed transition data) and pavement roughness ranges. Post-test analysis revealed that the roads were significantly smoother than previous studies, therefore the initial maximum value of IRI equaling 2.0 was reduced to a maximum value of 1.6. Fuel consumption data collected on pavements with an IRI greater than 1.6 were thus not taken into consideration in this phase. Pavement structure was represented in the model by two indicator values like for the LDVs, Pvash and Pvcomp:

- the first took on a value of one (1) for asphalt and zero (0) otherwise,
- the other took a value of one (1) for composite and zero (0) otherwise.

Thus, concrete pavement was defined as the base category or structure. The analysis developed a model which estimated fuel consumption rate (l/100km) as a function of

Institutional Repository - Library & Information Centre - University of Thessaly
09/12/2017 02:36:50 EET - 137.108.70.7

pavement structure, vehicle load, air or pavement temperature, vehicle speed, wind speed, IRI, grade, and various interactions among these variables. It was determined that the following single mathematical expression could be applied to all the seasonal subsets and to the combined data set:

$$FuelCon = Constant + Pvash \times (1 = asphalt) + Pvcomp \times (1 = composite) + IRIcoeff \times IRI + Gradecoeff \times Grade + Loadcoeff \times Load - Pavement\ temperature\ coeff \times Pavetemp - Speed\ coeff \times v + AirSpdSq\ coeff \times AirSpdSq \quad [139]$$

where

FuelCon:	fuel consumption rate in l/100km;
IRI:	International Road Roughness Index;
Grade:	Road grade in percent;
Load:	Total vehicle mass in kilograms;
Pavetemp:	Pavement or ambient temperature in degrees Celsius;
v:	Vehicle road speed in km/h;
AirSpdSq:	Absolute air speed (road speed plus relative wind speed) squared.

In order to quantify and compare the savings in fuel consumption on concrete relative to asphalt or composite pavements, point estimates and confidence bounds were determined for expected fuel consumption on each surface for a range of temperatures in each seasonal model. Calculations were performed using the following assumptions:

- an IRI of 1.0 to reflect a relatively smooth surface;
- percent grade of 0;
- speed of 100 km/h;
- loads of 16,000 (“empty”), 43,660 (“full”), and 49,400 kg (“max”); and
- relative wind speed of 0 km/h.

Results are shown in the tables below. Each table below gives point estimates. The resulting point estimates are provided along with their 95th percentile confidence for expected fuel consumption for cars on smooth road surfaces. The third column shows the mean value of the estimated fuel consumption between the 95% lower and upper bound.

Institutional Repository - Library & Information Centre - University of Thessaly
09/12/2017 02:36:50 EET - 137.108.70.7

Ambient Temp	Surface	Estimate FC(L/100 km)
-8.5	Asphalt	49.3
-12.7	Asphalt	50.3
-17	Asphalt	51.4
-8.9	Composite	49.6
-13.5	Composite	50.6
-18	Composite	51.7
-8.6	Concrete	48.9
-12.9	Concrete	49.9
-17.2	Concrete	50.0

Table 66: Full, Winter Point Estimates, 100km/h, IRI=1.0 (Taylor, Eng, & Patten, 2006).

Ambient Temp	Surface	Estimate FC(L/100 km)
17	Asphalt	44.9
12.7	Asphalt	44.9
8.5	Asphalt	44.9
18	Composite	44.5
13.5	Composite	44.6
8.9	Composite	44.6
17.2	Concrete	44.2
12.9	Concrete	44.2
8.6	Concrete	44.2

Table 67: Full, Spring Point Estimates, 100km/h, IRI=1.0 (Taylor, Eng, & Patten, 2006).

Ambient Temp	Surface	Estimate FC(L/100 km)
29.5	Asphalt	41.5
25.4	Asphalt	40.4
21	Asphalt	39.4
31.4	Composite	40.3
27	Composite	39.3
22.5	Composite	38.2
30	Concrete	40.8
26	Concrete	39.8
21.5	Concrete	38.8

Table 68: Full, Summer Day Point Estimates, 100km/h, IRI=1.0 (Taylor, Eng, & Patten, 2006).

Institutional Repository - Library & Information Centre - University of Thessaly
09/12/2017 02:36:50 EET - 137.108.70.7

Ambient Temp	Surface	Estimate FC(L/100 km)
25.4	Asphalt	39.0
21	Asphalt	39.7
17	Asphalt	40.5
27	Composite	39.7
22.5	Composite	40.4
18	Composite	41.2
26	Concrete	38.8
21.5	Concrete	39.6
17	Concrete	40.3

Table 69: Full, Summer Night Point Estimates, 100km/h (Taylor, Eng, & Patten, 2006).

Ambient Temp	Surface	Estimate FC(L/100 km)
4.2	Asphalt	47.0
0	Asphalt	46.6
-4.2	Asphalt	46.2
4.5	Composite	47.8
0	Composite	47.4
-4.5	Composite	47.0
4.3	Concrete	46.6
0	Concrete	46.2
-4.3	Concrete	45.8

Table 70: Full, Fall Point Estimates, 100km/h, IRI=1.0 (Taylor, Eng, & Patten, 2006).

Ambient Temp	Surface	Estimate FC(L/100 km)
-8.5	Asphalt	42.3
-12.7	Asphalt	43.3
-17	Asphalt	44.3
-8.9	Composite	42.6
-13.5	Composite	43.6
-18	Composite	44.7
-8.6	Concrete	41.8
-12.9	Concrete	42.9
-17	Concrete	43.9

Table 71: Empty, Winter Point Estimates, 100km/h, IRI=1.0 (Taylor, Eng, & Patten, 2006).

Institutional Repository - Library & Information Centre - University of Thessaly
09/12/2017 02:36:50 EET - 137.108.70.7

Ambient Temp	Surface	Estimate FC(L/100 km)
8.5	Asphalt	40.2
12.7	Asphalt	40.2
17	Asphalt	40.3
8.9	Composite	39.9
13.5	Composite	39.9
18	Composite	40.0
8.6	Concrete	39.6
12.9	Concrete	39.6
17	Concrete	39.6

Table 72: Empty, Spring Point Estimates, 100km/h, IRI=1.0 (Taylor, Eng, & Patten, 2006).

Ambient Temp	Surface	Estimate FC(L/100 km)
29.5	Asphalt	36.3
25.4	Asphalt	35.2
21	Asphalt	34.2
31.4	Composite	35.1
27	Composite	34.1
22.5	Composite	33.1
30	Concrete	35.7
26	Concrete	34.6
21.5	Concrete	33.6

Table 73: Empty, Summer Day Point Estimates, 100km/h, IRI=1.0 (Taylor, Eng, & Patten, 2006).

Institutional Repository - Library & Information Centre - University of Thessaly
09/12/2017 02:36:50 EET - 137.108.70.7

Ambient Temp	Surface	Estimate FC(L/100 km)
25.4	Asphalt	37.8
21	Asphalt	38.6
17	Asphalt	39.3
27	Composite	38.6
22.5	Composite	39.2
18	Composite	40.0
26	Concrete	37.6
21.5	Concrete	39.1
17	Concrete	38.4

Table 74: Empty, Summer Night Point Estimates, 100km/h, IRI=1.0 (Taylor, Eng, & Patten, 2006).

Ambient Temp	Surface	Estimate FC(L/100 km)
4.2	Asphalt	39.8
0	Asphalt	39.4
-4.2	Asphalt	39.0
4.5	Composite	40.6
0	Composite	40.2
-4.5	Composite	39.8
4.3	Concrete	39.5
0	Concrete	38.7
-4.3	Concrete	39.1

Table 75: Empty, Summer Night Point Estimates, 100km/h, IRI=1.0 (Taylor, Eng, & Patten, 2006).

Institutional Repository - Library & Information Centre - University of Thessaly
09/12/2017 02:36:50 EET - 137.108.70.7

Ambient Temp	Surface	Estimate FC(L/100 km)
30	Asphalt	19.2
21	Asphalt	17.8
12.7	Asphalt	16.3
0	Asphalt	15.3
-12.7	Asphalt	14.4
31.4	Composite	19
22.5	Composite	17.6
13.5	Composite	16.1
0	Composite	15.1
-13.5	Composite	14.2
30	Concrete	18.7
21.5	Concrete	17.3
12.9	Concrete	15.8
0	Concrete	14.9
-12.9	Concrete	13.9

Table 76: Empty, All Data Model Estimates, 60km/h, IRI=1.0 (Taylor, Eng, & Patten, 2006).

CSTT's conclusions, stemming from the tractor and van semi-trailer fuel consumption testing and subsequent statistical models, are summarized below. Unless noted otherwise, all values of absolute fuel consumption differences are mean values and all percentage differences are mean percentage differences:

- At 100 km/h, on smooth roads, fuel consumption reductions were realized on all concrete roads when compared to asphalt. The savings ranged from 0.4 l/100 km to 0.7 l/100 km (0.8% to 1.8%) when compared to asphalt roads. These savings were realized for both empty and fully loaded vehicle conditions for four of the five seasons. All these differences were found to be statistically significant at the 95% level. The savings during the fifth season, Summer Night, were 0.25l/100km (0.4%), however, these data were found to be not statistically significant.
- When comparing concrete roads to composite roads at 100 km/h, the results showed that fuel consumption savings ranged from 0.2l/100km to 1.5 L/100 km (0.8% to 3.1%) in favor of concrete. However, under Summer day conditions, less fuel was consumed on the composite roads, as compared to concrete. The value of these savings was roughly 0.5l/100km (1.5%). All composite to concrete comparisons were

Institutional Repository - Library & Information Centre - University of Thessaly
09/12/2017 02:36:50 EET - 137.108.70.7

found to be statistically significant except the Spring data, which was not statistically significant.

- The fuel savings for the empty trailer at 60 km/h when comparing concrete to asphalt roads ranged from 0.4 l/100km to 0.5 L/100km (1.7% to 3.9%) in favor of concrete and were all statistically significant in four of the five seasons. The fuel savings for the Summer Night data were 0.1 L/100 km (0.5%) but they were not statistically significant.
- The fuel savings for the full trailer at 60 km/h when comparing concrete to asphalt roads ranged from 0.2l/100km to 0.4 l/100km (1.3% to 3.0%) in favor of concrete and were all statistically significant in four of the five seasons. The fuel savings for the Summer Night data were 0.1 L/100 km (0.5%) but they were not statistically significant.
- The fuel savings for the empty trailer at 60 km/h in four of the five seasons when comparing concrete to composite roads ranged from 1.1 l/100km to 1.9 l/100km (2.0% to 6.0%), in favor of concrete. However, the summer day data indicated a savings in favor of composite, when compared to concrete, of 0.2 l/100 km (3.0%). All of these savings were statistically significant.
- The fuel savings for the full trailer at 60 km/h in four of the five seasons when comparing concrete to composite roads ranged from 0.6 l/100km to 1.4 l/100km (1.9% to 4.1%) in favor of concrete. However, the summer day data indicated a savings in favor of composite, when compared to concrete, of 0.2 l/100 km (2.4%). All of these savings were statistically significant except the Spring data.

100 km/h	**FC**
Concrete to Asphalt	0.8% to 1.8% less
Concrete to Composite	0.8% to 3.1% less
60 km/h / Empty	**FC**
Concrete to Asphalt	1.7% to 3.9%
Concrete to Composite	2.0% to 6.0%
60 km/h / Full	**FC**
Concrete to Asphalt	1.3% to 3.0%
Concrete to Composite	1.9% to 4.1%

Table 77: General conclusions.

Institutional Repository - Library & Information Centre - University of Thessaly
09/12/2017 02:36:50 EET - 137.108.70.7

5.2.2.2 Studies examining three parameters

All studies presented in this section focus on the same three parameters: the gradient, the rolling resistance and the air resistance. Each of them presents the impact of their correlation on the behavior of the vehicle.

In 1997, D. Hassel and Franz-Josef Weber studied the influence of the gradient, the rolling resistance and the air resistance on emission and fuel consumption behavior of heavy duty vehicles and also light duty vehicles that we mentioned previously (Hassel & Weber, 1997). The methods were different for light and heavy duty vehicles but here we present the results concerning the case of heavy duty vehicles as those concerning the light duty vehicles were presented earlier in our review. Emission measurements for gradient classes of -6%, -4%,-2%, 0%, 2%, 4% and 6% were conducted. In the case of the +2% gradient classes, the US Test 72 with warm start was operated. For the +4 % and +6 % gradient classes special driving cycles derived from the driving behavior data collected in highway roads in Switzerland were operated. Besides the experiments, there were also some useful mathematical expressions given concerning the computation of power needed for the vehicle to overcome gradient correlated with other important parameters.

The development of the emission and consumption functions for heavy duty vehicles is described in detail in the final report of the German Emission Factor Programme (Hassel, Jost, Weber, Dursbeck, Sonnborn, & Plettau, 1995). The parameters of the function are L_{WR} which is the power for overcoming the wind, rolling, and gradient resistance and L_B which is the power for overcoming the inertia of the mass during acceleration. In contrary to the parameters of the functions for the passenger cars the parameters of the function for heavy duty vehicles include gradient resistance according to the mathematical expression for L_{WR}:

$$L_{WR} = \left[\frac{\rho}{2} \times CD \times A_{Frontal} \times v^2 + m \times a_g \times (C_r + \sin(\theta)\right] \times v \quad [140]$$

where

ρ:	air density;
CD:	drag coefficient;
$A_{Frontal}$:	frontal area of vehicle;
a_g:	acceleration due to gravity;
C_r:	coefficient of rolling resistance;
θ:	gradient angle.

Institutional Repository - Library & Information Centre - University of Thessaly
09/12/2017 02:36:50 EET - 137.108.70.7

The heavy duty vehicle fleet is in analogy to the passenger vehicles analyzed before divided into layers (strata). The definition of the layers takes into account for each heavy duty vehicle category the following parameters:

- vehicle mass,
- body style,
- model year.

As described before, the gradient factors were derived for the Swiss and German driving patterns, which are representative for special traffic situations on different road categories. In the case of lacking information about detailed driving behavior there must be a possibility to calculate gradient factors only on the basis of the mean speed. There is a possibility to determine gradient factors by calculating the ratios of the emission factors at different gradients referring to gradient class 0%.

As the mean speeds in the single countries and for the single road categories may be different, one possibility to represent the gradient factors is in form of a regression analysis on the basis of the emission data from German work-book. By means of the following method it is possible to come to general relationships for the gradient factors:

- regression analysis for level, so that emission for level can be calculated for every speed of the gradient driving patterns,
- calculation of the emission ratio for each driving pattern in relation to the emission at gradient 0 %,
- regression analysis for each gradient class, based on the calculated emission ratios.

Due to the regression analysis there was a smoothening of the ratios, which can be neglected. Figure 62 shows, as an example, the NO_x emission ratios for a heavy duty vehicle layer (lorry 7,5 - 16 tons) and the respective regression lines.

Institutional Repository - Library & Information Centre - University of Thessaly
09/12/2017 02:36:50 EET - 137.108.70.7

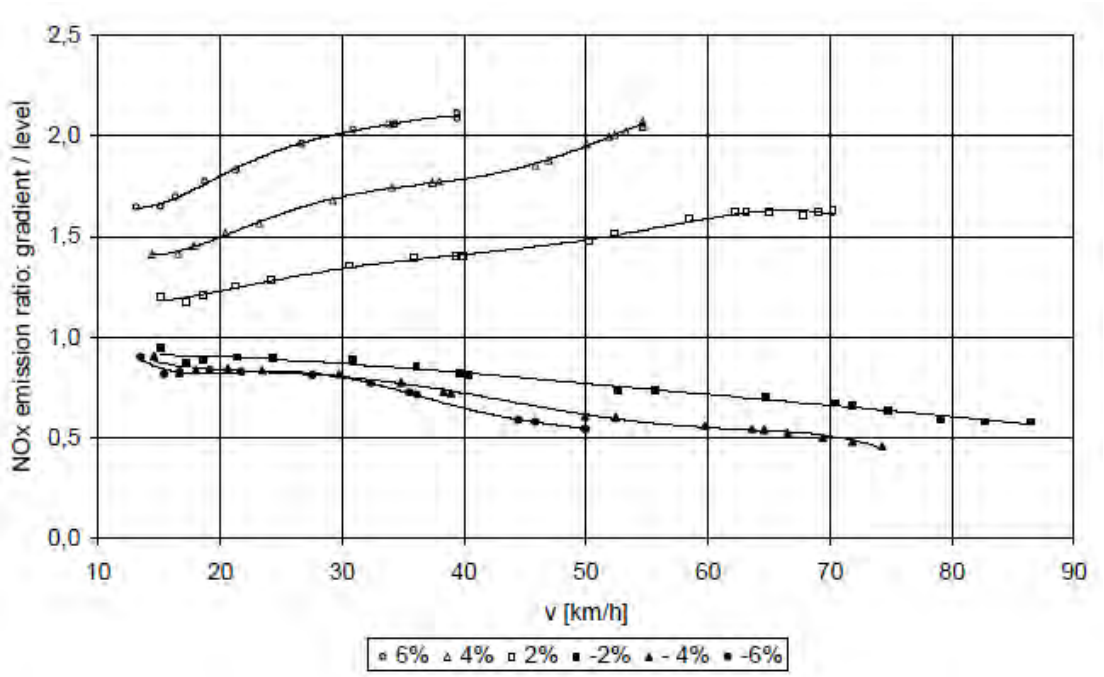

Figure 62: NOx emission ratios for the heavy duty vehicle layer - lorry 7,5 - 16 tons – for different gradient classes at mean vehicle load and the respective regression lines [Figure 3, (Hassel & Weber, 1997)].

In 2004, as we already mentioned in LDVs section above, a report conducted by EPA and Eurobitume, presented the impact of the above three parameters on the energy/fuel consumption for a vehicle, and gave different results for Light Duty and Heavy Duty Vehicles (EAPA & EUROBITUME, March 2004). We already presented the results about LDVs so below we will see the case of Heavy Duty Vehicles. There is no reference to the emission rates of the vehicle as well but there are results about the power consumption and the fuel consumption presented. The results come from experiments held in the past and no mathematical expressions are given, they are general and do not depend on a specific type of road surface (asphalt, concrete, composite). No assumptions depending on the age of the pavement were made.

Figure 63 and Figure 64, taken from a report published by Linköping University (Sandberg T. , 2001), show an example for a heavy truck. The potential energy available in the "fossil fuel" is transferred into mechanical power available for the engine crankshaft. This available mechanical power is then used for mastering driveline, air drag and rolling resistance losses at a constant speed. The potential left over mechanical power is available for climbing and/or acceleration of the vehicle mass. In Figure 63 a typical situation is presented for a 40-ton truck, driving at a constant speed of 80 km/h. Driveline loss accounts for 3%, air drag for 9%, rolling resistance for 12%. The left over mechanical power, 16%, is potentially available for climbing a slope and/or acceleration of the vehicle mass. Since the efficiency of the engine is

Institutional Repository - Library & Information Centre - University of Thessaly
09/12/2017 02:36:50 EET - 137.108.70.7

only approximately 40%, the rolling resistance counts for about 12% of the total fuel consumption of the heavy truck.

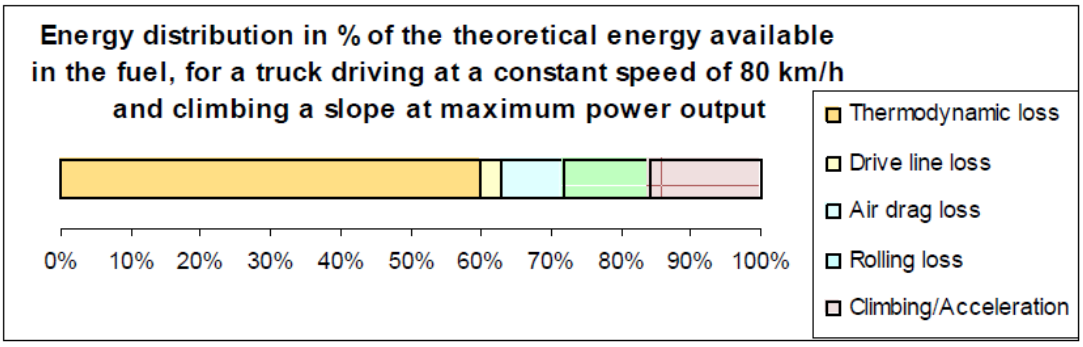

For a truck driving at a constant speed of 80 km/h and at maximum power output of the engine (Climbing/Acceleration means energy available for climbing a slope or accelerating the vehicle mass).

Figure 63: Energy distribution of the potential energy available in the fuel (Sandberg T. , 2001).

The same situation is presented again in Figure 64 but now expressed as a percentage of the potential available mechanical power at the engine crankshaft. Driveline losses are now 7%, air drag 23% and rolling resistance 30%. Potential available for climbing and/or acceleration of the vehicle mass is 40% of the engine output mechanical power at the crankshaft. Reducing the rolling resistance loss can contribute significantly to the overall fuel need: the smoother the road, the lower the fuel consumption.

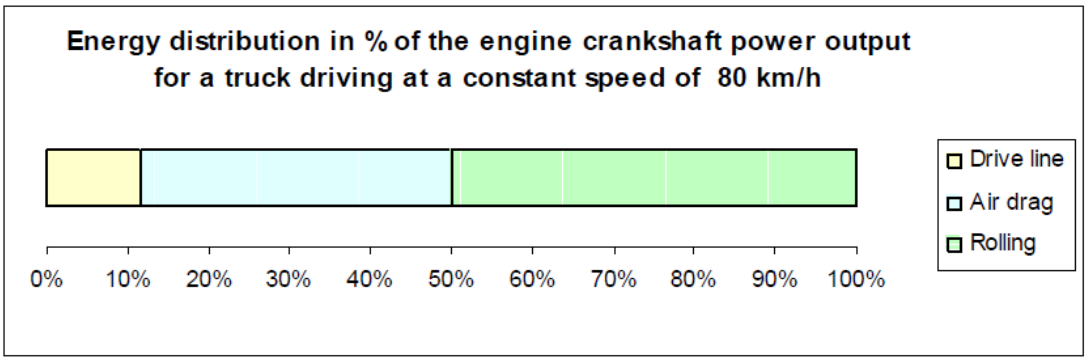

Figure 64: Energy distribution of the actual power output of a heavy truck driving at a constant speed of 80 km/h on an even road (Sandberg T. , 2001).

Approximately 12% of the fuel consumption for heavy trucks is accounted for by the rolling resistance losses in the tires at a constant speed of 80 km/h. This energy loss represents approximately 30% of the available mechanical power from the engine crankshaft.

Institutional Repository - Library & Information Centre - University of Thessaly
09/12/2017 02:36:50 EET - 137.108.70.7

In 2008 there was an energy system analysis of the fuel cell buses operated during the project Clean Urban Transport for Europe (CUTE), which ended in May 2006 where 27 fuel cell buses were operated in nine European cities (Saxe, Folkesson, & Alvfors, 2008). In this paper key performance parameters from the operation of the fuel cell buses in the project were reported, the energy system of the bus was analyzed and drive cycle tests in five cities were presented and analyzed. From the experiments carried out, the base consumption at different speeds was obtained and the power for traction as well as the power consumption of the unspecified auxiliaries were estimated. The constant speed test was performed at five different speeds 10, 20, 30, 40 and 50 km/h on a flat route (airport runway) and all auxiliaries possible to control were turned off (no AC, no door openings, etc.). The test mass of the vehicle was 14,520 kg, corresponding to the bus, the driver and the 3 test coordinators. The bus was accelerated to the designated speed, which was maintained as long as possible, limited by the length of the runway. Each test was performed four times to obtain reliable consumption figures. For the higher test speeds the acceleration period was longer and the time spent at constant speed was hence shorter; thus the data for the lower speeds are more reliable. Besides the experiments, there is also a mathematical expression used for the calculations that is going to be presented below. The study focuses on the power demands to overcome the above parameters in correlation and the fuel consumption but not other the emissions factors.

The largest demonstration project before the CUTE project was the Xcellsis/Ballard phase 3 programme, where six buses operated during 2 years (1998–2000) in regular service in Chicago and Vancouver.

The active force bringing a vehicle forward, F_x, equals the total running resistance:

$$F_x = 0.5 \times \rho \times A_{Frontal} \times CD \times v^2 + m \times c_g \times C_r + mg \times sin\theta \times (m + m_j) \times a \quad [141]$$

Where the first term represents the air resistance, the second the rolling and the third the gradient resistance and:

F_x: acting force in the x-direction [N];
v: vehicle speed in x-direction [m/s];
a: vehicle acceleration in x-direction [m/s^2];
m: vehicle mass [kg];
c_g: gravitational constant [9.81 m/s^2];
m_j: equivalent mass of rotating parts [kg];

Institutional Repository - Library & Information Centre - University of Thessaly
09/12/2017 02:36:50 EET - 137.108.70.7

θ: inclination of the road [deg];

C_r: coefficient of the rolling resistance [-];

CD: coefficient of air resistance [-];

$A_{Frontal}$: vehicle's frontal area [m^2];

ρ: air density [kg/m^3].

By letting the vehicle free-roll, i.e. F_x=0, from different speeds and measuring the distance travelled before coming to a stop, the rolling resistance coefficient (C_r) and drag resistance coefficient (CD) may be calculated. The drag resistance coefficient was found to be 0.7.

The rolling, drag and total (sum of the two) resistances in kW as function of the vehicle speed for the fuel cell bus are displayed in Figure 65.

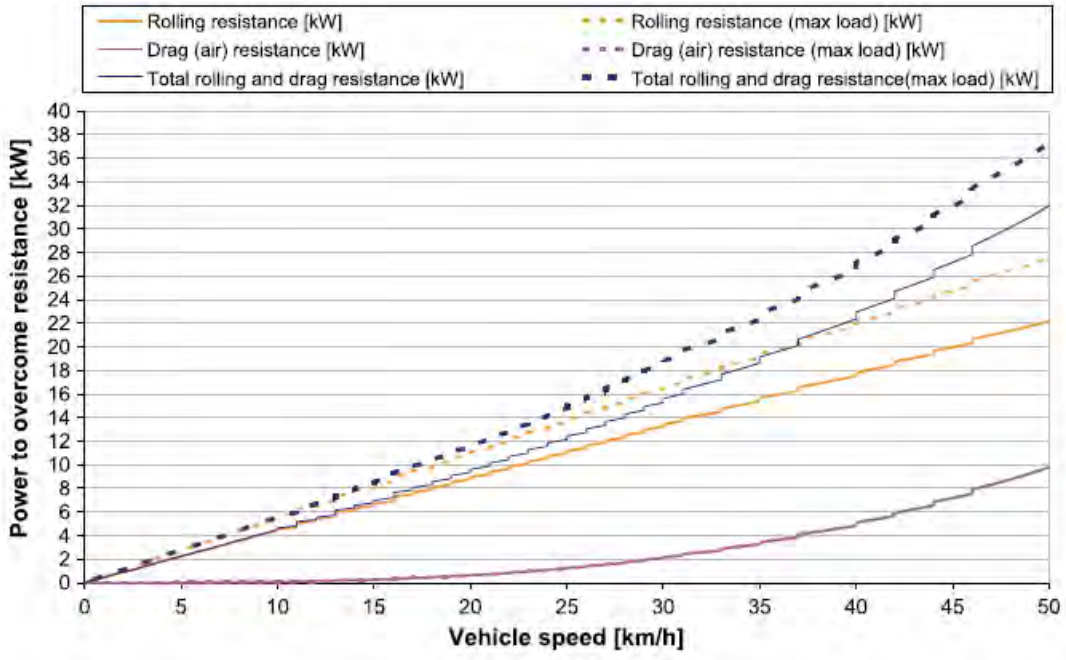

Figure 65: The air and rolling resistance in kW as function of vehicle speed for a vehicle with maximum load, 18,000 kg (calculated) and a vehicle with test load, 14,520 kg (measured/calculated). The drag resistance is load independent hence the drag resistance at maximum load is the same as the drag resistance at tested load (Saxe, Folkesson, & Alvfors, 2008).

During the study, there was also an analysis that showed that the minimum power consumption of the other auxiliaries (minimum because it does not include on-demand auxiliaries such as air conditioning or power for door opening and kneeling) would be 8–10kW at all times, see Figure 66.

Institutional Repository - Library & Information Centre - University of Thessaly
09/12/2017 02:36:50 EET - 137.108.70.7

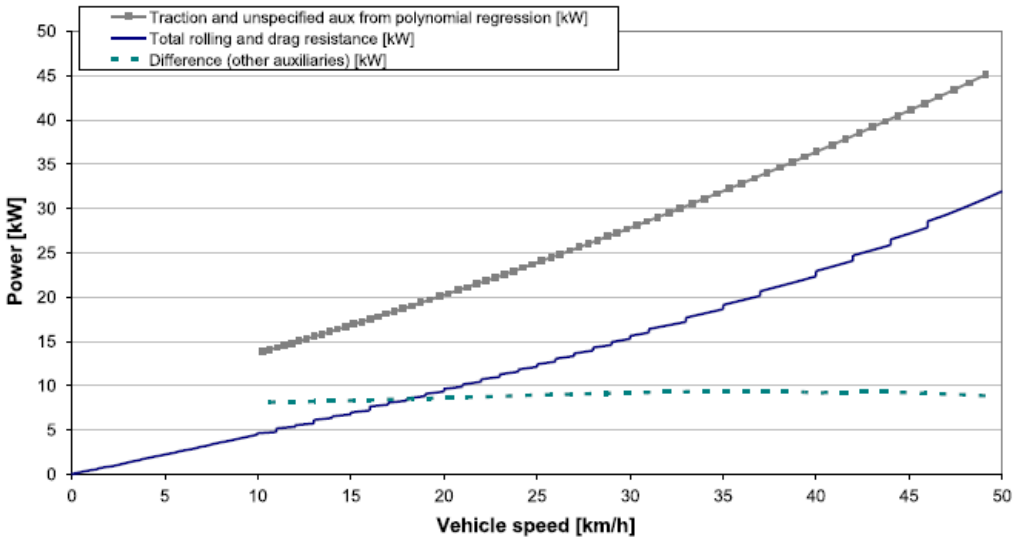

Figure 66: Total running resistance calculated with air and drag resistance coefficients from the roll-out test, compared with power for traction and unspecified auxiliaries calculated from Ballard data: fuel cell output minus dump, losses and specified auxiliaries (polynomial fit of data) from the constant speed test. The difference between the two representing the power consumption of auxiliaries is shown as a dotted line (Saxe, Folkesson, & Alvfors, 2008).

5.2.2.3 Studies examining four parameters

In 2001, a report conducted by T. Sandberg emphasized in the impact of several parameters on the fuel consumption of heavy duty vehicles. Using a simulation program, there were experiments carried out that showed how the rolling resistance, the air resistance, the gradient and auxiliary unites like A/C can affect the fuel consumption of a heavy truck on typical urban or on highway roads (Sandberg T. , 2001). There were also some mathematical expressions provided but those that refer to our subject are already mentioned before and give definitions about each of the parameters. There were references to the energy consumption of the vehicle (power and fuel) but not to the behavior of the vehicle considering the emissions.

According to the report, fuel consumption depends on a lot of factors; speed and weight of the vehicle are the most important because they effect the rolling resistance, air resistance and the resistance due to inclination of the road. This is illustrated in Figure 67 showing how the energy produced by the engine is divided into different energy losses. Data was generated with a simulation of a 40 ton truck on a typical road. Only points were the engine produced power were taken into account (no downhills). Due to the large weight, the largest loss was in potential energy when climbing up hills. About 30% of the energy was lost as rolling resistance in the tires and 23% was lost as air resistance. The rest, around 7%, came from losses in wheel bearings, the central gear, the gearbox, and engine auxiliary units.

Institutional Repository - Library & Information Centre - University of Thessaly
09/12/2017 02:36:50 EET - 137.108.70.7

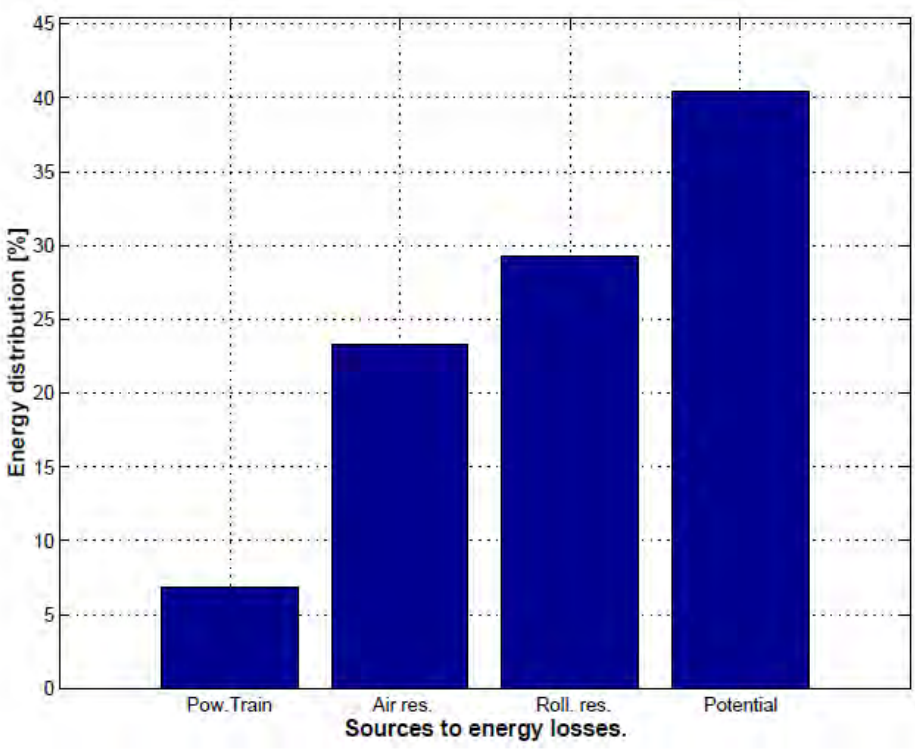

Figure 67: A simulation of a 40 ton truck on a typical road shows that most of the energy produced by the engine is used to climb the hills (Sandberg T. , 2001).

A good operational point is the combination of engine speed and load where the specific fuel consumption of the engine is low. The procedure of choosing good combinations of engine, gearbox, central gear ratio and tire dimension is called powertrain configuration. The potential of powertrain configuration is shown in Figure 68 where the same simulation as in Figure 67 is illustrated but here the base was the amount of energy put in to the engine through the fuel.

Institutional Repository - Library & Information Centre - University of Thessaly
09/12/2017 02:36:50 EET - 137.108.70.7

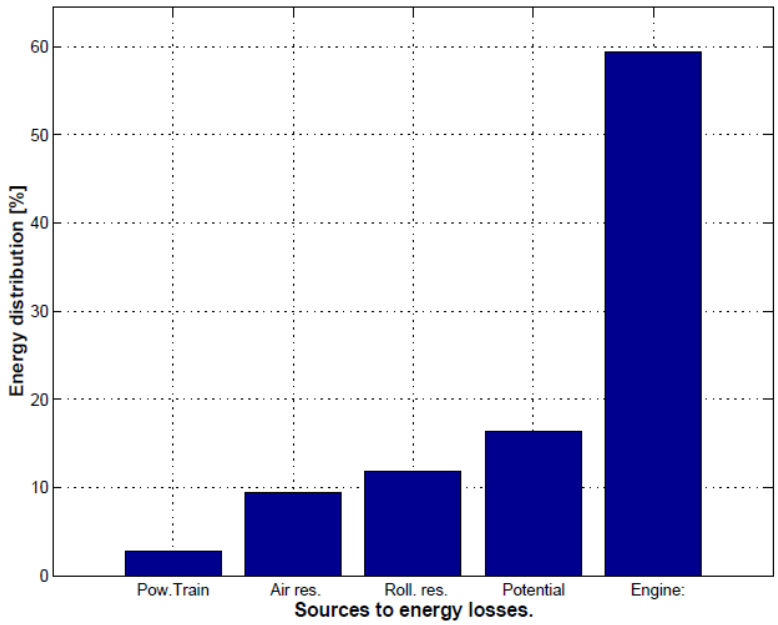

Figure 68: Distribution of the energy put in to (in the fuel) the engine for a 40 ton truck simulated on a typical road. Since the e_ciency of the engine is about 40% there is a large potential to improve this (Sandberg T. , 2001).

In another experiment the fuel consumption of a test truck in highway driving was measured. The altitude of the road was recorded with a barometer and used in the corresponding simulations. Despite of the limited accuracy of this equipment the simulation program managed to predict a level of fuel consumption only 2% lower than the real measurements. This was a satisfying result.

In 2005, a report of the European Cooperation in the field of Scientific and Technical Research was published with primary objective the development of an improved methodology for estimating pollutant emissions and fuel consumption from commercial (urban) road transport operated with Heavy Duty Vehicles in Europe (Sturm & Hausberger, 2005). There were no experiments conducted and no mathematical expressions about the fuel consumption and emission rates direct calculation. Mathematical expressions referring to the engine power needed for a vehicle to overcome road gradients were given though, taking in account also other parameters like the rolling resistance factor.

The resulting emission model PHEM (Passenger car and Heavy duty Emission model) is interpolating the fuel consumption and the emissions from the engine maps according to the course of engine power demand and engine speed in the driving cycles.

The actual engine power was calculated according to:

Institutional Repository - Library & Information Centre - University of Thessaly
09/12/2017 02:36:50 EET - 137.108.70.7

$$P = P_{rolling\ resistance} + P_{air\ resistance} + P_{acceleration} + P_{road\ gradient} + P_{transmission\ losses} + P_{auxiliaries} \quad [142]$$

The single parts of the total power demand from the engine are calculated as follows.

$$P_R = m \times a_g \times (C_{r0} + C_{r1} \times v + C_{r2} \times v^2 + C_{r3} \times v^3 \times C_{r4} \times v^4) \times v \quad [143]$$

where:

P_R:	power in [W];
m:	mass of vehicle plus loading [kg];
a_g:	gravitational acceleration [m/s²];
C_{r0}..C_{r4}:	rolling resistance coefficients;
v:	vehicle speed in [m/s], the vehicle speed is computed as average speed of second i and second (i+1) from the given driving cycle. The corresponding acceleration is ($v_{i+1} - v_i$).

The power for overcoming the air resistance was simulated as:

$$P_{air} = CD \times A_{Frontal} \times \frac{\rho}{2} \times v^3 \quad [144]$$

with

P_{air}:	power in [W];
CD:	drag coefficient [-];
$A_{Frontal}$:	frontal area of the HDV in [m²];
ρ:	density of the air [on average 1,2 kg/m³].

The values for CD and $A_{Frontal}$ were taken from the specifications given by the manufacturer. If no manufacturer specifications for the CD value were available the CD was set according to those of a similar HDV in a data bank of the TUG Institute.

The power for overcoming road gradients was calculated as:

$$P_g = m \times a_g \times Gradient \times 0.01 \times v \quad [145]$$

Institutional Repository - Library & Information Centre - University of Thessaly
09/12/2017 02:36:50 EET - 137.108.70.7

where

P_g:	power in [W];
a_g:	gravitational acceleration [m/s²];
Gradient:	road gradient in %;
m:	mass of the vehicle + loading in [kg].

The power demand of auxiliaries was given by:

$$P_{auxiliaries} = P_0 + P_{rated} \quad [146]$$

where

$P_{auxiliaries}$:	power in [kW];
P_0:	power demand of the auxiliaries as ratio to the rated power [-].

For average HDV this mathematical expression is sufficient from today's point of view. For special HDVs (e.g. garbage trucks) a more detailed approach may improve the model accuracy. Roads are rather seldom absolutely flat and the road gradient has a high influence on the engine loads pattern and the emission levels.

In 2010, a report by the U.S. Department of was published (NHTSA, 2010). The report presented the fundamental vehicle attributes that account for fuel consumption as a basis for discussing the technologies that could reduce fuel consumption. There was reference to urban but also highway conditions and there were conclusions concerning the fuel consumption, the power and the CO_2 emissions. Essentially, the committee described the force or power required to propel a vehicle at any moment in time as definable by a "road load equation," which evaluates the effect of tire rolling resistance, aerodynamic drag, acceleration, grade effects (both of which are affected by vehicle weight) but also accessories use like AC. The committee presented a visual depiction (Figure 69) to illustrate how the extremes of duty cycles can create a wide range of impacts of these specific vehicle attributes to overall fuel consumption, as follows:

Institutional Repository - Library & Information Centre - University of Thessaly
09/12/2017 02:36:50 EET - 137.108.70.7

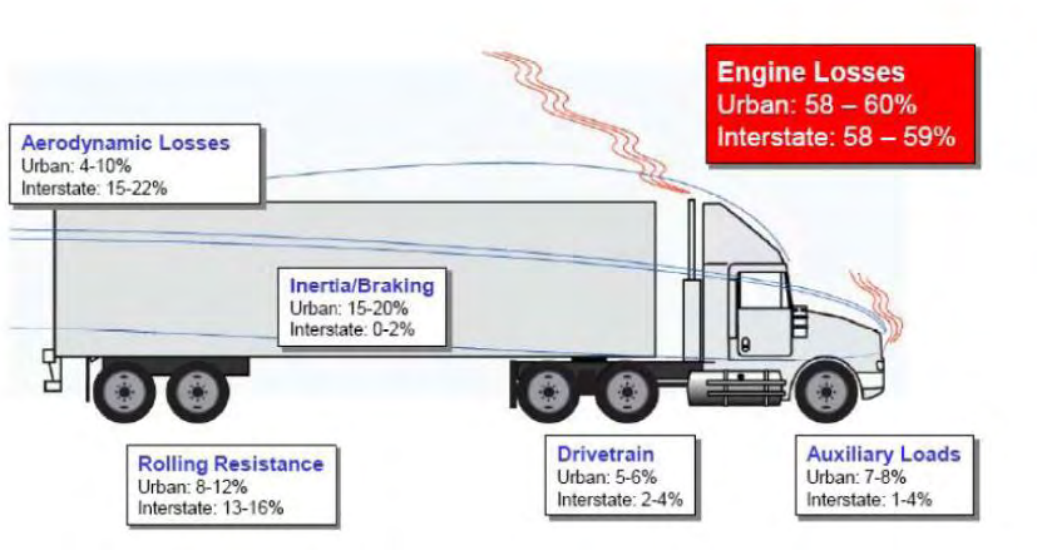

Figure 69: Energy "loss" range of vehicle attributes as impacted by duty cycle, on a level road (NHTSA, 2010).

The committee considered both physical testing and computer simulation as potential ways to evaluate fuel consumption and no mathematical expressions were provided. For physical testing, the committee explained that options included on-road testing and dynamometer testing. For measuring aerodynamics, the committee discussed coast-down testing, wind tunnel testing, and computation fluid dynamics (CFD). For on-road testing, the committee discussed SAE J1321, a fuel consumption procedure developed by the Society of Automotive Engineers and widely used by carriers and manufacturers for evaluating fuel economy, which measures on-road fuel consumption utilizing a similar control vehicle operated in tandem with a test vehicle to provide reference fuel consumption data.The committee's analysis suggested that the SAE procedure was roughly 3 percent accurate (99 percent confidence) between the test vehicle and the control vehicle.

The committee stated that at highway speeds, aerodynamic loads consume more power than any other load on current tractor-trailer vehicles and that auxiliary loads – such as compressed air needed for the braking systems, air conditioners, power-steering systems, and the alternator to charge the vehicle's battery – can consume up to 2.5 percent of fuel, so fuel consumption reductions of 1-2.5 percent are feasible. It was suggested that electrification of these auxiliaries, mostly in hybrid vehicles, would reduce some of this loss. The committee also stated that technological advances have lowered the coefficient of rolling resistance of tires by roughly 50 percent since 1990, but that further reductions are expected to be less dramatic.

Institutional Repository - Library & Information Centre - University of Thessaly
09/12/2017 02:36:50 EET - 137.108.70.7

Another important conclusion was fuel consumption, and therefore CO_2 emissions, are highly dependent on the drive cycle over which they are measured. Steady cruise conditions, such as highway driving, tend to be more efficient, having lower fuel consumption and CO_2 emissions. In contrast, highly transient operation, such as city driving, tends to lead to lower efficiency and therefore higher fuel consumption and CO_2 emissions.

5.2.3 Very Specific Type of Vehicles (VSVTs)

For this category of vehicles there were no studies found examining two or four parameters in correlation. Below we present the studies examining three parameters.

5.2.3.1 Studies examining three parameters

All the studies presented below examine the same three parameters in correlation: the gradient, the rolling resistance and the air resistance. The results show the impact of their combined activity on the vehicle's behavior.

In 1995, M. Barth, F. An, J. Osephnorbeck and M. Ross presented a new modal-emissions modeling approach that was deterministic and based on analytical functions that described the physical phenomena associated with vehicle operation and emissions productions (Barth, Norbeck, & Ross, 1995). They examined the influence of the three parameters mentioned above. This model relied on highly time-resolved emissions and vehicle operation data that had to be collected from a wide range of vehicles of varying emission control technologies using urban roads as data. The methodology of the presented model is described in Figure 70. There were mathematical expressions given for the calculation of the demanded power, the emissions of the vehicle and the fuel use. No experiments though were conducted. For the calculations there were also taken into account other parameters besides the gradient factor.

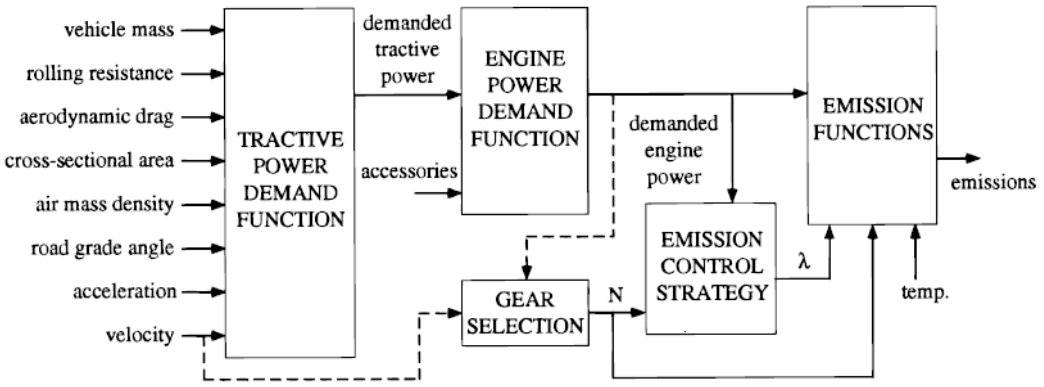

Figure 70: Power-demand emissions modeling methology
[Figure 2, (Barth, Norbeck, & Ross, 1995)]

Institutional Repository - Library & Information Centre - University of Thessaly
09/12/2017 02:36:50 EET - 137.108.70.7

An instantaneous power demand function was the fundamental basis of the physical model. By knowing the vehicle's mass and given a prescribed acceleration and velocity on a particular grade, the total tractive power requirements (in kilowatts) placed on a vehicle (at the wheels) is given in simplest form as:

$$P_{tractive} = \frac{M}{100} \times V \times (a + g \times sin\theta) + \left(m \times c_g \times C_r + \frac{\rho}{2} \times v^2 \times A_{Frontal} \times CD\right) \times v/1000 \quad [147]$$

where

m: vehicle mass (kg);

v: vehicle velocity (m/sec);

a: vehicle acceleration (m/s^2);

c_g: gravitational constant (9.81 m/s^2);

θ: road grade angle;

C_r: rolling resistance coefficient;

ρ: mass density of air (1.225 kg/m^3, depending on temperature and altitude);

A: frontal area of the vehicle (m^2);

CD: aerodynamic drag coefficient.

To translate this tractive power requirement to demanded engine power requirements, the following simple relationship can be used as a first approximation:

$$P_{engine} = \frac{P_{tractive}}{h_{tf}} + P_{accesories} \quad [148]$$

where h_{tf} is the combined efficiency of the transmission and final drive, and $P_{\text{accessories}}$ is the engine power demand associated with the operation of accessories, such as air conditioning, power steering and brakes and electrical loads. In the final model, $P_{\text{accessories}}$ may be modeled as a function of engine speed and h_{tf} can be modeled in terms of engine speed and P_{tractive}.

The speed of the engine in relation to the speed of the vehicle was determined by an internal gear selection strategy (or shift schedule) that depended on inputs such as engine and vehicle speeds and, possibly, other related inputs such as demanded engine power. Engine speed *N* (rps) played a role in fuel use and the emission control function. Gear selection and engine speed were complicated by the wide variety of automatic transmissions and their management.

Institutional Repository - Library & Information Centre - University of Thessaly
09/12/2017 02:36:50 EET - 137.108.70.7

One of the most important components of this physical model was approximating the emission control mechanisms of the vehicle. For older vehicles, engine control was accomplished through some combination of mechanical, pneumatic, or hydraulic systems. The engine control regulated fuel and air intake as well as spark timing and exhaust gas recirculation to achieve the desired performance in fuel economy, emissions, and power output. Due to the advent of automotive electronics, modern vehicles have complex emission control systems that closely regulate fuel injectors. For a hot-stabilized engine operating under normal conditions, the fuel mixture was maintained at the stoichiometric ratio, where the performance of the catalytic converter was maximized. However, there were several other vehicle operating modes that could affect the commanded air/fuel ratio. During engine start and warm up, the air/fuel ratio was typically commanded rich to improve combustion stability (older, carbureted vehicles use a choke). Another important operating mode was during high power episodes, such as those induced by hard accelerations and/or steep grades. When modeling the emission control function, we considered λ as the regulated output variable, where λ was the "equivalence ratio" and was defined as:

$$\lambda = \frac{(A/F)_0}{(A/F)} \qquad [149]$$

where $(A/F)_0$ is the air/fuel ratio at stoichiometry (≈14.7), and (A/F) is the commanded air/fuel ratio.

A model that determines the fuel use in any driving cycle for any vehicle model has previously been developed and is given as:

$$\frac{dF}{dt} \approx \lambda \times \left(k \,.N\,.D + \frac{P_{engine}}{\eta_{engine}} \right) \qquad [150]$$

where

k: engine friction factor (representing the fuel energy used at zero power output to overcome engine friction per engine revolution and unit of engine displacement);

N: engine speed;

D: engine displacement;

P_{engine}: demanded engine power;

η_{engine}: measure of indicated engine efficiency.

Institutional Repository - Library & Information Centre - University of Thessaly
09/12/2017 02:36:50 EET - 137.108.70.7

This mathematical expression is a simple but fairly accurate way to determine fuel use rate (in kilowatts).

A set of analytical functions that describes engine emissions rates were developed as functions of fuel consumption and air/fuel ratio. Under stoichiometric conditions, engine out emissions are basically proportional to fuel use. These functions change, however, with non-stoichiometric conditions (e.g., commanded enrichment). Tailpipe emissions can be modeled as:

$$Emissions_{tailpipe} = \frac{dF}{dt} . \frac{dCO/dt}{dF/dt} . CPF \quad [151]$$

where

dF/dt: the fuel-use rate in g/s;
dCO/dt: the engine-out emissions (for CO) in grams/s;
CPF: the catalyst pass fraction, a function primarily of temperature and equivalence ratio.

Also in 1995, the N.D. Lea International Ltd made a report about modeling road user effects in HDM4. This study was The Maintenance Standards Model (HDM) is widely used by consultants, lending agencies and government departments to investigate the economic consequences of investments in the road infrastructure (International Ltd., 1995). According to this report, the gradient resistance is the force component in the direction of travel necessary to propel a vehicle up a grade (positive resistance) or down a grade (negative resistance) either during driving in urban roads or highway roads. The study provided mathematical expressions referring to the power needed to overcome the gradient resistance in combination also with other parameters. There were also experimental results presented but no reference to the behavior of the vehicle concerning the emissions and the fuel consumption.

The weight of the vehicle can be resolved into both a parallel and perpendicular component with respect to the direction of travel. Therefore, the gradient resistance is given as:

$$Fg = m \times c_g \times \sin(\theta) \quad [152]$$

where

m: the mass of the vehicle;

Institutional Repository - Library & Information Centre - University of Thessaly
09/12/2017 02:36:50 EET - 137.108.70.7

c_g: the gravitational contant;

Fg: the gradient force in N;

θ: the angle of incline in radians.

Since θ is small, θ » sin(θ) » tan(θ), and tan(θ) = GR/100, where GR is the gradient as a percentage.

Using this approximation Fg can be written as:

$$Fg = m \times GR \times c_g \times 10^{-2} \quad [153]$$

The approximation that θ » sin(θ) » tan(θ) introduces a 1.1 per cent error on a gradient of 15 percent. In the figure below, there is a schematical description of the Fg acting on a vehicle.

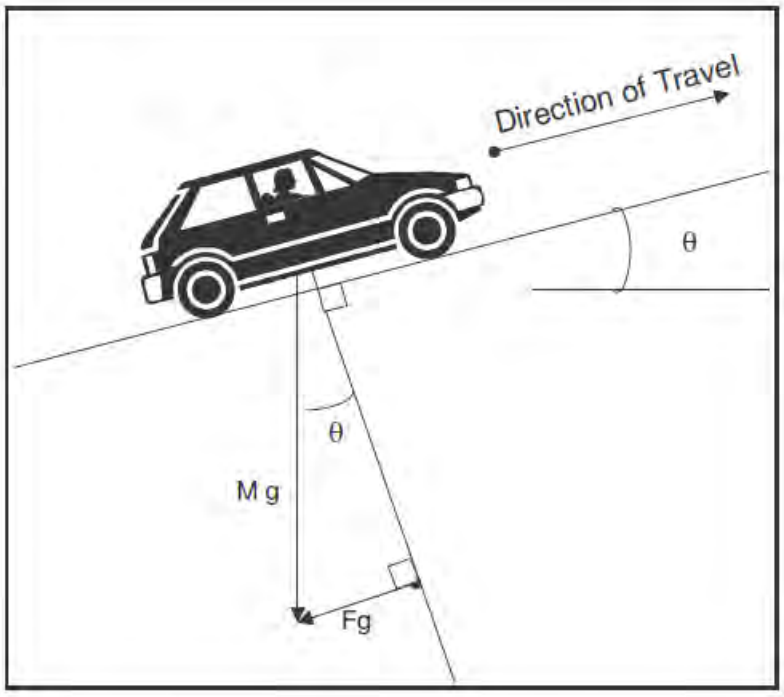

Figure 71: Resolving Forces on a Gradient [Figure 4.5, (International Ltd., 1995)].

The HDM-III speed prediction model assumed that the speed at any given time was the minimum of the various constraining speeds (Watanatada, Lima, & Dhareshwar, 1987b):

$$VSS = \min(VDRIVE, VBRAKE, VCURVE, VROUGH, VDESIR)$$

where

VSS: the steady-state velocity in m/s;

VDRIVE: the velocity limited by gradient and used driving power in m/s;

VBRAKE: the velocity limited by gradient and used braking power in m/s;

Institutional Repository - Library & Information Centre - University of Thessaly
09/12/2017 02:36:50 EET - 137.108.70.7

VCURVE: the velocity limited by curvature in m/s;

VROUGH: the velocity limited by roughness in m/s;

VDESIR: the desired velocity under ideal conditions in m/s.

Figure 72 shows the behavior of the above speeds referring to a heavy truck and Figure 73 presents the VDRIVE of two different types of vehicle: a passenger car and an articulated truck.

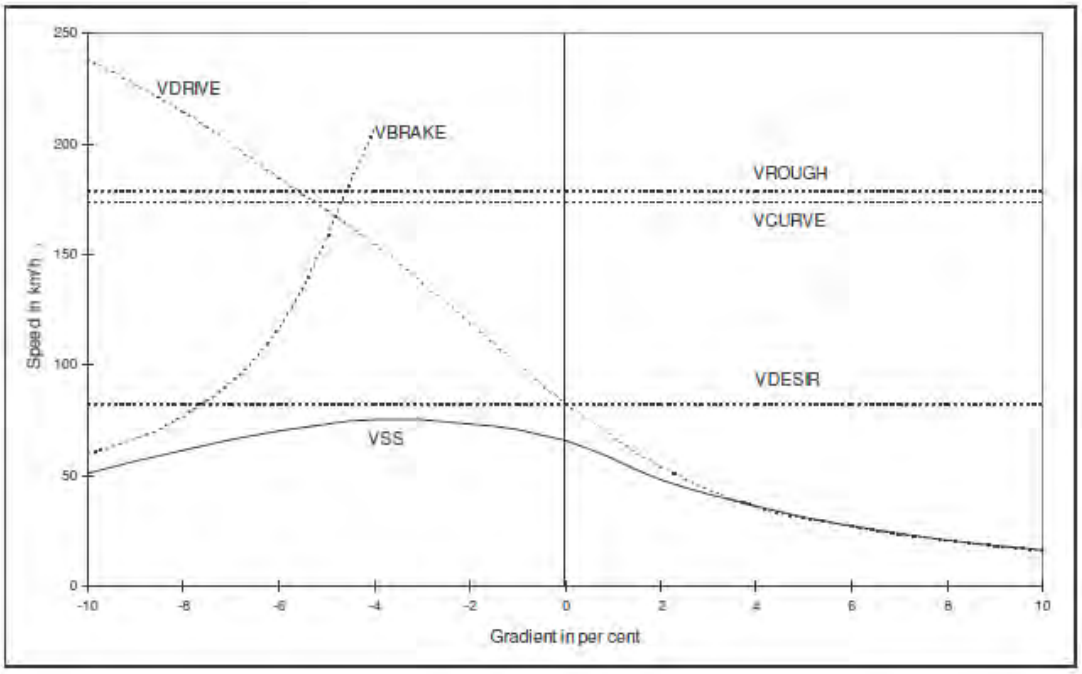

Figure 72 Constraining and Steady-state Velocities versus Gradient for a Heavy Truck [Figure 5.1, (Watanatada, Lima, & Dhareshwar, 1987b)].

VDRIVE is the constraining speed due to the used driving power. The used driving power is less than the maximum rated output power. The maximum driving power is typically between 60 and 80 percent of the maximum rated output power (Bennett, A speed prediction model for rural two-lane highways, 1994), with the lower values pertaining to vehicles with high power to weight ratios.

Institutional Repository - Library & Information Centre - University of Thessaly
09/12/2017 02:36:50 EET - 137.108.70.7

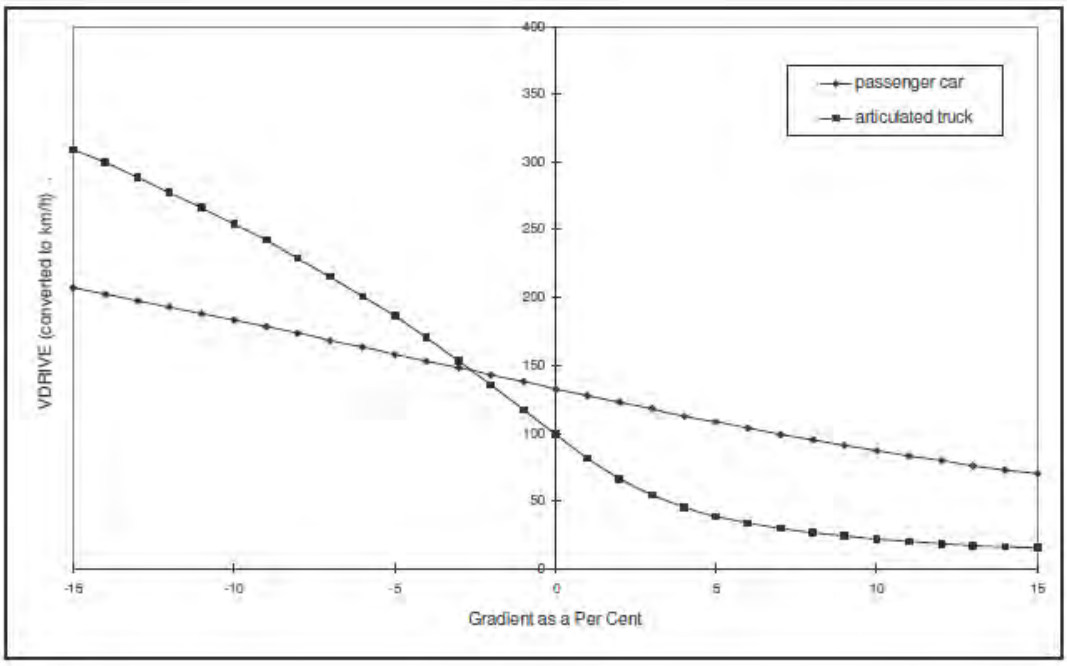

Figure 73 VDRIVE versus Gradient for a Passenger Car and an Articulated Truck [Figure 5.2, (Watanatada, Lima, & Dhareshwar, 1987b)].

The maximum driving power is calculated on steep upgrades with zero curvature resistance and inertial forces. This results in the following simplified expression for calculating the driving power:

$$P_d = \frac{v \times (Fa + Fr + Fg)}{1000} \quad [154]$$

where

P_d: the maximum utilised driving power in kW;

v: the vehicle velocity in m/s;

Fa: the aerodynamic resistance in N;

Fr: the rolling resistance in N;

Fg: the gradient resistance in N.

It is shown that the driving power dominates only on positive gradients or on minor negative gradients where power is required to overcome rolling and aerodynamic resistance. As shown in Figure 73, on positive gradients there is a marked difference in the predicted speeds. Because of their high power-to-weight ratios, the passenger car experiences a much lower speed reduction than the trucks. The truck speeds decrease rapidly to their "crawl speed" where the forces are in balance.

Institutional Repository - Library & Information Centre - University of Thessaly
09/12/2017 02:36:50 EET - 137.108.70.7

In 2007, a report about on-road remote sensing of automobile emissions in the Chicago area was published (Bishop, Stadtmuller, & Stedman, 2007). The Vehicle Specific Power was used again to show the impact of the gradient, rolling resistance and air resistance on the emissions of the vehicle. There have been measurements conducted on passing vehicles in a highway road. The study, besides the experimental results, presented a mathematical expression to evaluate this impact. There are results about the emissions based on the VSP but there is no reference to the behavior of the fuel consumption.

A mathematical expression for determining the instantaneous power of an on-road vehicle has been proposed by (Jimenez, McClintock, McRae, Nelson, & Zahniser, 1999), which takes the form:

$$VSP = 4.39 \times \sin(\theta) \times v + 0.22 \times v \times \mathrm{a} + 0.0954 \times v + 0.0000272 \times v^3 \quad [155]$$

where VSP is the vehicle specific power in kW/metric tonne, θ is the angle of the roadway (in degrees), v is vehicle speed in mph, and a is vehicle acceleration in mph/s. Derived from dynamometer studies, and necessarily an approximation, the first term represents the work required to climb the gradient, the second term is the $f = m\times$ a work to accelerate the vehicle, the third is an estimated friction term, and the fourth term represents aerodynamic resistance.

The emissions data were binned according to vehicle specific power, and illustrated in Figure 74. All of the specific power bins contain at least 100 measurements and the HC data have been offset adjusted.

Institutional Repository - Library & Information Centre - University of Thessaly
09/12/2017 02:36:50 EET - 137.108.70.7

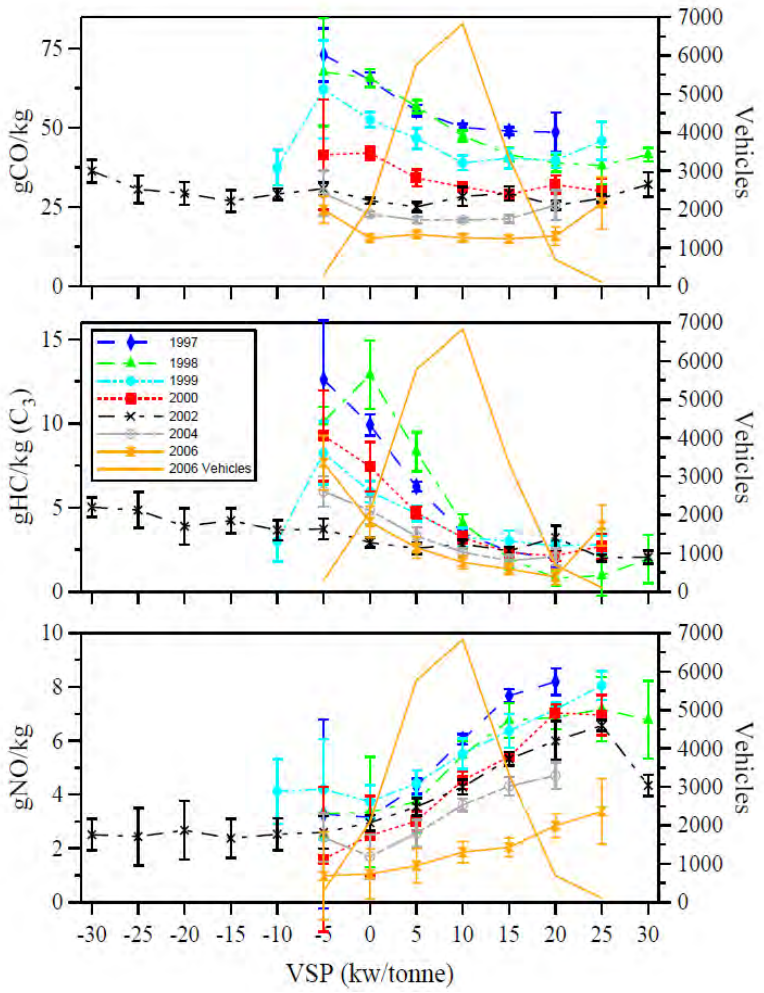

Figure 74: Vehicle emissions as a function of vehicle specific power for all of the Chicago E-23 data sets. Error bars are standard errors of the mean calculated from daily samples. The solid line without markers is the vehicle count profile for the 2006 data set [Figure 8, (Bishop, Stadtmuller, & Stedman, 2007)].

In 2012, Jian-Da Wu, Jun-Ching Liu proposed a predictive system for car fuel consumption using a radial basis function (RBF) neural network (Wu & Jun-Ching, 2012). The proposed work consisted of three parts: information acquisition, fuel consumption forecasting algorithm and performance evaluation. For the creation of the system there were mathematical expressions provided that compute the power demand of the vehicle but not the fuel consumption and emissions. The impact of correlation of the three parameters were studied and different type of roads were used (urban and highway roads). Although there are many factors affecting the fuel consumption of a car in a practical drive procedure, in the present system the relevant factors for fuel consumption were simply decided as make of car, engine style, weight of car, vehicle type and transmission system type which were used as input information for the neural network training and fuel consumption forecasting procedure.

Institutional Repository - Library & Information Centre - University of Thessaly
09/12/2017 02:36:50 EET - 137.108.70.7

The weight of cars and transmission types affect the physical characteristics that directly influence fuel consumption. For the weight of the car, a greater weight indicates higher engine loads. This can affect engine loads for fuel consumption. The tractive force F_T required at the interface between the tires of the driven wheels and the road is expressed with the following mathematical expression:

$$F_T = CD + C_r + m \times (\frac{dv}{dt}) + m \times a_g \times \sin(\theta) \quad [156]$$

where CD is the aerodynamic drag, C_r is the tire rolling resistance, m is the vehicle's mass, v is road speed, a_g is the acceleration of gravity, and a is the inclination angle of the road. The m×(dV/dt) is termed acceleration resistance and $m \times a_g \times \sin(\theta)$ is the climbing resistance. All resistances will reduce the power of the engine production.

For the weight of car and vehicle types, the two impact factors having to be overcome are rolling resistance and air resistance. The rolling resistance R of a vehicle depends on its mass and a coefficient of rolling resistance, and is expressed by the following mathematical expression:

$$R = C_r \times G \quad [157]$$

where C_r is coefficient of rolling resistance, G = m×g is the force that vehicle exerts on the ground, and m is the vehicle's mass.

The research successfully verified the effectiveness of the RBF (Radial Basis Function) network to forecast the fuel consumption of cars. The percentages of accuracy and prediction performance were used to estimate the forecasting efficiency of the proposed system.

5.3 Conclusions

From the presented studies, we conclude that parameters as the gradient, the rolling resistance, the air resistance and the use of the air conditioning system in correlation, can cause a high impact on the behavior of the vehicle, affecting its power/fuel consumption and/or the emissions.

The road gradient combined with one or more parameters and especially positive or very steep grades can have and even more serious impact in the fuel consumption or the emissions produced from the vehicle. Other factors such as the use of air conditioning system or the type of the vehicle (e.g. diesel, catalyst), the driving mode (e.g. stop and go or steady speed, acceleration), the type of road are also factors that combined with other parameters can affect the fuel consumption and the exhausts of a vehicle.

Institutional Repository - Library & Information Centre - University of Thessaly
09/12/2017 02:36:50 EET - 137.108.70.7

Weather conditions combined with the above parameters can also contribute to the behavior of the vehicle. Under dry surface conditions at urban driving speed of 30 mph, fuel consumption per unit distance was found to be lower on concrete pavements than on asphalt pavements. Although other studies showed no difference between different types of road (e.g. asphalt and concrete). In the study of (Taylor, Eng, & Patten, 2006), an LDV was found to consume more fuel on asphalt than concrete and less on a composite pavement during a winter test. On the other hand, in summer tests, it was found to consume more on a composite pavement than concrete and less on asphalt. It was also mentioned that when the ambient or pavement temperature increases, the fuel consumption decreases.

All the studies examining the air resistance were found to be in correlation with other parameters. The wind and the air density in combination with the size and the shape of the vehicle and also the gradient, rolling resistance and the use of A/C can cause a resistance that the vehicle has to overcome using more power and therefore consuming even more fuel. The reduction of fuel consumption of vehicles by aerodynamic means has become an accepted practice in the last decades by mounting add-on devices for the vehicles. Also modifications of the main shape of the vehicle improved the aerodynamic efficiency in a positive way. Besides extensive wind tunnel testing, road testing of the aerodynamic devices is needed to convince the transportation market of the effectiveness of the aids (Gandert, Raemdonck, & van Tooren, 2008).

Besides energy consumption decision makers need also to consider several other factors in order to satisfy the multiple requirements of protecting the environment (limiting greenhouse gas emission), saving energy, reducing traffic noise and ensuring good driving safety and comfort.

Institutional Repository - Library & Information Centre - University of Thessaly
09/12/2017 02:36:50 EET - 137.108.70.7

GENERAL CONCLUSIONS

Throughout the previous chapters, we studied the effect of some important parameters to the behavior of the vehicle concerning the fuel consumption and the emission rates. More specifically, our study was concentrated on the effect of the gradient, the rolling resistance, the air resistance (drag) and the use of accessories like the A/C and the impact of all these factors either separately or in correlation.

Other factors like the type of the vehicle, the type of road, the speed and the weather conditions were also taken into account in the majority of the information presented in the above chapters.

It is a fact that the road grade is a parameter that definitely affects the fuel consumption especially in uphill driving and even more if it is combined with higher speeds or heavier vehicles.

The A/C use also has an impact on the fuel consumption and the emissions of the vehicle as it consumes a percentage of the power of the vehicle in order to operate. It is important that it is used in a controlled way, taking into account the ambient temperature/humidity and keeping a stable temperature so that excessive use is avoided. The use of accessories like the A/C needs to be studied more than the previous years as the majority of the vehicles nowadays are occupied with A/C. It has become a significant parameter that definitely affects the behavior of the vehicle and also the environment.

The air resistance is also an important parameter but as we also mentioned during our review, there were no studies examining only this parameter separately but it was studies in correlation with other important parameters. The wind and the air density in combination with the size and the shape of the vehicle and also the gradient, rolling resistance and the use of A/C can cause a resistance that the vehicle has to overcome using more power and therefore consuming even more fuel.

In real life, it is a fact that more than one of these parameters act at the same time so it was important that we presented studies that examine more than one of these together. The combination of these parameters can cause a higher impact on the fuel consumption of the vehicle and the emission rates.

Other factors also in combination with the road gradient, the rolling resistance, the air resistance and the use of A/C can cause even higher effects. Weather conditions for example that affect the quality of the road or the ambient temperature can affect the impact of the rolling resistance or the use of A/C.

Institutional Repository - Library & Information Centre - University of Thessaly
09/12/2017 02:36:50 EET - 137.108.70.7

Also, the type of the road or was also taken into account in all the above studies. The impact of the above parameters is different in highway roads were the range of speed is higher than in urban roads that there are perhaps lower speeds, traffic and stop-and-go conditions. The quality of the road and the age of the pavement was also found to have an effect as the vehicle behaves in a different way depending on the surface it is on.

In order to come to some general conclusions it was important to examine different types of vehicles. It is a fact that all these parameters have a different effect in combination with heavy and light vehicles. It is obvious that heavy duty vehicles need more power to operate so when driving on steeper grades or in wind conditions, the impact will be much higher that light duty vehicles.

The examination of all these parameters and factors can help the increase of the fuel economy and can reduce the emission rates of the vehicles. It is important also for the driver but also for the environment to find driving modes and vehicles that have a well-balanced energy behavior.

Institutional Repository - Library & Information Centre - University of Thessaly
09/12/2017 02:36:50 EET - 137.108.70.7

Bibliography

Pierson, W., Gertler, A., Robinson, N., Zielinska, B., Bishop, G., Stedman, D., και συν. (1994). Summary of recent tunnel studies in the Fort McHenry and Tuscarora mountain tunnels. *Forth CRC On-Road Vehicle Emissions.* San Diego.

Influence of passenger car auxiliaries on pollutant emission factors within the Artemis model, 24 (2008).

Adem, F. (2009). Drag reduction of pickup truck using add-on devices. Sacramento: California State University.

Afotey, B. (2008). Statistical approach to the development of a micro scale model for estimating exhaust emissions from light duty gasoline vehicles. *Phd Dissertation*. Arlinghton: University of Texas.

Akcelik, R. (1980). Can traffic management reduce vehicle fuel consumption and emissions and affect vehicle design requirements. *Objectives in Traffic System Management. Proc. Conf.* Melbourn, Australia: National Science Centre / jointly organised by SAE-Australasia Energy Poligy. Advisory Committee and the Australian Road Research Board.

Akcelik, R. (1981). Fuel efficiency and other objectives in tragic system management. *Traffic Engine Control*, *22*, 54-65.

Akcelik, R. (1982). *Derivation and calibration of fuel consumption models.* Australian Road Research Board.

Ardekani, S. A., & Sumitsawan, P. (2010). *Effect of pavement type on fuel consumption and emissions in city driving.* The Ready Mixed Concrete Research & Education Foundation.

Barth, M., Norbeck, F. A., & Ross, M. (1995). modal emissions modeling: a physical aproach. *Transportation Research Record, 1520*, 81-88.

Bennett, C. (1989a). *The New Zealand vehicle operating cost model.* RRU Bulletin 82, Transit New Zealand, Wellington.

Bennett, C. (1994). *A speed prediction model for rural two-lane highways.* School of Engineering, Department of Civil Engineering, university of Auckland.

Institutional Repository - Library & Information Centre - University of Thessaly
09/12/2017 02:36:50 EET - 137.108.70.7

Biggs, D. (1987). *Estimating fuel consumption of light to heavy vehicles.* Nunawading: Australian Road Research Board.

Biggs, D. (1988). *ARFCOM- models for estimating light to heavy vehicle fuel consumption.* Research Report ARR 152, Australian Road Research Board.

Biggs, D. (1990). *Comparison of observed heavy vehicle fuel consumption in Canada with estimates.* Nunawading: Australian Road Research Board.

Biggs, D. (1995). Correspondence with HTRS Team.

Bishop, G. A., Stadtmuller, R., & Stedman, D. H. (2007). *On-road remote sensing of automobile emissions in the Chicago area.* Coordinating Research Council, CRC.

Boriboonsomsin, K., & Barth, M. (2009). Impacts of road grade on fuel consumption and carbon dioxide emissions evidenced by use of advanced navigation systems. *Journal of the Transportation Research, 2139,* 21-30.

Cadle, S. H., Ayala, A., Black, K. N., Fulper, C. R., Graze, R. R., Minassian, F., et al. (2007). Real-world vehicle emissions: a summary of the sixteenth coordinating research council on-road vehicle emissions workshop. *J. Air & Waste Manage Assoc., 57,* 139-145.

Cadle, S., Ayala, A., Black, K., Fulper, C., Graze, R., Minassian, F., et al. (2007). Real-world vehicle emissions: a summary of the sixteenth coordinating research council on-road vehicle emissions workshop. *J. Air & Waste Management,* 139-145.

Cicero-Fernandez, P., & Long, J. (1995). Motor vehicle episodic emissions due to high load driving and positive grades: an on-road, on-board sensing study. *A&WMA 88th Annual Meeting, Paper No. 95-TA37.03.* San Antonio, Texas.

Cicero-Fernandez, P., & Long, J. R. (1996). Assesment of commuting under grade loads and ramp meeting. *Preliminary On-road Emissions Findings World Car Conference.*

Cicero-Fernandez, P., & Long, J. R. (April 3-5, 1995). Grades and other loads effects on on-road emissions: an on-board analyzer study. *Fifth CRC On-Road Vehicle Emission Workshop San Diego.* El Monte, California: California Resources Board Mobile Source Division Analysis Section 9528.

Colberg, C. A., Tona, B., Catone, G., Sangiorgio, C., Stahel, W. A., Sturm, P., et al. (2005). Comparison of a road traffic emission model (HBEFA) with emissions derived from

Institutional Repository - Library & Information Centre - University of Thessaly
09/12/2017 02:36:50 EET - 137.108.70.7

measurements in the Gubrist road tunnel, Switzerland. *Atmospheric Environment*, 4703-4714.

Colberg, C. A., Tona, B., Catone, G., Sangiorgio, C., Stahel, W. A., Sturm, P., et al. (2005). Statistical analysis of the vehicle pollutant emissions derived from several european road tunnel studies. *Atmospheric Environment*, 2499-2511.

Colberg, C. A., Tona, B., Catone, G., Sangiorgio, C., Stahel, W. A., Sturm, P., et al. (2005). Statistical analysis of the vehicle pollutant emissions derived from several European road tunnel studies. *Atmospheric Environment, 39*, 2499-2511.

Colberg, C. A., Tona, B., Stahel, W. A., & Staehelin, J. (2005). Comparison of a road traffic emission model (HBEFA) with emissions derived from measurements in the Gubrist road tunnel, Switzerland. *Atmospheric Envoronment, 39*, 4703-4714.

Council, N. R. (2006). *Tires and passenger vehicle fuel economy.* Washington DC: Transportation Research Board.

De Graaff, D. (1999). *Rolling resistance of porous asphalt - a pilotstudy.* The Netherlands.

Delorme, A., Karbowski, D., & Sharer, P. (2009). *Evaluation of fuel consumption potential of medium & heavy duty vehicles through modeling and simulation.* National Academy of Sciences.

Denis, M. S., & Winer, A. (October 18-20, 1993). Prediction of on-road emissions and comparison of modeled on-road Emissions to federal test procedure emissions. *Specialty Conference on The Emiission Inventory: Perception and Reality of A&WMA*, (pp. 18-20). Pasadena California.

Denis, M. S., Cicero-Fernandez, P., Winer, A., & al, e. (1994). Effects of in-use driving conditions and vehicle/engine operating parameters on off-cycle events: comparison with federal test procedure conditions. *J. Air Waste Manage. Assoc., 44*, 31-38.

Department of Energy. (2009). *Advanced technologies and energy efficiency:where does the energy go?* Retrieved from http://www.fueleconomy.gov/feg/atv.shtml

Duleep, K. (November, 2005). Tires, technology, and energy consumption. PowerPoint presentation. Energy efficient tires: improving the on-road performance of motor vehicles. Paris, France: International Energy Agency.

EAPA, & EUROBITUME. (March 2004). *Environmental impacts and fuel efficiency of road pavements.*

Institutional Repository - Library & Information Centre - University of Thessaly
09/12/2017 02:36:50 EET - 137.108.70.7

Enns, P., German, J., & Markey, J. (October 18-20, 1993). EPA's survey of in-use driving patterns: implications for mobile source emission inventories. *Specialty Conference on The Emission Inventory: Perception and Reality of A&WMA.* Pasadena California: A&WMA.

EPA. (2006). *Fuel economy labeling of motor vehicle revisions to improve calculation of fuel economy estimates.* Office of Transportation and Air Quality.

EPA. (2010). *MOVES2010 Highway vehicle temperature, humidity, air conditioning, and inspection and maintenance adjustments.*

Frey, H. C., Rouphail, N. M., Zhai, H., Farias, T. L., & Goncalves, G. A. (2007). Comparing real-world fuel consumption for diesel- and hydrogen-fueled transit buses and implication for emissions. *Transportation Research, 12,* 281-282.

Frey, H. C., Unal, A., Rouphail, N. M., & James D., C. (2003). On-road measurement of vehicle tailpipe emissions using a portable instrument. *J. Air & Waste Manage. Assoc., 53,* 992-1002.

Frey, H. C., Zhang, K., & Rouphail, A. M. (2008). Fuel use and emissions comparisons for alternative routes, time of day, road grade, and vehicles based on in-use measurements. *42,* 2483-2489.

G.W. Taylor Consulting. (2002). *Additional analysis of the effect of pavement structure on truck fuel consumption.* Government of Canada.

Gandert, M., Raemdonck, V., & van Tooren, M. (2008). Data acquisition of a tractor-trailer combination to register aerodynamic performances. *Faculty of Aerospace Engineering*.

Gibbons, J. (1999). Pavements and surface materials. *UConn Extension Land Use Educator*.

Gillespie, J. S., & McGhee, K. K. (2007). Get in, get out, come back!What the relationship between pavement roughness and fuel consumption means for the length of the resurfacing cycle. *Journal of the Transportation Research Board,* 32-39.

Goodyear. (2012). *Factor affecting truck fuel economy.*

Hammarstrom, U., & Yanya, M. (2011). *A method for estimation of average engine fuel maps. Power measurements at drive wheels.* Linkoping: Swedish Road and Transport Institute.

Institutional Repository - Library & Information Centre - University of Thessaly
09/12/2017 02:36:50 EET - 137.108.70.7

Hammarstrom, U., Eriksson, J., Karlsson, R., & Yahya, M.-R. (2012). *Rolling resistance model, fuel consumption model and the traffic energy saving potential from changed road surface conditions.* The Swedish Transport Administration.

Hammarstrom, U., Karlsson, R., & Sorenssen, H. (2008). *Road surface effects on rolling resistance - coastdown measurements with uncertainty anaysis in focus.* Linkoping: The Swedish Road and Transport Research Institute/EIE/06/039/S12.448265-ECRPD.

Harris, B. (2005). Comments on modelling procedures and a proposed partial one-way traffic-flow system. *Capita Symonds air quality modeling results for Bradford on Avon: a commentary*.

Hassel, D., & Weber, F.-J. (1997). Gradient influence on emission and consumption behavior of light and heavy duty vehicles. MEET Project/Action COST 319.

Hassel, D., Brosthaus, J., Dursbeck, F., Jost, P., Sonnborn, K. S., & Rheinland, T. (1983). *Das abgas emissionsverhalten von nutzfahrzeugen in der bundesrepublik Deutschland im bezugsjahr 1980.* Berlin: Umweltbundesamt.

Hassel, D., Jost, P., Weber, F., Dursbeck, F., Sonnborn, K., & Plettau, D. (1995). *.: Abgas-Emissionsfaktoren von Nutzfahrzeugen in der Bundesrepublik Deutschland Abschlußbericht des TÜV Rheinland.* Berlin.

Hausberger , S., Rexeis, M., Zallinger, M., Luz , R., & Eichlsede, H. (2009). *Emission factors from the model PHEM for the HBEFA Version 3.* Graz University of Technology.

Helms, H., & Lambrecht, U. (2006). The potential contribution of light-weighting to reduce transport energy consumption. *International Journal of Life Cycle Assessment*.

Hickman, A. (1999). *methodology for calculating transport emissions and energy consumption.* Deliverably 22 for the MEET project.

Hucho, W.-H. (1998). *Aerodynamics of road vehicles.* Warrendale,PA: SAE International.

Hugrel, C., & Joumard, R. (September 17-19, 2001). The contribution of passenger cars to the greenhouse effect: the influence of air-conditioning and ACEA's commitment (JAMA and KAMA included) on the CO2 emissions. *Proceedings of 10th International Symposium "Transport and Air Pollution.* Boulder, Colorado USA.

Ihs, A., & Velin, H. (2002). *Vägytans inverkan på fordonshastigheter.* Statens väg- och transportforskningsinstitut.

Institutional Repository - Library & Information Centre - University of Thessaly
09/12/2017 02:36:50 EET - 137.108.70.7

Ingram, K. (1978). *The wind-averaged drag coefficient applied to heavy goods vehicles.* Crowthorne, Berkshire.

International Ltd., N. L. (1995). *Modeling road user effects in HDM4.* RETA 5549-REG Higway Development and Management Research.

Jest, P., Hassel, D., & Sonnbrn, K. (1995). A new method to determine exhaust emission factors for heavy duty vehicles. *The Science of the Total Enviromnment, 169*, 213-217.

Jimenez, J., McClintock, P., McRae, G., Nelson, D., & Zahniser, M. (1999). *Proceedings of the 9th CRC On-Road Vehicle Emissions Workshop.* CA: Coordinating Research Council.

John, S., & Kobett, D. (1978). *Grade effects on traffic flow stability and capacity.* Washinghton D.C.: Transportation Research Board.

Karlsson, R., Hammarström, U., Sörensen, H., & Eriksson, O. (2011). *Road surface influence on rolling resistance. Coastdown measurements for a car and an HGV.* Linköping: The Swedish Road and Transport Research Institute.

Keller, M., Evequoz, R., Heldstab, J., & Kessler, H. (1995). Luftschadstoffemissionen des straßenverkehrs 1950-2010. *Bundesamt fur Umwelt, Wald and Landschaft*. Bern.

Kelly, N., & Groblicki, P. (1993). Real-world emmisions from a modern production vehicle driven in Los Angeles. *J. Air Waste Manage. Assoc., 43*, 1351-1357.

Koupal, J. (2001). Air conditioning activity effects in MOBILE6. *Air and radiation*.

Koupal, J., & Kremer, J. (2001). Air conditioning correction factors in MOBILE6. *Air and Radiation*.

LaClair, T. (2006). *The Pneumatin Tire: roling resistance.* (A. Gent, & J. Walter, Eds.) Washington DC: National Highway Traffic Safety Administration.

Larry, R. E., MacIsaac Jr., J. D., Harris, J. R., Yates, K., Dudek, W., Holmes, J., et al. (2009). *NHTSA tire fuel efficiency consumer information program development: phase 2 – effects of tire rolling resistance levels on traction, treadwear, and vehicle fuel economy*. National Highway Traffic Safety Administration.

Institutional Repository - Library & Information Centre - University of Thessaly
09/12/2017 02:36:50 EET - 137.108.70.7

Leung, D., & Williams, D. (2000). modeling of motor vehicle fuel consumption and emissions using a power-based model. *Environmental Monitoring and Assessment, 65*, 21-29.

Manning, F., & Kilareski, W. (1990). *Principles of highway engineering and traffic analyses.* Brisbane: John Wiley and Sons.

McLean, J., & Ramsay, E. (October 1996). *Interpretations of road profile-roughness data: review and research needs.* Australia: ARR 295, ARRB Transport Research Ltd.

Michelin. (2003). *The Tire Encyclopedia* (Vol. 3). France.

Nam , E. (2000). *Understanding and modeling NOx emissions from air conditioned automobiles.* SAE paper 2000-01-0858.

NHTSA. (2010). *Factors and considerations for establishing a fuel efficiency regulatory program for commercial medium -and heavy- duty vehicles.* U.S Department of Transportation.

NOAA website. (n.d.). Retrieved from NOAA's National Weather Service: http://www.nws.noaa.gov/om/heat/index.shtml#heatindex.

OECD. (2004). *Can cars come clean?Strategies for low-emission vehicles.* Organisation for Economic Co-Operation & Development.

Ongel, & Aybike. (2007). Experimental analysis of open-graded asphalt concrete mixes in terms of safety, durability, and noise. 385. University of California.

Park, J., Kong, J., Jo, H., Park, Y., & Lee, J. (2001). Measurement of road gradients for the development of driving modes including road gradients. *Journal of Automobile Engineering*(9), 977-986.

Park, J., Kong, J., Jo, H., Park, Y., & Lee, J. (2001). Measuremnts of road gradients for the development of driving modes including road gradients. *Journal of Automobile Engineering*(9), 977-986.

Park, J., Kong, J., Park, Y., & Lee, J. (2012, January 31). measurement of road gradients for the development of driving modes including road gradients. *Journal of Automobile Engineering*.

Park, S., & Rakha, H. (2005). Energy and environmental impacts of roadway grades. *Journal of the Transportation Research Board*, 148-160.

Institutional Repository - Library & Information Centre - University of Thessaly
09/12/2017 02:36:50 EET - 137.108.70.7

Pierson, W. R., Gertler, A. W., Robinson, N. F., sagebiel, J. C., Zielinska, B., Bishop, G. A., et al. (1996). Real-world automotive emissions:sSummary of studies in the Fort McHenry and Tuscarora mountain tunnels. *Atmospheric Environment, 30*(12), 2233-2256.

Pierson, W., Gertler, A., Robinson, N., Zielinska, B., Bishop, G., Stedman, D., et al. (1994). Summary of recent tunnel studies in the Fort McHenry and Tuscarora mountain tunnels. *Forth CRC On-Road Vehicle Emissions.* San Diego.

Post, K., Kent, J., Tomlin, J., & Carruther, N. (1984). Fuel consumption and emission modelling by power demand and a comparison with other models. *Transportation Research Record , 18A*(3), 191-213.

Post, K., Tomlin, J., Pitt, D., Carruthers, N., Maunder, A., Kent, J., et al. (1981). *Fuel Economy and Emissions Results.* Charles Kolling Res. Lab., University of Sydney.

Reimpell, J., Stoll, H., & Betzler, J. (2001). Engineering principles 2nd Edition. *The Automotive Chassis* , 123.

Ribau, J. P., Silva, C. M., & Farias, T. L. (2010). Electric and hydrogen consumption analysis in plug-in road vehicles. *International Journal of Energy and Environment, 1*(1).

Roujol, S. (2005). *Influence of passenger car auxiliaries on pollutant emissions.* Institute National De Recherche sur Les Transportes et Leur Securite.

Roujol, S., & Joumard, R. (2009). Influence of passenger car auxiliaries on pollutant emission factors within the Artemis model. *Atmospheric Environment, 43*, 1008–1014.

Sahlholm, P. (2008). Iterative road grade estimation for heavy duty vehicle control. KTH School of Electrical Engineering.

Sandberg, T. (2001). *Heavy truck modelling for fuel consumption. Simulations and measurements.* Linköping University.

Sandberg, U. S. (1990). Road macro- and megatexture influence on fuel consumption. *Environmental Impacts and Fuel Efficiency of Road Pavements*, 460-479.

Saxe, M., Folkesson, A., & Alvfors, P. (2008). Energy system analysis of the fuel cell buses operated in the project: Clean Urban Transport for Europe. *Elsevier Ltd.*, 689–711.

Schmidt, W., Dahlquist, E., Finkbeiner, M., Krinke, S., Lazzari, S., Oschmann, D., et al. (2004). Life cycle assessment of lightweight and end-of-life scenarios for generic

Institutional Repository - Library & Information Centre - University of Thessaly
09/12/2017 02:36:50 EET - 137.108.70.7

compact class passenger vehicles. *The International Journal of Life Cycle Assessment, 9*(6), 405-416.

Silva, C., & Farias, T. (2006). Evaluation of numerical models for simulation of real-world hot-stabilized fuel consumption and emissions of gasoline light-duty vehicles. *Transportation Research Part D, 11*, 377-385.

Singer, B. C., & Harley, R. .. (1996). A fuel-based motor vehicle emission inventory. *Journal of the Air & Waste Management Association, 46*, 581-593.

Singer, B. C., Kirchstetter, T. W., Harley, R. A., Kendall, G. R., & Hesson, J. M. (n.d.). A fuel-based approach to estimating motor vehicle cold-start emissions. *Journal of the Air & Waste Management Association, 49*, 125-135.

Smith, P. (1963). Past performance of composite pavements. *Highway Research Record, 37*, 14-30.

Sovran. (1984). The effect of ambient wind on a vehicle's aerodynamic work requirement and fuel consumption. *SAE Technical Paper*(840298).

Sovran, G., & Bohn, M. (1981). Formula for tractive energy requirements of vehicles during the EPA-Schedules. *Society of Automotive Engineers*(810184).

Sturm, P., & Hausberger, S. (2005). *Emissions and fuel consumption from heavy duty vehicles.*

Sullivan, & Edward, C. (1993, October). Vehicle speeds and accelerations along on-ramps: inputs to determine the emissions effects of ramp metering. California: Caltrans Office of Traffic improvement.

Sumitsawan, P., Romanoschi, S., & Ardekani, S. A. (August 2009). Effect of pavement type on fuel consumption and emissions. *Proceedings of the 2009 Mid-Continent Transportation Research Symposium.* Ames, Iowa: Iowa State University.

Taylor, G., Eng, P., & Patten, J. (2006). *Effects of pavement structure on vehicle fuel consumption - Phase III.* National Research Council of Canada & Conseil national de recherches.

U.S. Department of Energy. (n.d.). Retrieved from Energy Efficiency and Renewable Energy: http:/www.fueleconomy.gov/feg/atv.shtml

Institutional Repository - Library & Information Centre - University of Thessaly
09/12/2017 02:36:50 EET - 137.108.70.7

U.S. Environmental Protection Agency. (1994). *Air conditioning survey data.* Retrieved from http://www.epa.gov/otaq/sftp.htm#phoenix

van Raemdock, G. (2006). Design of an aerodynamic aid for a tractor-trailer combination. Delft University of Technology, Faculty of Aerospace Engineering.

Visser, A., & Curtayne, P. (1985). *A pilot study on the effect of road surface properties on the fuel consumption of a passenger car.* Pretoria: NITRR Contract Report C/PAD/46.5.

Watanatada, T., Lima, P. R., & Dhareshwar, A. M. (1987b). *Vehicle Speeds and Operating Costs.* Washington DC: World Bank Publications.

Watson, H. (1980). Can traffic management reduce fuel consumption and emissions and affect vehicle requirements. *Sensitivity of fuel consumption and emissions to driving patterns and vehicle design.* Australia.

Weilenmann, M., Vasic, A.-M., Stettler, P., & Novak, P. (2005). Influence of mobile air-conditioning on vehicle emissions and fuel consumption: a model approach for modern gasolinecars used in Europe. *Environ. Sci. Technol.*(39), 9601-9610.

Welstand, J., Haskew, H., Gunst, R., & Bevilacqua, O. (2003). *Evaluation of the effects of air conditioning operation and associated environmental conditions on vehicle emissions and fuel economy.* SAE Paper 2003-01-2247.

Wong, J. (1993). *Theory of ground vehicles.* Wiley.

Woodside, A., & al., e. (2003). Rolling resistance of surface materials affected by surface type, tyre load and inflation pressure. *Mairepav'03 Symposium.* Portugal.

Wu, J.-d., & Jun-Ching, L. (2012). A forecasting system for car fuel consumption using a radial basis function neural network. *Expert Systems with Applications, 39*, 1883-1888.

Yang, Z., & Khalighi, B. (2005). CDF simulation for flow over pickup trucks. *Society of Automotive Engineers*(2005-01-0547).

Zhang, K., & Frey, H. (2005). Road grade estimation for on-road vehicle emissions modeling using LIDAR data. *Proceedings, Annual Meeting od the Air & Waste Management Association.* Minneapolis, MN.

Institutional Repository - Library & Information Centre - University of Thessaly
09/12/2017 02:36:50 EET - 137.108.70.7

Zhang, K., & H.C., F. (June 20-23, 2005). road grade estimation for on-road vehicle emissions modeling using LIDAR data. *Proceedings, Annual Meeting od the Air & Waste Management Association.* Minneapolis, MN.

Institutional Repository - Library & Information Centre - University of Thessaly
09/12/2017 02:36:50 EET - 137.108.70.7